NRC Publications Archive
Archives des publications du CNRC

Performance of Protected Ceiling/Floor Assemblies and Impact on Tenability with a Basement Fire Scenario
Su, J. Z.; Taber, B. C.; Leroux, P.; Bénichou, N.; Lougheed, G. D.; Bwalya, A. C.

NRC Publications Archive Record / Notice des Archives des publications du CNRC :
https://nrc-publications.canada.ca/eng/view/object/?id=b001a3aa-0894-4046-a7d7-03c68300fa14
https://publications-cnrc.canada.ca/fra/voir/objet/?id=b001a3aa-0894-4046-a7d7-03c68300fa14

National Research Council Canada   Conseil national de recherches Canada

Performance of Protected Ceiling/Floor Assemblies and Impact on Tenability with a Basement Fire Scenario

IRC-RR-307

Su, J.Z.; Taber, B.C.; Leroux, P.; Bénichou, N.; Lougheed, G.D.; Bwalya, A.C.

May 2011

National Research Council Canada   Conseil national de recherches Canada

Canada

NRC · CNRC

Performance of Protected Ceiling/Floor Assemblies and Impact on Tenability with A Basement Fire Scenario

Research Report: IRC-RR-307

Date: May 13, 2011

Authors: Joseph Z. Su, Bruce C. Taber, Patrice Leroux, Noureddine Bénichou, Gary D. Lougheed, Alex C. Bwalya

ACKNOWLEDGMENTS

NRC·CNRC

EXECUTIVE SUMMARY

After the Phase-1 project of the Fire Performance of Houses (FPH), which had focused on the fire performance of unprotected floor assemblies above a basement and impact on occupant safety in single-family houses, a further study was conducted to investigate the fire performance of protected ceiling/floor systems in a basement fire scenario.

A series of full-scale fire experiments were conducted using four types of floor assemblies (wood I-joist, steel C-joist and metal-web wood truss assemblies, as well as solid-sawn wood joist assemblies), which were selected from the assemblies that had been tested in Phase 1 of the FPH research. The test assemblies were protected on the basement side with direct-applied regular gypsum board, residential sprinkler systems or a suspended ceiling. The study focused on the impact of the protection measures on the life safety of occupants from the perspective of tenability within the test house and structural integrity of floor systems for use as egress routes.

The experiments conducted using the test assemblies with regular gypsum board protection exhibited the same chronological sequence of fire events — fire initiation, smoke alarm activation, onset of untenable conditions, and finally structural failure of the test assemblies. The sequence was the same between the experiments conducted in this series of the full-scale fire experiments and also the same as the experiments conducted in Phase 1 of the FPH research for the fire scenario with an open basement doorway. Smoke obscuration was the first hazard to arise. Untenable (incapacitation) conditions were reached shortly after smoke obscuration. Compared to the experiments conducted in Phase 1 using the same floor structures without gypsum board protection, the times during which tenable conditions were maintained were similar or improved slightly whilst the structural performance was improved significantly with the gypsum-board-protected ceiling/floor assemblies. The times taken to reach structural failure for the gypsum-board-protected assemblies were much longer than those Phase 1 experiments with no protection. Also, with regular gypsum board protection, all test assemblies provided similar durations of structural fire endurance under the test fire scenario.

The experiment using the test assembly with the suspended ceiling followed the same sequence of fire events. However, the benefit of the suspended ceiling as a floor protection measure was marginal since the structural collapse of the test assembly was delayed only slightly and tenability conditions were similar to those found in Phase 1 tests of the same floor assembly without protection.

In the experiments with residential sprinkler-protected assemblies, the structural integrity of the test assemblies was protected, there was no structural failure or damage to the test assemblies in the test scenario and the fire was effectively suppressed. The residential sprinkler systems also maintained the conditions tenable in the test house during the experiments. Additional experiments were conducted with different and more challenging fuel package and fire location (a separate report RR-308 contains details and results of two such experiments [18]).

NRC·CNRC

TABLE OF CONTENTS

LIST OF FIGURES

NRC·CNRC

NRC·CNRC

NRC·CNRC

LIST OF TABLES

NRC·CNRC

PERFORMANCE OF PROTECTED CEILING/FLOOR ASSEMBLIES AND IMPACT ON TENABILITY WITH A BASEMENT FIRE SCENARIO

Joseph Z. Su, Bruce C. Taber, Patrice Leroux, Noureddine Bénichou, Gary D. Lougheed, Alex C. Bwalya

1   INTRODUCTION

1.1   Background

National Research Council Canada's Institute for Research in Construction (NRC-IRC) has been conducting a multiphase research project on the fire performance of houses (FPH). One of the primary objectives of the research is to determine the impact of products and systems used in construction of single-family houses on life safety of occupants under fire conditions.

The recently completed Phase 1 of the FPH research [1-7] was undertaken in response to a request from the Canadian Commission on Building and Fire Codes and the Canadian Commission on Construction Materials Evaluation to gain better understanding of the factors that affect the life safety of occupants in the event of a fire. The Phase-1 study focused on basement fires and their impacts on the structural integrity of unprotected floor assemblies above a basement and tenability conditions on upper storeys in the test house. A range of floor systems available in the marketplace was used in the Phase-1 research.

After the Phase-1 study, a group of industrial and governmental bodies expressed an interest in pursuing further studies to investigate the performance of protected floor systems and the effect of different protection measures on tenability conditions. In response, NRC-IRC's Fire Research (FR) Program formed a consortium to undertake the further studies (Phase 1b). This report documents the Phase-1b research project.

1.2   Objectives of the Research

A series of full-scale fire experiments were conducted in an experimental facility representing a typical two-storey detached single-family house with protected ceiling/floor assemblies above the basement under a basement fire scenario. The objectives of this consortium project are:
1. To study the fire performance of ceiling/floor systems protected by measures such as regular gypsum board, residential sprinkler systems or suspended ceiling; and
2. To understand the impact of the protection measures on the tenability conditions for occupants on the upper storeys.
3. To determine the sequence of events such as fire initiation, smoke alarm activation, onset of untenable conditions, and structural failure.

2   EXPERIMENTS

2.1   Experimental Facility

The experimental facility used represented a typical two-storey detached single-family house with a basement. Figure 1 and Figure 2 show an elevation view and a plan view, respectively, of the facility with basement, first storey and second storey. Each storey had a floor area of

NRC·CNRC

95 m^2 and a ceiling height of 2.4 m. There was no heating, ventilating and air-conditioning or plumbing system installed in the test house, i.e., no associated mechanical openings.

The basement was partitioned to create a fire room representing a 27.6 m^2 basement living area (the remaining area was not used during the experiments). This was the average size of basement rooms based on survey results [8]. A rectangular exterior opening measuring 2.0 m wide x 0.5 m high and located 1.8 m above the floor was provided in the south wall of the fire room. The size of the opening is equivalent to the area of two typical basement windows (1.0 x 0.5 m). A removable noncombustible panel was used to cover the opening at the beginning of each experiment. The walls of the fire room were lined with 12.7-mm-thick regular gypsum board.

A 0.91-m-wide x 2.05-m-high doorway opening located on the north wall of the fire room led into an empty stairwell enclosure (without a staircase). At the top of this stairwell, a 0.81-m-wide x 2.05-m-high doorway led into the first storey. This doorway leading to the first storey either had a door in the closed position (closed basement doorway) or had no door (open basement doorway), depending on the scenario being studied. There is no requirement for a basement door in the National Building Code of Canada (NBCC) [9].

The first storey had an open-plan layout. A test ceiling/floor assembly was constructed directly above the fire room for each experiment (more details are provided in Sections 4.2 - 4.9). The remainder of the floor on the first storey was constructed out of noncombustible materials. A 0.89-m-wide x 2.07-m-high doorway led to the exterior. The staircase to the second storey was not enclosed. There were no window openings on the first storey.

Figure 1. The test facility
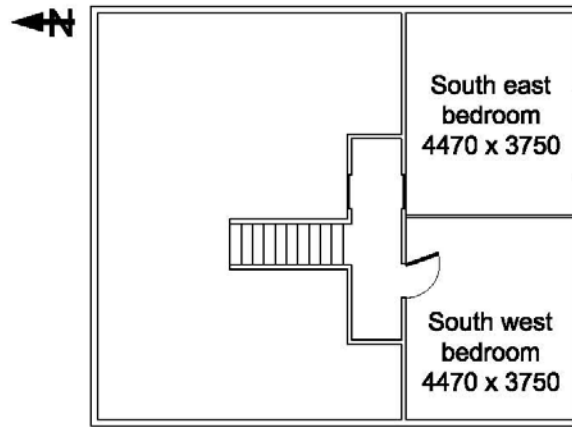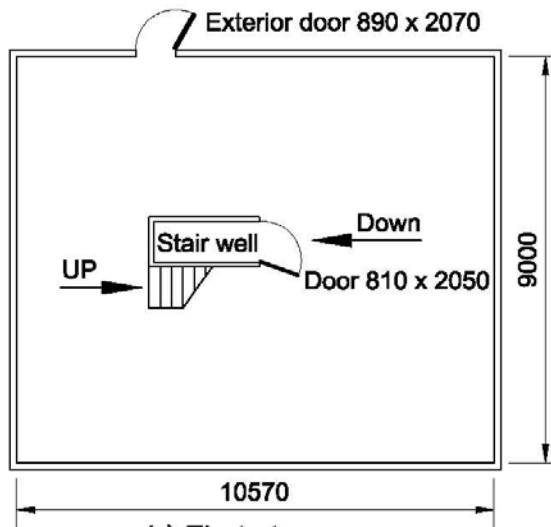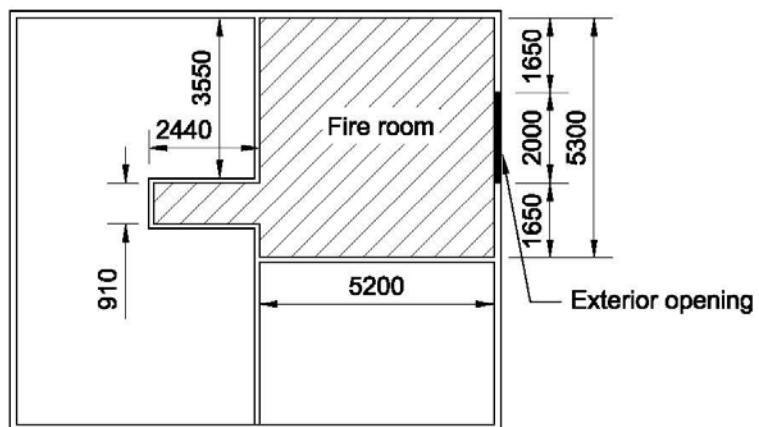
Figure 2. Facility plan view (all dimensions in mm)

The second storey was partitioned to contain bedrooms, which were connected by a corridor (measuring 4.45 m long x 1.10 m wide). The experiments involved two target bedrooms of the same size. The door of the southeast bedroom remained closed whereas the door on the southwest bedroom was kept open. Each bedroom doorway was 0.81 m wide x 2.05 m high. There were no window openings on the second storey.

For the first and second storeys, cement board covered the walls, and the ceilings were covered with 12.7-mm-thick regular gypsum board.

2.2   Fuel Package

A simple and repeatable fuel package, which had been developed for Phase 1 of the FPH research [10, 11], was used in the full-scale experiments. This fuel package consisted of a mock-up sofa constructed with 9 kg of exposed polyurethane foam (PUF), the dominant combustible constituent of upholstered furniture, and 190 kg of wood cribs beside and underneath the mock-up sofa. A photograph of the fuel package is shown in Figure 3.

The mock-up sofa was constructed with 6 blocks of flexible polyurethane foam (with a density of 32.8 kg/m^3) placed on a metal frame. Each block was 610 mm long x 610 mm wide and 100 mm or 150 mm thick. The 150-mm-thick foam blocks were used for the backrest and the 100-mm-thick foam blocks for the seat cushion. The PUF was used without any upholstery fabric that is used in typical upholstered furniture.

The wood cribs were made with spruce lumber pieces, each piece measuring 38 mm x 89 mm x 800 mm. For the small cribs located under the mock-up sofa, four layers with six pieces per layer were used. The other two cribs used eight layers.

Figure 3. Fuel package

The placement of the fuel package in the basement fire room is illustrated in Figure 4. The fuel quantity used in each experiment is listed in Table 1. The mock-up sofa was located at the center of the floor area. The mock-up sofa was ignited in accordance with the ASTM 1537 test protocol [12] and the wood cribs provided the remaining fire load to sustain the fire for the desired period of time. This fuel package provided a relatively-severe, fast-growing basement fire with a very reproducible fire exposure [10, 11, 13].
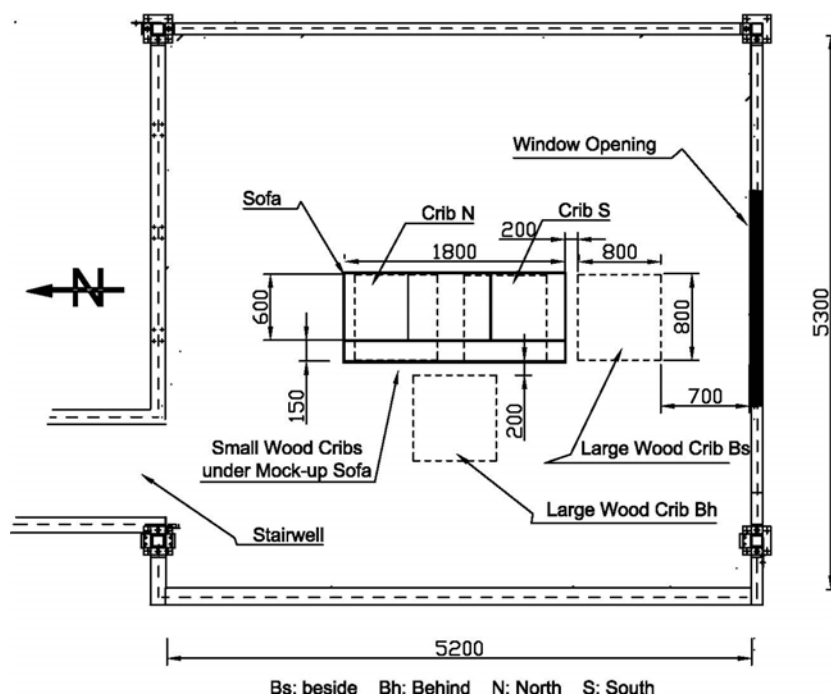
Figure 4. Layout of the fuel package (all dimensions in mm)

Table 1. Fuel Quantities in Experiments (kg)

Test	Foam	Crib Bs	Crib Bh	Crib N + Crib S	Moisture Content of Cribs
PF-01 (March 19, 2009)	9.31	63.2	62.7	32.1 + 30.7	6%
PF-02 (May 6, 2009)	9.32	63.2	63.5	31.2 + 30.9	6%
PF-03 (Sep. 24, 2009)	9.25	64.5	63.4	33.3 + 33.0	10%
PF-03B (Oct. 8, 2009)	9.27	64.1	65.2	33.7 + 32.2	8%
PF-04 (Jan. 28, 2010)	9.30	61.3	61.0	31.3 + 31.3	6%
PF-05 (April 14, 2010)	9.53	59.8	62.4	32.1 + 31.9	7%
PF-06 (June 1, 2010)	9.66	65.7	65.7	32.8 + 32.1	7%
PF-06C (Sep. 14, 2010)	9.57	63.3	64.9	32.9 + 32.3	8%

NRC·CNRC

2.3 Fire Scenario

The fire scenario used in the experiments was one of the scenarios used in Phase 1 of the FPH research [7, 13]. In this scenario, the doorway from the first storey to the open stairwell to the basement fire room had no door. Since there is no requirement for a basement door in the NBCC, this scenario was considered the code minimum. On the second storey, the door to the southwest bedroom was open and the door to the southeast bedroom was closed.

The exterior window opening in the basement fire room and the exterior door on the first storey were initially closed. The mock-up sofa was ignited using a gas burner in accordance with the ASTM 1537 test protocol [12]. The noncombustible panel that covered the fire room's exterior window opening was manually removed if and when the temperature measured at the top-center of the opening reached 300°C. This would provide the ventilation air required for combustion and simulate the fire-induced breakage and complete fall-out of the window glass. To simulate occupants evacuating the test house, the exterior door on the first storey was opened at 180 s after ignition and left open.

It is acknowledged that this fire scenario does not represent a frequent household fire scenario. The fire scenario was used in the project to provide a reasonable challenge to the structural integrity of the test ceiling/floor assembly above the basement.

2.4 Protected Ceiling/Floor Assemblies Used

Table 2 shows the ceiling/floor systems used in the full-scale fire experiments with the open basement doorway fire scenario. The four types of assemblies were selected from the assemblies that had been tested in Phase 1 of the FPH research [1-7]. The test floor assemblies were constructed in the same way as in Phase 1 of the FPH research but the floor assemblies were protected on the basement side with regular gypsum board, residential sprinkler systems or a suspended ceiling. There were discussions on other protection systems, e.g., spray on insulation, and the consortium decided not to pursue these further, given a fixed number of tests.

For each experiment, a ceiling/floor assembly was constructed on the first storey directly above the 5.3 m long x 5.2 m wide basement fire room. A single layer of oriented strandboard (OSB) was used for the subfloor of all assemblies without additional floor finishing materials on the test assemblies since there are no specific requirements for floor finishing materials atop an OSB subfloor in the NBCC. This was considered the code minimum and reduced the number of experimental variables.

Each assembly selected for testing was designed on the basis of an imposed load of 1.90 kPa, self-weight of 0.5 kPa and the span of the basement room. For the assemblies using solid-sawn wood joists and steel C-joists, the maximum allowable design spans for those members under residential occupancy loading resulted in the use of an intermediate support beam. For the wood I-joist and metal-web wood truss assemblies, they were designed and constructed to span the full width of the room, which resulted in them being at or near to their maximum allowable design span.

NRC·CNRC

In the experiments, actual loading was applied on the test assembly, as follows: the self-weight (dead load) of the assembly, plus an imposed load (live load) of 0.95 kPa (i.e., half of the imposed load of 1.90 kPa prescribed by the NBCC [9] for residential occupancies). This was based on the fact that in a fire situation, only part of the imposed load is available. This was also consistent with a number of international standards (Eurocode [14], New Zealand and Australian standards [15, 16], and ASCE [17]). The total imposed load applied to the test assembly was 25 kN (i.e., 0.95 kPa multiplied by the floor area) using uniformly distributed concrete blocks.

A primary fire test was conducted with each ceiling/floor assembly. For those ceiling/floor assemblies that survived the primary tests, where possible, the floor/ceiling systems were refitted for secondary fire tests such as tests of another protection configuration, or tests of another protection system (a secondary test was denoted by a letter after the test number, as shown in Table 2). Specific details of the design and construction of the protected assemblies are provided in Sections 4.2 - 4.9.

Table 2. Fire Tests with Protected Ceiling/Floor Assemblies (open basement doorway)

Assemblies	Protection	Primary test	Protection	Secondary test
Solid-sawn wood joist (235 mm depth)	Gypsum	PF-01 (March 19, 2009)	-	-
Steel C-joist (203 mm depth)	Gypsum	PF-02 (May 6, 2009)	-	-
Wood I-joist* (302 mm depth)	Sprinkler (2 sprinklers)	PF-03 (Sep. 24, 2009)	Sprinkler (1 sprinkler)	PF-03B (Oct. 8, 2009)
Wood I-joist (302 mm depth)	Gypsum	PF-04 (Jan. 28, 2010)	-	-
Wood I-joist (302 mm depth)	Suspended Ceiling	PF-05 (April 14, 2010)	-	-
Metal-web wood truss* (302 mm depth)	Sprinkler (1 sprinkler)	PF-06 (June 1, 2010)	Gypsum	PF-06C (Sep. 14, 2010)

Notes:
1. The wood I-joist were referred as wood I-joist A in Phase 1 of the FPH research;
2. *Additional secondary tests with the residential sprinkler system were conducted for these test assemblies (see a separate report for details [18]).

2.5 Instrumentation

Extensive thermocouple arrays were installed in the test house to measure temperatures. Vertical arrays of thermocouples (at heights of 0.4, 0.9, 1.4, 1.9 and 2.4 m above the floor) were located at the four quarter points of the fire room, basement doorway, four quarter points on the first storey, centre of the corridor on the second storey, and centre of the two bedrooms on the second storey.

NRC·CNRC

Thermocouples were installed at the basement exterior opening to monitor the temperature. A heat flux meter was installed on the west wall (near the centre, 2.05 m above the floor) in the fire room.

Extensive thermocouple arrays were also installed on the test assemblies, including thermocouples on the unexposed side of the assemblies and in the floor cavities. In addition, flame-sensing devices [19] and floor deflection devices [20] were installed on the unexposed surface of the test assemblies. The floor deflection was measured at nine locations on the test assembly. The flame-sensing device was placed at the central tongue-and-groove joint of the subfloor.

Smoke and gas measurements focused on upper storeys with four gas sampling locations. On the first storey, gas sampling ports were located at the southwest quarter point at 0.9 m and 1.5 m above the floor. On the second storey, gas sampling ports were located at the centre of the corridor at 0.9 m and 1.5 m above the floor. Gas samples from these sampling locations were connected to nondispersive infrared CO/CO_2 gas analyzers, O_2 gas analyzers and smoke density meters.

Residential ionization and photoelectric smoke alarms were installed on each level and in each bedroom, which were powered by batteries and were not interconnected (new smoke alarms were used in each experiment).

Airflow velocities at the various openings and the differential pressure between the fire room and the first storey were also measured but are not included in this report. This data may be useful for fire modeling purposes in the future.

2.6   Experimental Procedure

The mock-up sofa was ignited in accordance with the ASTM 1537 test protocol [12] and data was collected at 5 s intervals throughout each test.

The noncombustible panel that covered the fire room's exterior window opening during the initial stage of each test was manually removed if the temperature measured at the top-center of the opening reached 300°C. The removal of the panel simulated the fire-induced breakage and complete fall-out of the window glass and provided the ventilation air necessary for combustion.

The exterior door on the first storey was opened in each test at 180 s after ignition and left open, simulating a situation where some occupants, who would have been in the test house, escaped leaving the exterior door open while other occupants may still have been inside the house.

A test was terminated after structural failure of any part of the test assembly or after a predetermined test duration (20~30 minutes), whichever came first.

3   METHODOLOGY FOR TENABILITY ANALYSIS

Heat, narcotic and irritant gases, and smoke produced from fires can individually or collectively create conditions that are potentially untenable for occupants. An approach based on ISO 13571 and the SFPE Handbook [21, 22] was used to conduct tenability analysis, which has

NRC·CNRC

been fully described in reports on Phase 1 of the FPH research [1-7]. The objective of the tenability analysis was to estimate the time available for occupants to escape from a fire before the onset of incapacitating conditions.

The fractional effective dose (FED) was calculated using measured data on potential heat and gas exposure to determine the time available for escape. The calculated time available for escape depends not only on the time-dependent temperatures, concentrations of combustion gas products and density of smoke in the test house, but also on the characteristics of occupants. This report presents the results of the analysis for two typical FED values: FED = 1 and FED = 0.3.

The time available for escape calculated based on FED = 1 represents the time available for a healthy adult of average susceptibility. To examine the effect on a more susceptible person, the threshold can be lower, e.g. FED=0.3, and the time available for escape would be shorter than for an average healthy adult. The time available for escape associated with other FED values can also be calculated, if required.

The location of the occupant in the test house has an effect on the time available for escape. The analysis focused on the fire conditions affecting tenability, as measured on the first and second storeys of the test facility, and the impact on any occupant assumed to be present at the time of ignition. The tenability analysis focused on potential impact on any occupants on the upper storeys of the test house. The conditions in the basement fire room are not survivable once flashover occurs.

Heat, combustion gas products and smoke obscuration are treated as acting independently on the occupant to create incapacitating conditions and the time available for escape is the shortest of the times estimated from consideration of exposure to combustion gas products, heat and visual obscuration.

3.1   Exposure to Toxic Gases

The tenability analysis on gas exposure involved CO and CO_2 and oxygen vitiation only, since flaming combustion of polyurethane foam and wood cribs primarily produced toxic carbon monoxide (CO) and asphyxiant carbon dioxide (CO_2) in a vitiated oxygen (O_2) environment. Given the amount of polyurethane foam in the fuel package and the volume of the test house, hydrogen cyanide (HCN) produced from the combustion of polyurethane foam would not reach a concentration of concern for occupant life safety. The fuel package contained no chemical components that would produce acid halides in the combustion gases.

Detailed analysis indicated that the toxic effect of CO would be capable of causing incapacitation at an earlier time than the effect of O_2 vitiation and the asphyxiant effect of CO_2. The fractional effective dose for incapacitation due to CO was calculated using the approach given in ISO TS 13571 for short exposure to CO at high concentrations [21]:

$$FED = \sum_{t1}^{t2} \frac{[CO] \cdot \Delta t}{35000} \exp(\frac{\%CO_2}{5})$$

where *[CO]* is the inhaled carbon monoxide concentration in *parts per million*, *Δt (minutes)* is the discrete increment of time (i.e. the time interval for data sampling), 35000 *(ppm·min)* is the

NRC·CNRC

incapacitation dose for the CO exposure, and *exp(%CO$_2$/5)* is a CO_2-induced hyperventilation factor for breathing [21, 22]. The uncertainty in the calculation of FED due to the CO exposure is estimated to be ±40% [21].

3.2 Exposure to Heat

The rate of convected heat transfer from hot gases to the skin depends on temperature, ventilation, humidity of the enclosure and clothing over the skin [22]. For hot air at temperatures above 120°C and with water vapour of less than 10%, pain and skin burns would be likely to occur in a few minutes. Assuming unclothed or lightly clothed subjects, the fractional effective dose for incapacitation due to the convected heat exposure was calculated using the following equation [21, 22]:

$$FED = \sum_{t1}^{t2} \frac{T^{3.4}}{5 \times 10^7} \Delta t$$

where *T (°C)* is the temperature and *Δt (minute)* is the discrete increment of time (i.e. the time interval for data sampling). The uncertainty in the calculation of FED due to convected heat is estimated to be ±25%. Since there was temperature stratification, the temperatures at the 1.4 m height from the floor were used for the analysis of convected heat exposure on each storey, as this is the height of the nose/mouth of an average-height individual.

Radiant heat is important when the hot smoke layer is over 200°C, which corresponds to the threshold radiant heat flux of 2.5 kW·m^{-2} to produce second degree burning of skin [23]. The calculation indicated that the convected heat exposure would result in incapacitation before the radiant heat began to play a major role on the first and second storeys. Convected heat was the most important source of heat exposure for occupants on the first and second storeys for the fire scenarios used.

3.3 Visual Obscuration by Smoke

Visual obscuration by the optically-dense smoke tended to be the first hazard to arise that could impede evacuation by the occupants. Although visual obscuration would not directly cause incapacitation, it would cause delays in movement by the occupants and thus prolong their exposure to other hazards. Visibility through smoke and the optical density of smoke are related (the visibility is proportional to the reciprocal of the *OD* for non-irritating smoke, for example) [24]. In this report, the smoke obscuration is expressed as the optical density per meter (*OD* in *m^{-1}*):

$$OD = \frac{1}{L} \log_{10}\left(\frac{I_0}{I}\right)$$

where *I$_0$* is the intensity of the incident light, *I* is the intensity of the light transmitted through the path length, *L* (m), of the smoke. The optical density is related to the extinction coefficient *k (m^{-1})* by *OD = k/2.303*.

Various threshold *OD* values have been suggested as the tenability limit for smoke obscuration for small buildings with occupants familiar with the egress route [22, 24-27]. In ISO 13571[21],

the minimum visible brightness difference between an object and its background is used to estimate the smoke obscuration limit at which occupants cannot see their hands in front of their faces (a distance of 0.5 m or less). These calculations indicate that occupants cannot see their hands in front of their faces and become disoriented at an optical density of 3.4 m^{-1}. For an occupant whose vision is impaired, this can happen at an optical density of 2 m^{-1} or lower. Psychological effects of smoke on occupants may accelerate the loss of visibility [24]. Possible reduction of time to untenable smoke level due to psychological effect is not addressed in this report. A tenability limit of $OD_{Limit} = 2$ m^{-1} is used in this study.

4   RESULTS OF EXPERIMENTS AND ANALYSIS

This section provides the results of measurements and analysis, a summary of the findings of the performance of protected ceiling/floor assemblies and the effect of the protection measures on tenability conditions.

4.1   Smoke Alarm Response

Table 3 shows the activation times of the smoke alarms installed in the test facility. There was a significant delay for the smoke alarms in the second storey to activate, compared to the smoke alarm in the basement fire room. This highlights the importance of having the smoke alarms interconnected to activate simultaneously when one of them detects a fire.

Table 3. Smoke Alarm Activation Times (in seconds) After Ignition

Location	Basement fire room	1st storey		2nd storey corridor		2nd storey SW bedroom (door open)		2nd storey SE bedroom (door closed)	
Smoke alarm type	P 2	I 3	P 4	I 5	P 6	I 9	P 10	I 7	P 8
Test PF-01	27	37	57	102	112	117	127	242	282
Test PF-02	30	45	55	110	125	145	140	235	265
Test PF-03	45	95	105	175	175	210	na	na	na
Test PF-03B	34	79	94	196	176	na	na	na	na
Test PF-04	30	40	55	115	125	140	na	235	255
Test PF-05	47	67	87	127	137	147	na	267	282
Test PF-06	55	85	95	185	195	360	410	na	na
Test PF-06C	30	75	90	140	145	150	160	220	250

Notes:
1. I: Ionization   P: Photoelectric   na: no activation;
2. The ionization smoke alarm was not installed in the basement fire room to avoid dealing with radioactive materials in the cleanup of debris after fire tests.

NRC·CNRC

4.2 Solid-Sawn Wood Joist Assembly with Gypsum Protection – Test PF-01

Test PF-01 was conducted using a solid-sawn wood joist assembly with direct-applied regular gypsum board on the exposed side (gypsum board ceiling in the fire room).

4.2.1   Construction Details of the Test Assembly

The overall dimensions of the solid-sawn wood joist assembly were 5250 mm x 5150 mm. Specific dimensions of the components of the assembly are provided in Figure 5 to Figure 10.

The solid-sawn wood joists were manufactured using spruce-pine-fir (SPF) lumber bearing a grade-stamp 'No.2 and better'. The structural members were 235 mm deep x 38 mm wide (nominal 2" x 10"), and were spaced at 400 mm on centre (Figure 5). The joist span length was 4.17 m (Figure 5) based on the span tables of the NBCC [9]. This corresponds to the maximum span allowed for wood floor joists of SPF lumber graded as 'No.2 and better', and constructed with cross-bridging mid-span and the joists spaced at 400 mm o.c. Since the maximum span allowed for the solid-sawn wood joists was shorter than the length of the fire room, a beam was used as an intermediate support at the end of the 4.17-m span and a set of shorter joists were used to increase the span of the floor to extend to the end of the fire room.

The test assembly was supported by three horizontal steel beams, each of which was supported by two steel columns. The beams were bolted to the columns, which were stiffened by steel bars and rested stably on the floor under the weight of the test assembly and steel beams.

Figure 6 shows the details of the joint overlap and the supporting steel beams, as well as the end connection. Ceramic fibre blankets were used to fill any gaps between the assembly and the end walls. Ceramic fibre blankets were also used to protect the steel beams and columns so that they were not subjected to fire and would not fail during the test.

Rim boards (headers) made of solid lumber that were 38 mm thick x 235 mm deep, were placed at the east and west sides of the test assemblies as shown in Figure 5. One row of diagonal wood cross-bracing, 38 mm thick x 38 mm wide, was placed at the centre of the longer span of the assembly between the joists. Details of the cross-bracing and its location within the joist layout for the above-mentioned assembly are shown in Figure 5 and Figure 6.

NRC·CNRC
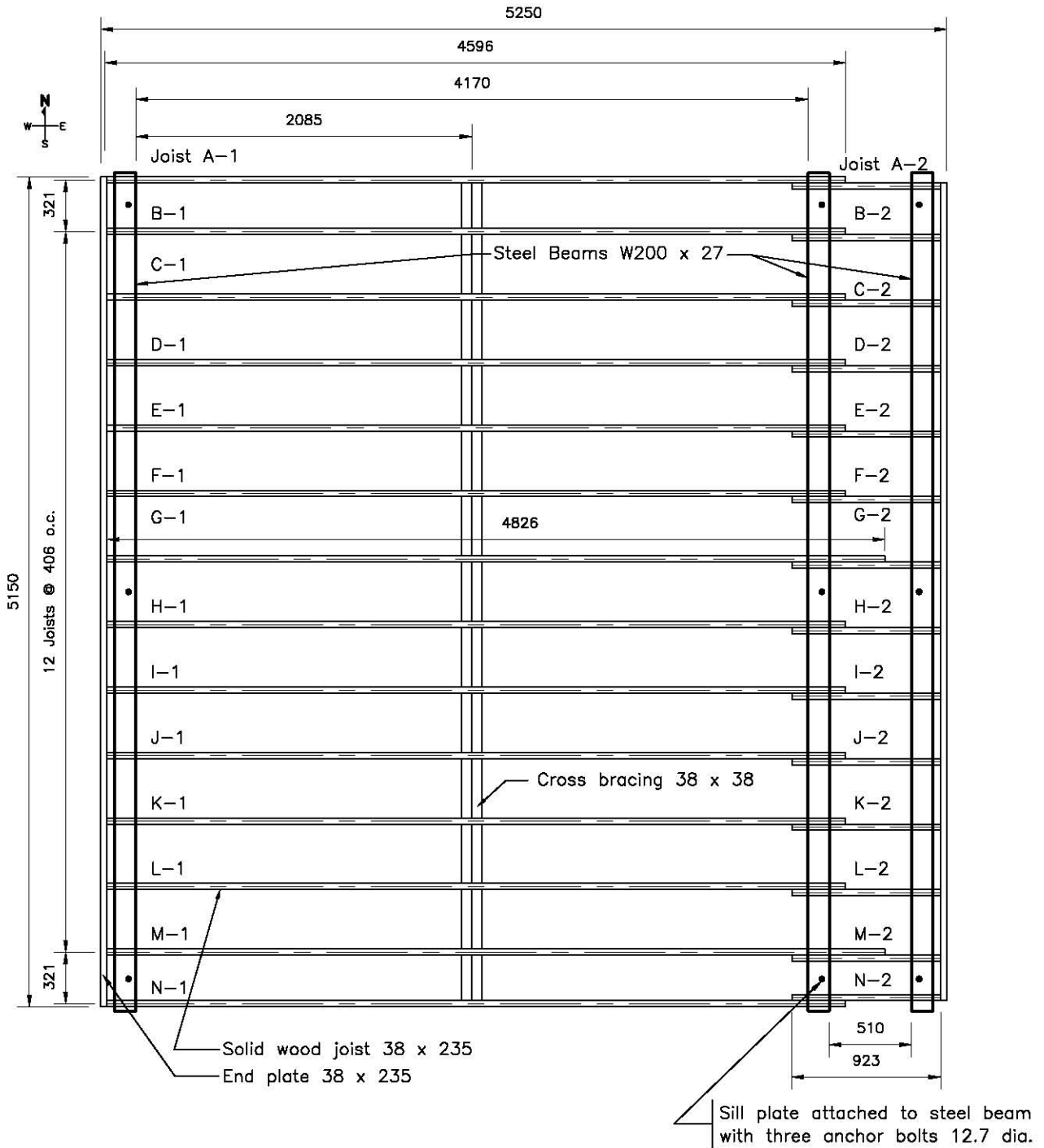
Figure 5. Solid-sawn wood joist layout details (PF-01) (all dimensions in mm)

NRC·CNRC

OSB 15.1 thick — Solid wood joist 38 x 235

Header toenailed to sill plate with 12 d common 83 long nails at 600 o.c.

Floor joists toenailed to sill plate with two 12 d common nails 83 long

Steel beam/column W200 x 27 Protected with ceramic fibre blankets

Sill plate 38 x 133 attached to steel beam with three anchor bolts 12.7 dia. by 63 long

207

207

End connection details (East view)

12 d common nails 83 long
Gypsum board 12.7 thick

Anchor bolts

Solid wood joists 38 x 235

Ceramic fibre blanket

Gypsum Board 12.7 thick
Cement Board 12.7 thick
Steel stud 89 deep
Glass fibre insulation 89 thick
Sheet metal 18 ga

Wall

End connection details (North view)

Two 8 d common nails 64 long at each end

Cross bracings 38 x 38

Cross bracing details (East view)

12 d common nails 83 long

50

133

207

100

38
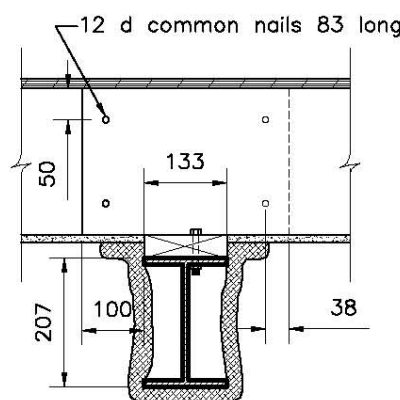
Joist overlap details (North view)

12 d common nails 83 long
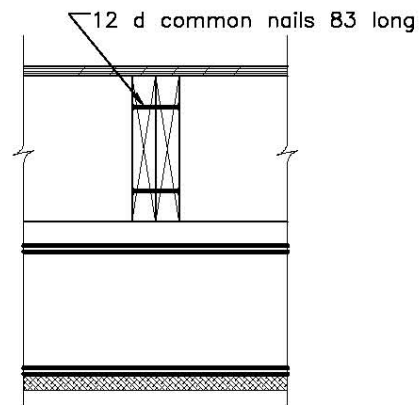
Joist overlap details (East view)

Figure 6. Details of end connection, supports, cross-bracing and joist overlap (PF-01) (all dimensions in mm)

14

NRC·CNRC

OSB was used as the subfloor material in the test assembly. The specific OSB material used was selected based on a separate study documented in reference [28]. The subfloor panels were 15.1 mm thick, with a full panel size of 1.2 x 2.4 m. The longer panel edges had a tongue-and-groove profile while the short panel edges were square butt ends. Figure 7 shows the layout of the subfloor. The nailing pattern and description of nails used to attach the OSB panels to the solid-sawn wood joists and rim board (header) are shown in Figure 8.
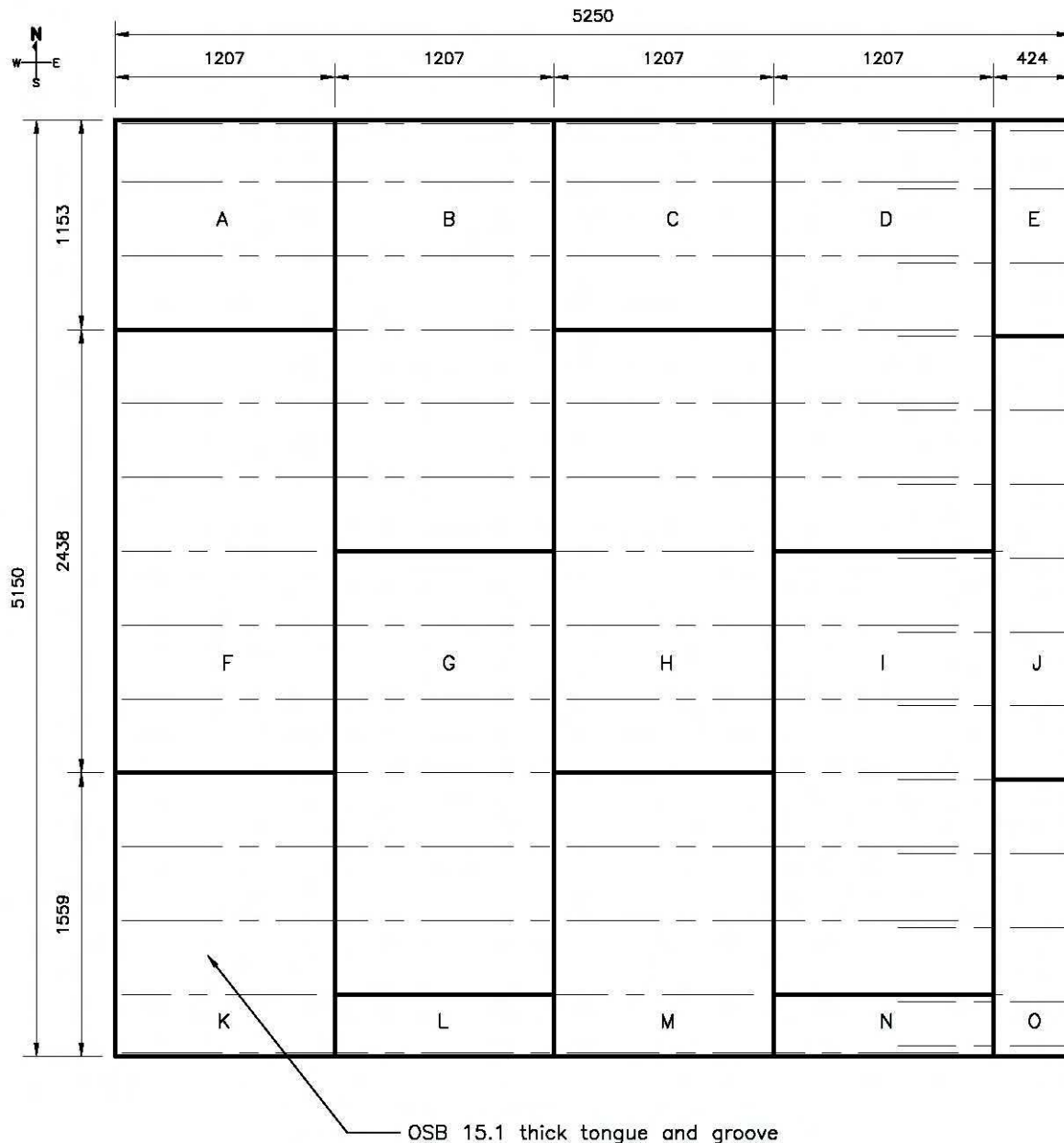
Figure 7. OSB subfloor layout (PF-01, PF-03, PF-03B, PF-04 and PF-05) (all dimensions in mm)

NRC·CNRC

8d common nails 64 long
6d common nails 51 long
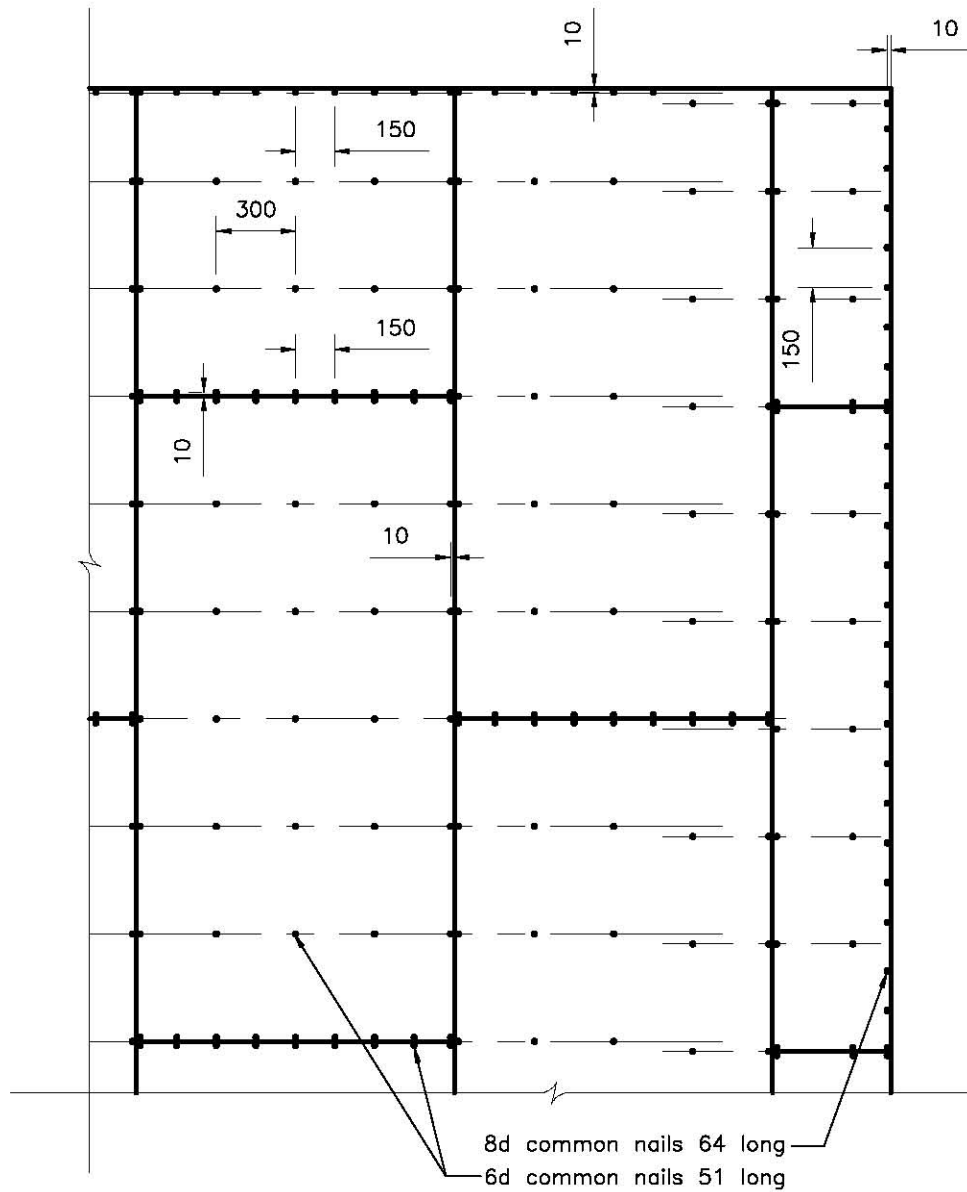
PARTIAL VIEW

Figure 8. Subfloor nail pattern and nail description (PF-01) (all dimensions in mm)

NRC·CNRC
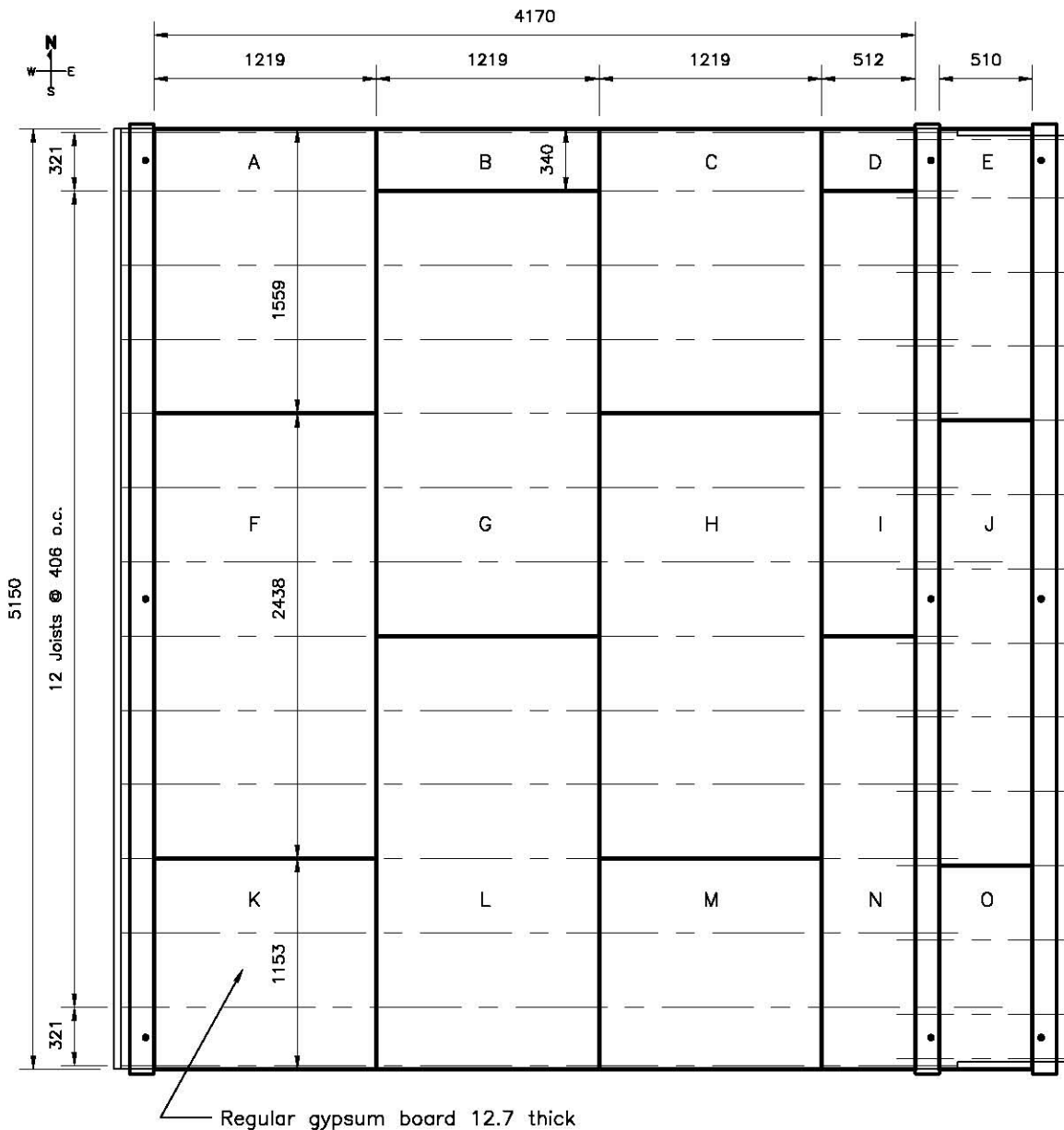
Figure 9. Gypsum board layout on the assembly as the basement ceiling (PF-01) (all dimensions in mm)

Regular gypsum board was installed on the basement side of the ceiling/floor assembly by being fastened directly to the bottom of the joists. The gypsum board was 12.7 mm thick, with a full sheet size of 1.2 x 2.4 m. Figure 9 shows the layout of the gypsum board on the assembly. The joints of the gypsum board were finished with joint compound and tape. The screw pattern and description of screws used to fasten the gypsum board to the solid-sawn wood joists and rim board (header) are shown in Figure 10.

NRC·CNRC
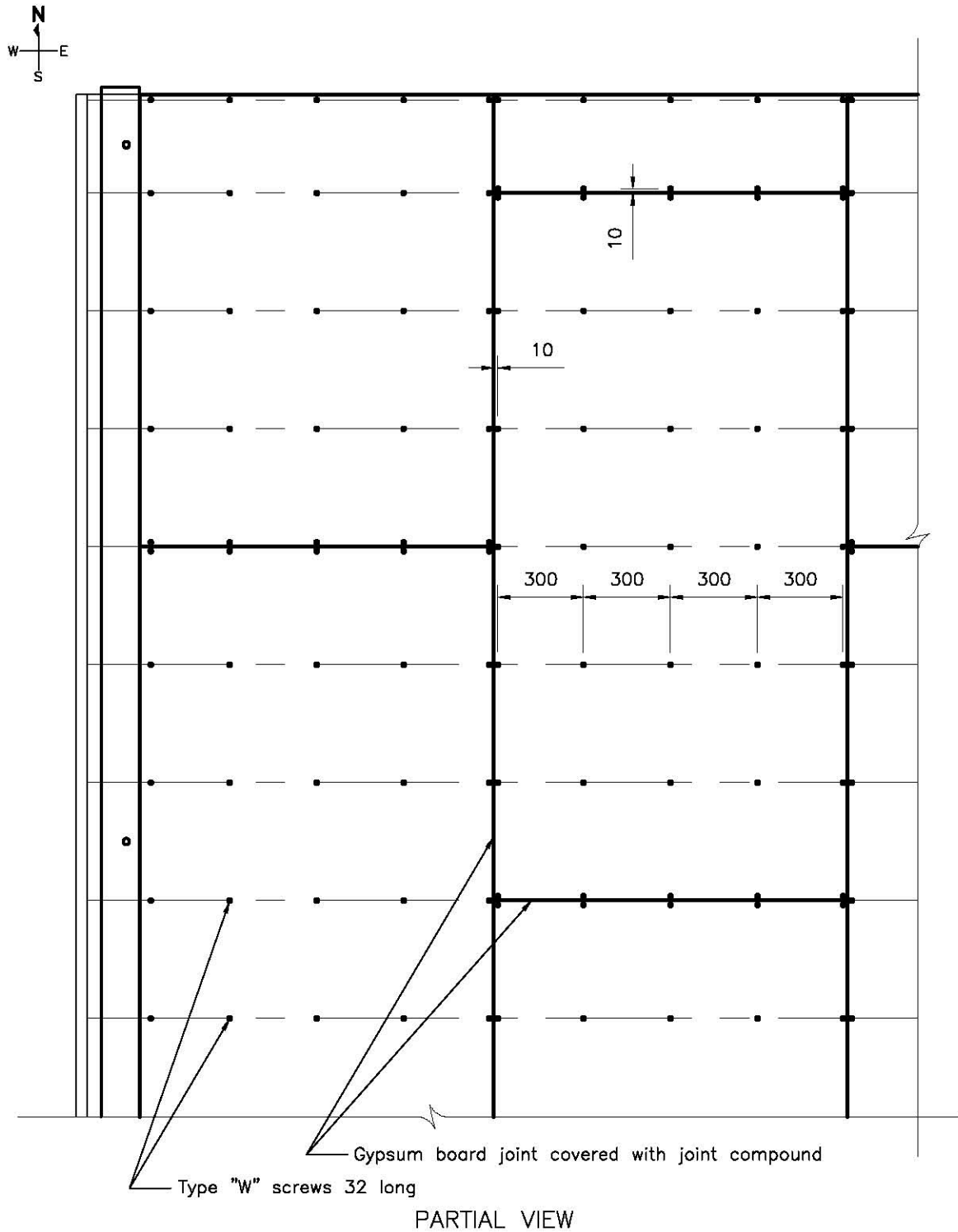
Figure 10. Gypsum board screw layout (PF-01, PF-04 and PF-06C) (all dimensions in mm)

N
W — E
S

10

10

300 300 300 300

Gypsum board joint covered with joint compound

Type "W" screws 32 long

PARTIAL VIEW

NRC·CNRC

Sixty-one Type K (20 gauge) chromel-alumel thermocouples, with a thickness of 0.91 mm, were used for measuring temperatures at a number of locations throughout the assembly. The thermocouples were located on the unexposed side and in the cavities of the assembly as shown in Figure 11 and Figure 12. These locations were chosen to monitor the conditions of the assembly at critical locations during the fire tests.
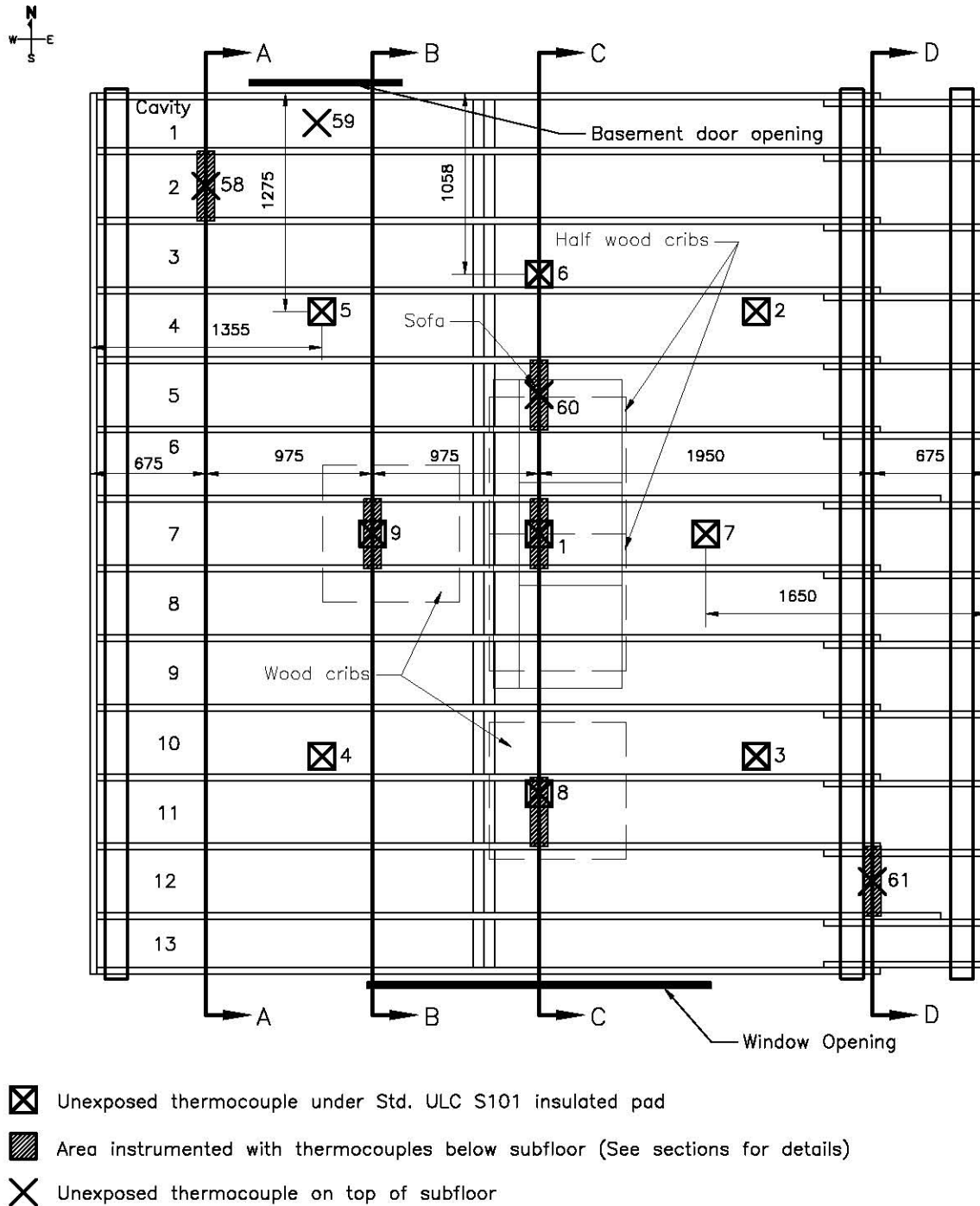
Figure 11. Thermocouples locations in PF-01 assembly (all dimensions in mm)
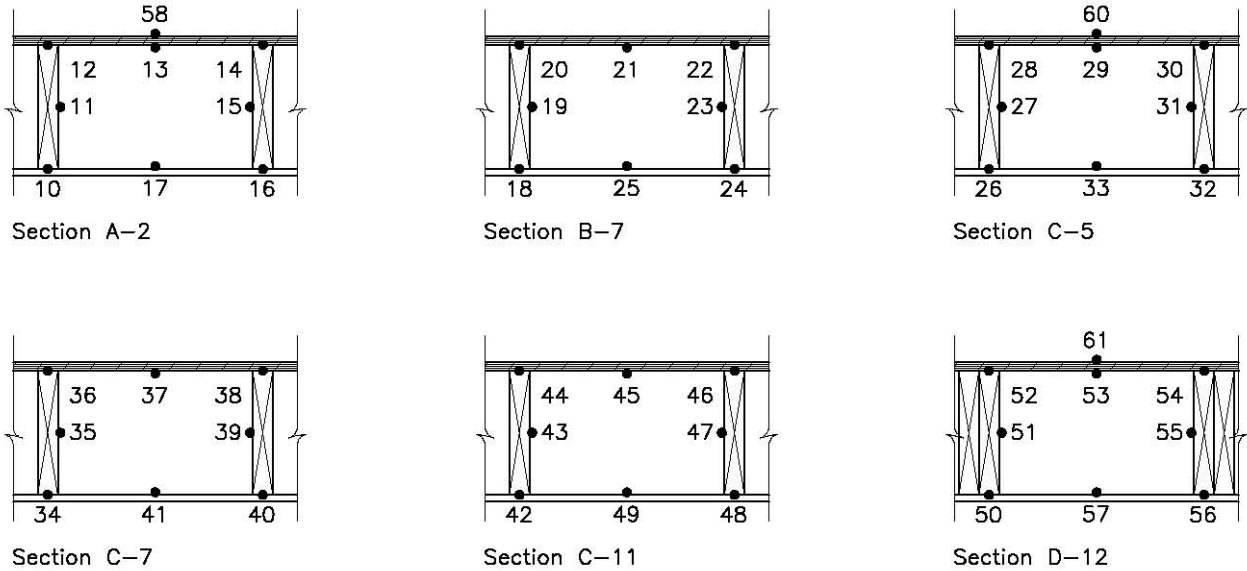
Figure 12. Thermocouples locations reflecting the different sections shown in Figure 11
(Test PF-01)

The floor deflection was measured at 9 points. The measurement technique utilized 9 rods that were touching the tops of 9 concrete blocks placed on the unexposed surface of the test assembly at the locations shown as circles in Figure 13. This ensured that the downward movement of the subfloor was monitored during the fire exposure. The deflections were recorded using an electro-mechanical method described in Reference [20].
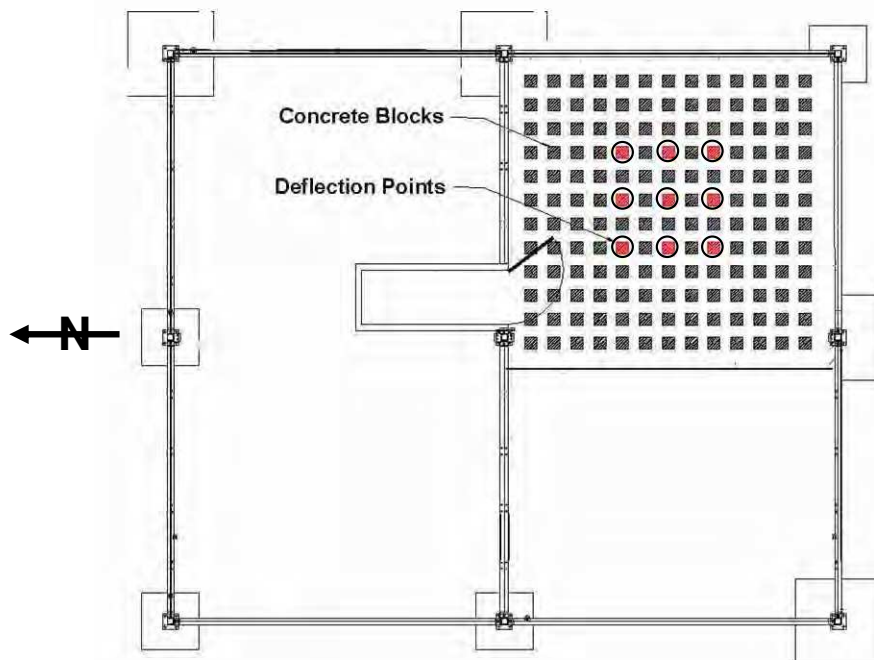
Figure 13. Loading blocks and deflection measurement points on the unexposed side of the assembly

4.2.2 Fire Development in Basement

Figure 14 shows the temperatures measured in the basement fire room. The polyurethane foam used for the mock-up sofa dominated the initial fire growth. The temperatures at the window quickly reached 300°C and the noncombustible window covering panel was removed at 97 s. The temperatures at the 2.4 m height exceeded 600°C within 140 s, indicating that the fire room reached flashover conditions. The fast development of the fire from ignition to attainment of the first temperature peak was consistent with the experiments in Phase 1 of FPH research. Following this initial stage of fire growth, the fire became wood-crib-dominated. There was a quick transition from a well-ventilated flaming fire to an under-ventilated fire. (Note that the significant temperature drop in the NW quadrant around 1000 s was unknown.) Figure 14 also shows the heat flux measured at the west wall (near the centre, 2.05 m above the floor). The maximum heat flux was 150 kW·m^{-2}, indicating post-flashover conditions in the fire room.
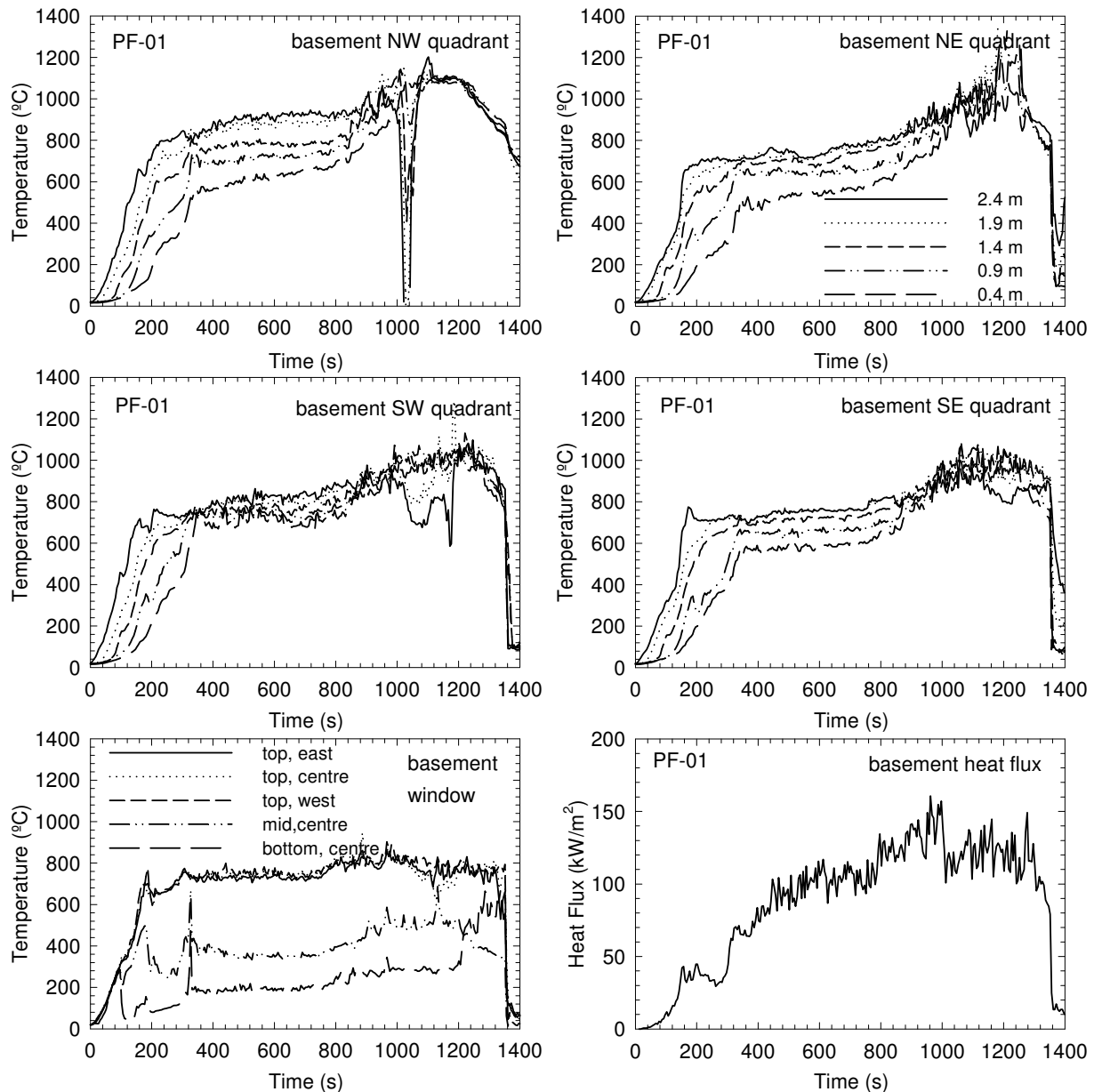
Figure 14. Temperatures and heat flux in the basement fire room in Test PF-01

NRC·CNRC

4.2.3 Visual Obscuration

The optical density was measured at 0.9 and 1.5 m heights (simulating the height of the nose/mouth of an average height individual crawling and standing, respectively) above the floor on the first and second storeys. Table 4 shows the times to reach OD = 2 m^{-1}. Figure 15 shows the optical density-time profiles. It must be pointed out that the video records show no signs of decrease in the optical density after the first peak, indicating that the smoke density meters started the self purging cycle. The smoke density meter has an operation temperature limit of 80°C in its gas chamber; when this temperature is reached, the flow is reversed to cool the chamber to protect the electronic components. The smoke meter resumes operation once the gas chamber is cooled down below 80°C. In this experiment, only the initial part of the curves (up to the first peaks) represents valid measurements.

Table 4. Time (in seconds) to the Smoke Optical Density Limit in Test PF-01

Test PF-01	1st storey SW quadrant	2nd storey corridor
OD =	2 m^{-1}	2 m^{-1}
1.5 m above floor	192	257
0.9 m above floor	212	237
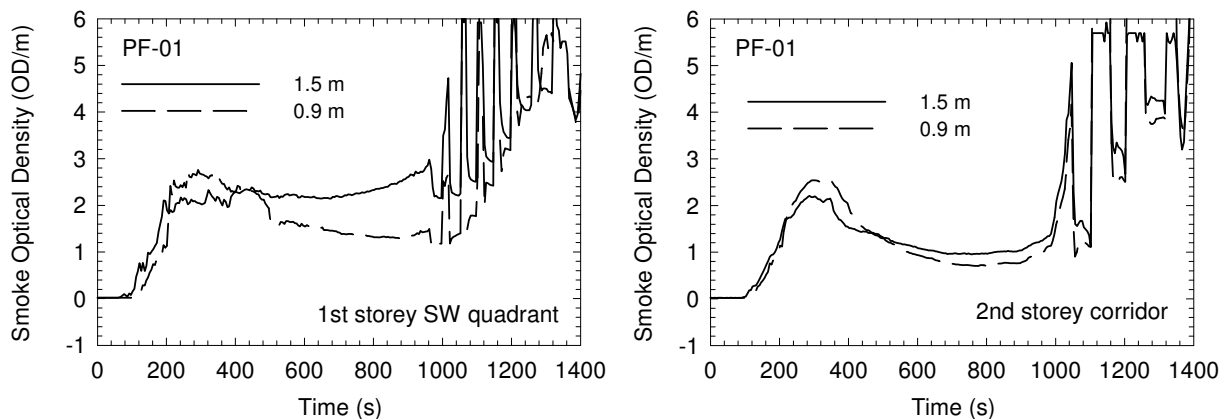
Figure 15. Smoke optical density measurements in Test PF-01

4.2.4 Gas Measurements and Analysis (CO, CO$_2$ and O$_2$)

Figure 16 shows the CO, CO$_2$ and O$_2$ concentration-time profiles measured at the southwest quarter point on the first storey and at the centre of the corridor on the second story during the experiment. Within approximately 400 s, oxygen was diminished to below 10% and CO$_2$ increased to above 10%, which could cause incapacitation and lead to rapid loss of consciousness due to lack of oxygen alone or due to the CO$_2$ asphyxiant effect alone [22]. The concentrations were below 5% O$_2$ and above 16% CO$_2$ near the end of the experiment. Note that two gas analyzers used had an upper limit of 10% for CO$_2$ measurements and one gas analyzer used had an upper measurement limit of 1% CO. All other gas analyzers had higher measurement limits.

NRC·CNRC

The tenability analysis indicated that the toxic effect of CO would be capable of causing incapacitation at an earlier time than the effect of O_2 vitiation and the asphyxiant effect of CO_2. The times to reach the specified FED for exposure to O_2 vitiation, CO_2 and CO are shown in Table 5.
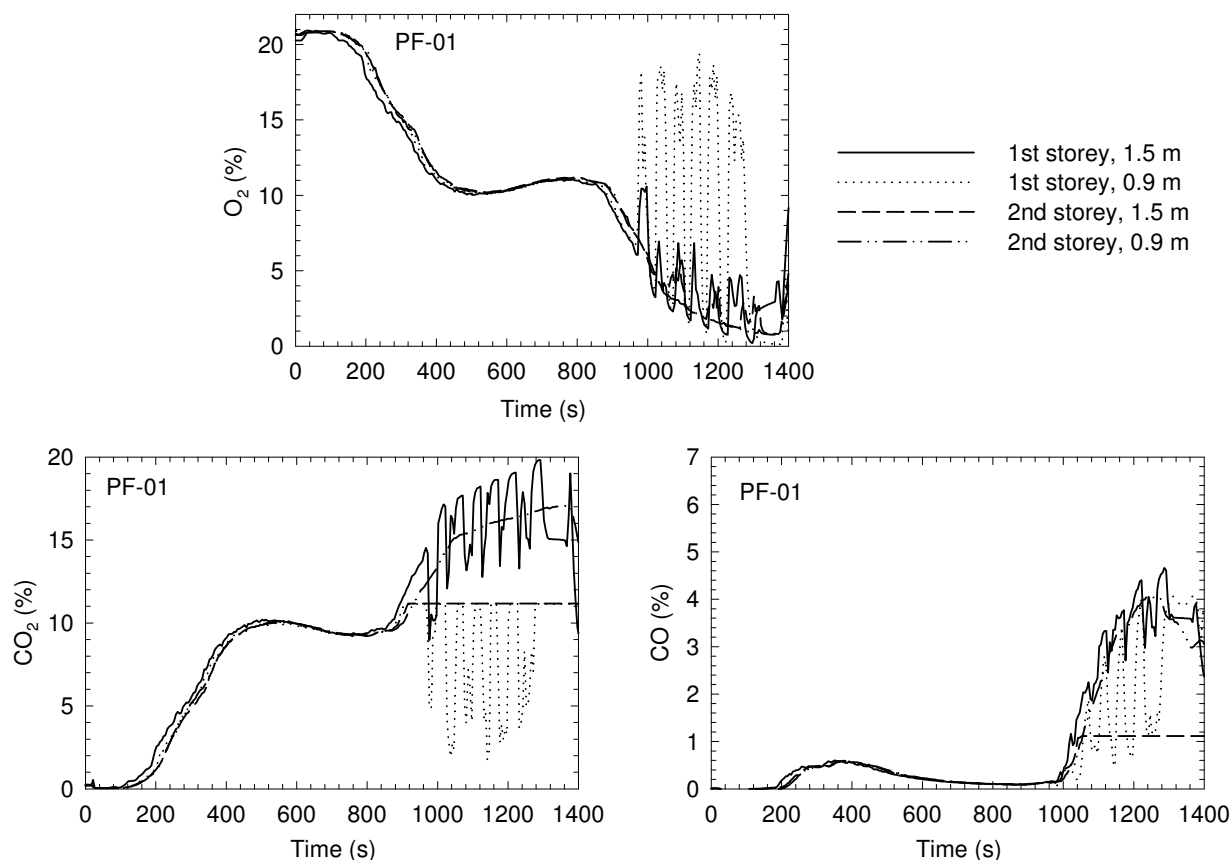
Figure 16. CO, CO_2 and O_2 concentrations in Test PF-01

Table 5. Time (in seconds) to the Specified FED for Exposure to O_2 Vitiation, CO_2 and CO in Test PF-01

Fractional Effective Dose	FED = 0.3	FED = 1.0
CO alone – 1st storey	337	922
CO with CO_2 hyperventilation – 1st storey	272±20	352±30
Low O_2 hypoxia – 1st storey	557	947
CO alone – 2nd storey corridor	357	967
CO with CO_2 hyperventilation – 2nd storey corridor	297±20	377±30
Low O_2 hypoxia – 2nd storey corridor	592	977
High CO_2 hypercapnia – 1st storey	412	527
High CO_2 hypercapnia – 2nd storey corridor	432	552

Note:
1. Values determined using concentrations at 1.5 m height.

NRC·CNRC

4.2.5 Temperature-Time Profiles on the Upper Storeys

Figure 17 and Figure 18 show temperature profiles measured on the first and second storeys during the experiment. The temperatures depended on the locations inside the test house. In the bedroom with the door closed, the temperatures never exceeded 60°C during the experiment.
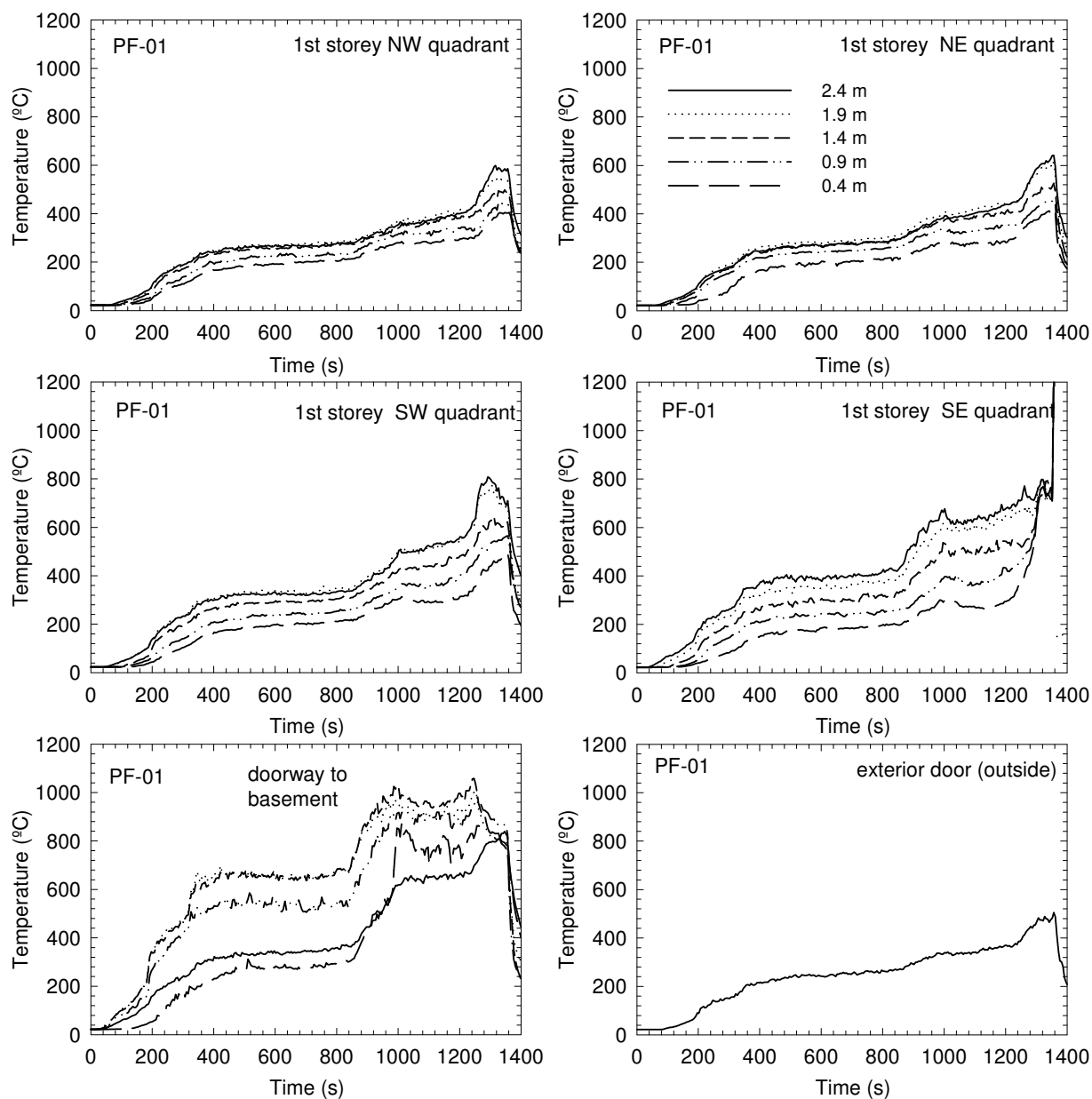
Figure 17. Temperatures on the first storey in Test PF-01

NRC·CNRC
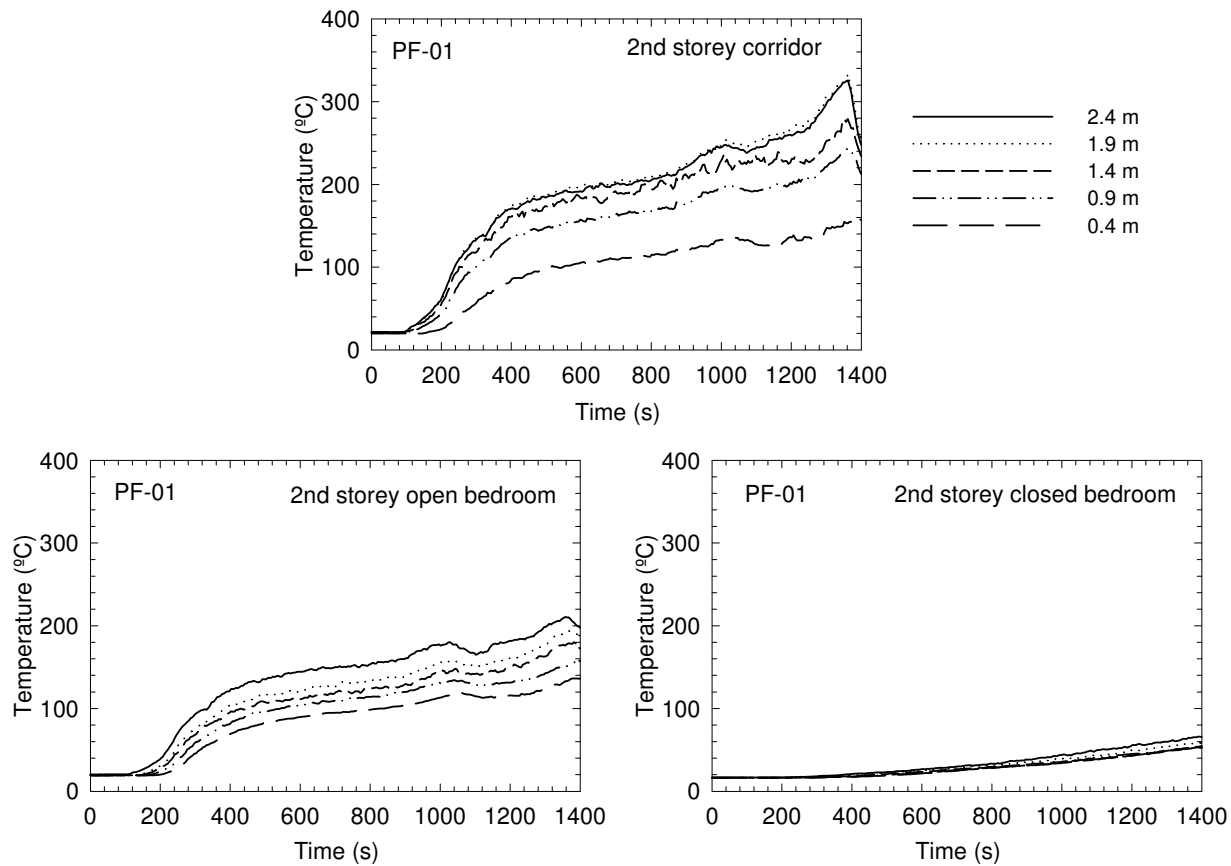
Figure 18. Temperatures on the second storey in Test PF-01

The convective heat exposure depended on the location in the test house. In the closed bedroom, heat exposure would not cause incapacitation. On the first storey, in the corridor or in the open bedroom on the second storey, the calculated times to incapacitation due to exposure to the convected heat are given in Table 6 for FED = 0.3 and 1. The calculated times to reach the heat incapacitation doses on the first storey were shorter than those for CO exposure; the time difference for FED to change from 0.3 to 1.0 due to the heat exposure was also shorter than that for CO exposure. In the corridor on the second storey, the calculated times to reach the incapacitation doses for heat exposure were slightly longer than those for CO exposure.

Table 6. Time (in seconds) to the Specified FED for Convected Heat in Test PF-01

Fractional Effective Dose	FED = 0.3	FED = 1.0
1st storey SE quadrant	242	292
1st storey SW quadrant	242±10	287±15
1st storey NE quadrant	257	312
1st storey NW quadrant	257	317
2nd storey corridor	317±15	407±25
2nd storey open bedroom	472	697
2nd storey closed bedroom	not reached (FED<0.06)	not reached (FED<0.06)

Note:
1. Values determined using temperatures at 1.4 m height.

NRC·CNRC

4.2.6 Estimation of Time to Incapacitation

Table 7 summarizes the results of tenability analysis with the estimated times to the onset of various conditions for Test PF-01. Smoke obscuration was the first hazard to arise. The calculated time for reaching the specific FED either due to the heat exposure or due to the CO exposure (exacerbated by CO_2-induced hyperventilation), whichever occurred first, is listed in Table 7. Heat exposure reached the specific FED on the first storey at times shorter than for CO exposure. On the second storey (in the corridor), CO exposure reached the specific FED earlier than heat exposure. The time difference for heat exposure and CO exposure to reach the specific FED was not significant. Note that for the closed bedroom on the second storey, based on the temperatures and the heat exposure calculation, the conditions in the closed bedroom would not reach untenable conditions.

Table 7. Summary of Estimation of Time to Specified FED and OD (in seconds) for Test PF-01

Test	$OD = 2\ m^{-1}$		$FED = 0.3$		$FED = 1$	
	1st storey	2nd storey	1st storey	2nd storey	1st storey	2nd storey
PF-01	192±5	257±5	**242±10**	*297±20*	**287±15**	*377±30*

Notes:
1. Values determined using the measurements at 1.5 m height (for gas concentrations and OD) or 1.4 m height (for temperatures);
2. The number with the *Italic* typeface represents the calculated time for reaching the CO incapacitation dose, while the number in **bold** represents the calculated time for reaching the heat incapacitation dose, whichever occurred first.

4.2.7 Performance of Test Assembly

A floor system provides an egress route for occupants and its structural integrity directly impacts the safe evacuation of the occupants from the house during a fire emergency. During the fire experiment, the conditions of the test assembly were monitored.

Figure 19 shows temperatures in the cavities of the test assembly. The thermocouples installed in the six sections of the floor cavities aimed to monitor the temperatures inside the cavities and provide an indication of the effectiveness of the gypsum board protection for the test assembly. The time when the temperatures in the floor cavities begun approaching the fire room temperature indicated likely opening of cracks and subsequent fall off of the gypsum membrane protection for the floor structure. This happened from about 700 s to 1100 s depending on the position. This was accompanied by a slow but regular increase in room temperatures in the basement (Figure 14), which was likely a result of an increase in the burning rate due to the additional fuel from ignited areas of the test assembly that were left exposed to the fire as portions of the gypsum ceiling fell off.   Visual observation confirmed that small gypsum pieces started falling from the centre of the ceiling shortly after 700 s, followed by larger gypsum pieces falling off after 800 s. Subsequently, the fire started to involve the joists and subfloor.

NRC·CNRC
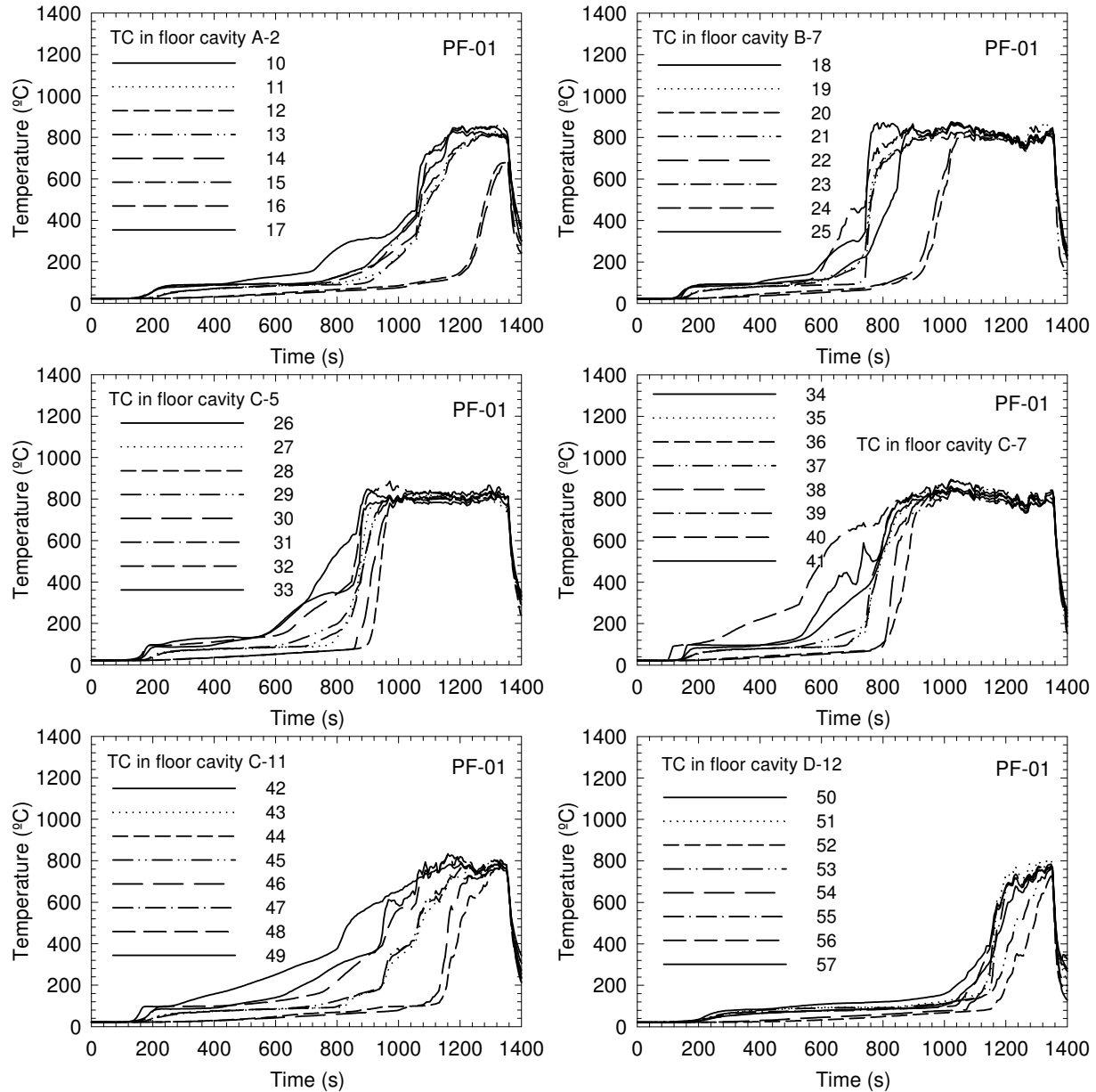
Figure 19. Temperatures in floor cavities in Test PF-01

Figure 20 shows results of the measurements using thermocouples, flame-sensing devices and deflection devices on the unexposed side the test assembly on the first storey.

The deflection of the ceiling/floor assembly was measured at nine points located in the central area of the test assembly just above the fuel package where the impact of the fire on the assembly was anticipated to be the greatest. The test assembly reached the maximum deflection capacity of the measurement devices at 1000 s prior to its structural failure.

The temperature measurements by nine thermocouples under insulated pads on top of the subfloor (on the first storey) are consistent with the measurements in the standard fire-resistance test with respect to thermocouple type, installation and layout [29]. A rapid

NRC·CNRC

increase in temperature indicates that the test assembly was significantly breached. The subsequent rapid decrease in temperature was due to the termination of the experiment by extinguishing the fire with water. It is worth mentioning that on the basis of temperature, failure under standard fire-resistance test conditions is defined as a temperature rise of 140°C on average of the nine padded thermocouples or a temperature rise of 180°C at any single point. Based on this criterion, the floor failure time would be 1100 s (single-point temperature rise of 180°C). Four bare thermocouples were also installed on the unexposed side of the test assembly for temperature measurements.

The flame-sensing device [19] at the central tongue-and-groove joint on the unexposed side of the OSB subfloor provided detection of flame penetration through the test assembly. Figure 20 shows a noticeable voltage signal after 1000 s and a large voltage spike after 1230 s, indicating that the device was detecting flames that had penetrated the test assembly. Flame penetration of the test assembly is also a failure criterion in standard fire-resistance testing [29].
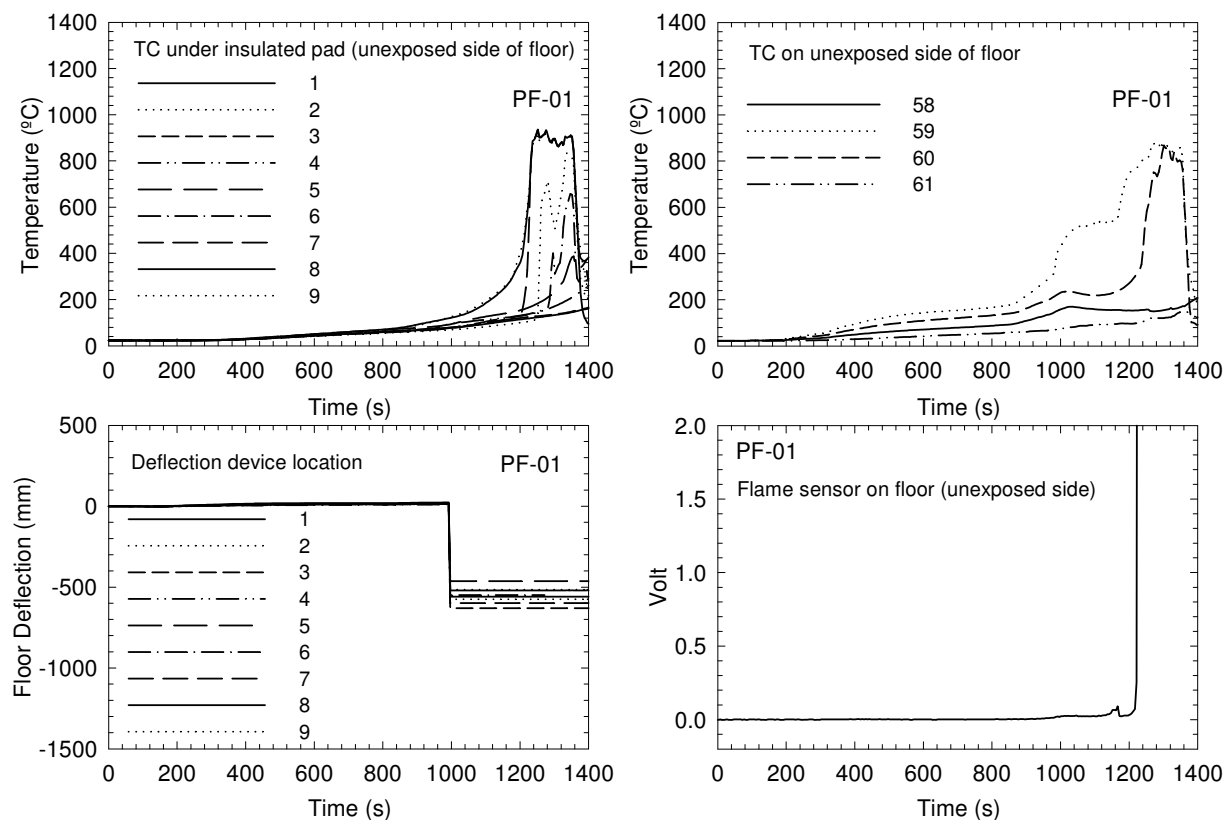
Figure 20. Temperatures, deflections and flame sensor on the unexposed side of the assembly on the first storey in Test PF-01

Although the failure time of the test assembly could be slightly different using other criterion, visual observation through the window opening of the fire room confirmed that structural failure occurred at 1320 s. After this time, the test assembly lost function as an egress route. The fire consumed the OSB subfloor in many areas, particularly in areas directly above the fuel package. Several concrete blocks, which were used to apply loading to the test assembly, fell through the subfloor. There was a partial collapse of the test assembly with one floor joist consumed by the fire. Most other solid-sawn wood joists although significantly charred, deflected but did not collapse.

NRC·CNRC

4.2.8   Sequence of Events

Table 8 summarizes the chronological sequence of the fire events in Test PF-01 — fire initiation, smoke alarm activation, onset of untenable conditions, and structural failure of the test assembly. Smoke obscuration was the first hazard to arise. It must be pointed out that people with impaired vision could become disoriented earlier at an optical density lower than 2 m^{-1}. The incapacitation conditions were reached shortly after smoke obscuration. The structural failure of the test assembly occurred well after the untenable conditions were reached.

For comparison purposes, Table 8 also shows data from the test conducted in Phase 1 using the same floor structure but no gypsum board protection (UF-01). The data indicates that tenability conditions are only slightly improved whilst the structural performance is improved significantly with the protected ceiling/floor assembly.

Table 8. Summary of Sequence of Events in Test PF-01 (in seconds)

Assembly Type	Test	First Alarm	OD = 2 m^{-1}	FED=0.3-1 1st storey	FED=0.3-1 2nd storey	Structural Failure
Gypsum protected solid-sawn wood joists	PF-01	27	192	**242-287**	*297-377*	1320*
Unprotected solid-sawn wood joists	UF-01	40	185	*205-235*	*225-255*	740

Notes:
1. Values determined using the measurements at 1.5 m height (for gas concentrations and OD) or 1.4 m height (for temperatures);
2. The number with the *Italic* typeface represents the calculated time for reaching the CO incapacitation dose, while the number in **bold** represents the calculated time for reaching the heat incapacitation dose, whichever occurred first;
3. *Values of the structural failure time of the test assemblies determined by visual observation;
    a. The maximum deflection capacity of the measurement devices reached at 1000 s;
    b. A single-point temperature rise of 180°C occurred on the unexposed side of the test assembly at 1100 s;
    c. A large voltage spike detected using the flame-sensing device at 1230 s.

4.3   Steel C-Joist Assembly with Gypsum Protection – Test PF-02

Test PF-02 was conducted using a steel C-joist assembly with regular gypsum board on the basement side (i.e. gypsum board ceiling in the fire room).

4.3.1   Construction Details of the Test Assembly

The overall dimensions of the steel C-joist assembly were 5250 mm x 5150 mm. Specific dimensions of the various components of the assembly are provided in Figure 21 to Figure 27. The light-gauge steel C-joists were 203 mm x 41 mm, 1.438 mm (gauge 17), and were spaced at 400 mm on centre (see Figure 21). Based on calculations of maximum strength and deflection, the C-joist span length chosen was 4.477 m [9]. Since the maximum span allowed for the steel C-joists does not extend across the entire length of the fire room, a steel beam was used as an intermediate support at the end of the 4.477-m span and a set of shorter C-joists were used to increase the span of the test assembly to the end of the room. Figure 21, Figure 22 and Figure 23 show the details of the joist overlaps and the supporting steel beams. This

NRC·CNRC

assembly was constructed with blocking and continuous flat strap at the mid span and at the joist overlaps. The assembly was supported by three steel beams, which were in turn supported by six steel columns (two columns for each beam). The beams were bolted to the columns, which were stiffened by steel bars and rested stably on the floor under the weight of the tests assembly and steel beams.

Figure 21. Steel C-joist layout details (PF-02) (all dimensions in mm)
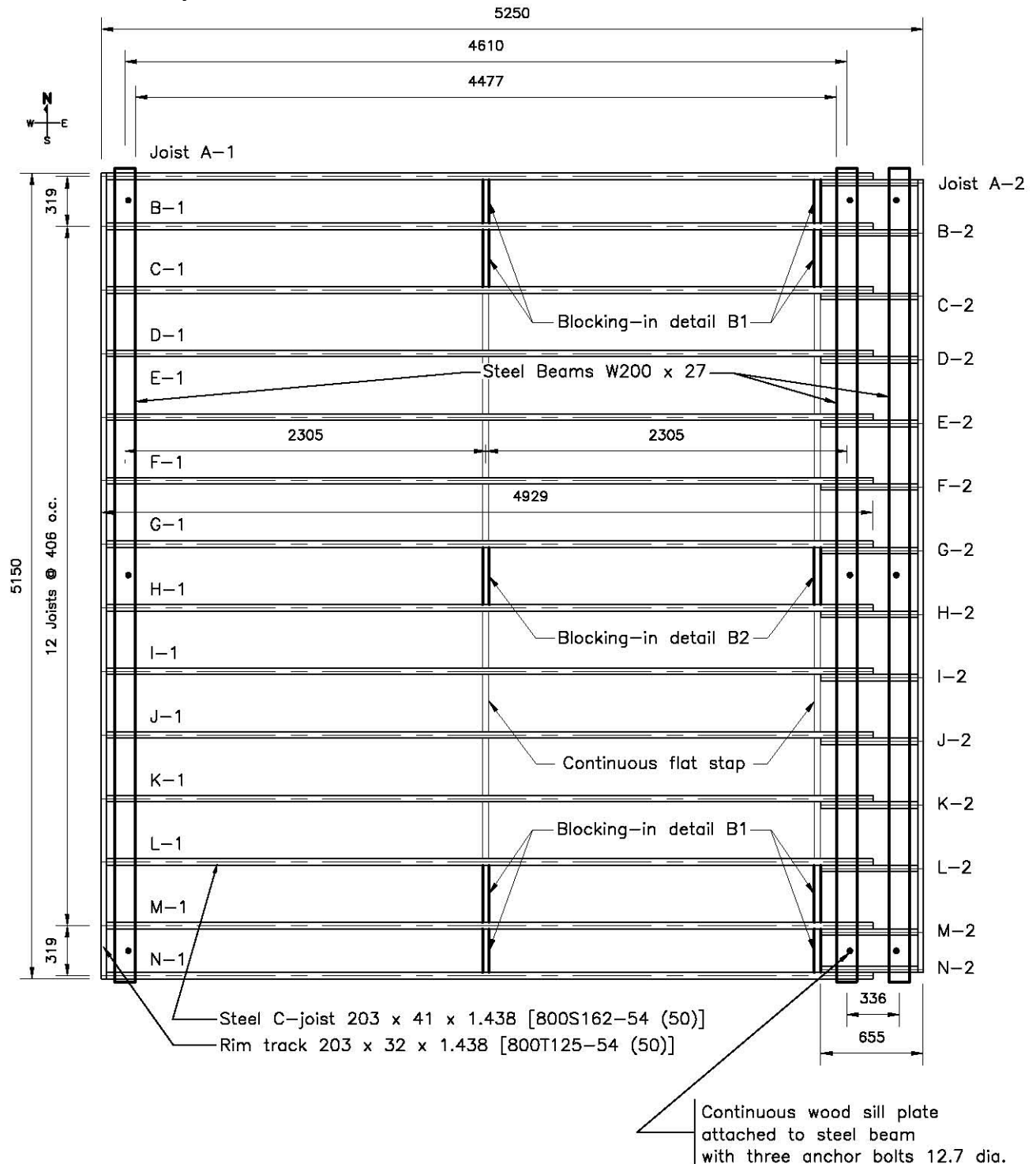
Figure 22 also shows the end connection details. Ceramic fibre blankets were used to fill any gaps between the assembly and the end walls, and to protect the beams and columns so that they were not subjected to fire and would not fail during the test.

Rim tracks (headers) made of steel 203 mm x 32 mm and 1.438 mm thick, were placed at the east and west sides of the test assemblies as shown in Figure 21. Blocking-in, stiffeners and a continuous strap were used. Details are shown in Figure 21 to Figure 23.

#8-18 screws 19 long top and bottom of rim track
Rim track 203 x 32 x 1.438 [800T125-54 (50)]
Steel C-joist 203 x 41 x 1.438 [800S162-54 (50)]
Structural adhesive between C-joist and OSB
Web stiffener 32 x 92 x 1.146 x 194 long [362S125-43]
                                    centred over W200 beam

#10-16 screws 19 long

Anchor bolts

Gypsum board 12.7 thick
C-joist secured to sill plate with 2-#8 wood screws
Ceramic fibre blanket

Gypsum Board 12.7 thick
Cement Board 12.7 thick
Steel stud 89 deep
Glass fibre insulation 89 thick
Sheet metal 18 ga

Wall

End connection details

Steel C-joist 203 x 41 x 1.438 [800S162-54 (50)]
Steel C-joist overlap
#10-16 screws through stiffener and both C-joists

Stiffener inside the joist with the longer span length

167

Anchor bolts

Gypsum board 12.7 thick
C-joist secured to sill plate with 2-#8 wood screws

207

133

Overlap details

Figure 22. Details of end connection and joist overlap (PF-02) (all dimensions in mm)

31

NRC·CNRC

OSB 15.1 thick
Clip angles 38 x 38 x 1.438 x 140 long
Blocking-in [600S162-54 (50)]

#8-18 typical screws

13

Gypsum board 12.7 thick
C-joist 203 x 41 x 1.438 [203S162-54 (50)]
Continuous flat strap 38 x 0.879 connected to typical C-joist with 1- #8-18 screws and to C-joists with blocking-in with 2-#8-18

Blocking-in detail B1

OSB 15.1 thick
Clip angles 38 x 38 x 1.438 x 140 long
Blocking-in [600S162-54 (50)]

Gypsum board 12.7 thick
continuous flat strap attached to blocking-in with 2-#8-18 screws

Blocking-in detail B2

Figure 23. Blocking-in details (PF-02) (all dimensions in mm)

NRC·CNRC
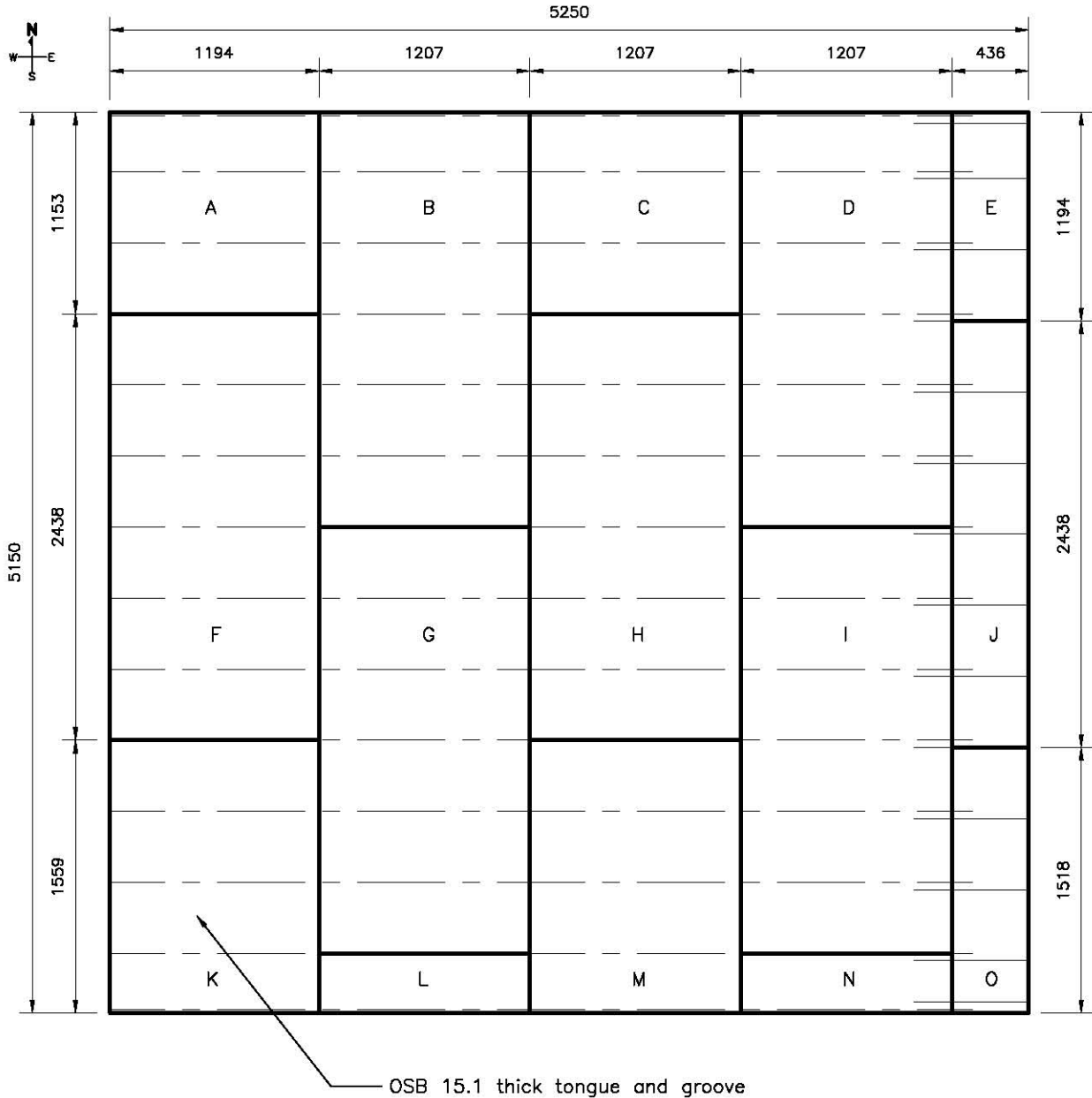
Figure 24. Subfloor layout (PF-02) (all dimensions in mm)

OSB was used as the subfloor material in the test assembly. The specific OSB material used was selected based on a separate study documented in reference [28]. The subfloor panels were 15.1 mm thick in the assembly, with a full panel size of 1.2 x 2.4 m. The longer panel edges had a tongue-and-groove profile while the short panel edges were square butt ends. Figure 24 shows the layout of the subfloor. The screw pattern and description of screws used to attach the OSB panels to the steel C-joists and rim track are shown in Figure 25.

NRC·CNRC
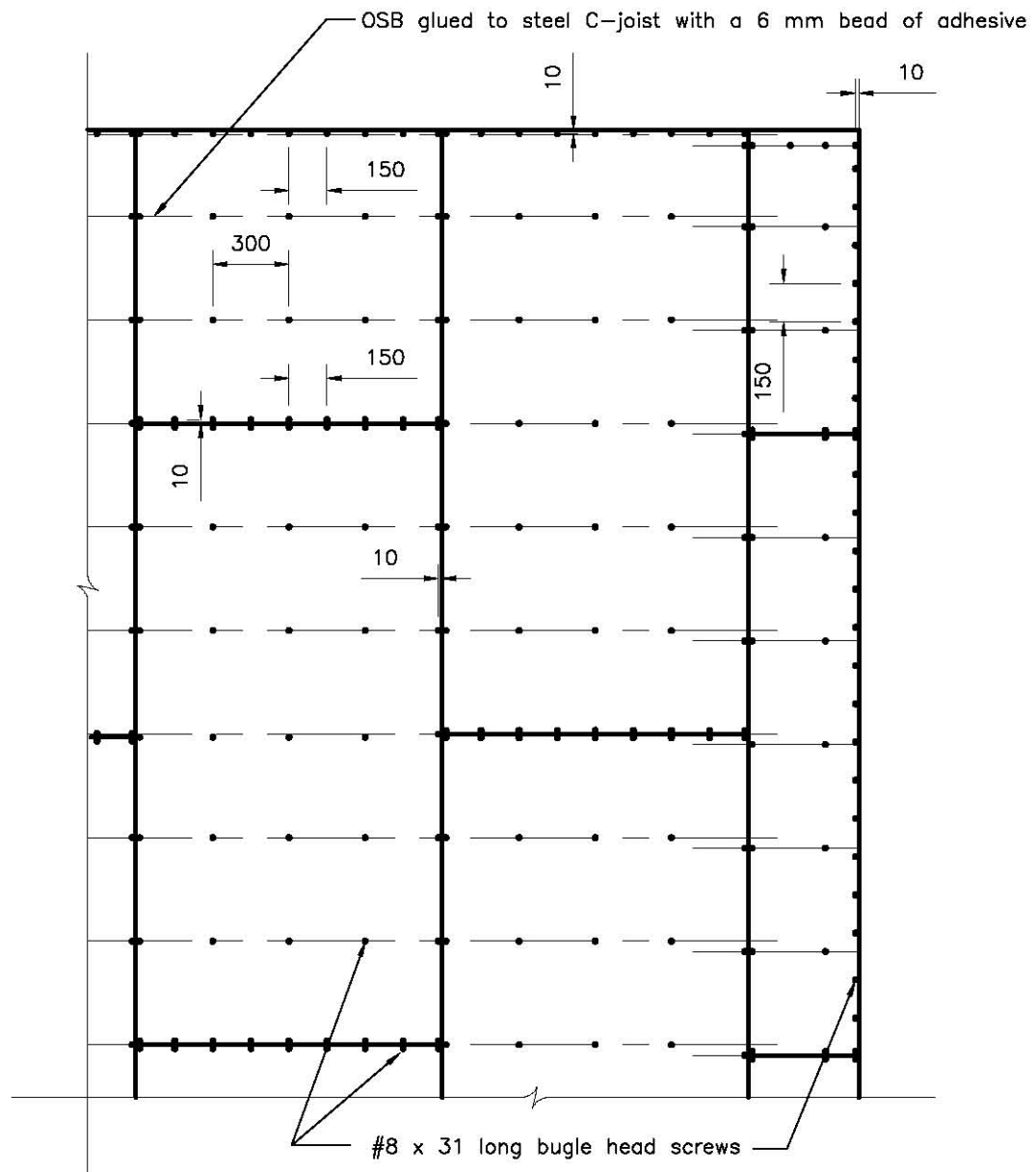
Figure 25. Subfloor screw pattern and screw description (PF-02) (all dimensions in mm)
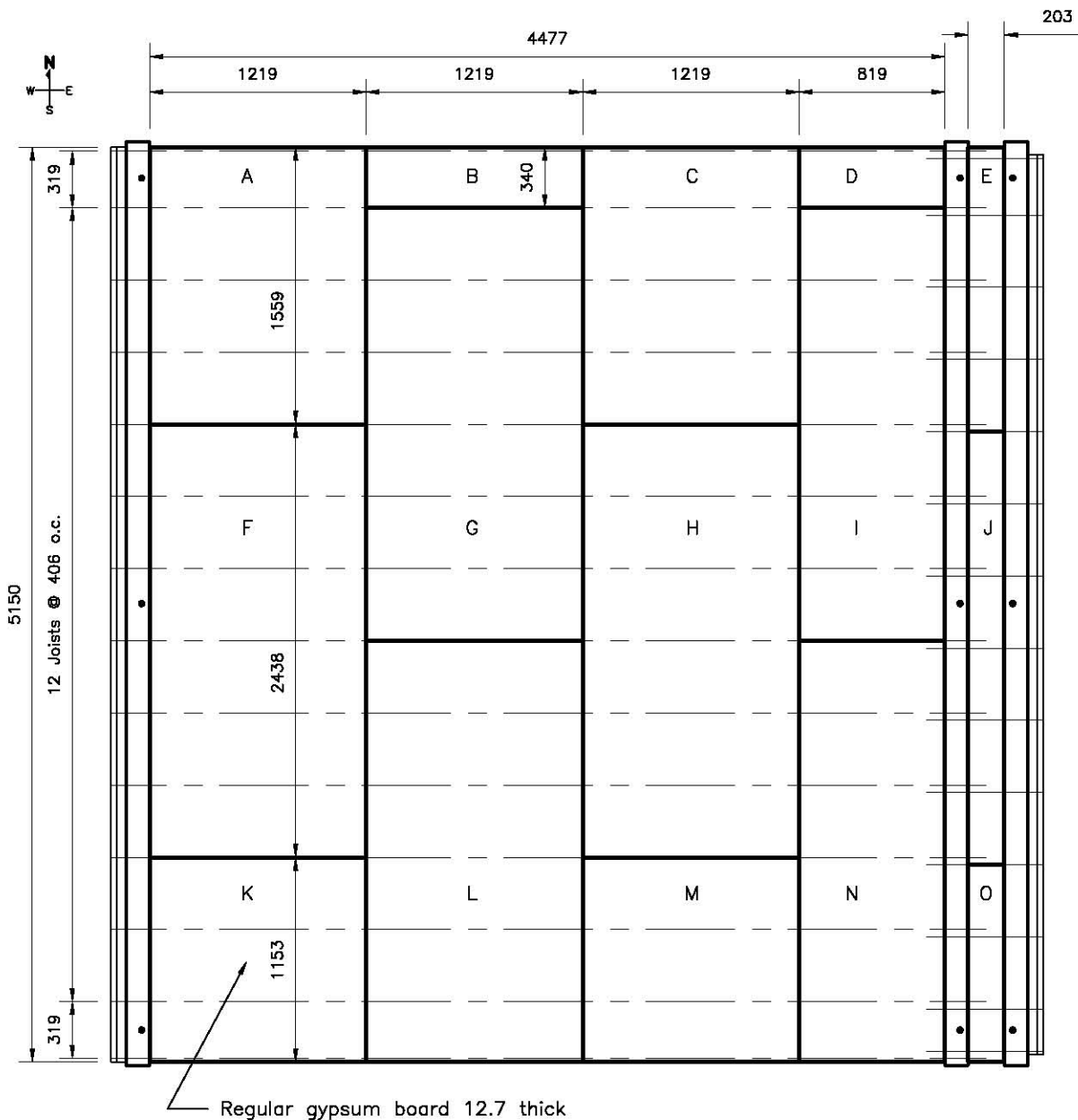
Figure 26. Gypsum board layout on the assembly as the basement ceiling (PF-02) (all dimensions in mm)

Regular gypsum board was installed on the basement side of the test assembly by being fastened directly to the bottom of the steel C-joists. The gypsum board was 12.7 mm thick, with a full sheet size of 1.2 x 2.4 m. Figure 26 shows the layout of the gypsum board on the assembly. The joints of the gypsum board were finished with joint compound and tape. The screw pattern and description of screws used to fasten the gypsum board to the steel C-joists and rim track are shown in Figure 27.

NRC·CNRC
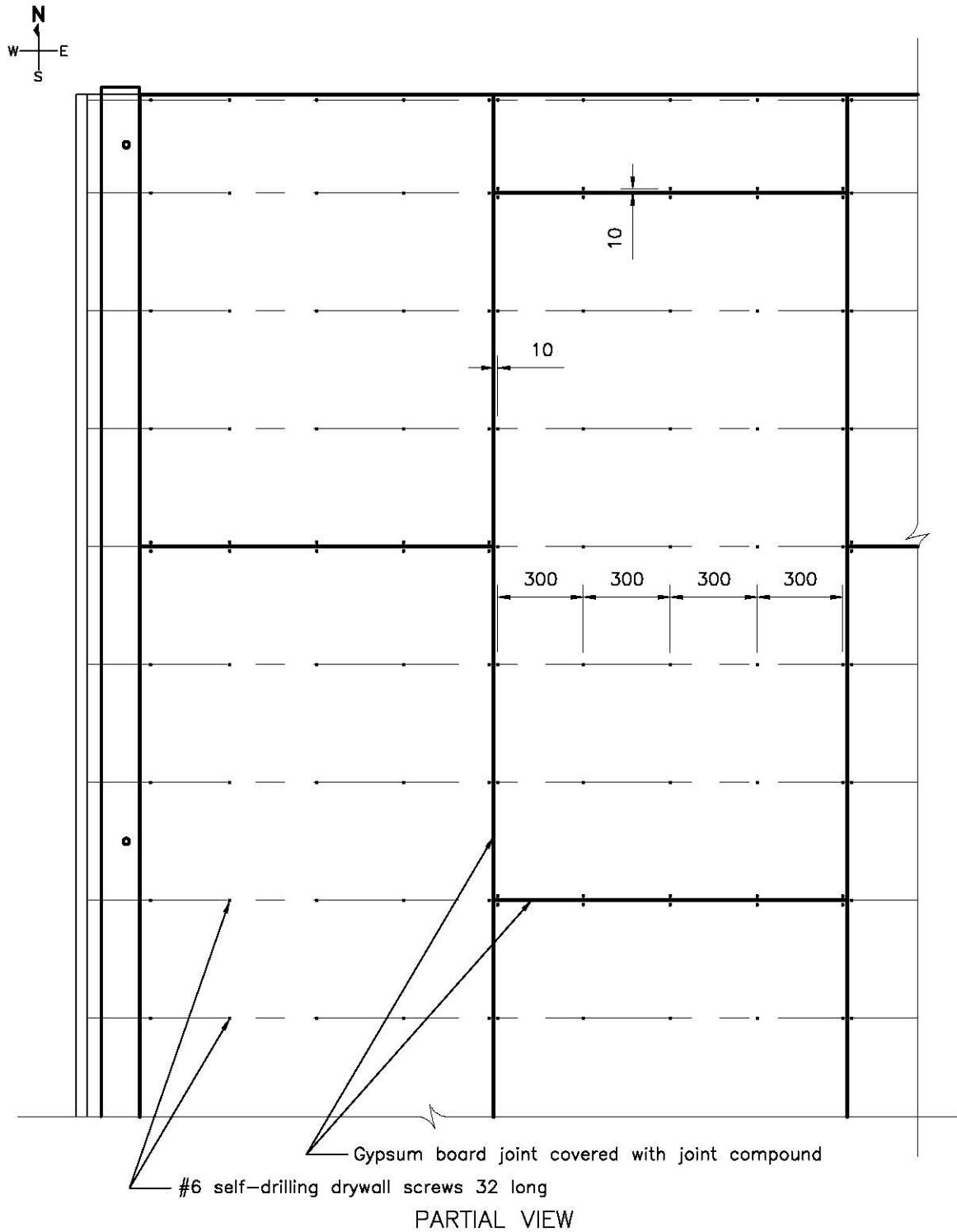
Figure 27. Gypsum board screw layout for steel C-joist assembly (PF-02) (all dimensions in mm)

Text labels within the figure:

N
W—E
S

10

10

300 300 300 300

Gypsum board joint covered with joint compound

#6 self-drilling drywall screws 32 long

PARTIAL VIEW

NRC·CNRC

Sixty-one Type K (20 gauge) chromel-alumel thermocouples, with a thickness of 0.91 mm, were used for measuring temperatures at a number of locations throughout the assembly. The thermocouples were located on the unexposed side and in the cavities of the assembly as shown in Figure 28 and Figure 29. These locations were chosen to monitor the conditions of the assembly at critical locations during the fire tests. The floor deflection was measured at 9 points on the unexposed surface of the test assembly at the locations as shown in Figure 13.
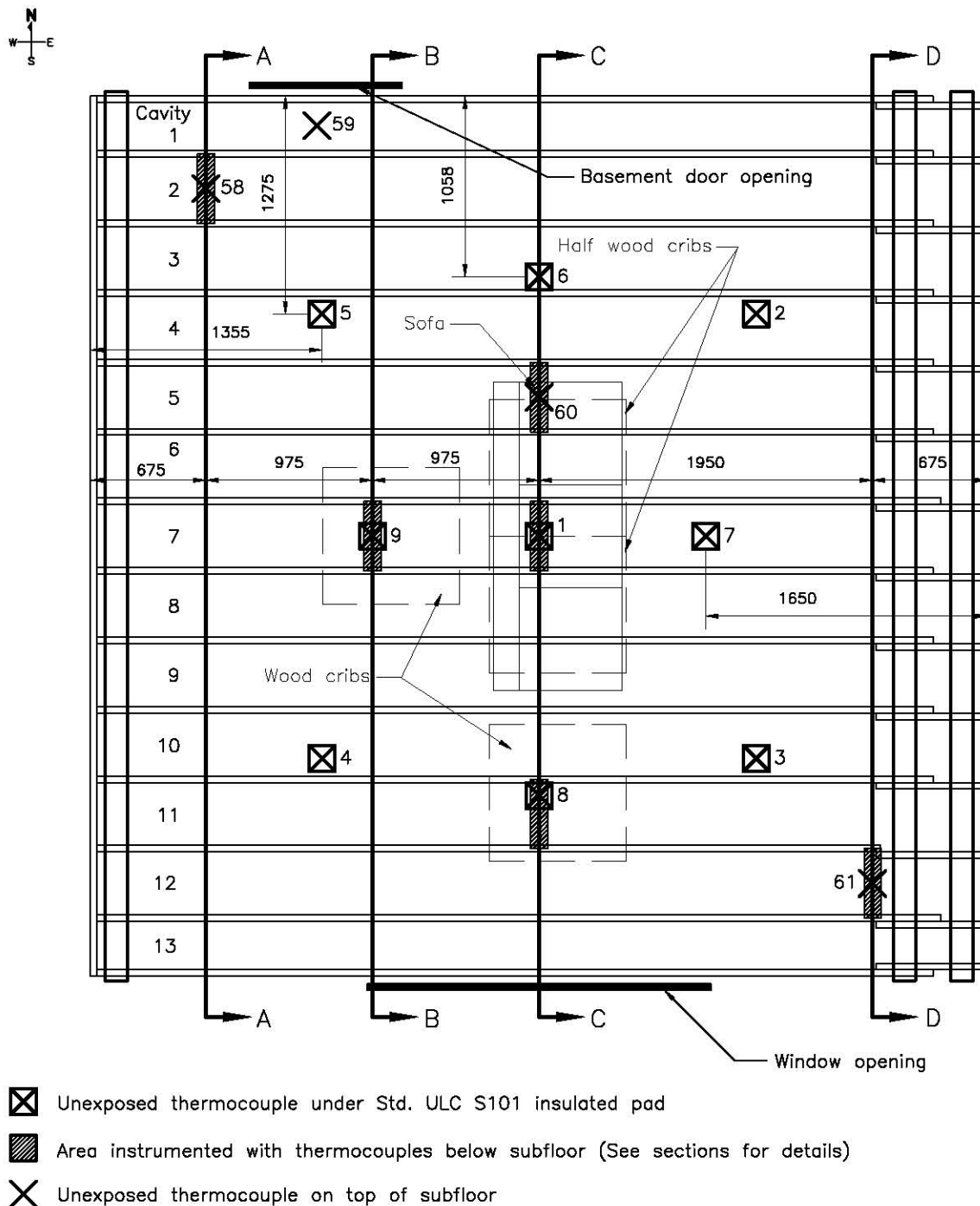
Figure 28. Thermocouples locations in PF-02 assembly (all dimensions in mm)

NRC·CNRC
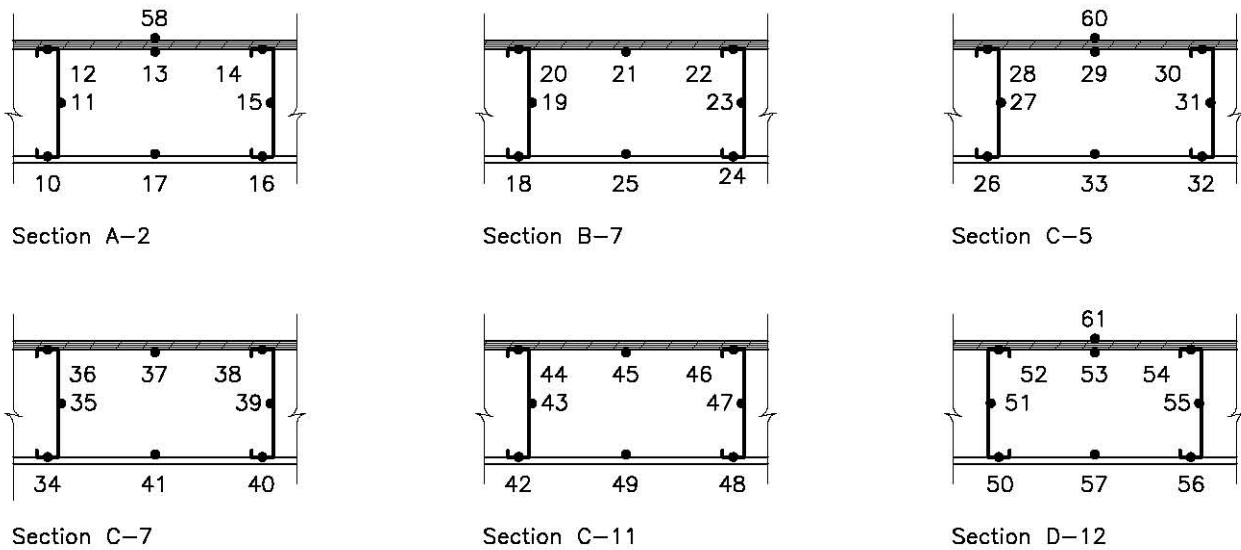
Figure 29. Thermocouples locations in the different sections shown in Figure 28 (PF-02)

4.3.2   Fire Development in Basement

Figure 30 shows temperatures measured in the basement fire room. The polyurethane foam used for the mock-up sofa dominated the initial fire growth. The temperatures at the window quickly reached 300°C and the noncombustible window covering panel was removed at 120 s. The temperatures at the 2.4 m height exceeded 600°C within 140-160 s, indicating that the fire room reached flashover conditions. The fast development of the fire from ignition to attainment of the first temperature peak was consistent with the experiments in Phase 1 of FPH research. Following this initial stage of fire growth, the fire became wood-crib-dominated. There was a quick transition from a well-ventilated flaming fire to an under-ventilated fire.

Figure 30 also shows the heat flux measured at the west wall (near the centre, 2.05 m above the floor). The maximum heat flux was 150 kW·m^{-2}, indicating post-flashover conditions in the fire room.

NRC·CNRC
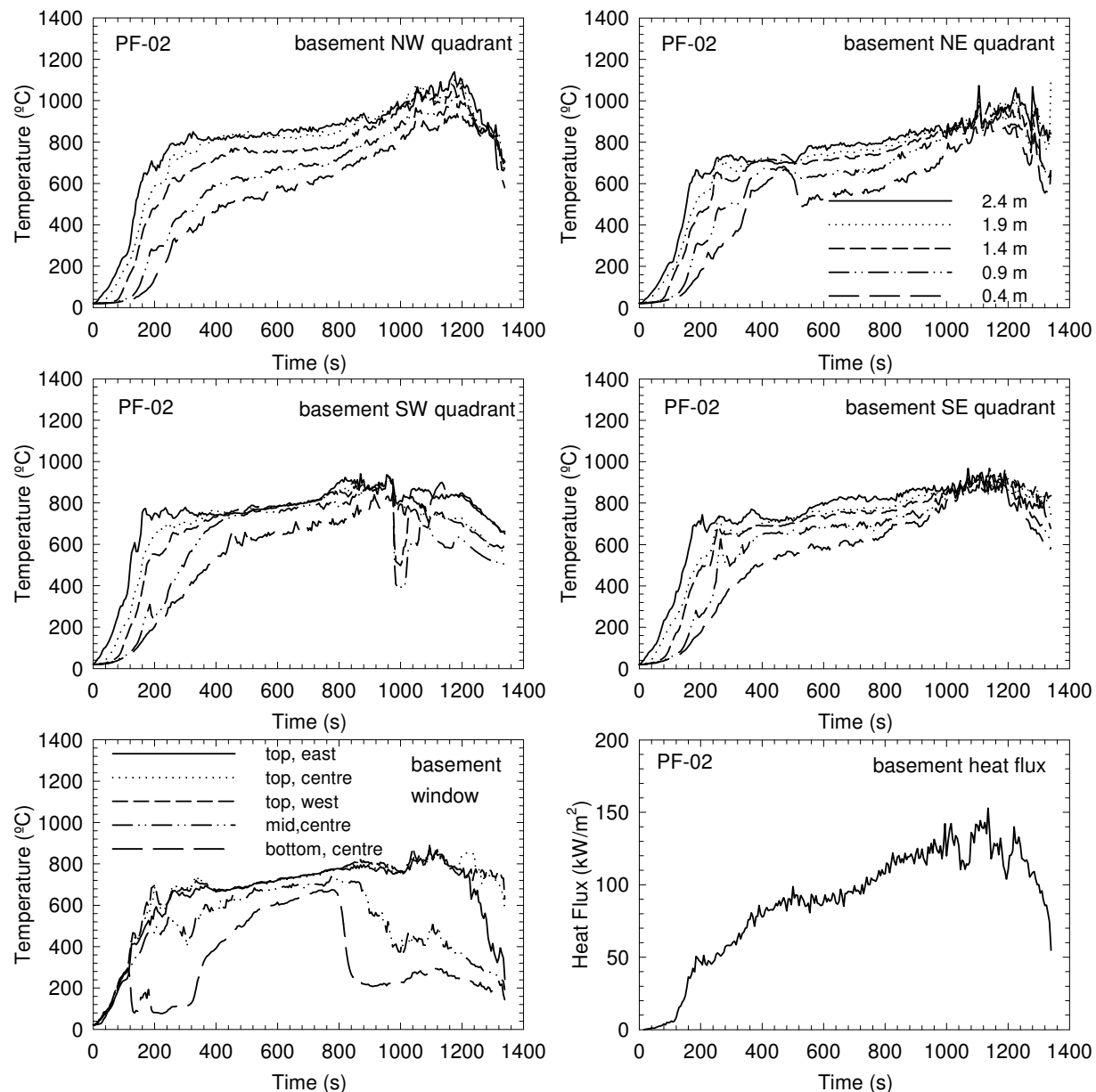
Figure 30. Temperatures and heat flux in the basement fire room in Test PF-02

4.3.3 Visual Obscuration

The optical density was measured at 0.9 and 1.5 m heights (simulating the height of the nose/mouth of an average height individual crawling and standing, respectively) above the floor on the first and second storeys. Figure 31 shows the optical density-time profiles. The second storey reached OD = 2 m^{-1} after 220 s. It must be pointed out that the video records show complete darkness in the test house on both storeys after 200 s. The smoke density meter has an operation temperature limit of 80°C in its gas chamber; when this temperature is reached,

the flow is reversed to cool the chamber to protect the electronic components. The smoke meter resumes operation once the gas chamber is cooled down below 80°C. In this experiment, only the initial part of the curves (up to 200 s) represents valid measurements.
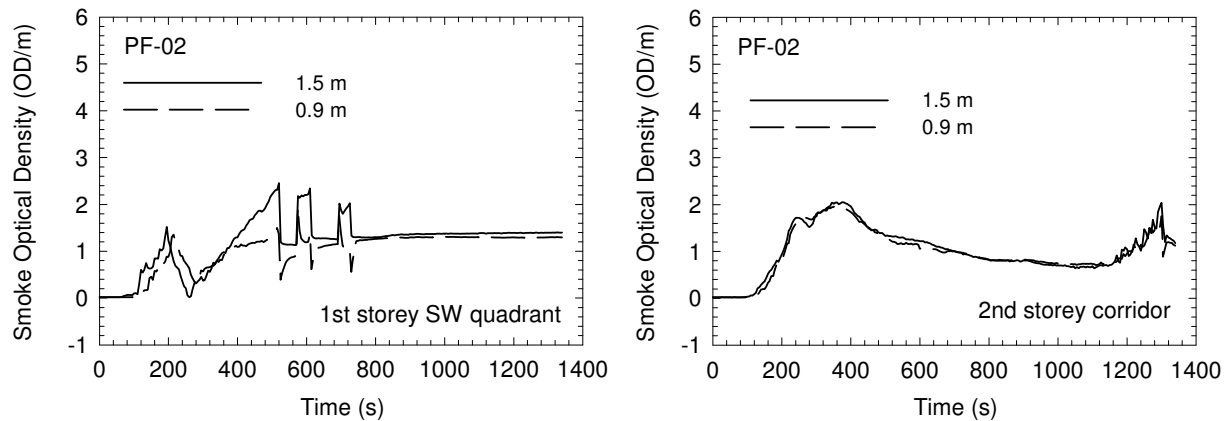
Figure 31. Smoke optical density measurements in Test PF-02

4.3.4   Gas Measurements and Analysis (CO, CO_2 and O_2)

Figure 32 shows the CO, CO_2 and O_2 concentrations measured at the southwest quarter point on the first storey and at the centre of the corridor on the second story during the experiment. Within approximately 400 s, oxygen was diminished to below 12% and CO_2 increased to above 8%. The concentrations were below 5% O_2 and above 15% CO_2 near the end of the experiment. The tenability analysis indicated that the toxic effect of CO would be capable of causing incapacitation at an earlier time than the effect of O_2 vitiation and the asphyxiant effect of CO_2. Table 9 shows the times to reach the specified FED for exposure to O_2 vitiation, CO_2 and CO.

NRC·CNRC
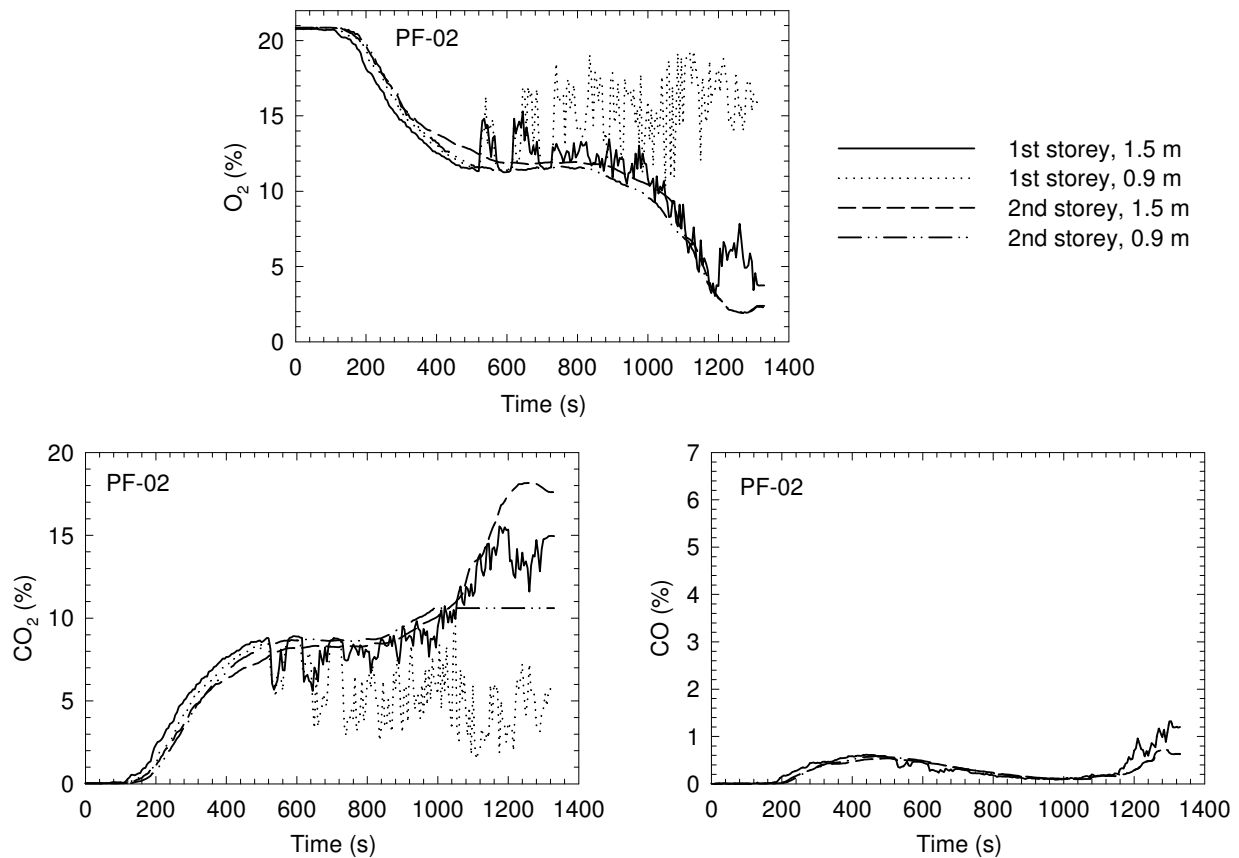
Figure 32. CO, CO_2 and O_2 concentrations in Test PF-02

Table 9. Time (in seconds) to the Specified FED for Exposure to O_2 Vitiation, CO_2 and CO in Test PF-02

Fractional Effective Dose	FED = 0.3	FED = 1.0
CO alone – 1st storey	360	670
CO with CO_2 hyperventilation – 1st storey	285±20	375±35
Low O_2 hypoxia – 1st storey	895	1135
CO alone – 2nd storey corridor	400	720
CO with CO_2 hyperventilation – 2nd storey corridor	325±20	420±45
Low O_2 hypoxia – 2nd storey corridor	895	1130
High CO_2 hypercapnia – 1st storey	460	760
High CO_2 hypercapnia – 2nd storey corridor	540	815

Note:
1. Values determined using concentrations at 1.5 m height.

41

NRC·CNRC

4.3.5 Temperature-Time Profiles on the Upper Storeys

Figure 33 and Figure 34 show temperature profiles measured on the first and second storeys during the experiment. These profiles demonstrate that temperatures vary depending on the locations inside the test house. In the bedroom with the door closed, the temperatures never exceeded 80°C at the ceiling height during the experiment.
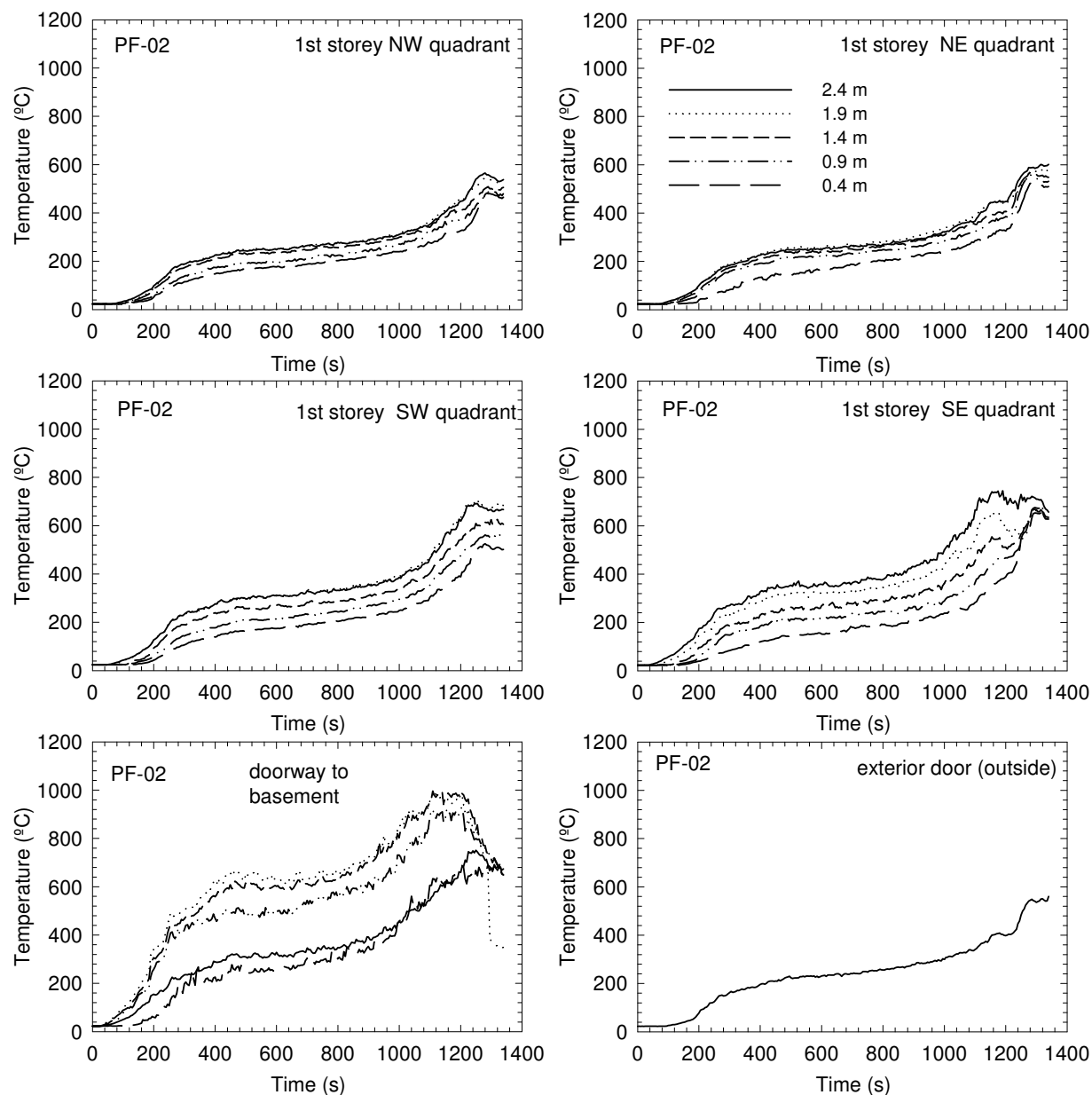
Figure 33. Temperatures on the first storey in Test PF-02

42

NRC·CNRC
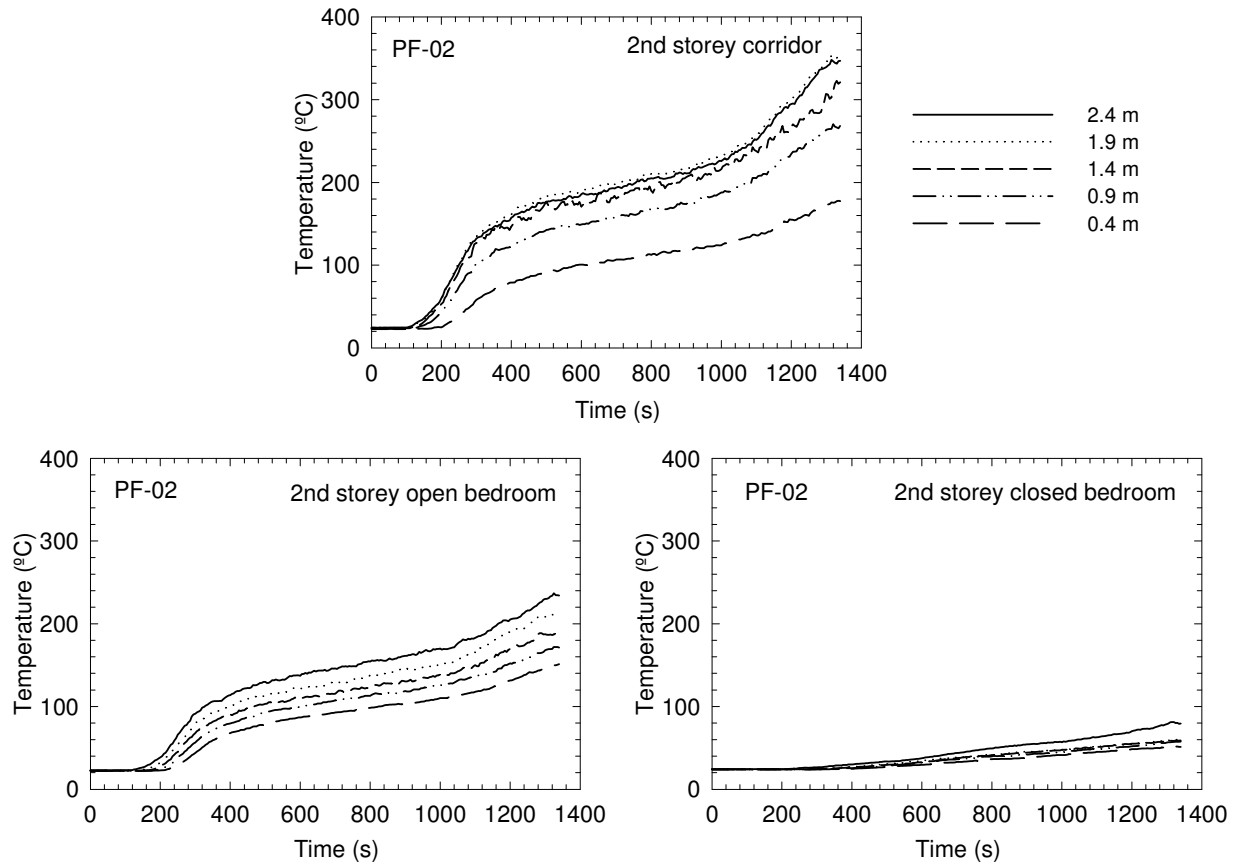
Figure 34. Temperatures on the second storey in Test PF-02

In the closed bedroom, heat exposure would not cause incapacitation. On the first storey, in the corridor and in the open bedroom on the second storey, the calculated times to incapacitation due to exposure to the convected heat are given in Table 10 for FED = 0.3 and 1. The calculated times to reach the heat incapacitation doses on the first storey were shorter than those for CO exposure. In the corridor on the second storey, the calculated times to reach the incapacitation doses for heat exposure were similar to those for CO exposure.

Table 10. Time (seconds) to the Specified FED for Exposure to Convected Heat in Test PF-02

Fractional Effective Dose	FED = 0.3	FED = 1.0
1st storey SE quadrant	260	305
1st storey SW quadrant	255±10	300±15
1st storey NE quadrant	270	320
1st storey NW quadrant	265	320
2nd storey corridor	320±15	415±25
2nd storey open bedroom	490	725
2nd storey closed bedroom	not reached (FED<0.13)	not reached (FED<0.13)

Note:
1. Values determined using temperatures at 1.4 m height.

4.3.6   Estimation of Time to Incapacitation

Table 11 summarizes the results of tenability analysis with the estimated times to the onset of various conditions for Test PF-02. The timing to reach the OD values of 2 m^{-1} on the first storey was unknown since the smoke meters installed on the first storey reversed the flow to cool and protect the devices. But, this timing must have been earlier than that on second storey, which is listed in the table. Smoke obscuration was the first hazard to arise. The calculated time for reaching the specific FED either due to the heat exposure or due to the CO exposure (exacerbated by CO_2-induced hyperventilation), whichever occurred first, is listed in Table 11. Heat exposure reached the specific FED on the first storey at times shorter than for CO exposure. On the second storey (in the corridor), CO exposure and heat exposure reached the specific FED at similar times. The time difference for heat exposure and CO exposure to reach the specific FED was not significant. Note that for the closed bedroom on the second storey, based on the temperatures and the heat exposure calculation, the conditions in the closed bedroom would not reach untenable conditions.

Table 11. Summary of Estimation of Time to Specified FED and OD (in seconds) for Test PF-02

Test	OD = 2 m^{-1}		FED = 0.3		FED = 1	
	1st storey	2nd storey	1st storey	2nd storey	1st storey	2nd storey
PF-02	not available	220	**255±10**	**320±15**	**300±15**	420±45

Notes:
1. Values determined using the measurements at 1.5 m height (for gas concentrations and OD) or 1.4 m height (for temperatures);
2. The number with the *Italic* typeface represents the calculated time for reaching the CO incapacitation dose, while the number in **bold** typeface represents the calculated time for reaching the heat incapacitation dose, whichever occurred first.

4.3.7   Performance of Test Assembly

A floor system provides an egress route for occupants and its structural integrity directly impacts the safe evacuation of the occupants from the house during a fire emergency. During the fire experiment, the conditions of the test assembly were monitored.

Figure 35 shows temperatures in the cavities of the test assembly. The thermocouples installed in the six sections of the floor cavities aimed to monitor the temperatures inside the cavities and provide an indication of the effectiveness of gypsum board protection for the test assembly. The moment that temperatures in the floor cavities approached the fire room temperature indicates the loss of the gypsum board membrane protection for the floor structure. This happened around 800 – 1100 s depending on the position. Visual observation confirmed that gypsum board pieces started falling from the centre of the ceiling shortly after 800 s, followed by larger gypsum board pieces falling. Then flame started to involve the subfloor.
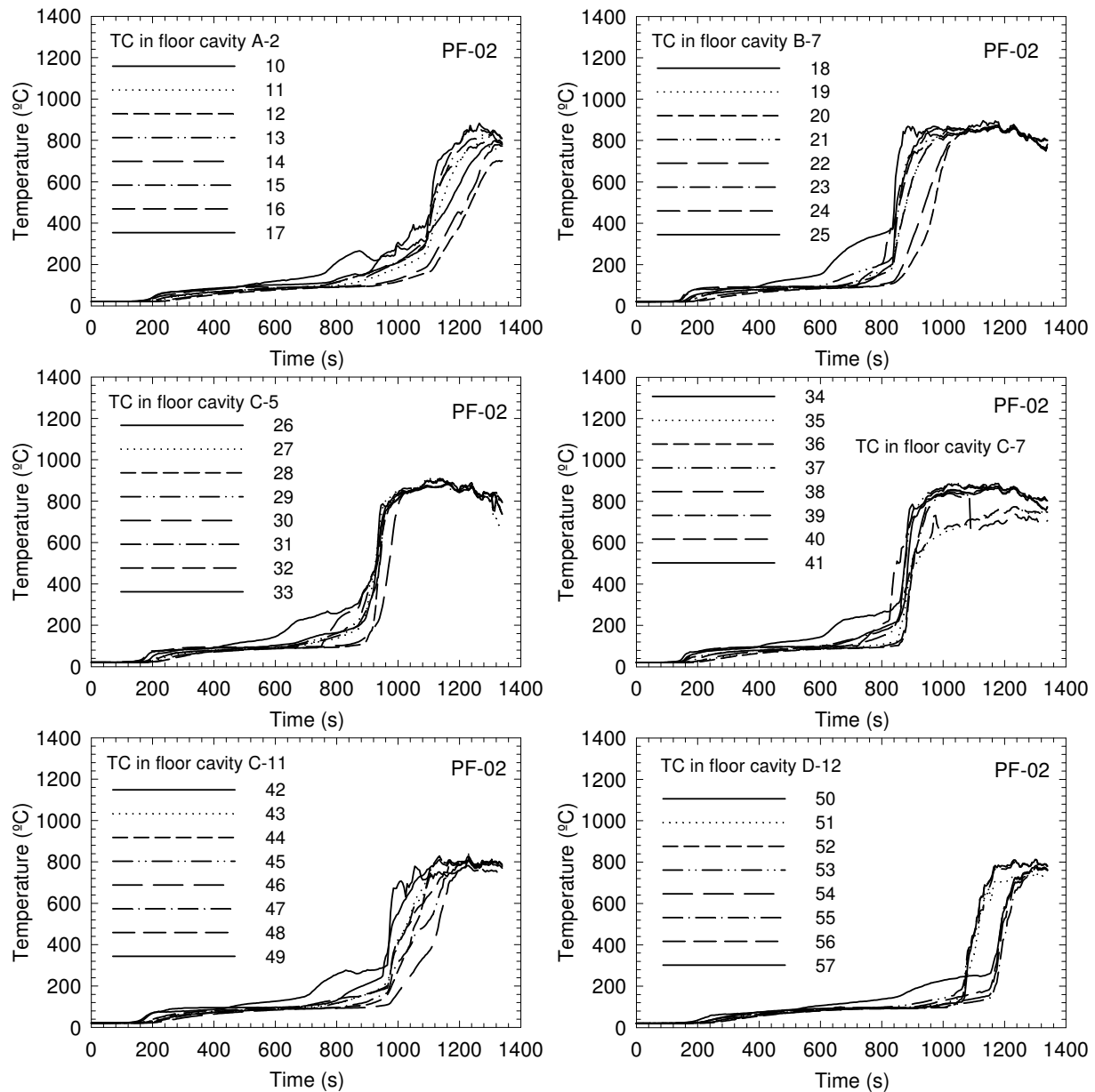
Figure 35. Temperatures in floor cavities in Test PF-02

The flame-sensing device was installed at the central tongue-and-groove joint on the unexposed side of the OSB subfloor to detect flame penetration. However, there was an instrument malfunction for the flame-sensing device in this experiment. Figure 36 shows results of the measurements using thermocouples and deflection devices on the unexposed side the test assembly on the first storey.

The temperature measurements by nine thermocouples under insulated pads on top of the subfloor (on the first storey) are comparable to the measurements in the standard fire-resistance test with respect to thermocouple type, installation and layout [29]. Based on the criterion of 180°C temperature rise at any single point, the structural failure time would be 1140 s. Four

45

bare thermocouples were also installed on the unexposed side of the test assembly for temperature measurements.

The floor deflection of the test assembly was measured at nine points located in the central area of the test assembly just above the fuel package where the impact of the fire on the assembly was anticipated to be the greatest. There was floor deflection of the test assembly prior to its structural failure. Based on visual observation, the test assembly started sagging around 1000 s and failed at 1300 s when many concrete blocks, which were used to apply loading to the test assembly, fell through the subfloor. These observations are consistent with the deflection measurements.

Although the structural failure time could be slightly different using different criterion, visual observation of the assembly failure at 1300 s is taken as the failure time. The fire consumed the OSB subfloor in most areas and many concrete blocks fell to the basement. The steel C-joists deformed and deflected approximately 0.5 m but did not collapse, as they were held in place by the connections to the rim track.
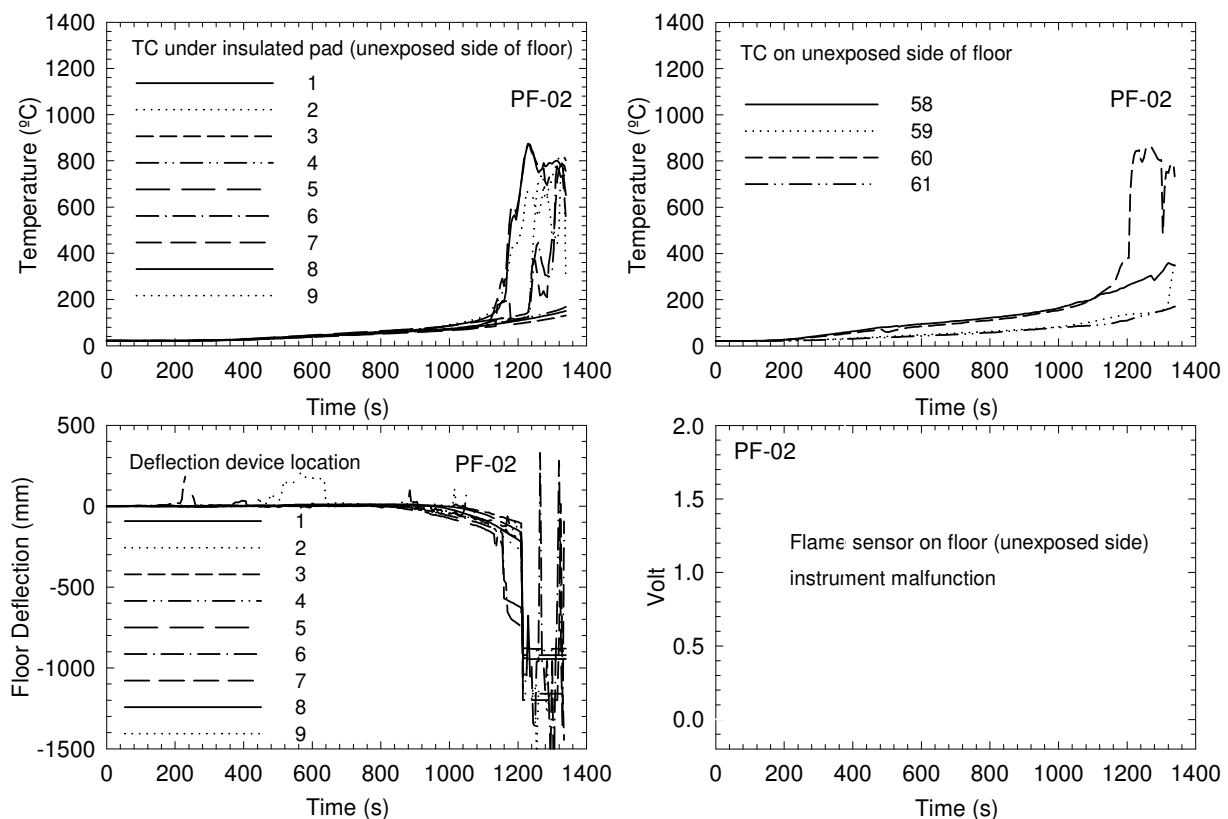
Figure 36. Temperatures, deflections and flame sensor on the unexposed side of the assembly on the first storey in Test PF-02

46

NRC·CNRC

4.3.8 Sequence of Events

Table 12 summarizes the chronological sequence of the fire events in Test PF-02 — fire initiation, smoke alarm activation, onset of untenable conditions, and structural failure of the test assembly. Smoke obscuration was the first hazard to arise. It must be pointed out that people with impaired vision could become disoriented earlier at an optical density lower than 2 m^{-1}. The incapacitation conditions were reached shortly after smoke obscuration. The structural failure of the test assembly occurred well after the untenable conditions were reached.

For comparison purposes, Table 12 also shows data from the test conducted in Phase 1 using the same floor structure but no gypsum board protection (UF-04). The data indicates that tenability conditions are only slightly improved whilst the structural performance is improved significantly with the protected ceiling/floor assembly.

Table 12. Summary of Sequence of Events in Test PF-02 (in seconds)

Assembly Type	Test	First Alarm	OD = 2 m^{-1}	FED=0.3-1 1st storey	FED=0.3-1 2nd storey	Structural Failure
Gypsum protected steel C-joists	PF-02	30	220	**255-300**	**320**-*420*	1300*
Unprotected steel C-joists	UF-04	30	195	**207-215**	*245-280*	462

Notes:
1. Values determined using the measurements at 1.5 m height (for gas concentrations and OD) or 1.4 m height (for temperatures);
2. The number with the *Italic* typeface represents the calculated time for reaching the CO incapacitation dose, while the number in **bold** typeface represents the calculated time for reaching the heat incapacitation dose, whichever occurred first;
3. *Values of the structural failure time of the test assemblies determined by visual observation;
   a. The maximum deflection capacity of the measurement devices reached at 1215 s;
   b. A single-point temperature rise of 180°C occurred on the unexposed side of the test assembly at 1140 s.

4.4 Wood I-Joist Assembly with Gypsum Protection – Test PF-04

Test PF-04 was conducted using a wood I-joist assembly with regular gypsum board fastened directly to the bottom flange of the wood I-joists on the basement side (i.e. gypsum board ceiling in the fire room). Except that the basement side had a different protection measure, the PF-04 test assembly was identical to those used in Tests PF-03, PF-03B and PF-05.

4.4.1 Construction Details of the Test Assembly

The overall dimensions of the wood I-joist assemblies were 5250 mm x 5150 mm. Specific dimensions of the various components of the assemblies are provided in Figure 37 to Figure 40. The wood I-joists were 302 mm deep, with an OSB web of 9.5 mm thick and the flanges were laminated veneer lumber (32 mm x 59 mm). The I-joists were spaced at 400 mm on centre. Based on calculations of maximum strength and deflection, the I-joist span length chosen was 4.813 m. This span allowed the wood I-joists to extend across the entire length of the fire room (with no need for an intermediate support). Laminated strand lumber (LSL) rim boards

NRC·CNRC

(headers) 32 mm thick x 302 mm deep (grade 1.3E), were placed around the perimeter of the assemblies as shown in Figure 37. It should be noted that, compared to the wood I-joists A used in Phase 1 of the FPH research, the wood I-joists used for current experiments were slightly modified by the manufacturer – the depth of the top and bottom flanges of the wood I-joist were changed from 35 mm to 32 mm. This change did not result in any change to the structural design values assigned to the wood I-joist members.
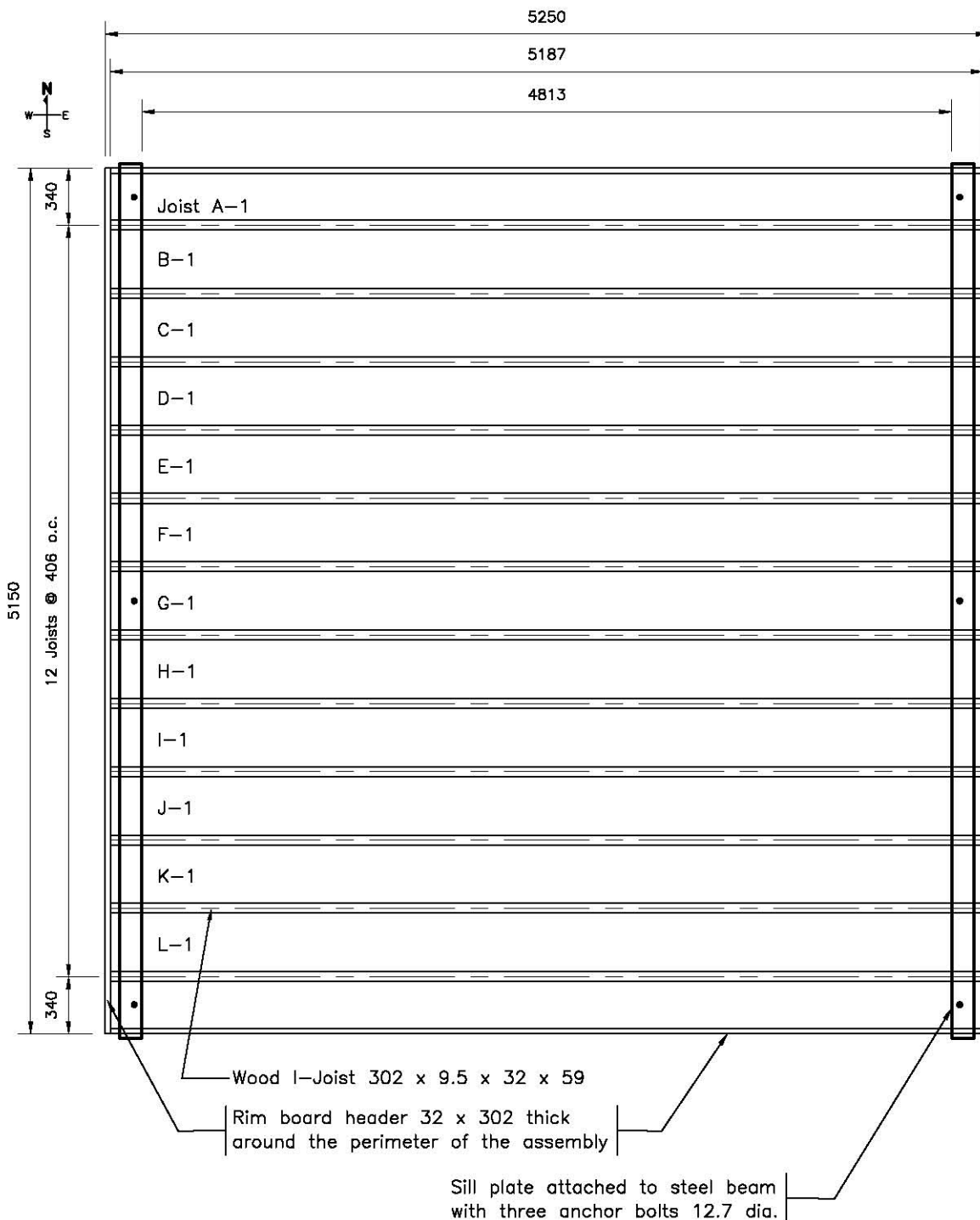
Figure 37. Wood I-joist layout details for Tests PF-03, PF-03B, PF-04 and PF-05 (all dimensions in mm)

The wood I-joist assembly was supported by two horizontal steel beams, each of which was supported by two steel columns (a total of four columns for each assembly). The beams were bolted to the columns, which were stiffened by steel bars and rested stably on the floor under the weight of the test assembly and steel beams.

End connection details (East view)

OSB 15.1 thick
Wood I-joist 302 x 9.5 x 32 x 59
Rim board header toenailed to sill plate with 10d 76 long box nails at 150 o.c.
LVL flange
Floor I-joists toenailed to sill plate with one 8 d box nails 64 long driven in at angle each side of the web
207
Steel beam/column W200 x 27 Protected with ceramic fibre blankets
Sill plate 38 x 230 attached to steel beam with three anchor bolts 12.7 dia. by 63 long
207

End connection details (North view)

Rim board header 32 thick
One 16 d box nails 89 long in each flange
Structural adhesive between I-joist and OSB
140
Anchor bolts
Gypsum board 12.7 thick
Wood I-joist 302 x 9.5 x 32 x 59
Ceramic fibre blanket
Gypsum Board 12.7 thick
Cement Board 12.7 thick
Steel stud 89 deep
Glass fibre insulation 89 thick
Sheet metal 18 ga
Wall

Figure 38. Details of end connection and supports for Test PF-04 (gypsum board protection) (all dimensions in mm)

NRC·CNRC

Regular gypsum board was installed on the basement side of the PF-04 assembly to provide a finished gypsum board ceiling in the basement fire room. The gypsum board was 12.7 mm thick, with a full sheet size of 1.2 x 2.4 m. Figure 38 shows details of the gypsum board installation, end connection and the supporting beams. Figure 39 shows the layout of the gypsum board on the assembly. The joints of the gypsum board were finished with joint compound and tape. The screw pattern and description of screws used to fasten the gypsum board to the solid-sawn wood joists and rim board (header) are shown in Figure 10. Ceramic fibre blankets were used to fill any gaps between the assemblies and the end walls, and also to protect the steel beams and columns from the fire, so that they would not fail during the experiments.
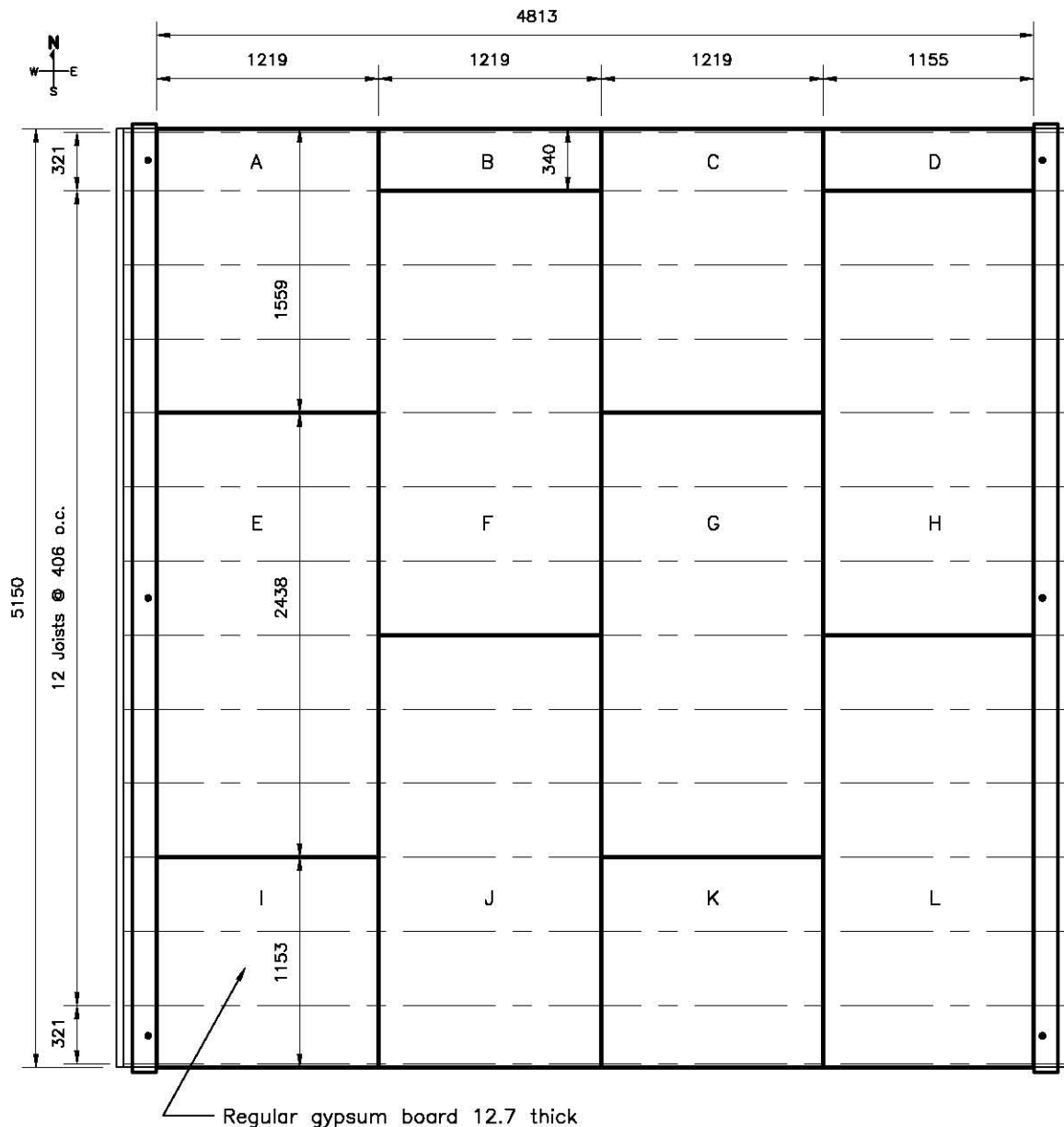
Figure 39. Gypsum board layout on basement ceiling (Tests PF-04 and PF-06C) (all dimensions in mm)

OSB was used as the subfloor material in the test assemblies. The specific OSB material used was selected based on a separate study documented in reference [28]. The subfloor panels were 15.1 mm thick, with a full panel size of 1.2 x 2.4 m. The longer panel edges had a tongue-and-groove profile while the short panel edges were square butt ends. Figure 7 shows the layout of the subfloor. The nailing pattern and description of nails used to attach the OSB panels to the wood I-joists and rim board (header) are shown in Figure 40.
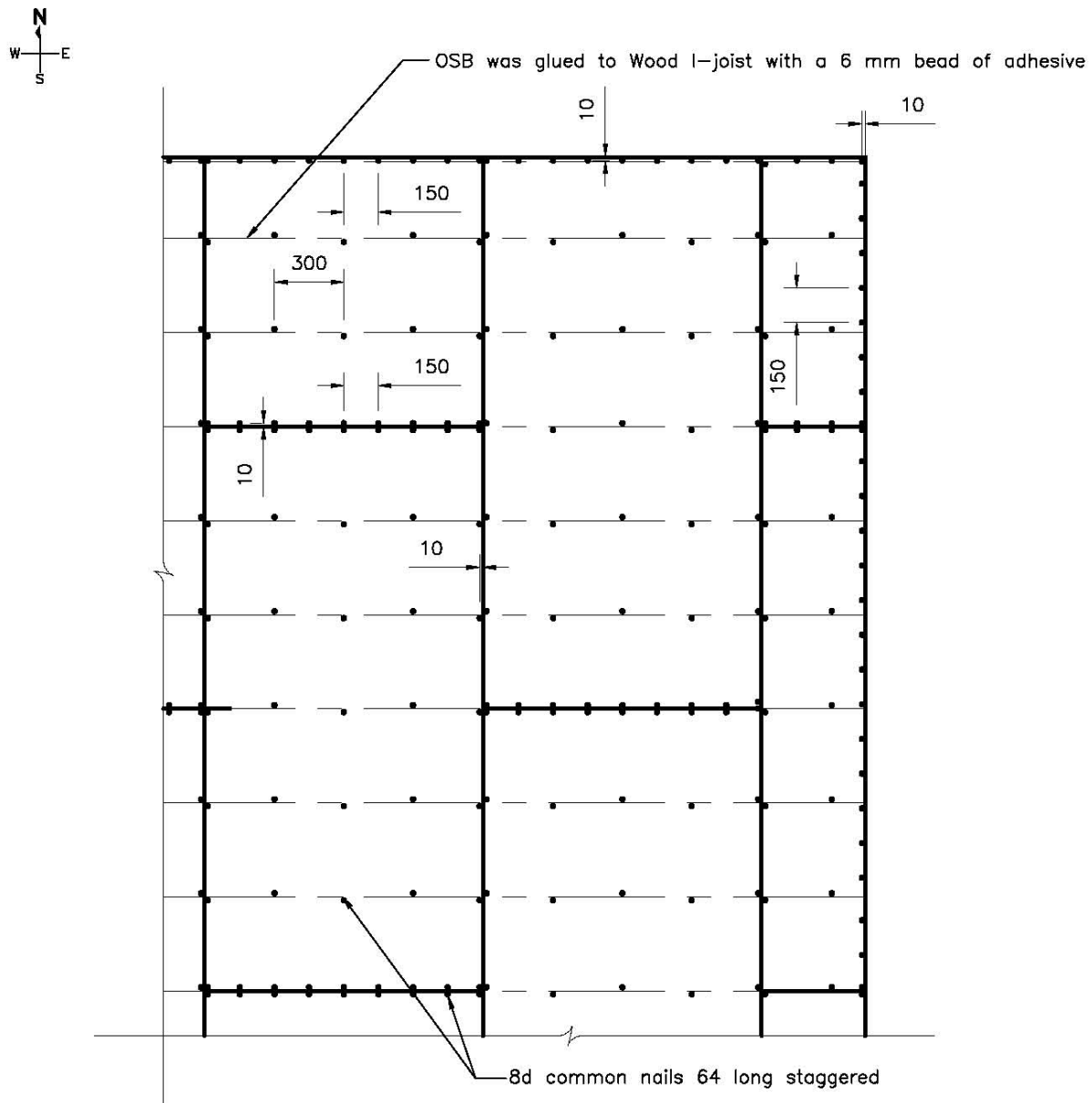
Figure 40. Subfloor nail pattern (Tests PF-03, PF-03B, PF-04 and PF-05) (all dimensions in mm)

Sixty-one Type K (20 gauge) chromel-alumel thermocouples, with a thickness of 0.91 mm, were used for measuring temperatures at a number of locations throughout the assembly. The thermocouples were located on the unexposed side and in the cavities of the assembly as shown in Figure 41 and Figure 42. These locations were chosen to monitor the conditions of the assembly at critical locations during the fire tests. The floor deflection was measured at 9 points on the unexposed surface of the test assembly at the locations shown in Figure 13.

Figure 41. Thermocouples locations (Tests PF-03, PF-03B, PF-04 and PF-05) (all dimensions in mm)

NRC·CNRC
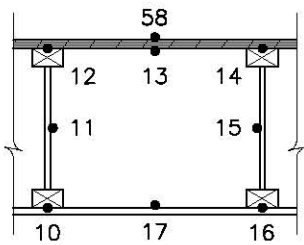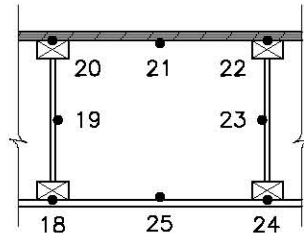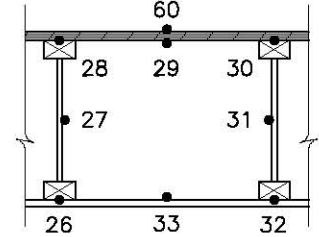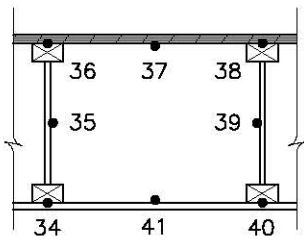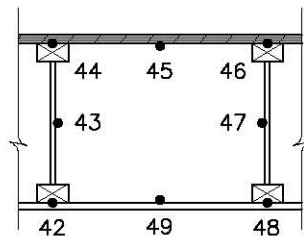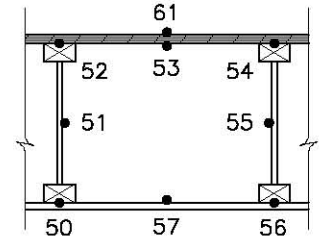
Figure 42. Thermocouples installed in the sections shown in Figure 41 (Test PF-04)

4.4.2   Fire Development in Basement

Figure 43 shows the temperature profiles measured in the basement fire room. The polyurethane foam used for the mock-up sofa dominated the initial fire growth. The temperatures at the window quickly reached 300°C and the noncombustible window covering panel was removed at 135 s. The temperatures at the 2.4 m height exceeded 600°C within 140-160 s, indicating that the fire room reached flashover conditions. The fast development of the fire from ignition to attainment of the first temperature peak was consistent with the experiments in Phase 1 of the FPH research. Following this initial stage of fire growth, the fire became wood-crib-dominated. There was a quick transition from a well-ventilated flaming fire to an under-ventilated fire. Figure 43 also shows the heat flux measured at the west wall (near the centre, 2.05 m above the floor). The maximum heat flux was 130 kW·m^{-2}, indicating post-flashover conditions in the fire room.
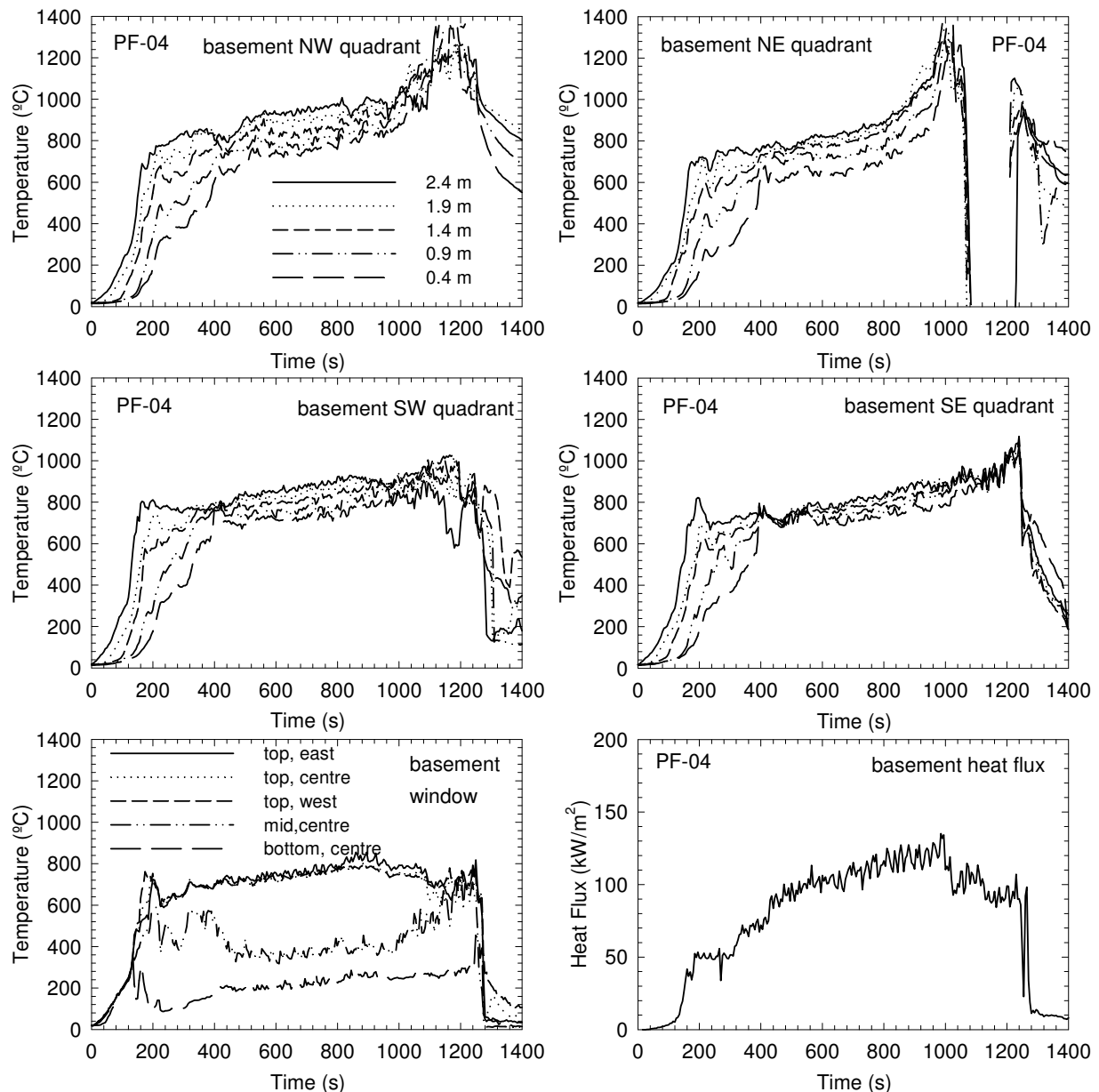
Figure 43. Temperatures and heat flux in the basement fire room in Test PF-04

4.4.3 Visual Obscuration

The optical density was measured at 0.9 and 1.5 m heights (simulating the height of the nose/mouth of an average height individual crawling and standing, respectively) above the floor on the first and second storeys. Table 13 shows the times to reach OD = 2 m^{-1}. Figure 44 shows the optical density-time profiles. It must be pointed out that the video records show no signs of decrease in the optical density after the first peak, indicating that the smoke density meters started the self purging cycle after that time. The smoke density meter has an operation temperature limit of 80°C in its gas chamber; when this temperature is reached, the flow is reversed to cool the chamber to protect the electronic components. The smoke meter resumes

operation once the gas chamber is cooled down below 80°C. In this experiment, the initial part of the curves (up to the first peaks) represents valid measurements. For the second storey, the second peaks near the end also represent valid measurements, as the self-purging cycle had ended.

Table 13. Time (in seconds) to the Smoke Optical Density Limit in Test PF-04

Test PF-04	1st storey SW quadrant	2nd storey corridor
OD =	2 m^{-1}	2 m^{-1}
1.5 m above floor	200	220
0.9 m above floor	265	265
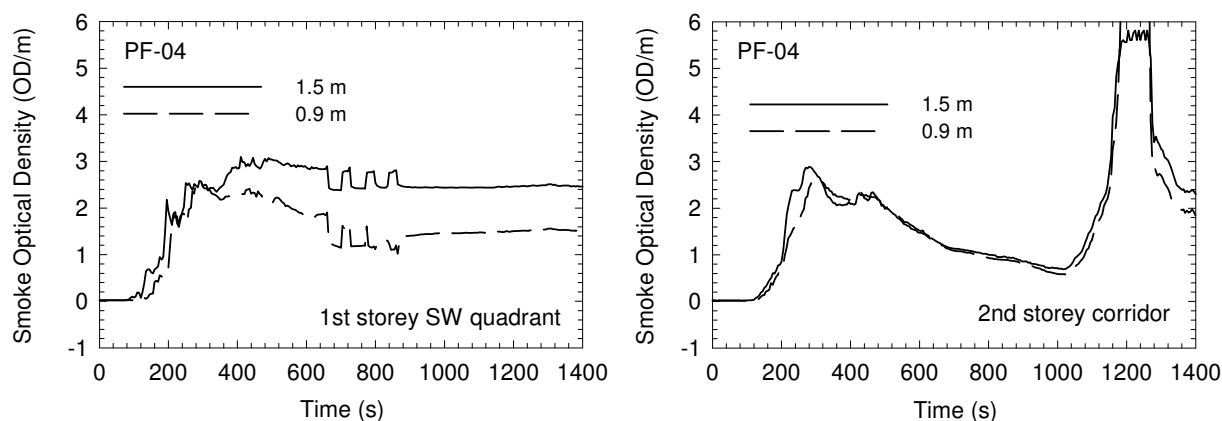
Figure 44. Smoke optical density measurements in Test PF-04

4.4.4   Gas Measurements and Analysis (CO, CO$_2$ and O$_2$)

Figure 45 shows the CO, CO$_2$ and O$_2$ concentration-time profiles measured at the southwest quarter point on the first storey and at the centre of the corridor on the second story during the experiment. Within approximately 400 s, oxygen was diminished to 11% and CO$_2$ increased to close to 10%, which could cause incapacitation and lead to loss of consciousness rapidly due to lack of oxygen alone or due to the CO$_2$ asphyxiant effect alone [22]. The concentrations were below 5% O$_2$ and above 15% CO$_2$ near the end of the experiment. The tenability analysis indicated that the toxic effect of CO would be capable of causing incapacitation at an earlier time than the effect of O$_2$ vitiation and the asphyxiant effect of CO$_2$. The times to reach the specified FED for exposure to O$_2$ vitiation, CO$_2$ and CO are shown in Table 14.

NRC·CNRC
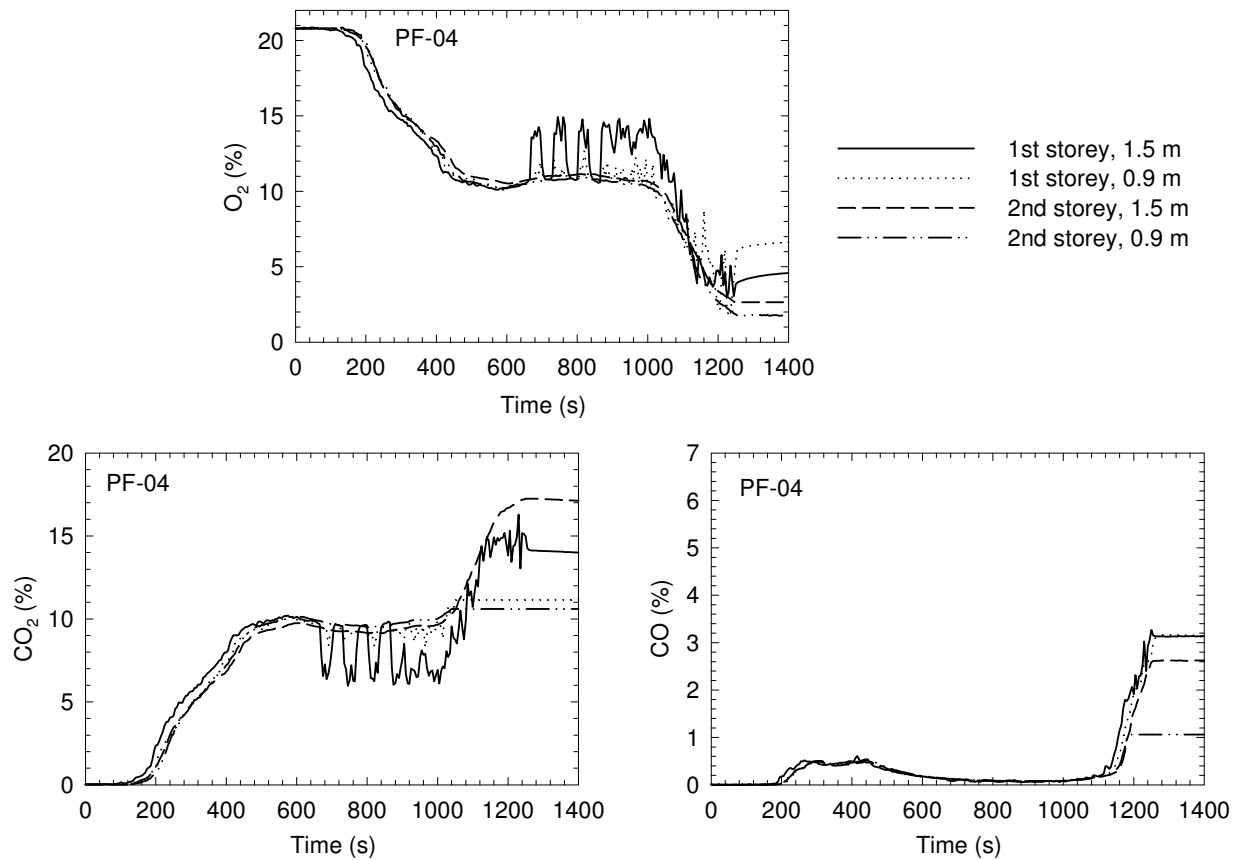
Figure 45. CO, CO_2 and O_2 concentrations in Test PF-04

Table 14. Time (in seconds) to the Specified FED for Exposure to O_2 Vitiation, CO_2 and CO in Test PF-04

Fractional Effective Dose	FED = 0.3	FED = 1.0
CO alone – 1st storey	340	1115
CO with CO_2 hyperventilation – 1st storey	270±20	365±40
Low O_2 hypoxia – 1st storey	600	1130
CO alone – 2nd storey corridor	370	1170
CO with CO_2 hyperventilation – 2nd storey corridor	295±20	400±50
Low O_2 hypoxia – 2nd storey corridor	670	1110
High CO_2 hypercapnia – 1st storey	435	565
High CO_2 hypercapnia – 2nd storey corridor	475	625

Note:
1. Values determined using concentrations at 1.5 m height.

NRC·CNRC

4.4.5 Temperature-Time Profiles on the Upper Storeys

Figure 46 and Figure 47 show temperature profiles measured on the first and second storeys during the experiment. The temperatures depended on the locations inside the test house. In the bedroom with the door closed, the temperatures never exceeded 60°C during the experiment.
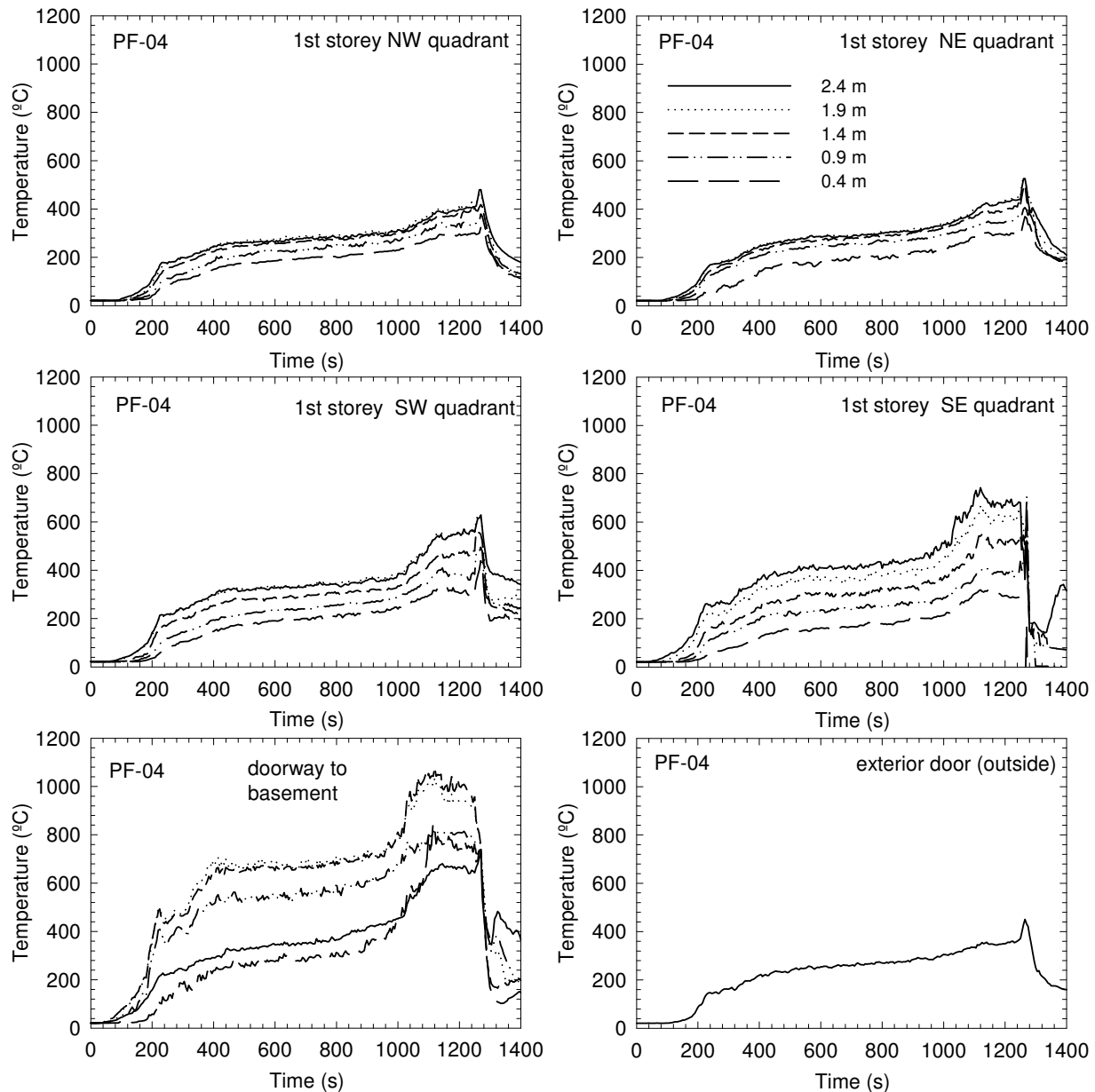
Figure 46. Temperatures on the first storey in Test PF-04

NRC·CNRC
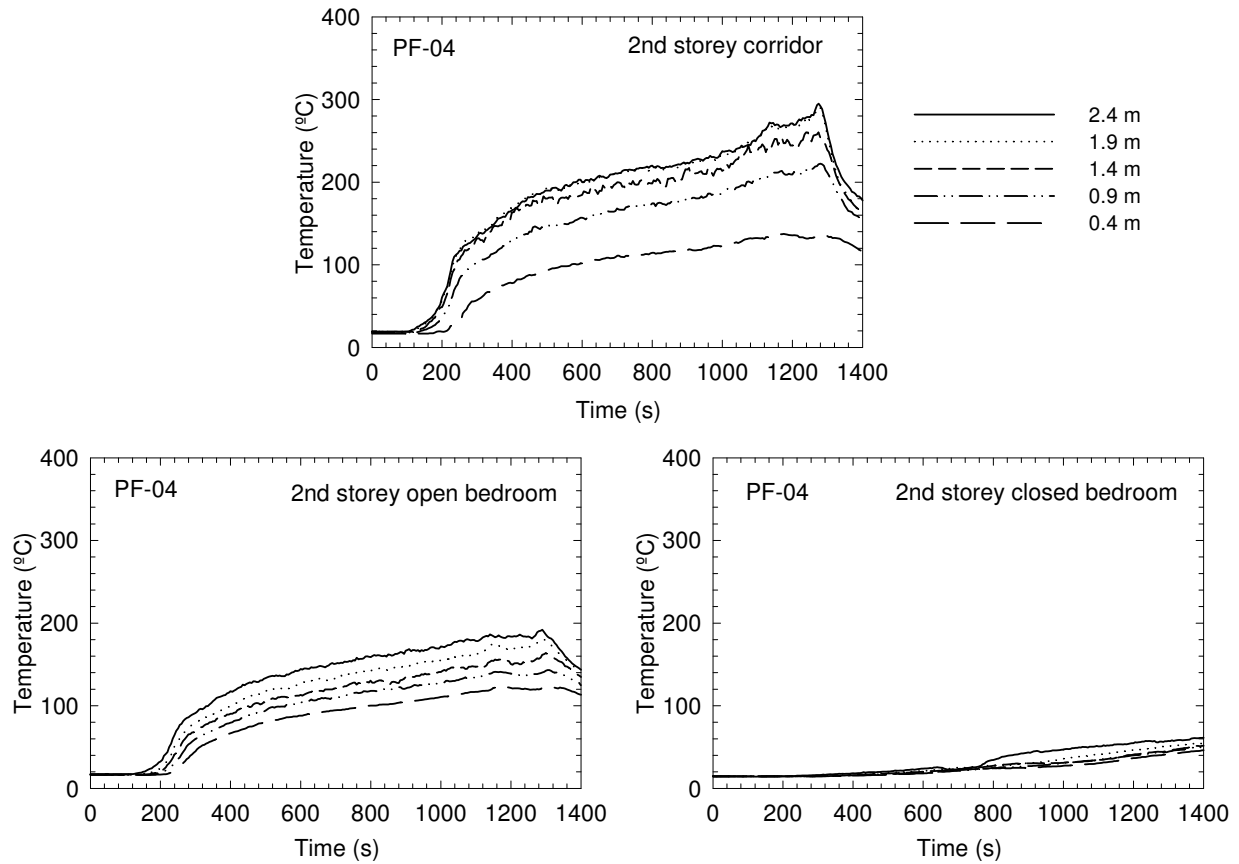
Figure 47. Temperatures on the second storey in Test PF-04

The convective heat exposure depended on the location in the test house. In the closed bedroom, heat exposure would not cause incapacitation. On the first storey, in the corridor or in the open bedroom on the second storey, the calculated times to incapacitation due to exposure to the convected heat are given in Table 15 for FED = 0.3 and 1. The calculated times to reach the heat incapacitation doses on the first storey were shorter than those for CO exposure; the time difference for FED to change from 0.3 to 1.0 due to the heat exposure was also shorter than that for CO exposure. In the corridor on the second storey, the calculated times to reach the incapacitation doses for heat exposure were similar to those for CO exposure.

Table 15. Time (in seconds) to Specified FED for Exposure to Convected Heat in Test PF-04

Fractional Effective Dose	FED = 0.3	FED = 1.0
1st storey SE quadrant	245	295
1st storey SW quadrant	235±5	280±10
1st storey NE quadrant	255	310
1st storey NW quadrant	250	310
2nd storey corridor	305±10	400±20
2nd storey open bedroom	485	705
2nd storey closed bedroom	not reached (FED < 0.03)	not reached (FED < 0.03)

Note:
1. Values determined using temperatures at 1.4 m height.

58

4.4.6 Estimation of Time to Incapacitation

Table 16 summarizes the results of tenability analysis with the estimated times to the onset of various conditions for Test PF-04. Smoke obscuration was the first hazard to arise. The calculated time for reaching the specific FED either due to the heat exposure or due to the CO exposure (exacerbated by CO_2-induced hyperventilation), whichever occurred first, is listed in Table 16. Heat exposure reached the specific FED on the first storey at times shorter than for CO exposure. On the second storey (in the corridor), CO exposure and heat exposure reached the specific FED at similar times. Note that for the closed bedroom on the second storey, based on the temperatures and the heat exposure calculation, the conditions in the closed bedroom would not reach untenable conditions.

Table 16. Summary of Estimation of Time to Specified FED and OD (in seconds) for Test PF-04

Test	$OD = 2\ m^{-1}$		$FED = 0.3$		$FED = 1$	
	1st storey	2nd storey	1st storey	2nd storey	1st storey	2nd storey
PF-04	200	220	**235±5**	*295±20*	**280±10**	*400±50*

Notes:
1. Values determined using the measurements at 1.5 m height (for gas concentrations and OD) or 1.4 m height (for temperatures);
2. The number with the *Italic* typeface represents the calculated time for reaching the CO incapacitation dose, while the number in **bold** typeface represents the calculated time for reaching the heat incapacitation dose, whichever occurred first.

4.4.7 Performance of Test Assembly

A floor system provides an egress route for occupants and its structural integrity directly impacts the safe evacuation of the occupants from the house during a fire emergency. During the fire experiment, the conditions of the test assembly were monitored.

Figure 48 shows temperatures in the cavities of the test assembly. The thermocouples installed in the six sections of the floor cavities monitored the temperatures inside the cavities and provided an indication of the effectiveness of gypsum board protection for the test assembly. The moment that the temperatures in the floor cavities approached the fire room temperature indicates the loss of the gypsum board membrane protection for the floor structure. This happened around 800 – 1100 s depending on the position. This was accompanied by a slow but regular increase in room temperatures in the basement, which was likely a result of an increase in the burning rate due to the additional fuel from ignited areas of the floor assembly that were left exposed to the fire as portions of the gypsum ceiling fell off. Visual observation confirmed that gypsum board pieces started falling from the centre of the ceiling shortly after 800 s, followed by larger gypsum board pieces falling. Then flame started to involve the joists and subfloor.

NRC·CNRC
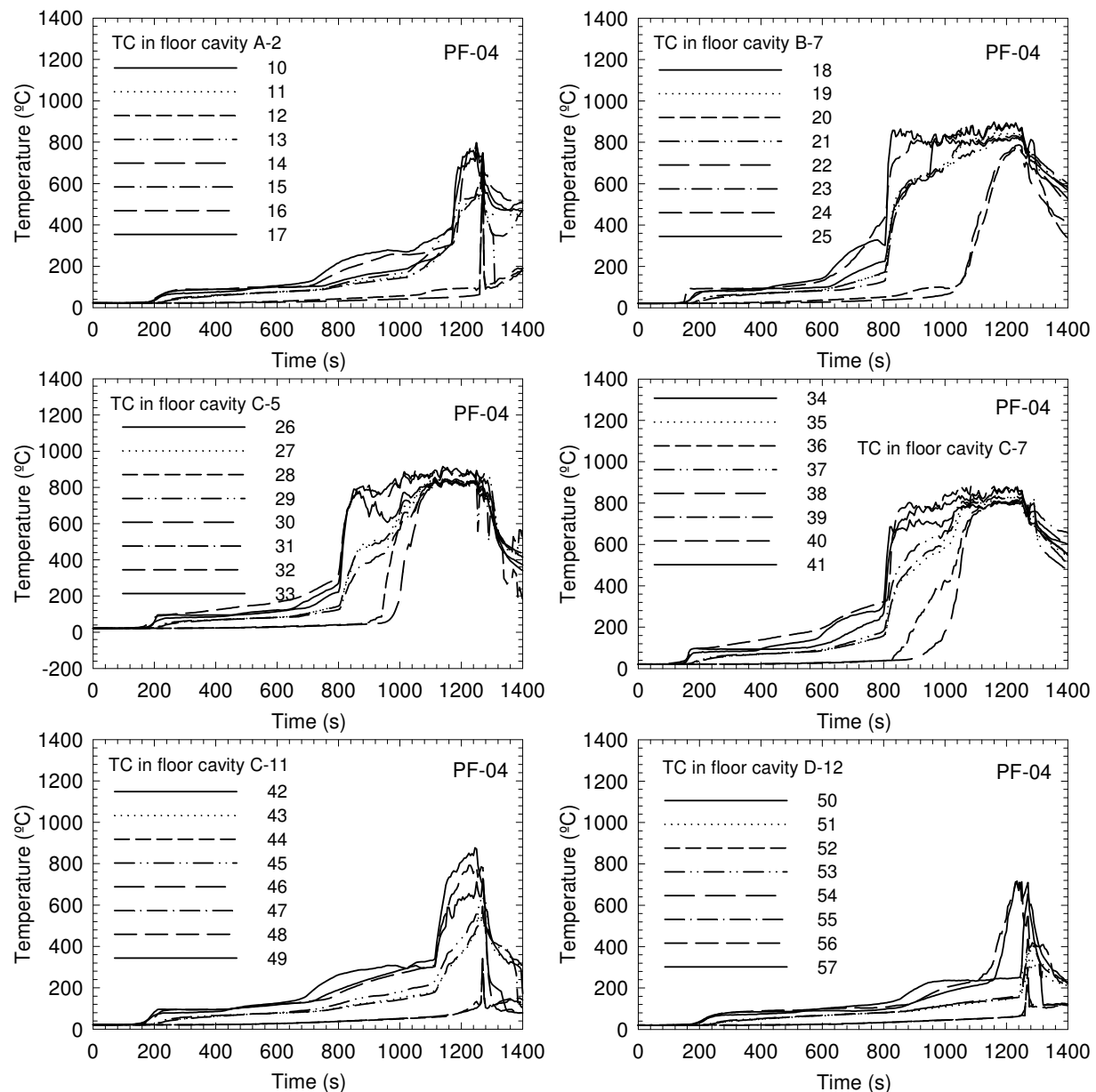
Figure 48. Temperatures in floor cavities in Test PF-04

Figure 49 shows results of the measurements using thermocouples, flame-sensing devices and deflection devices on the unexposed side of the test assembly on the first storey. There was a malfunction of the devices for the floor deflection measurements but the flame sensing and temperature measurements provided consistent data for structural performance of the test assembly.

The temperature measurements by nine thermocouples under insulation pads on top of the subfloor (on the first storey) are similar to the measurements in the standard fire-resistance test with respect to thermocouple type, installation and layout [29]. Rapid temperature rises occurred at 1240 s, indicating that the test assembly was significantly breached. The

subsequent rapid decrease in temperature was due to the termination of the experiment by extinguishing the fire with water. At the same time, four bare thermocouples and the flame-sensing device at the central tongue-and-groove joint on the unexposed side of the test assembly also captured sharp temperature rise and flame signal, respectively.

Visual observation through the window opening of the fire room confirmed that the test assembly collapsed at 1247 s. The test assembly collapsed into the basement in the form of a "V" shape with wood I-joists broken at the mid-points.
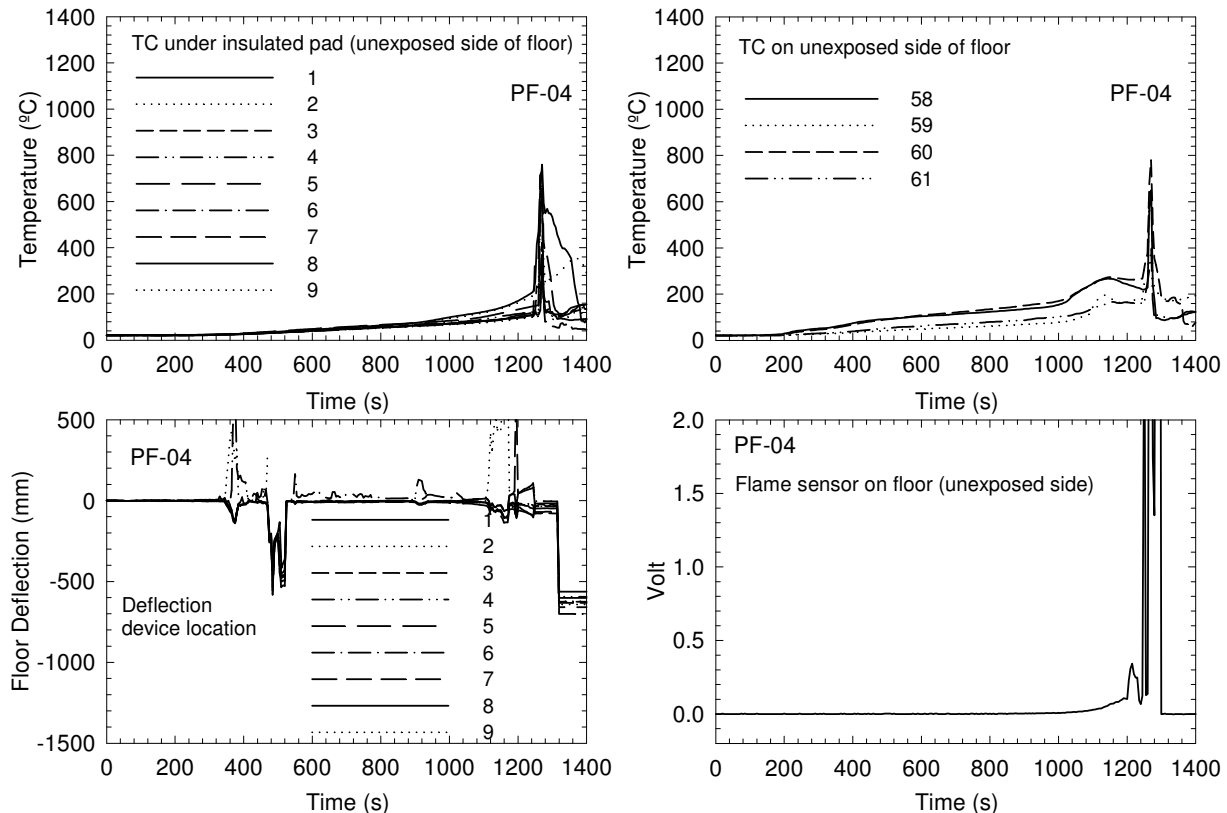
Figure 49. Temperatures, deflections and flame sensor on the unexposed side of the assembly on the first storey in Test PF-04

4.4.8   Sequence of Events

Table 17 summarizes the chronological sequence of the fire events in Test PF-04 — fire initiation, smoke alarm activation, onset of untenable conditions, and structural failure of the test assembly. Smoke obscuration was the first hazard to arise. It must be pointed out that people with impaired vision could become disoriented earlier at an optical density lower than 2 m^{-1}. The incapacitation conditions were reached shortly after smoke obscuration. The structural failure of the test assembly occurred well after the untenable conditions were reached.

For comparison purposes, Table 17 also shows data from the test conducted in Phase 1 using the same floor structure but no gypsum board protection (UF-03). The data indicates that tenability conditions are improved slightly whilst the structural performance is improved significantly with the protected ceiling/floor assembly.

61

NRC·CNRC

Table 17. Summary of Sequence of Events in Test PF-04 (in seconds)

Assembly Type	Test	First Alarm	OD = 2 m^{-1}	FED=0.3-1 1st storey	FED=0.3-1 2nd storey	Structural Failure
Gypsum board protected wood I-joists	PF-04	30	200-220	**235-280**	*295-400*	1247*
Unprotected wood I-joists	UF-03	48	183	**205-213**	*225-247*	490

Notes:
1. Values determined using the measurements at 1.5 m height (for gas concentrations and OD) or 1.4 m height (for temperatures);
2. The number with the *Italic* typeface represents the calculated time for reaching the CO incapacitation dose, while the number in **bold** typeface represents the calculated time for reaching the heat incapacitation dose, whichever occurred first;
3. *Values of the structural failure time of the test assemblies determined by visual observation;
   a. A single-point temperature rise of 180°C occurred on the unexposed side of the test assembly at 1240 s;
   b. A large voltage spike detected using the flame-sensing device at 1265 s.

4.5 Wood I-Joist Assembly with Suspended Ceiling – Test PF-05

Test PF-05 was conducted using a wood I-joist assembly with suspended ceiling in the basement fire room. Except that the exposed side (basement side) had a different protection measure, the PF-05 assembly was identical to those used in Tests PF-03, PF-03B and PF-04. Materials for the suspended ceiling were selected based on a survey of available products in local stores and on intermediate-scale fire tests.

4.5.1 Selection of Materials for Suspended Ceiling

A survey was conducted on available products for suspended ceilings in local stores in Ottawa. Three types of ceiling panels made of mineral fibre, fibreglass and wood fibre were available. The suspension systems included both metal and plastic tracks. The most commonly used metal tracks were made of galvanized steel. There were also aluminum and stainless steel tracks. The plastic tracks were made of PVC. Staples were normally used with wood fibre ceiling tiles.

In order to select ceiling materials for use as a protection measure for the test assembly in the full-scale fire experiment, a series of intermediate-scale fire experiments were conducted for different ceiling materials using a 1.33 m x 1.94 m horizontal furnace. A full description of the intermediate-scale furnace facility is provided by Sultan et al. [30].

The test assemblies used for the intermediate scale tests were all constructed using a 1260 mm x 1950 mm lightweight steel frame. This frame consisted of four 203-mm-deep steel C-joists spaced 406 mm on centre. The steel joists were fastened together using two lengths of 203 mm x 1260 mm steel rim tracks. A single 12.7-mm-thick OSB panel was used as the subfloor for each assembly. Wood strapping was installed every 305 mm perpendicular to the joists on the underside of the assemblies. Ceiling materials were installed under the wood strapping.

NRC·CNRC

The ceiling protection measures used for the intermediate-scale test assemblies included fibreglass ceiling panels, wood fibre ceiling tiles, mineral fibre panels and regular gypsum board. The fibreglass panels (610 mm x 1220 mm x 15 mm thick) were inserted into the plastic tracks that were fastened to the wood strapping. The wood fibre ceiling tiles (305 mm x 305 mm x 12 mm thick with tongue and groove) were stapled directly to the wood strapping. The mineral fibre panels (610 mm x 1220 mm x 13 mm thick) were suspended in metal tracks under the wood strapping. Regular gypsum board was fastened to the wood strapping as a protection measure for the assembly in the intermediate scale test.

Four dual-element Chromel-Alumel K-type thermocouple probes were used to measure the temperature inside the furnace chamber. These furnace thermocouples were located approximately 150 mm below the underside of the test assembly. The average temperature measured using these four thermocouples was used to control the furnace. The temperature in the furnace initially followed the standard time-temperature curve given in CAN/ULC S101 [29]. Once the test assembly ignited, the temperature in the furnace varied relative to the standard time-temperature curve.

Nine thermocouples were installed in the floor cavities of each test assembly at 3 locations. At each location, 3 thermocouples were used to monitor the temperatures in the cavity: temperature on the OSB surface (underside, facing cavity), temperature in the middle of the cavity, and temperature on the ceiling panel inner surface (facing cavity).

The temperatures inside the furnace and inside the central cavities of the test assemblies as well as the standard S101 time-temperature curve are shown in Figure 50. The time at which the temperatures in the floor cavity increased abruptly is taken as an indication of flames overcoming the ceiling membrane and entering the floor cavity. For the test assemblies with the fibreglass panels, mineral fibre panels and regular gypsum board, the time at which the furnace temperatures diverged from the standard time-temperature relationship is taken as an indication of the ignition time for the OSB subfloor. For the test assembly with the wood fibre tiles, the time at which the furnace temperature diverged from the standard time-temperature relationship is taken as an indication of the ignition time for the wood fibre tiles since they are combustible; the ignition time for the OSB subfloor is when the furnace temperature increased again after the initial peak.

Table 18 shows the times for flame entering the floor cavities and ignition of the OSB subfloor. The results of an intermediate-scale test assembly with the same OSB subfloor and steel framing but without any ceiling membrane [28], are also shown. The primary parameter that was studied using the intermediate-scale tests was the protection time offered by different ceiling materials. The protection time is calculated as the difference in the OSB ignition times between the protected and unprotected test assemblies, which are also shown in the table. Based on this parameter, it was decided to use the mineral fibre panels with metal tracks as suspended ceiling in the construction of the full-scale test assembly.

NRC·CNRC

Table 18. Intermediate Scale Furnace Results for Ceiling Materials (time in seconds)

Assembly	Hot Gases Cavity* (s)	OSB Ignited (s)	Protection Time** (s)
Unprotected	0	240	0
Fibreglass ceiling panel in plastic track	185	385	145
Wood fibre ceiling tile	250	340	100
Suspended mineral fibre ceiling panel in metal track	580	605	365
Gypsum board	1195	1270	1030

Notes:
1. *Also an estimate of protection time;
2. **Values determined using OSB subfloor ignition: OSB subfloor ignition time of protected assembly minus OSB ignition time of unprotected assembly.
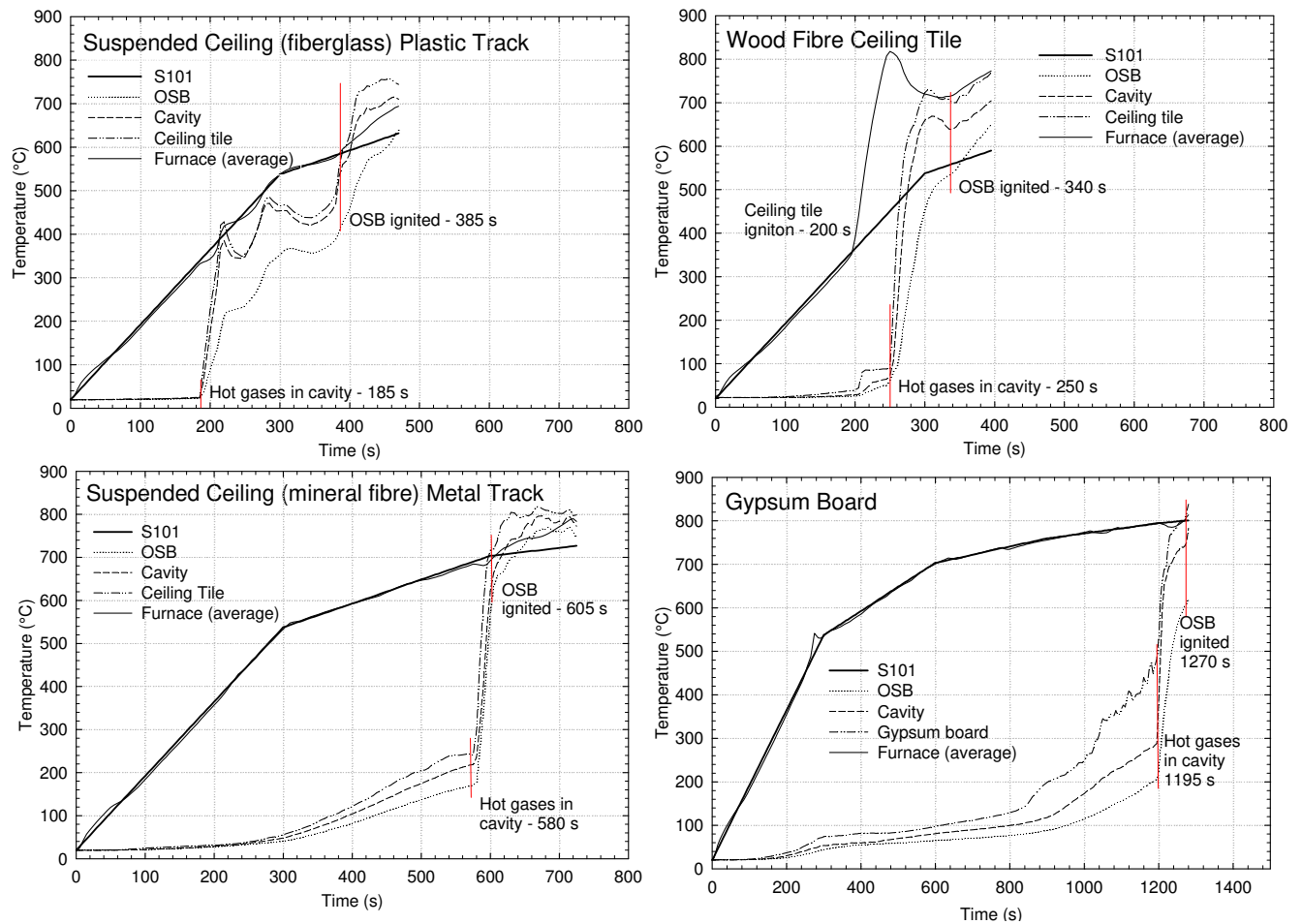
Figure 50. Temperature profiles in intermediate-scale tests for selection of suspended ceiling

NRC·CNRC

4.5.2 Construction Details of the Test Assembly

The test assembly used in Test PF-05 was identical to those used in Tests PF-03, PF-03B and PF-04 conducted using wood I-joists (see Figure 37 and Figure 40) except that the basement side had different protection measures. In Test PF-05, a suspended ceiling with the mineral fibre panels on metal track was installed below the test assembly in the basement fire room. The installation of the suspended ceiling followed the recommendations of the manufacturer. The mineral fibre panels were 12.7 mm thick, with a full-panel size of 0.6 x 1.2 m. Figure 51 and Figure 52 show details of the suspended ceiling layout, end connection and the supporting beams.
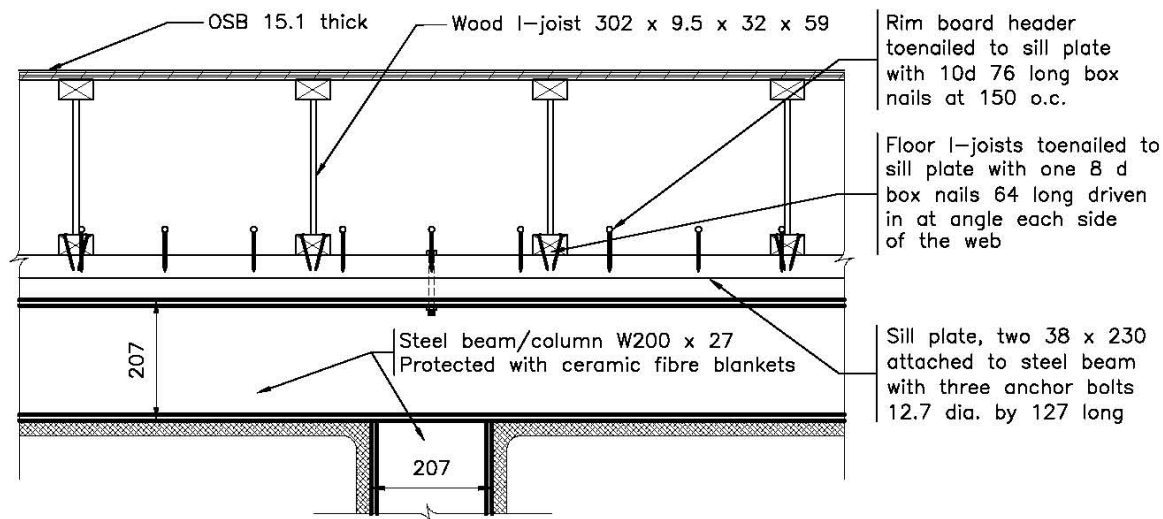
End connection details (East view)
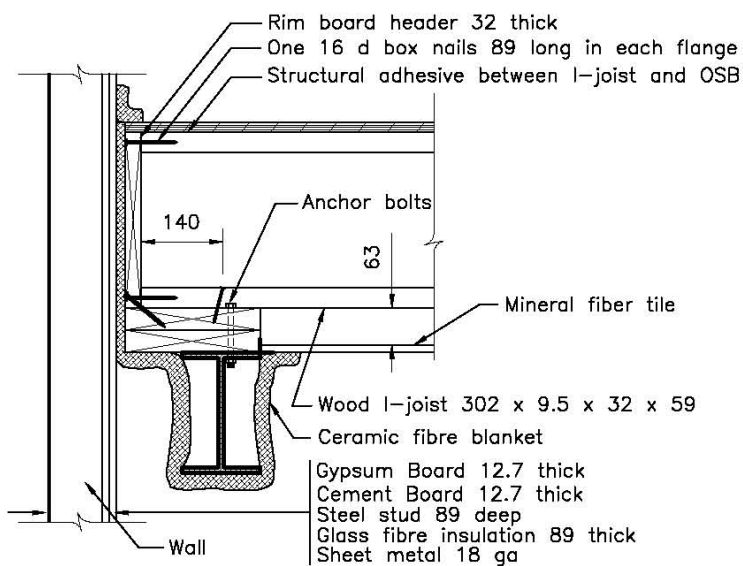
End connection details (North view)

Figure 51. Details of end connection and supports for Test PF-05 (suspended ceiling) (all dimensions in mm)

NRC·CNRC
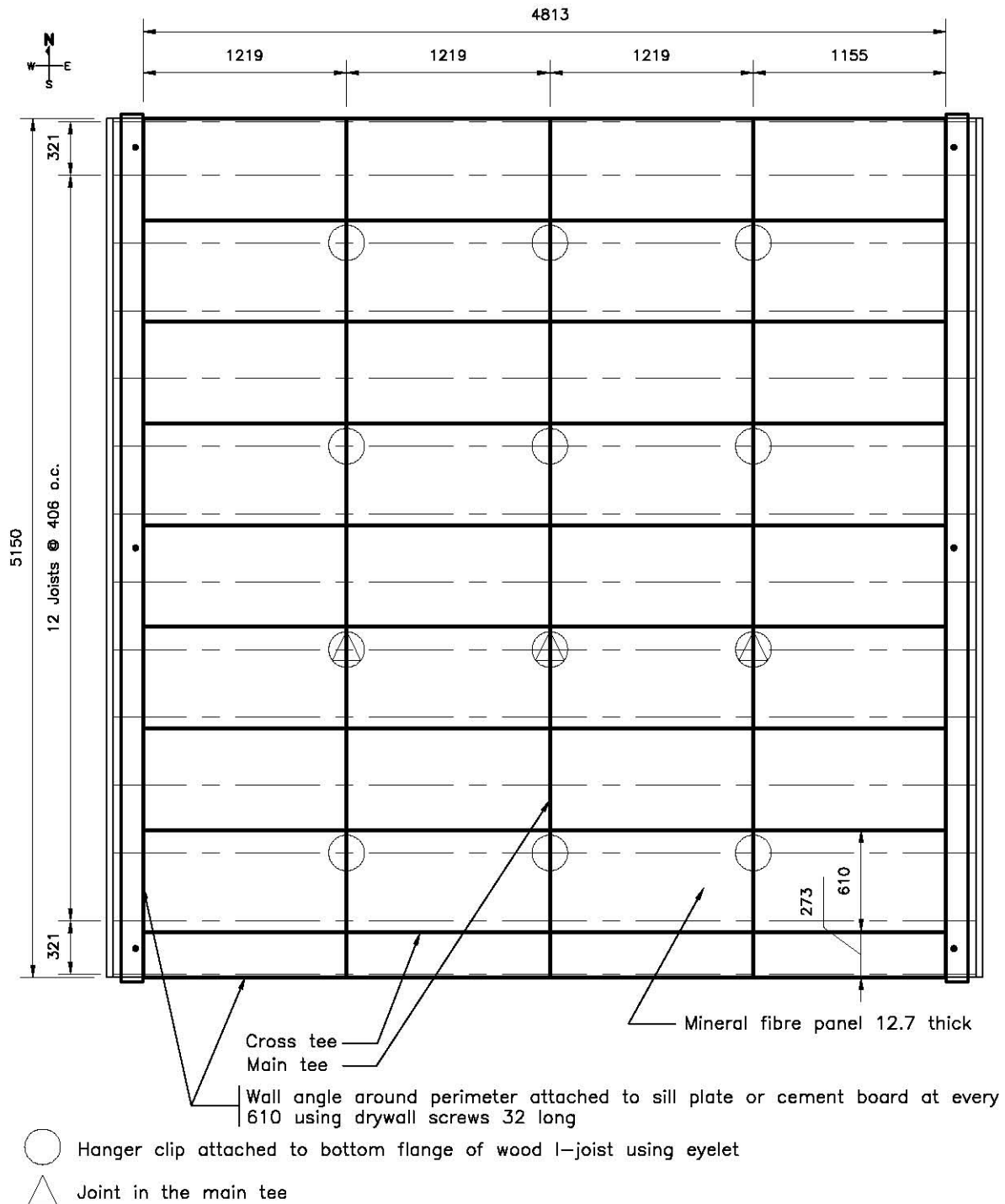
Figure 52. Mineral fibre panel layout as suspended ceiling (Test PF-05) (all dimensions in mm)

NRC·CNRC

The thermocouples for measuring temperatures throughout the assembly were located on the unexposed side and in the cavities of the assembly as shown in Figure 41 and Figure 53.
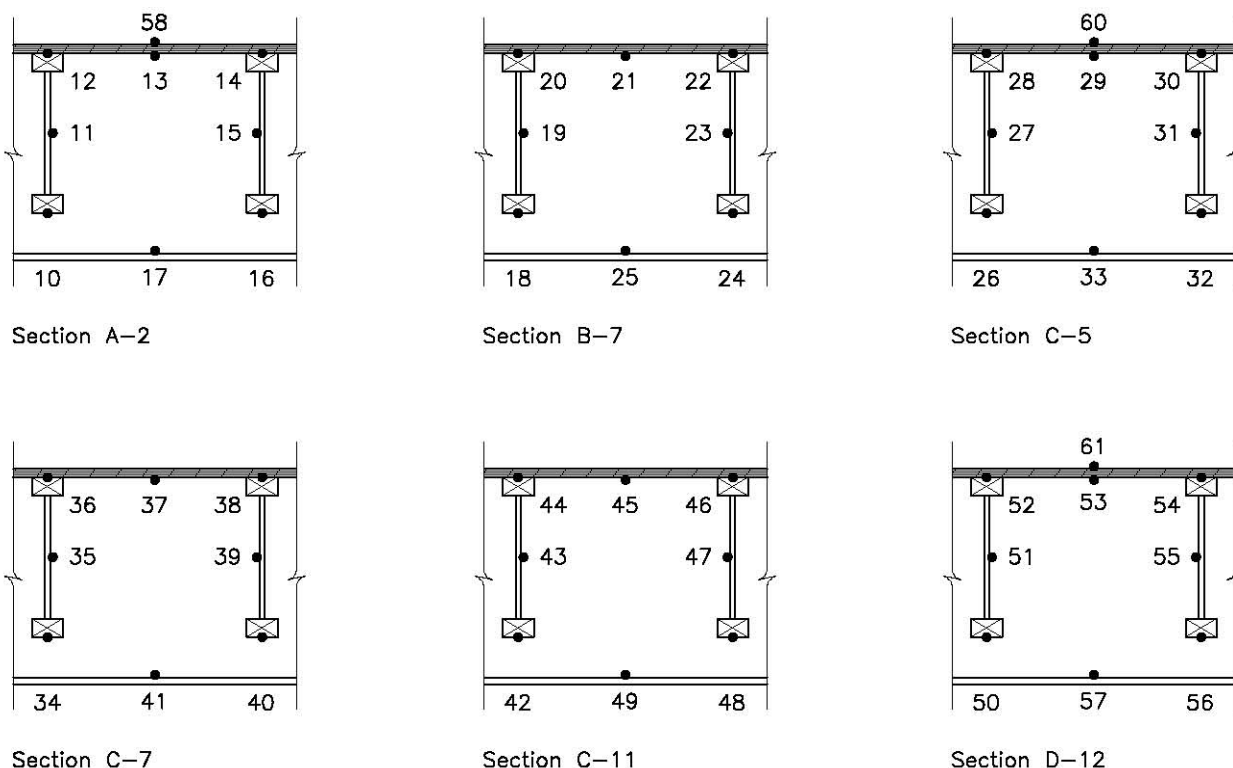
Figure 53. Thermocouples installed in the sections shown in Figure 41 (Test PF-05)

4.5.3 Fire Development in Basement

Figure 54 shows the temperature profiles measured in the basement fire room. The polyurethane foam used for the mock-up sofa dominated the initial fire growth. The temperatures at the window quickly reached 300°C and the noncombustible window covering panel was removed at 102 s. The temperatures at the 2.4 m height exceeded 600°C within 120-140 s, indicating that the fire room reached flashover conditions. The fast development of the fire from ignition to attainment of the first temperature peak was consistent with the experiments in Phase 1 of FPH research. Following this initial stage of fire growth, the fire became wood-crib-dominated. There was a quick transition from a well-ventilated flaming fire to an under-ventilated fire. Figure 54 also shows the heat flux measured at the west wall (near the centre, 2.05 m above the floor). The maximum heat flux was 105 kW·m^{-2}, indicating post-flashover conditions in the fire room.

NRC·CNRC
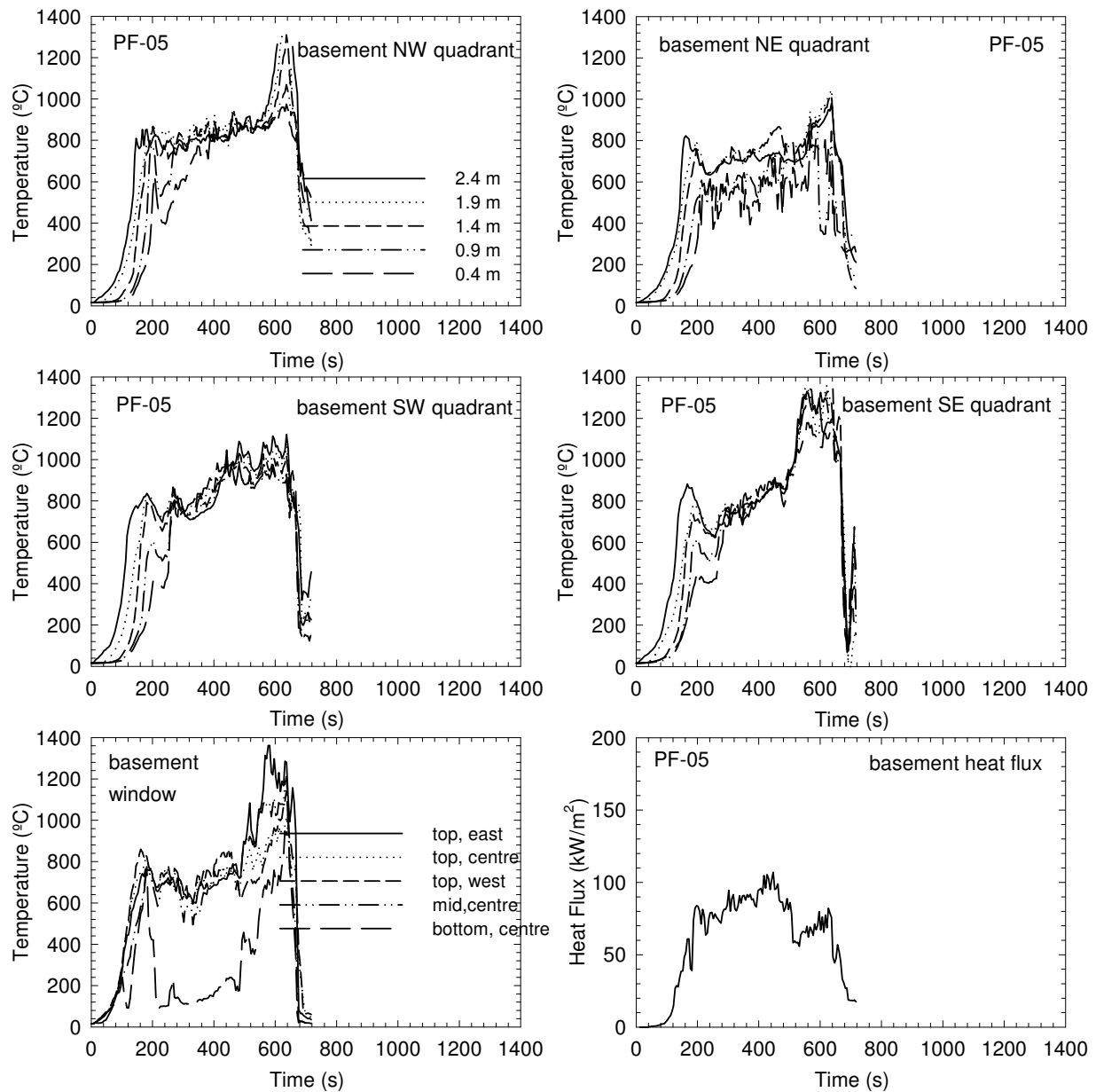
Figure 54. Temperatures and heat flux in the basement fire room in Test PF-05

4.5.4   Visual Obscuration

The optical density was measured at 0.9 and 1.5 m heights (simulating the height of the nose/mouth of an average height individual crawling and standing, respectively) above the floor on the first and second storeys. Table 19 shows the times to reach OD = 2 m^{-1}. Figure 55 shows the optical density-time profiles. It must be pointed out that the video records show no signs of decrease in the optical density after the first peak, indicating that the smoke density meters started the self-purging cycle. The smoke density meter has an operation temperature limit of 80°C in its gas chamber; when this temperature is reached, the flow is reversed to cool

68

the chamber to protect the electronic components. The smoke meter resumes operation once the gas chamber is cooled down below 80°C. In this experiment, the initial part of the curves (up to the first peaks) represents valid measurements. The second peaks near the end also represent valid measurements, as the self-purging cycle had ended.

Table 19. Time (in seconds) to the Smoke Optical Density Limit in Test PF-05

Test PF-05	1st storey SW quadrant	2nd storey corridor
OD =	**2 m^{-1}**	**2 m^{-1}**
1.5 m above floor	192	222
0.9 m above floor	212	232
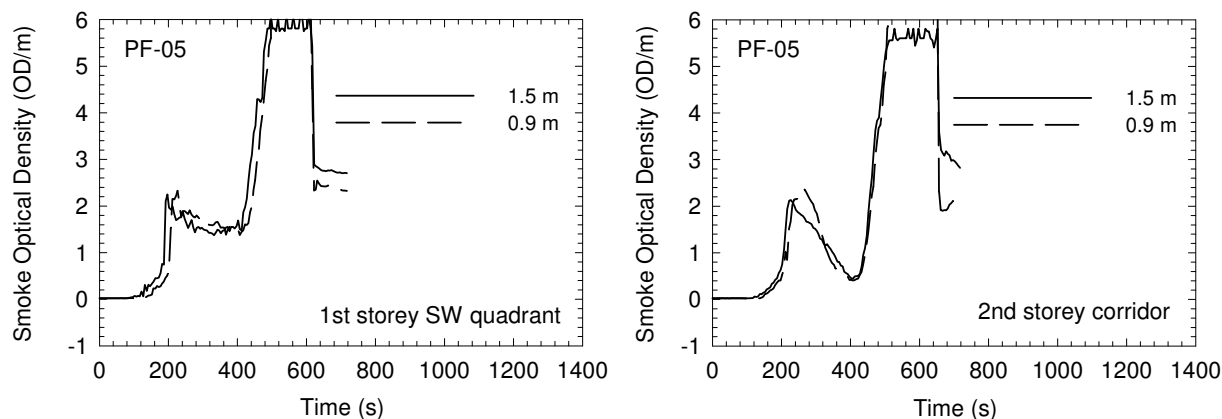
Figure 55. Smoke optical density measurements in Test PF-05

4.5.5 Gas Measurements and Analysis (CO, CO$_2$ and O$_2$)

Figure 56 shows the CO, CO$_2$ and O$_2$ concentration-time profiles measured at the southwest quarter point on the first storey and at the centre of the corridor on the second story during the experiment. Within approximately 350 s, oxygen was diminished to below 10% and CO$_2$ increased to above 10%, which could cause incapacitation and lead to rapid loss of consciousness due to lack of oxygen alone or due to the CO$_2$ asphyxiant effect alone [22]. The concentrations were below 5% O$_2$ and above 16% CO$_2$ near the end of the experiment. The tenability analysis indicated that the toxic effect of CO would be capable of causing incapacitation at an earlier time than the effect of O$_2$ vitiation and the asphyxiant effect of CO$_2$. The times to reach the specified FED for exposure to O$_2$ vitiation, CO$_2$ and CO are shown in Table 20.

NRC·CNRC
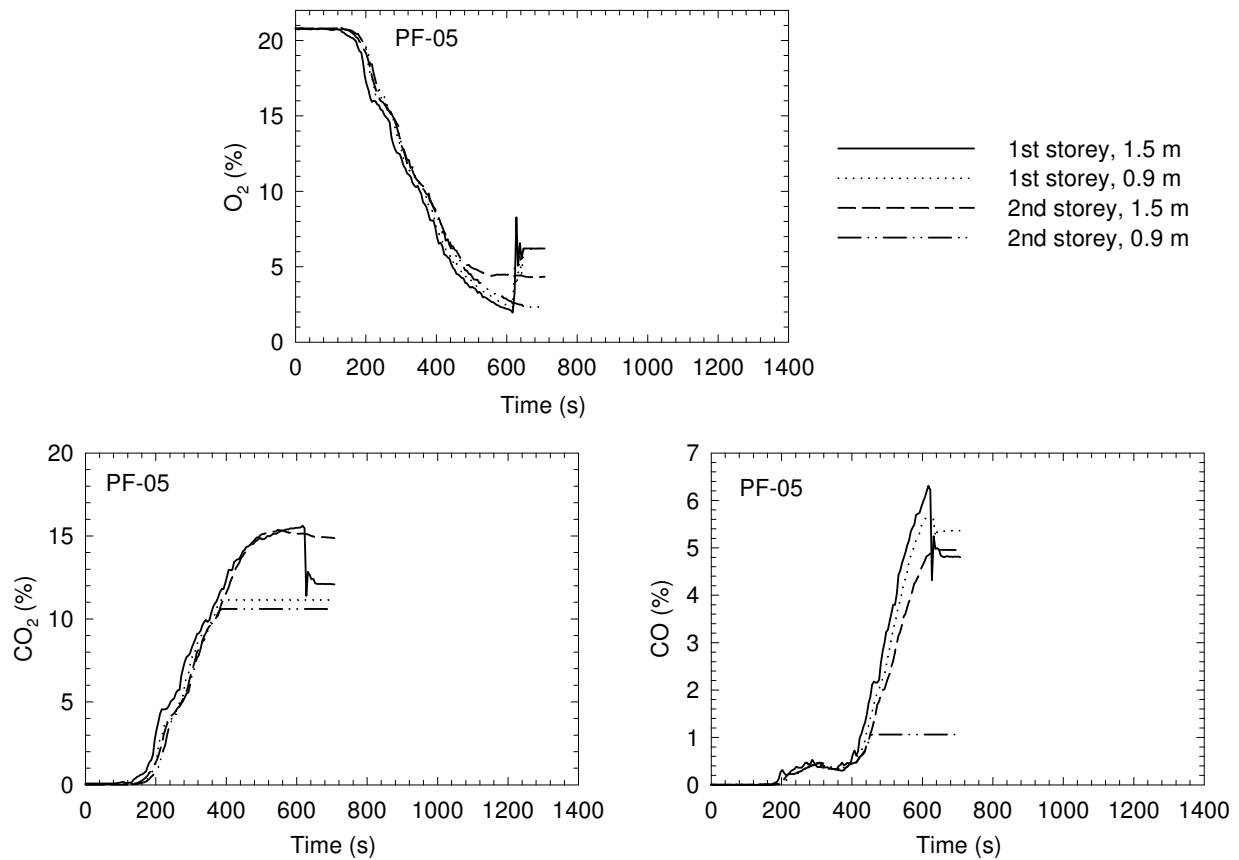
Figure 56. CO, CO_2 and O_2 concentrations in Test PF-05

Table 20. Time (in seconds) to the Specified FED for Exposure to O_2 Vitiation, CO_2 and CO in Test PF-05

Fractional Effective Dose	FED = 0.3	FED = 1.0
CO alone – 1st storey	362	487
CO with CO_2 hyperventilation – 1st storey	267±20	337±40
Low O_2 hypoxia – 1st storey	402	447
CO alone – 2nd storey corridor	392	512
CO with CO_2 hyperventilation – 2nd storey corridor	292±20	367±40
Low O_2 hypoxia – 2nd storey corridor	427	477
High CO_2 hypercapnia – 1st storey	347	402
High CO_2 hypercapnia – 2nd storey corridor	372	422

Note:
1. Values determined using concentrations at 1.5 m height.

NRC·CNRC

4.5.6   Temperature-Time Profiles on the Upper Storeys

Figure 57 and Figure 58 show temperature profiles measured on the first and second storeys during the experiment. The temperatures depended on the locations inside the test house. In the bedroom with the door closed, the temperatures never exceeded 60°C during the experiment.
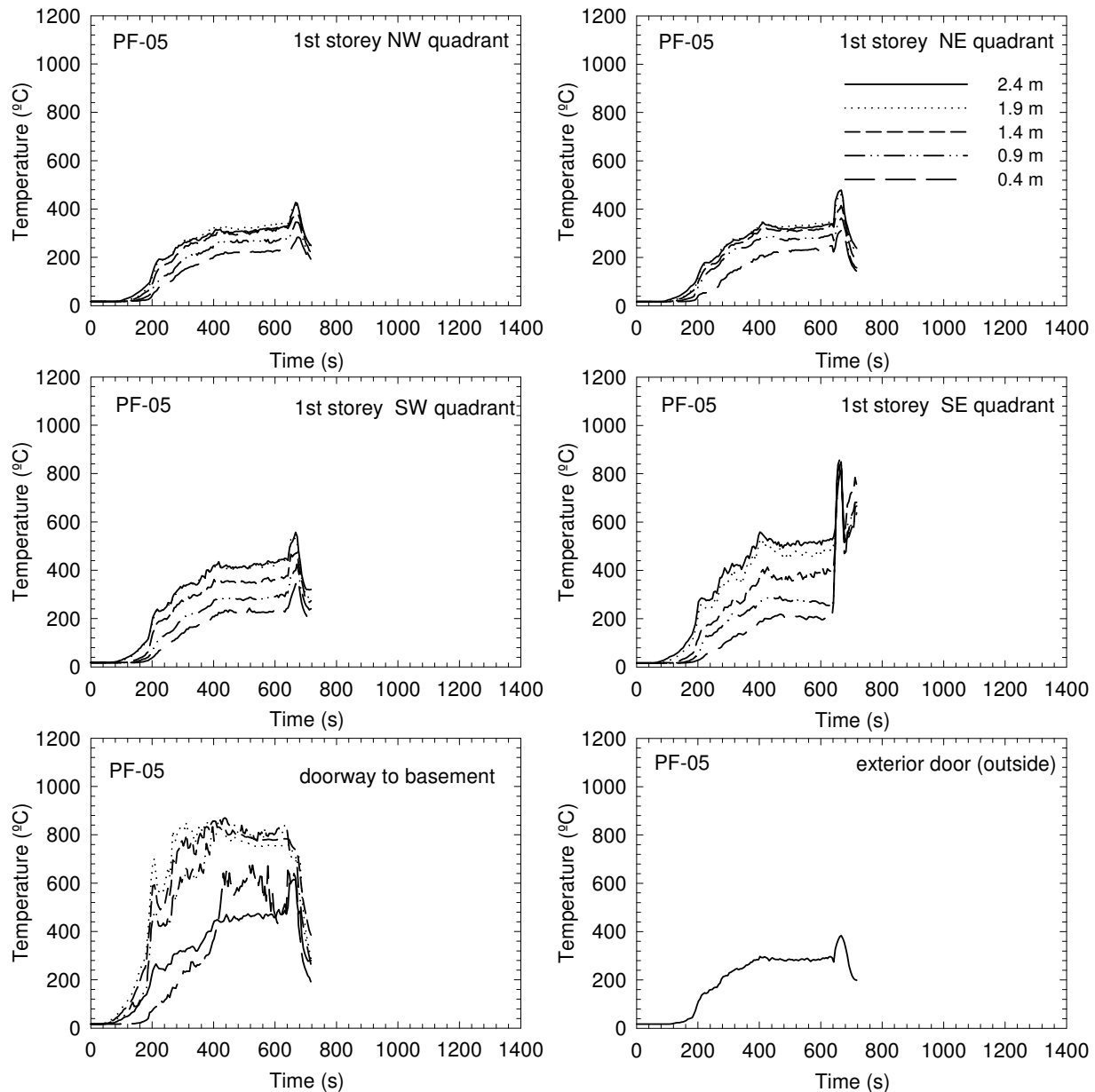
Figure 57. Temperatures on the first storey in Test PF-05
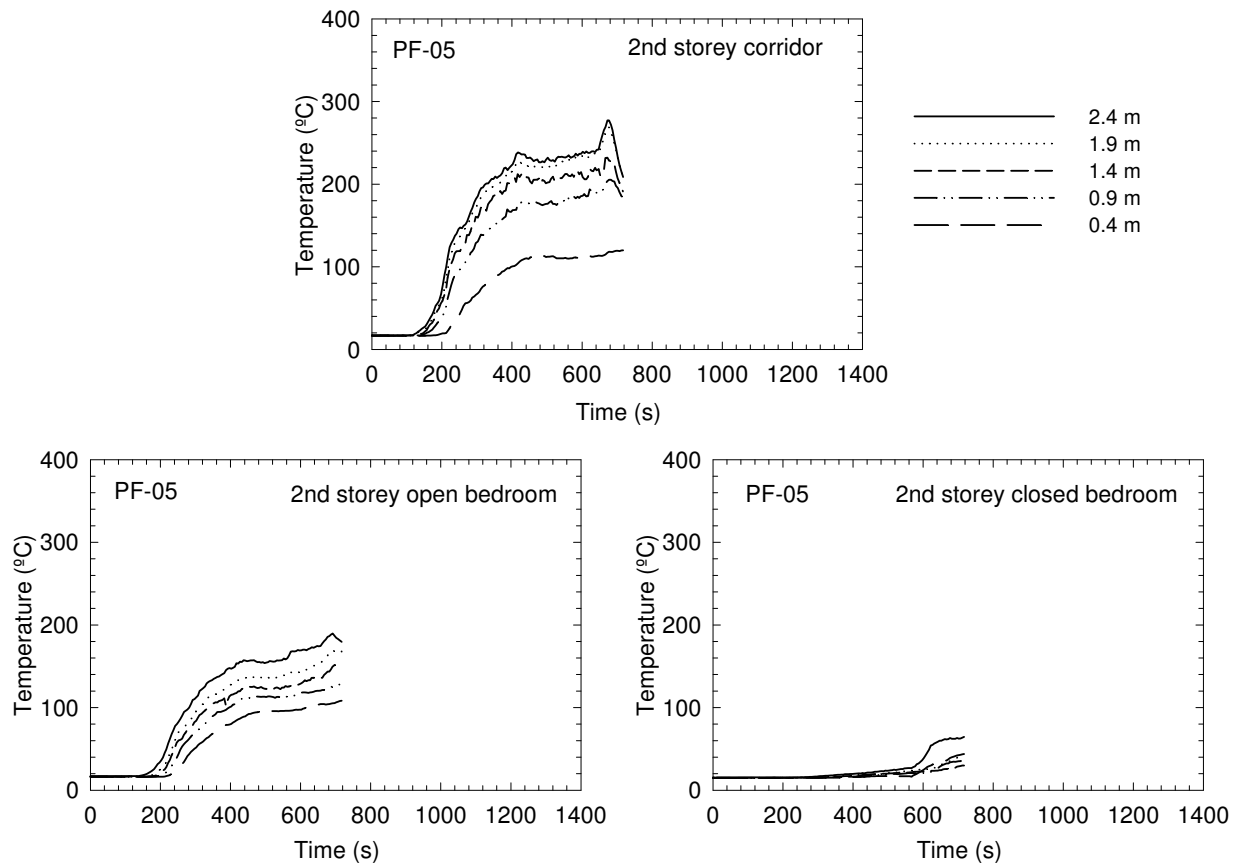
Figure 58. Temperatures on the second storey in Test PF-05

The convective heat exposure depended on the location in the test house. In the closed bedroom, heat exposure would not cause incapacitation. On the first storey, in the corridor or in the open bedroom on the second storey, the calculated times to incapacitation due to exposure to the convected heat are given in Table 21 for FED = 0.3 and 1. The calculated times to reach the heat incapacitation doses on the first storey were shorter than those for CO exposure; the time difference for FED to change from 0.3 to 1.0 due to the heat exposure was also shorter than that for CO exposure. In the corridor on the second storey, the calculated times to reach the incapacitation doses for heat exposure were also slightly shorter than those for CO exposure.

Table 21. Time (in seconds) to the Specified FED for Convected Heat in Test PF-05

Fractional Effective Dose	FED = 0.3	FED = 1.0
1st storey SE quadrant	227	267
1st storey SW quadrant	220±5	255±10
1st storey NE quadrant	237	282
1st storey NW quadrant	237	282
2nd storey corridor	282±10	342±20
2nd storey open bedroom	407	572
2nd storey closed bedroom	not reached (FED < 0.01)	not reached (FED < 0.01)

Note:
1. Values determined using temperatures at 1.4 m height.

NRC·CNRC

4.5.7 Estimation of Time to Incapacitation

Table 22 summarizes the results of tenability analysis with the estimated times to the onset of various conditions for Test PF-05. Smoke obscuration was the first hazard to arise. The calculated time for reaching the specific FED either due to the heat exposure or due to the CO exposure (exacerbated by CO_2-induced hyperventilation), whichever occurred first, is listed in Table 22. Heat exposure reached the specific FED at the times shorter than for CO exposure on the first storey and in the corridor on the second storey. The time difference for heat exposure and CO exposure to reach the specific FED was not significant. Note that for the closed bedroom on the second storey, based on the temperatures and the heat exposure calculation, the conditions in the closed bedroom would not reach untenable conditions.

Table 22. Summary of Estimation of Time to Specified FED and OD (in seconds) for Test PF-05

	OD = 2 m^{-1}		FED = 0.3		FED = 1	
Test	1st storey	2nd storey	1st storey	2nd storey	1st storey	2nd storey
PF-05	192	222	**220±5**	**282±10**	**255±10**	**342±20**

Notes:
1. Values determined using the measurements at 1.5 m height (for gas concentrations and OD) or 1.4 m height (for temperatures);
2. The number with the *Italic* typeface represents the calculated time for reaching the CO incapacitation dose, while the number in **bold** represents the calculated time for reaching the heat incapacitation dose, whichever occurred first.

4.5.8 Performance of Test Assembly

A floor system provides an egress route for occupants and its structural integrity directly impacts the safe evacuation of the occupants from the house during a fire emergency. During the fire experiment, the conditions of the test assembly were monitored.

Figure 59 shows temperatures in the cavities of the test assembly. The thermocouples installed in the six sections of the floor cavities aimed to monitor the temperatures inside the cavities and provide an indication of the effectiveness of suspended ceiling protection for the test assembly. The moment that the temperatures in the floor cavities approached the fire room temperature indicates the loss of the suspended ceiling membrane protection for the floor structure. This happened starting from 200 s depending on the position. Visual observation confirmed that mineral fibre ceiling panels started falling from the centre of the ceiling at 225 s, followed by more panels falling afterwards. Then flames started to involve the joists and subfloor.
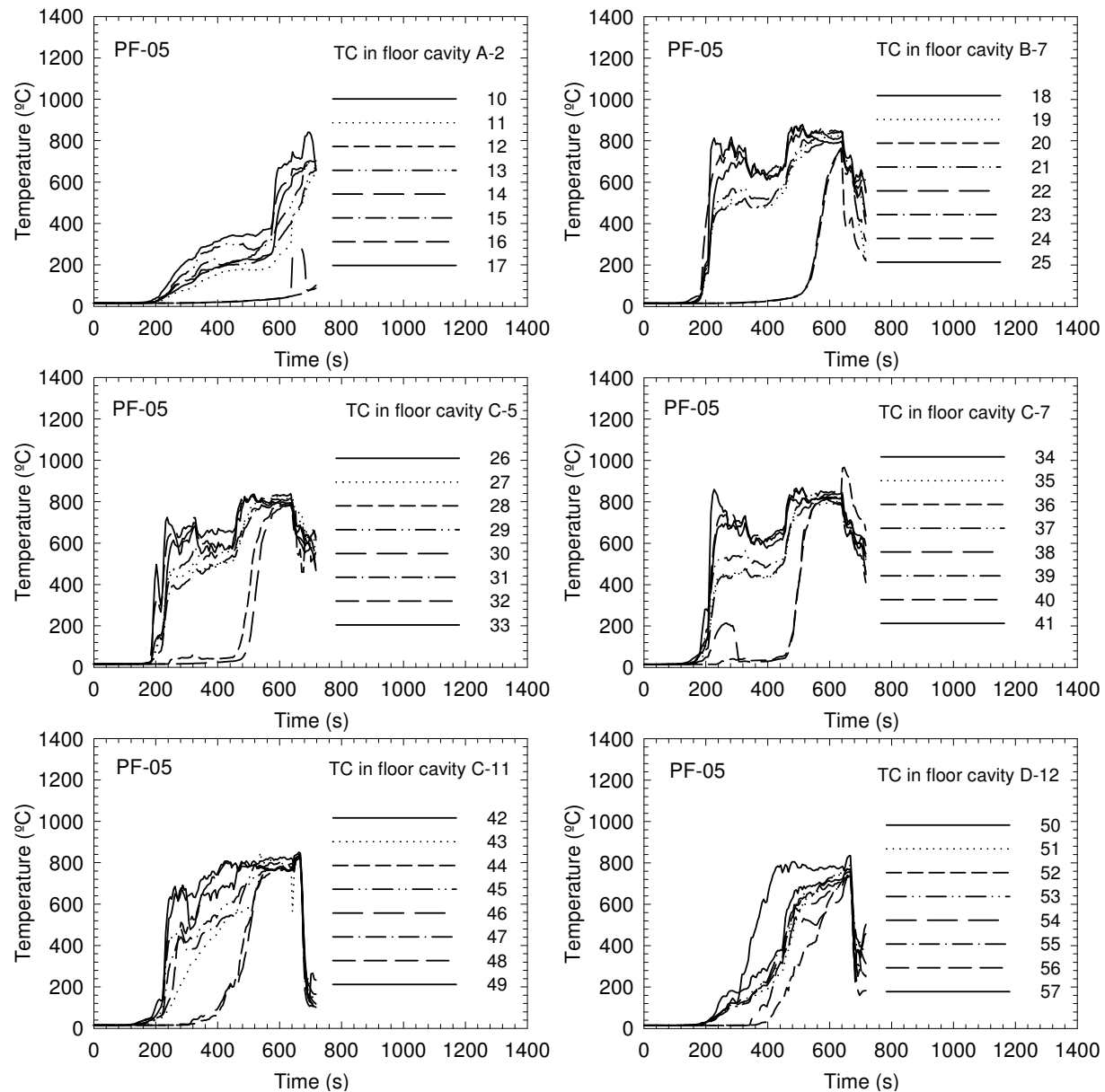
Figure 59. Temperatures in floor cavities in Test PF-05

Figure 60 shows results of the measurements using thermocouples, flame-sensing devices and deflection devices on the unexposed side of the test assembly on the first storey.

The temperature measurements by nine thermocouples under insulation pads on top of the subfloor (on the first storey) are similar to the measurements in the standard fire-resistance test with respect to thermocouple type, installation and layout [29]. A rapid increase in temperature on the unexposed side around 640 s indicates that the test assembly was significantly breached. The subsequent rapid decrease in temperature was due to the termination of the experiment by extinguishing the fire with water. Four bare thermocouples were also installed on the unexposed side of the test assembly for temperature measurements, which also indicated a rapid increase in temperature around 640 s.

The floor deflection of the test assembly was measured at nine points in the central area of the test assembly just above the fuel package where the impact of the fire on the assembly was anticipated to be the greatest. The test assembly reached the maximum deflection capacity of the measurement devices just before its structural failure.

The flame-sensing device [19] at the central tongue-and-groove joint on the unexposed side of the OSB subfloor provided detection of flame penetration through the test assembly. The figure shows a large voltage spike near 640 s, indicating the device being struck by flames that penetrated through the test assembly.
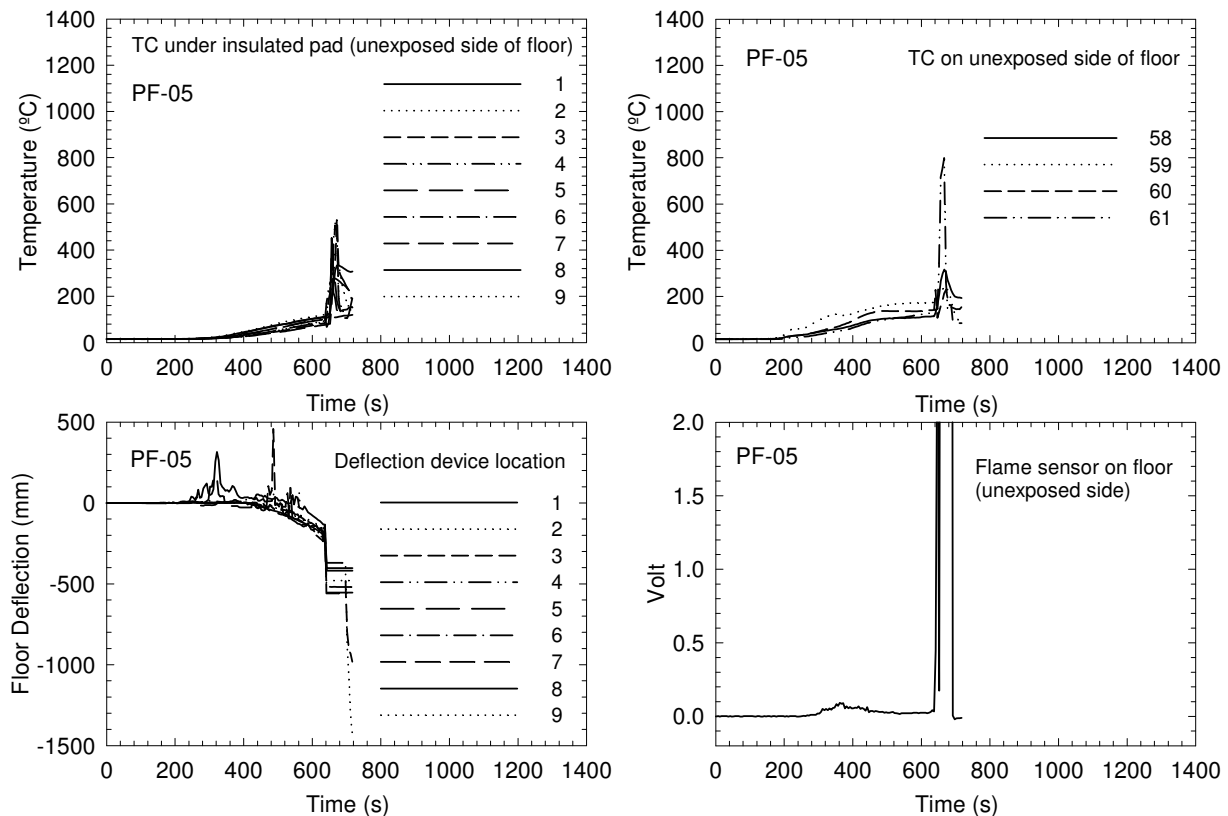
Figure 60. Temperatures, deflections and flame sensor on the unexposed side of the assembly on the first storey in Test PF-05

Visual observation through the window opening of the fire room confirmed the structural failure at 638 s. The test assembly collapsed into the basement in the form of a "V" shape with wood I-joists broken at the mid-points.

4.5.9 Sequence of Events

Table 23 summarizes the chronological sequence of the fire events in Test PF-05 — fire initiation, smoke alarm activation, onset of untenable conditions, and structural failure of the test assembly. Smoke obscuration was the first hazard to arise. It must be pointed out that people

NRC·CNRC

with impaired vision could become disoriented earlier at an optical density lower than 2 m^{-1}. The incapacitation conditions were reached shortly after smoke obscuration. The structural failure of the test assembly occurred well after the untenable conditions were reached.

For comparison purposes, Table 23 also shows data from the test conducted in Phase 1 using the same floor structure but no ceiling protection (UF-03). The data indicates that tenability conditions are only slightly improved whilst the structural performance is also improved with the protected ceiling/floor assembly.

Table 23. Summary of Sequence of Events in Test PF-05 (in seconds)

Assembly Type	Test	First Alarm	OD = 2 m^{-1}	FED=0.3-1 1st storey	FED=0.3-1 2nd storey	Structural Failure
Suspended ceiling protected wood I-joists	PF-05	47	192-222	**220-255**	**282-342**	638*
Unprotected wood I-joists	UF-03	48	183	**205-213**	*225-247*	490

Notes:
1. Values determined using the measurements at 1.5 m height (for gas concentrations and OD) or 1.4 m height (for temperatures);
2. The number with the *Italic* typeface represents the calculated time for reaching the CO incapacitation dose, while the number in **bold typeface** represents the calculated time for reaching the heat incapacitation dose, whichever occurred first;
3. *Values of the structural failure time of the test assemblies determined by visual observation;
    a. The maximum deflection capacity of the measurement devices reached at 640 s;
    b. A single-point temperature rise of 180°C occurred on the unexposed side of the test assembly at 640 s;
    c. A large voltage spike detected using the flame-sensing device at 640 s.

4.6   Wood I-Joist Assembly with Residential Sprinkler Protection – Test PF-03

Test PF-03 was conducted using a wood I-joist assembly with residential sprinkler protection in the basement fire room.

4.6.1   Construction Details of the Test Assembly

Except that the exposed side (basement side) had no finished ceiling, the wood I-joist assembly used in Test PF-03 was identical to those used in Tests PF-04 and PF-05 (see Figure 37, Figure 38, Figure 40 and Figure 41). The wood I-joists were exposed in the basement fire room. The thermocouples for measuring temperatures throughout the assembly were located on the unexposed side and in the exposed cavities of the test assembly as shown in Figure 41 and Figure 61.

NRC·CNRC
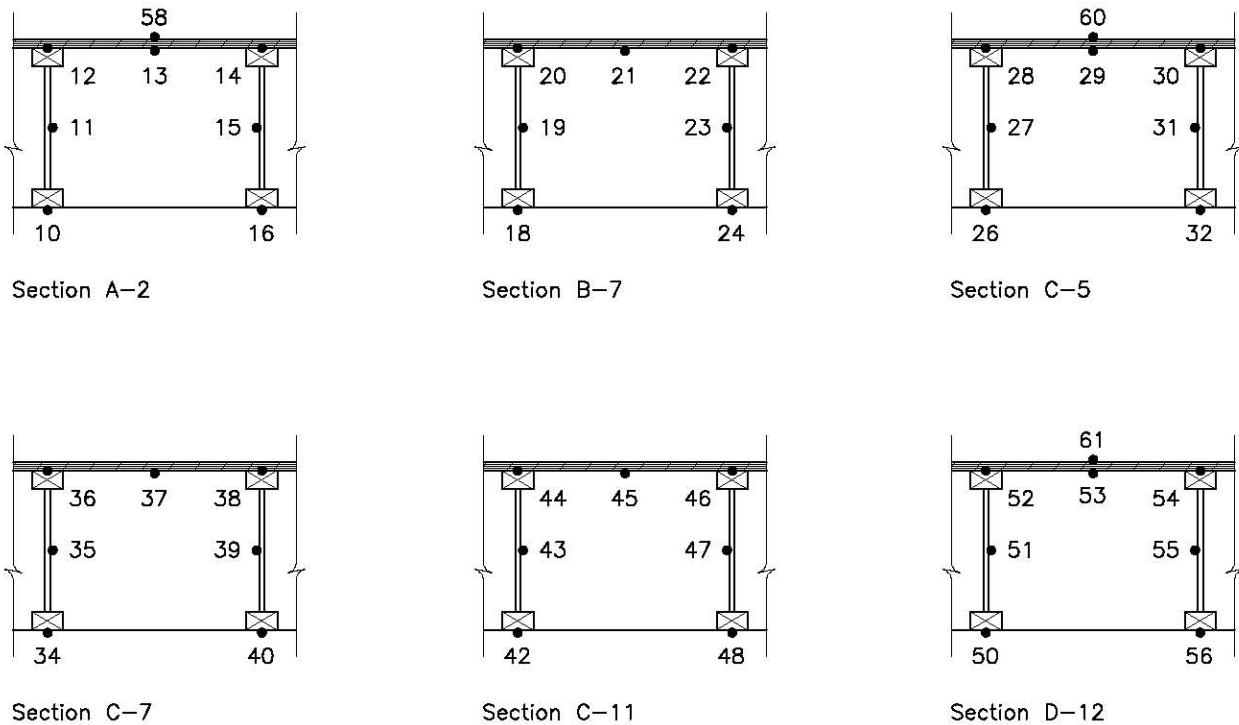
Figure 61. Thermocouples in the sections shown in Figure 41 (Tests PF-03 and PF-03B only)

4.6.2   Residential Sprinkler Design

The consortium members had extensive discussions on automatic sprinkler design issues, including spray density, water demand, available water flow, experiment duration, operating pressure, and possibility of reusing the same assembly for additional secondary experiments. These issues focused on what is the typical residential basement sprinkler installation with exposed joists, what compensating design factors have to be included for going beyond the product listings, and how many sprinklers should be used to protect the fire room.

Several design options were proposed. In the end, the consortium approved a residential sprinkler system design for the primary experiment (Test PF-03). This design used a two-sprinkler layout with CPVC plastic piping of 25.4 mm in diameter. Two Reliable F1 Residential 49[*] pendent sprinklers, which had a K factor of 4.9 and a temperature rating of 68°C (155°F), were located 3.66 m (12 ft) apart along the centerline of the fire room. Figure 62 and Figure 63 show the sprinkler locations relative to the wood I-joists and fuel package in the experiment. The deflector of each sprinkler was approximately 25.4 mm (1") below the bottom of the wood I-joists and 330 mm (13") below the subfloor. The sprinklers and piping were installed per NFPA 13D and APA Technical Note J745 [31, 32].

---

[*] Certain commercial products are identified in this paper in order to adequately specify the experimental procedure. In no case does such identification imply recommendations or endorsement by the National Research Council of Canada.

77

NRC·CNRC

The residential sprinkler system was designed to operate at 1.0×10^5 Pa (15 psi) with minimum 72 Lpm (19 USgpm) flow from each sprinkler (for a total operating flow of 144 Lpm (38 USgpm) from 2 sprinklers). The water supply had a static pressure of 3.45×10^5 Pa (50 psi). Although in many regions municipal water supply would be capable of providing an operating pressure above 1.0×10^5 Pa (15 psi), the consortium decided to conduct the experiment at that operating pressure. The consortium also decided that, as a minimum, the duration of the experiment should be comparable to Tests PF-01 and PF-02.

Flow tests were conducted to ensure the operating pressure and flow equal to or greater than the design values. With the two sprinklers simultaneously open, the hydraulically-most-remote sprinkler (north sprinkler) gave a pressure of 1.0×10^5 Pa (15 psi), and the two sprinklers provided a total flow of 144 Lpm (72 Lpm each). With the north sprinkler open only, it provided a pressure of 1.9×10^5 Pa (27.9 psi) and a flow of 98 Lpm (25.9 USgpm).
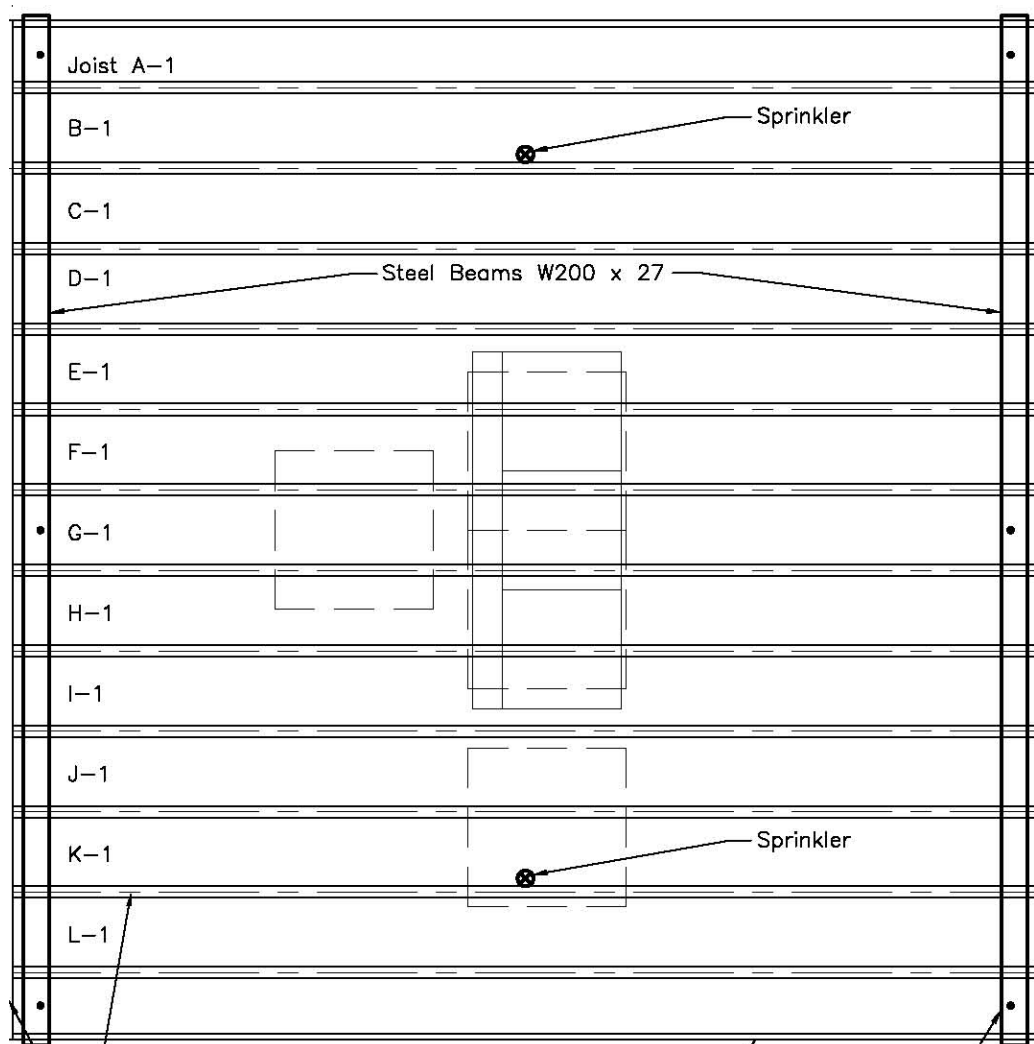
Figure 62. Sprinkler locations related to wood I-joists and fuel in Test PF-03 (all dimensions in mm)

Figure 63. Sprinkler and CPVC piping installation with exposed wood I-joists in Test PF-03

For applications within the listing conditions (assuming a smooth ceiling finish with 178 mm (7") deep exposed beams spaced over 2.3 m (7.5 ft) on center), a single sprinkler at the design conditions could cover a 5.5 m x 5.5 m (18 ft x 18 ft) area, which is bigger than the fire room (5.3 m x 5.2 m). NFPA 13D (Clause 8.1.3.1.2) allows the use of residential sprinklers beyond their listings '*where construction features or other special conditions exist that are outside the scope of sprinkler listings'*. It was recognized that the CPVC piping is only listed for use under exposed solid-sawn wood joists; the use of the CPVC piping below exposed wood-I joists would be beyond its listing conditions. In light of these 'listing' issues, it was agreed that using two sprinklers would compensate for the use of the residential sprinkler system components beyond their listing conditions and is consistent with the provisions of NFPA 13D.

NRC·CNRC

4.6.3 Fire Development in Basement

The polyurethane foam used for the mock-up sofa was ignited and dominated the initial fire growth. Figure 64 shows the temperatures measured beside the two sprinklers and on the wood cribs underneath the mock-up sofa in the basement fire room. The south sprinkler was activated by the heat at 106 s and quickly suppressed the fire. Based on observation and video records, visible flame disappeared in the fire room at 150 s. There was small flame re-appearing from 340 to 525 s then subsiding. The sprinkler discharge continued for 1200 s (20 min). The north sprinkler did not activate during the experiment.
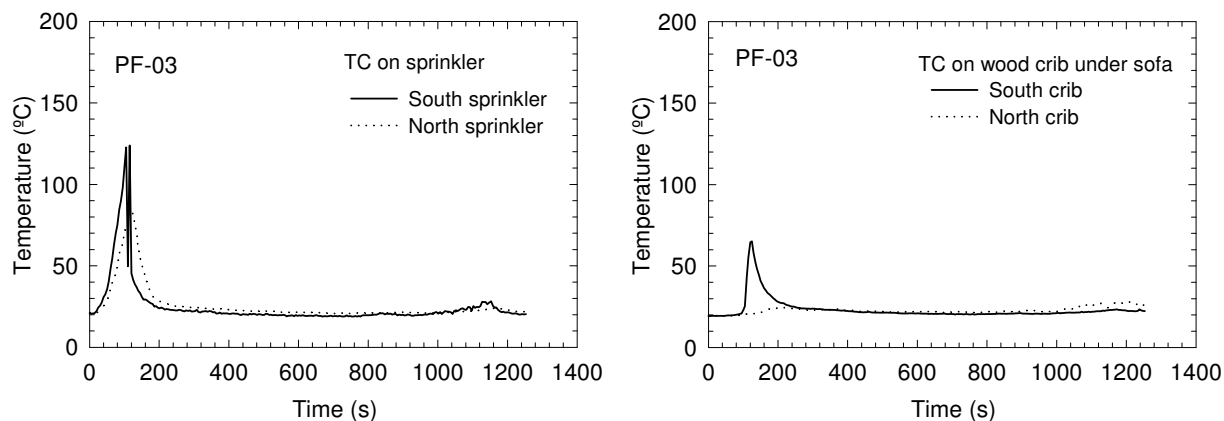
Figure 64. Temperatures on sprinklers and wood cribs in the fire room in Test PF-03

Figure 65 shows the temperature profiles measured in the basement fire room. Prior to the sprinkler activation, the peak temperatures at the 2.4 m height were 77°C at the NW quadrant, 71°C at the NE quadrant, 110°C at the SW quadrant, and 96°C at the SE quadrant. The peak temperatures at the window were 115°C. Upon the sprinkler activation, the temperatures in the fire room quickly reduced to close to ambient temperature. Figure 65 also shows the heat flux measured at the west wall (near the centre, 2.05 m above the floor). The maximum heat flux was 4 kW·m^{-2} for less than 20 s prior to the sprinkler activation.

The single sprinkler activation was able to suppress the fire and keep the temperature in the fire room close to the ambient level. Because the temperature at the window did not reach 300°C, the noncombustible window covering panel was not removed during the experiment.
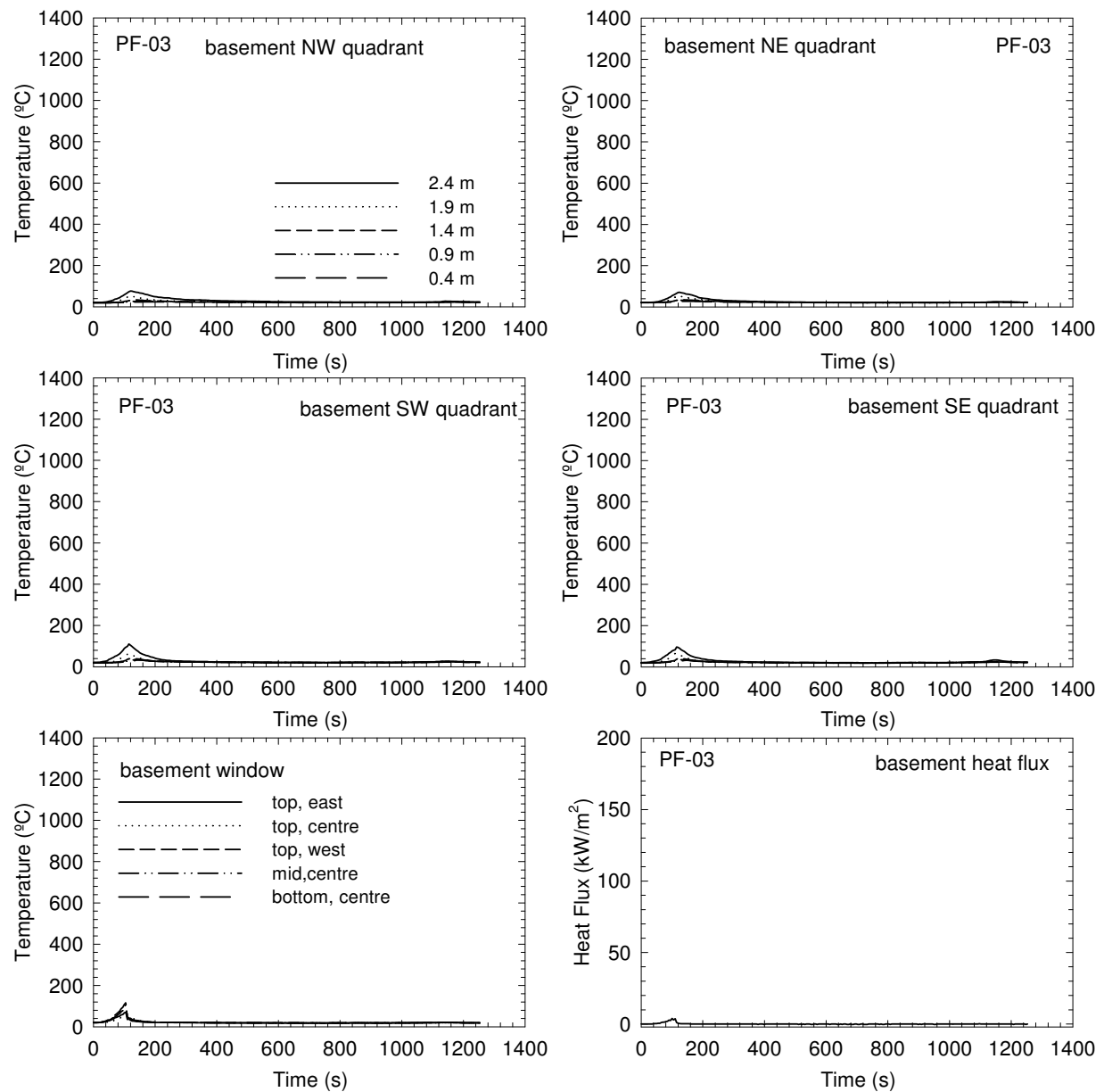
Figure 65. Temperatures and heat flux in the basement fire room in Test PF-03

4.6.4 Visual Obscuration

The optical density was measured at 0.9 and 1.5 m heights (simulating the height of the nose/mouth of an average height individual crawling and standing, respectively) above the floor on the first and second storeys. Figure 66 shows the optical density-time profiles; OD remained under 0.2 m^{-1} throughout the upper storeys during the experiment. At this smoke level, a normal person should still be able to see the surroundings.

NRC·CNRC
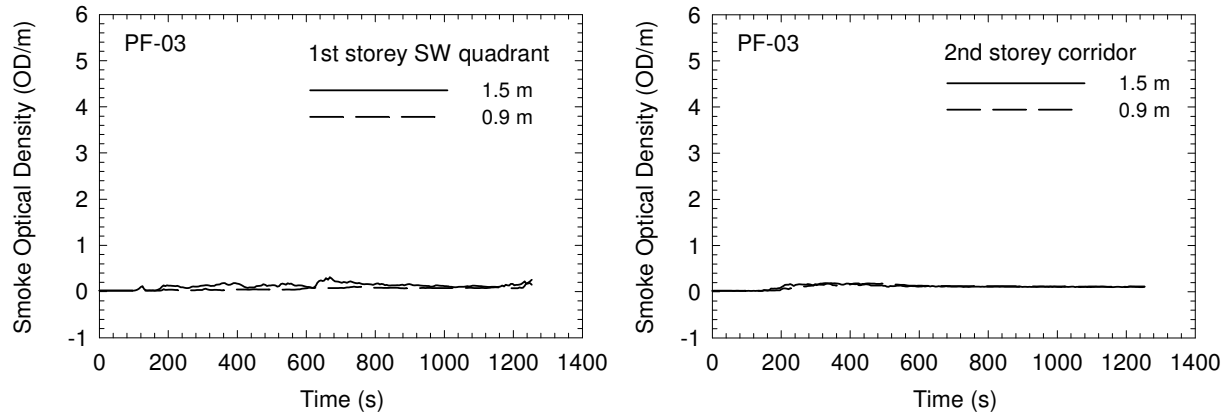
Figure 66. Smoke optical density measurements in Test PF-03

4.6.5   Gas Measurements and Analysis (CO, CO_2 and O_2)

Figure 67 shows the CO, CO_2 and O_2 concentrations at the southwest quarter point on the first storey and at the centre of the corridor on the second story during the experiment. The oxygen concentrations were above 20.5%. The CO_2 concentrations were below 0.2%, and CO below 0.01%. These conditions would not cause incapacitation or any reduction in tenable conditions.
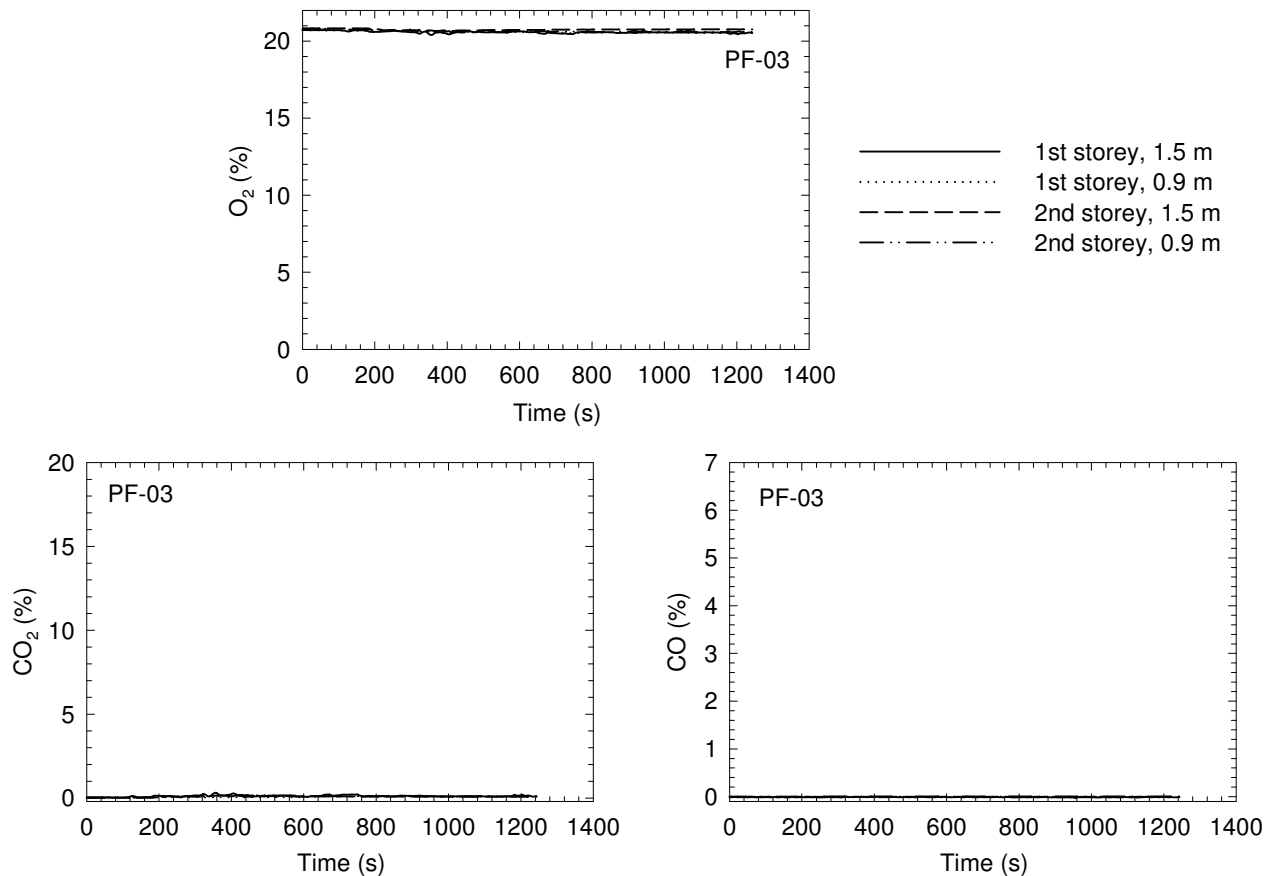
Figure 67. CO, CO_2 and O_2 concentrations in Test PF-03

NRC·CNRC

4.6.6 Temperature-Time Profiles on the Upper Storeys

Figure 68 and Figure 69 show temperature profiles measured on the first and second storeys during the experiment. On the first storey, the maximum temperature of 55°C was measured at the doorway to the basement prior to the sprinkler activation; the maximum temperatures at the four quadrants were less than 35°C. Upon the sprinkler activation, the temperatures on the first storey quickly reduced to ambient temperature. On the second storey, there was hardly any noticeable temperature change. These conditions would not cause incapacitation or any reduction in tenable conditions.
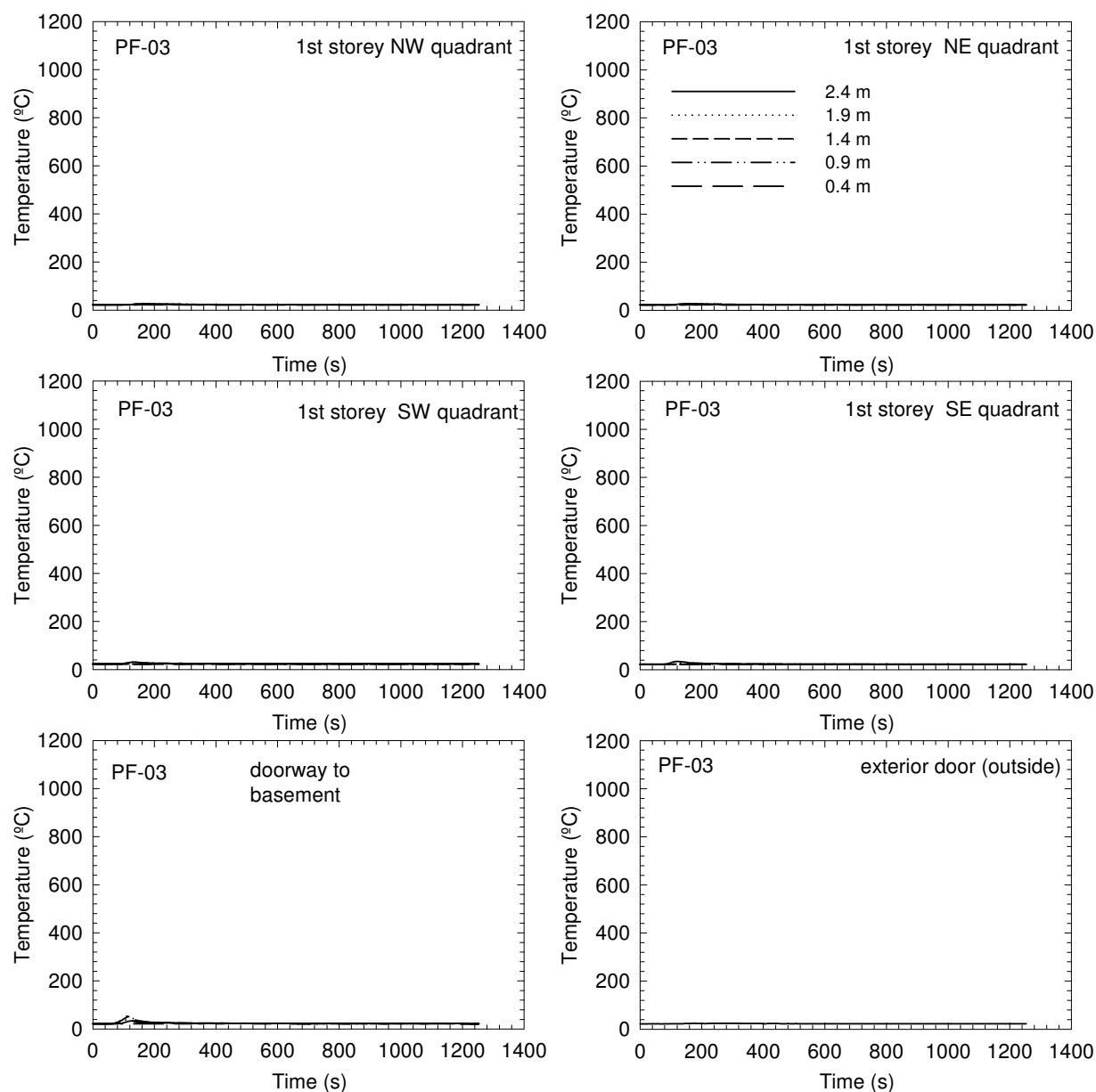
Figure 68. Temperatures on the first storey in Test PF-03

NRC·CNRC
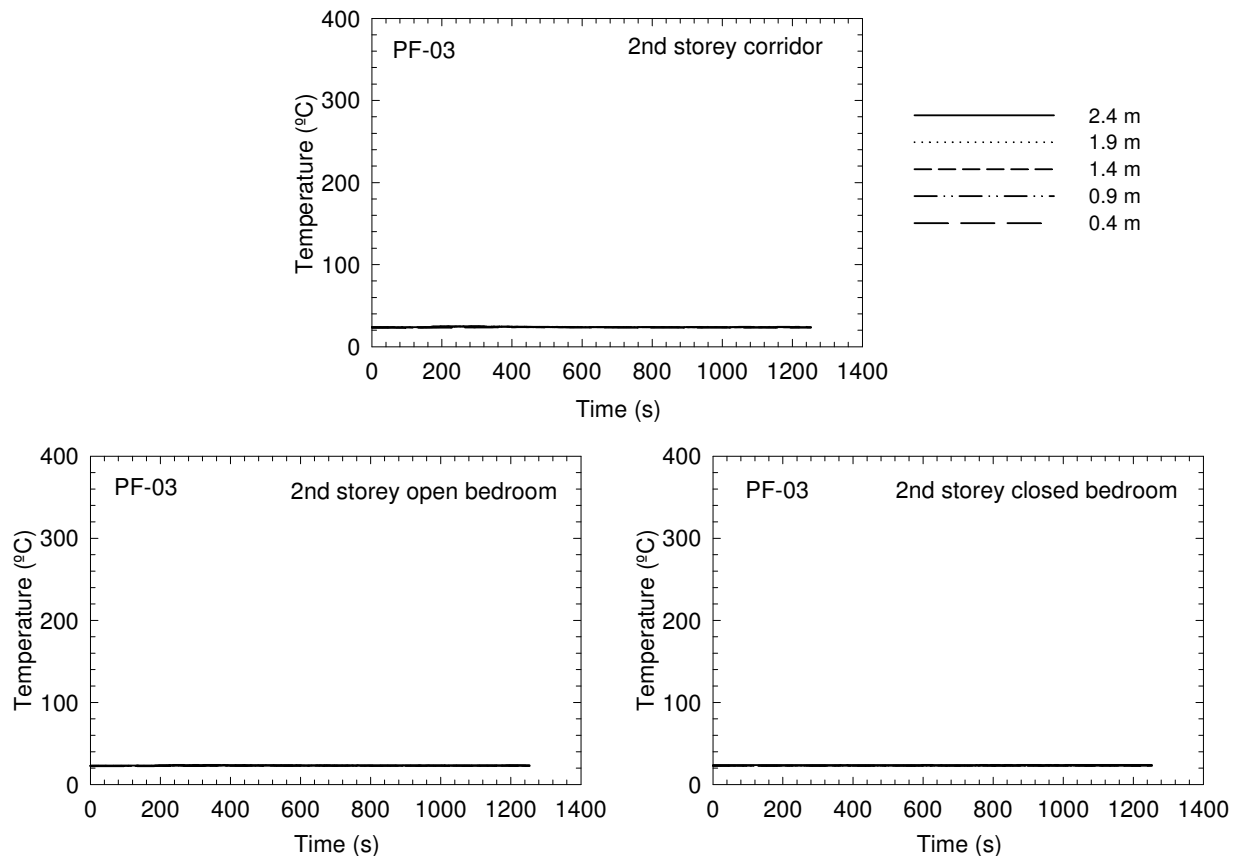
Figure 69. Temperatures on the second storey in Test PF-03

4.6.7   Performance of Test Assembly

A floor system provides an egress route for occupants and its structural integrity directly impacts the safe evacuation of the occupants from the house during a fire emergency. During the fire experiment, the conditions of the test assembly were monitored.

Figure 70 shows temperatures in the cavities of the test assembly. The thermocouples installed in the six sections of the floor cavities monitored the temperatures within the cavities and provided an indication of the effectiveness of residential sprinkler protection for the test assembly. Depending on the position, the maximum temperatures in the floor cavities were in the range of 60-160°C prior to the sprinkler activation. Upon the sprinkler activation, the temperatures in the floor cavities quickly reduced to ambient temperature. There was no ignition of the test assembly during the experiment.

NRC·CNRC
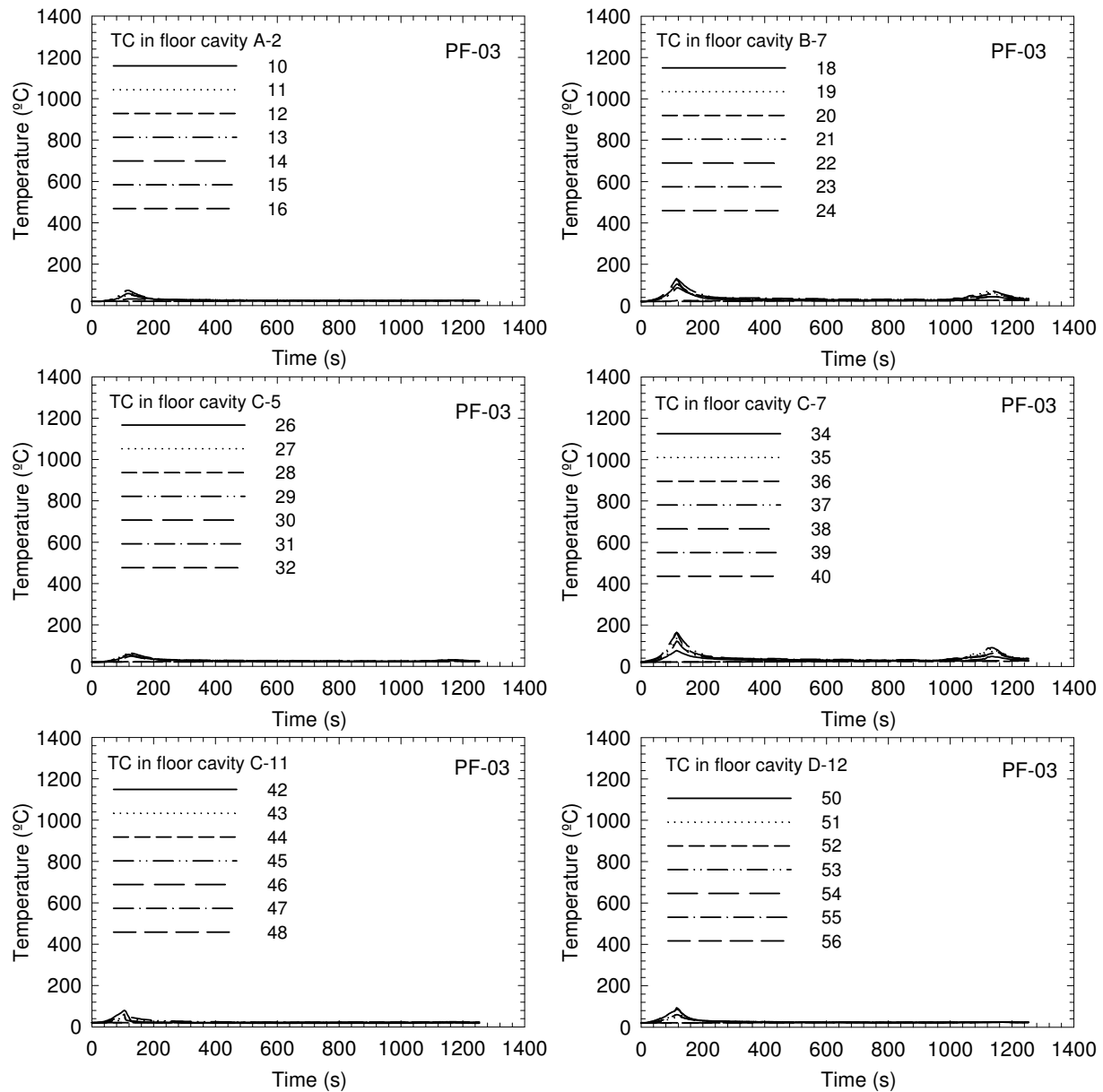
Figure 70. Temperatures in floor cavities in Test PF-03

Figure 71 shows results of the measurements using thermocouples, flame-sensing devices and deflection devices on the unexposed side the test assembly on the first storey.

The temperature measurements by nine thermocouples under insulated pads on top of the subfloor (on the first storey) are similar to the measurements in the standard fire-resistance test with respect to thermocouple type, installation and layout [29]. There were also four bare thermocouples installed on top of the subfloor. The increase in these temperatures was less than 10°C during the experiment.

The floor deflection of the test assembly was measured at nine points located in the central area of the test assembly just above the fuel package where the impact of the fire on the assembly was anticipated to be the greatest. There was no floor deflection of the test assembly during the experiment.

The flame-sensing device [19] at the central tongue-and-groove joint on the unexposed side of the OSB subfloor provided detection of flame penetration through the test assembly. There was no noticeable change in the voltage signal.
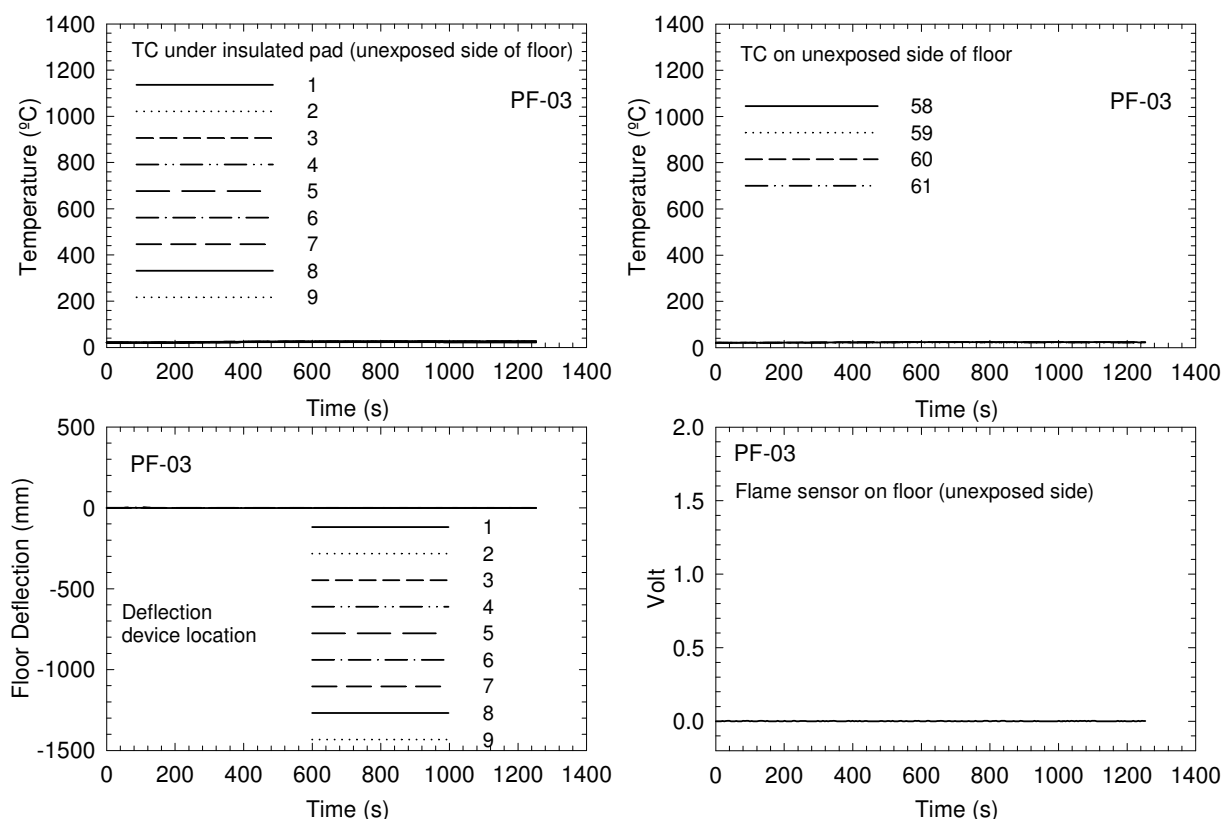
Figure 71. Temperatures, deflections and flame sensor on the unexposed side of the assembly on the first storey in Test PF-03

4.6.8 Sequence of Events

Table 24 summarizes the results for Test PF-03. The incapacitation conditions were not reached. Visual observation after the experiment confirmed that, other than soot deposition from the burning of the fuel package, no ignition or damage occurred with the test assembly and the CPVC piping system.

For comparison purposes, Table 24 also shows data from the test conducted in Phase 1 using the same floor structure but no protection (UF-03). The data indicates that the residential sprinkler system maintained tenable conditions and protected the structural integrity of the test assembly during the experiment.

NRC·CNRC

Table 24. Summary of Sequence of Events in Test PF-03 (in seconds)

Assembly Type	Test	First Alarm	OD = 2 m⁻¹	FED=0.3-1 1st storey	FED=0.3-1 2nd storey	Structural Failure
Sprinkler protected wood I-joists	PF-03*	45	not reached	not reached	not reached	not reached
Unprotected wood I-joists	UF-03	48	183	**205-213**	*225-247*	490

Notes:
1. *The sprinkler activated at 106 s;
2. Values determined using the measurements at 1.5 m height (for gas concentrations and OD) or 1.4 m height (for temperatures);
3. The number with the *Italic* typeface represents the calculated time for reaching the CO incapacitation dose, while the number in **bold** typeface represents the calculated time for reaching the heat incapacitation dose, whichever occurred first.

Since this PF-03 wood I-joist assembly survived the primary fire experiment (Test PF-03), two additional fire experiments (secondary Tests PF-03B and PF-03C) were conducted using this survived test assembly. (See a separate report for details on Test PF-03C [18].)

4.7   Wood I-Joist Assembly with Residential Sprinkler Protection – Test PF-03B

Test PF-03B was a secondary sprinklered fire experiment conducted using the wood I-joist assembly that survived Test PF-03.

4.7.1   Residential Sprinkler Design

The consortium discussed various automatic fire sprinkler design options for use in the "secondary" experiments. This included reconsideration of a single-sprinkler arrangement, among others, due to the fact that one sprinkler suppressed the fire in Test PF-03. The Consortium decided to conduct a secondary sprinkler test using a single-sprinkler system, which is typical for sprinklering this size of fire room (5.3 m x 5.2 m).

A Reliable F1 Residential 49[†] pendent sprinkler, which had a K factor of 4.9 and a temperature rating of 68°C (155°F), was located 3.05 m (10 ft) from both the south and east walls of the fire room. Figure 72 and Figure 73 show the sprinkler location relative to the wood I-joists and fuel package in the experiment. The deflector of the sprinkler was approximately 25.4 mm (1") below the bottom of the wood I-joists and 330 mm (13") below the subfloor. The sprinkler and CPVC plastic piping (25.4 mm in diameter) were installed per NFPA 13D and APA Technical Note J745 [31, 32]. It should be noted that a portion of the CPVC piping ran right above the fuel package.

[†] Certain commercial products are identified in this paper in order to adequately specify the experimental procedure. In no case does such identification imply recommendations or endorsement by the National Research Council of Canada.

NRC·CNRC

The residential sprinkler was designed to operate at 1.4×10^5 Pa (20.2 psi) with an 83.2 Lpm (22 USgpm) flow. The water supply had a static pressure of 3.45×10^5 Pa (50 psi). Flow tests were conducted and the design operating pressure and flow were confirmed.

For applications within the listing conditions, this single sprinkler at the design conditions could cover a 6.1 m x 6.1 m (20 ft x 20 ft) area, which is bigger than the fire room (5.3 m x 5.2 m). This greater coverage would provide some compensation for use of the residential sprinkler system components beyond their listing conditions and is consistent with the provisions of NFPA 13D.
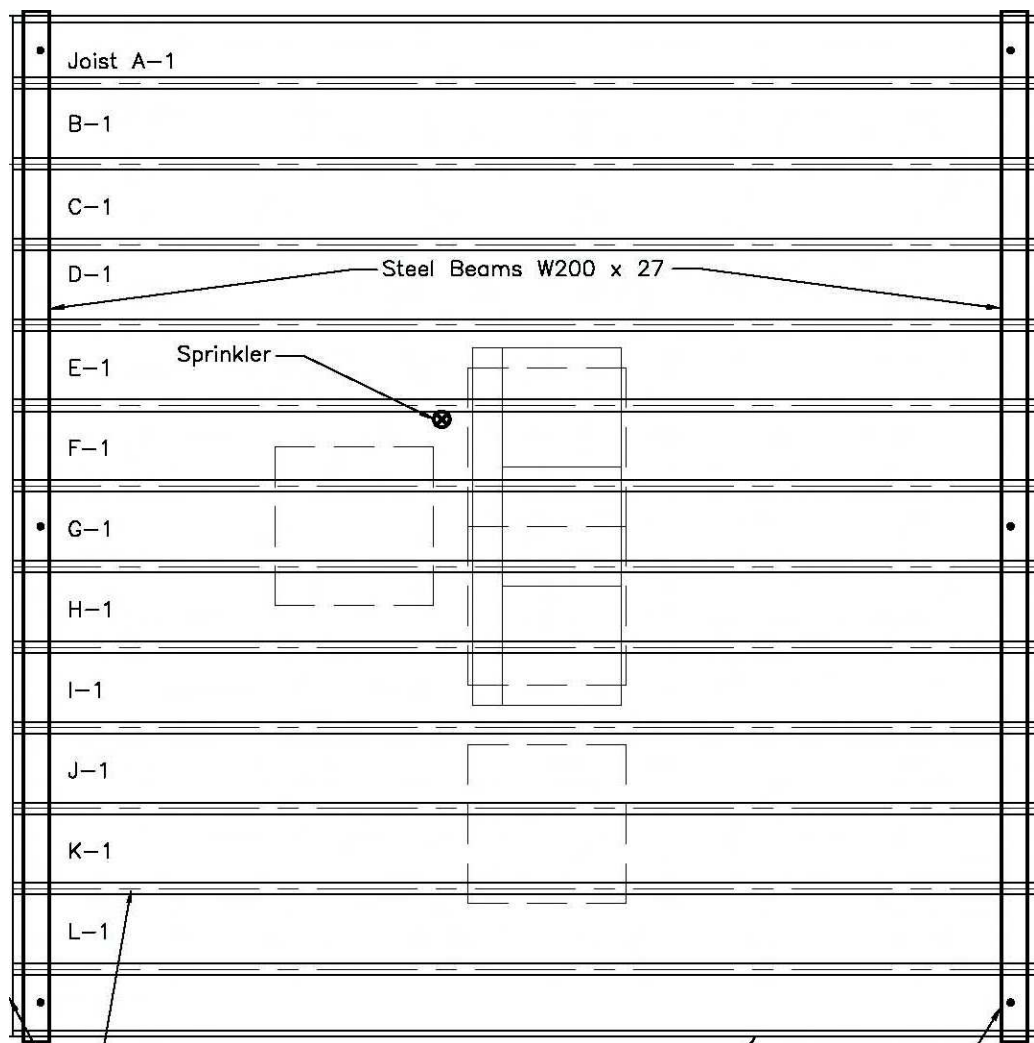
Figure 72. Sprinkler location related to wood I-joists and fuel in Test PF-03B (all dimensions in mm)

NRC·CNRC

Figure 73. Sprinkler and CPVC piping relative to exposed wood I-joists and fuel (Test PF-03B)

4.7.2 Fire Development in Basement

The polyurethane foam used for the mock-up sofa was ignited and dominated the initial fire growth. Figure 74 shows the temperature measured beside the sprinkler and on the wood cribs underneath the mock-up sofa in the basement fire room. The sprinkler activated at 87 s and quickly suppressed the fire. Based on observation and video records, visible flame disappeared in the fire room at 135 s. There was small flame re-appearing from 200 to 640 s then subsiding. The sprinkler discharge continued for 1800 s (30 min).
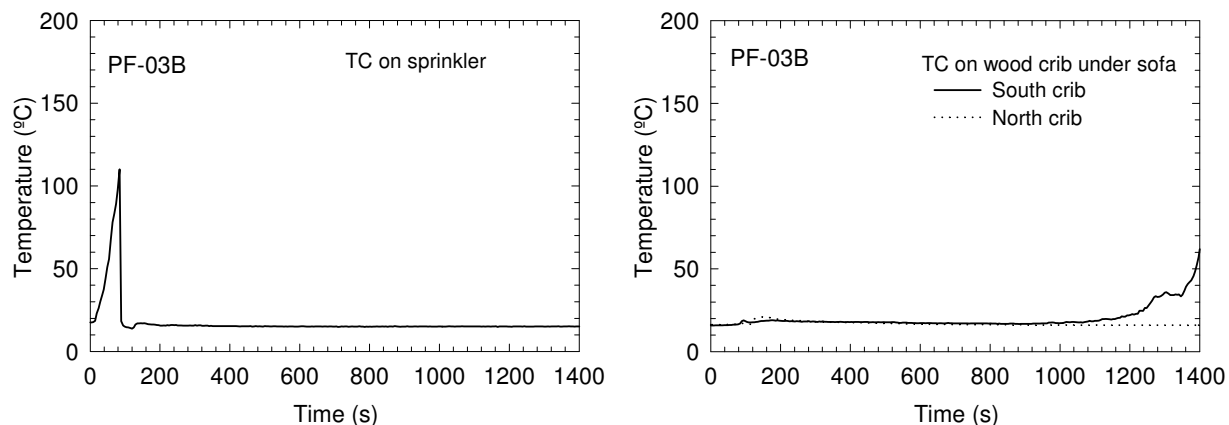
Figure 74. Temperatures at sprinkler and wood cribs in the fire room in Test PF-03B

Figure 75 shows the temperature profiles measured in the basement fire room. Prior to the sprinkler activation, the peak temperatures at the 2.4 m height were 58°C at the NW quadrant, 57°C at the NE quadrant, 81°C at the SW quadrant, and 79°C at the SE quadrant. The peak temperatures at the window were 108°C. After sprinkler activation, the temperatures in the fire room quickly reduced to close to the ambient temperature. Figure 75 also shows the heat flux measured at the west wall (near the centre, 2.05 m above the floor). The maximum heat flux was 2.8 kW·m^{-2} for less than 10 s prior to the sprinkler activation.

The sprinkler discharge was able to suppress the fire and keep the temperature in the fire room close to the ambient level during the 1800-s experiment. Because the temperature at the window did not reach 300°C, the noncombustible window covering panel was not removed during the experiment.
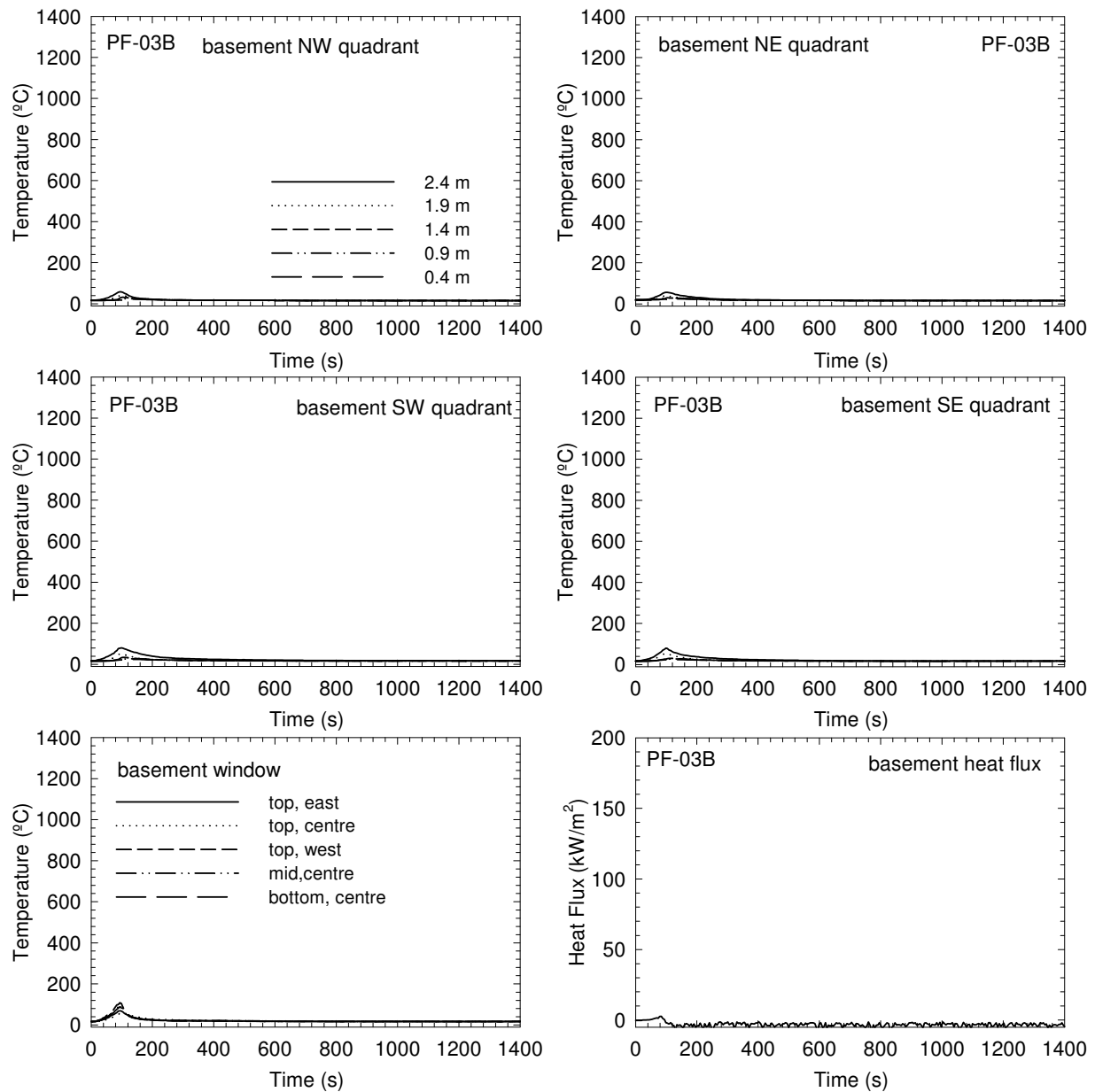
Figure 75. Temperatures and heat flux in the basement fire room in Test PF-03B

4.7.3 Visual Obscuration

The optical density was measured at 0.9 and 1.5 m heights (simulating the height of the nose/mouth of an average height individual crawling and standing, respectively) above the floor on the first and second storeys. Figure 76 shows the optical density-time profiles; OD remained under 0.15 m^{-1} throughout the upper storeys during the experiment. At this smoke level, a normal person should still be able to see the surroundings.

NRC·CNRC
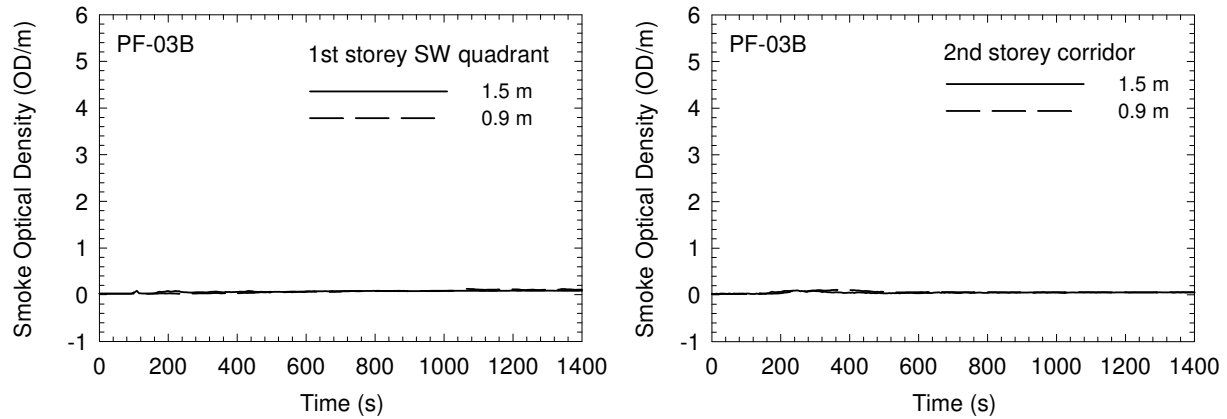
Figure 76. Smoke optical density measurements in Test PF-03B

4.7.4   Gas Measurements and Analysis (CO, CO_2 and O_2)

Figure 77 shows the CO, CO_2 and O_2 concentrations at the southwest quarter point on the first storey and at the centre of the corridor on the second story during the experiment. The oxygen concentrations were above 20.6%. The CO_2 concentrations were below 0.15%, and CO below 0.01%. These conditions would not cause incapacitation or any reduction in tenable conditions.
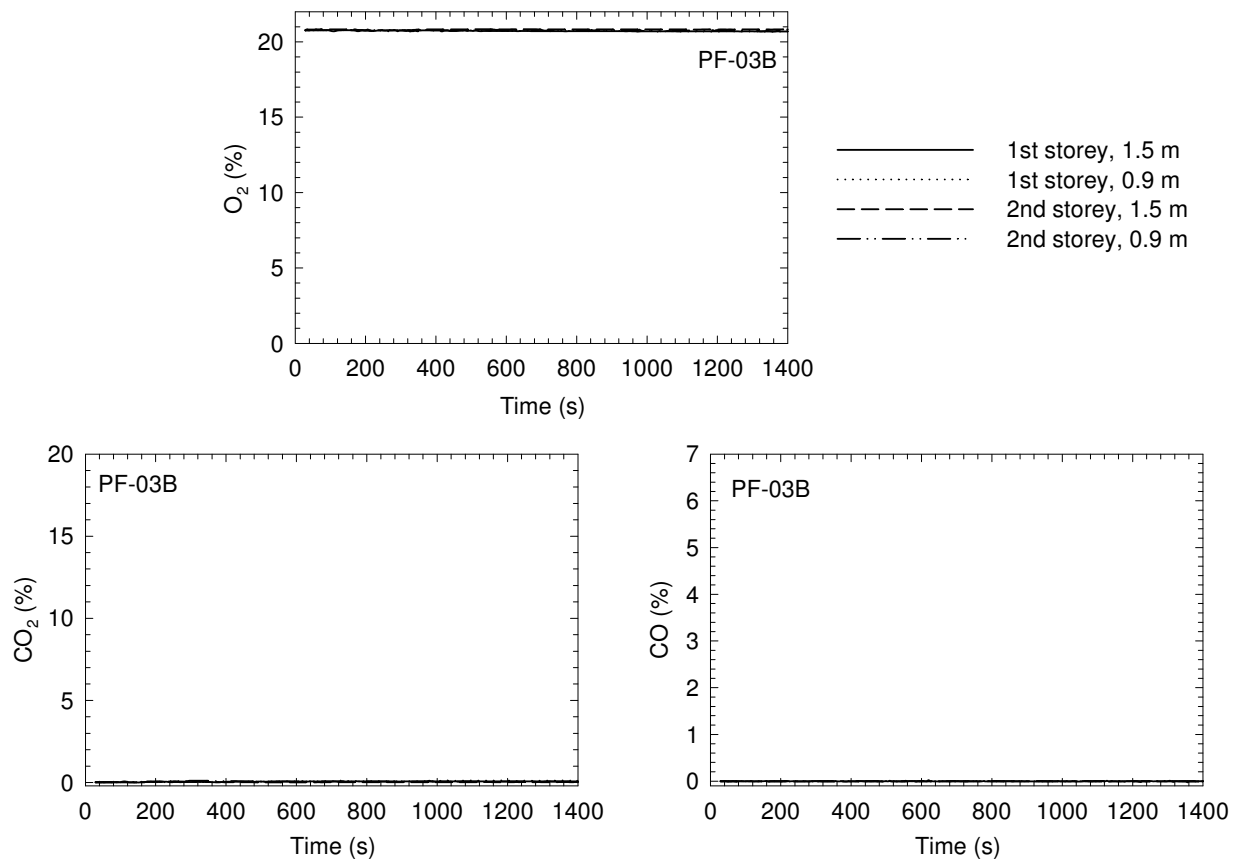
Figure 77. CO, CO_2 and O_2 concentrations in Test PF-03B

NRC·CNRC

4.7.5 Temperature-Time Profiles on the Upper Storeys

Figure 78 and Figure 79 show temperature profiles measured on the first and second storeys during the experiment. On the first storey, the maximum temperature of 44°C was measured at the doorway to the basement prior to the sprinkler activation; the maximum temperatures at the four quadrants were less than 28°C. After sprinkler activation, the temperatures on the first storey quickly reduced to the ambient temperature. On the second storey, there was hardly any noticeable temperature change. These conditions would not cause incapacitation or any reduction in tenable conditions.
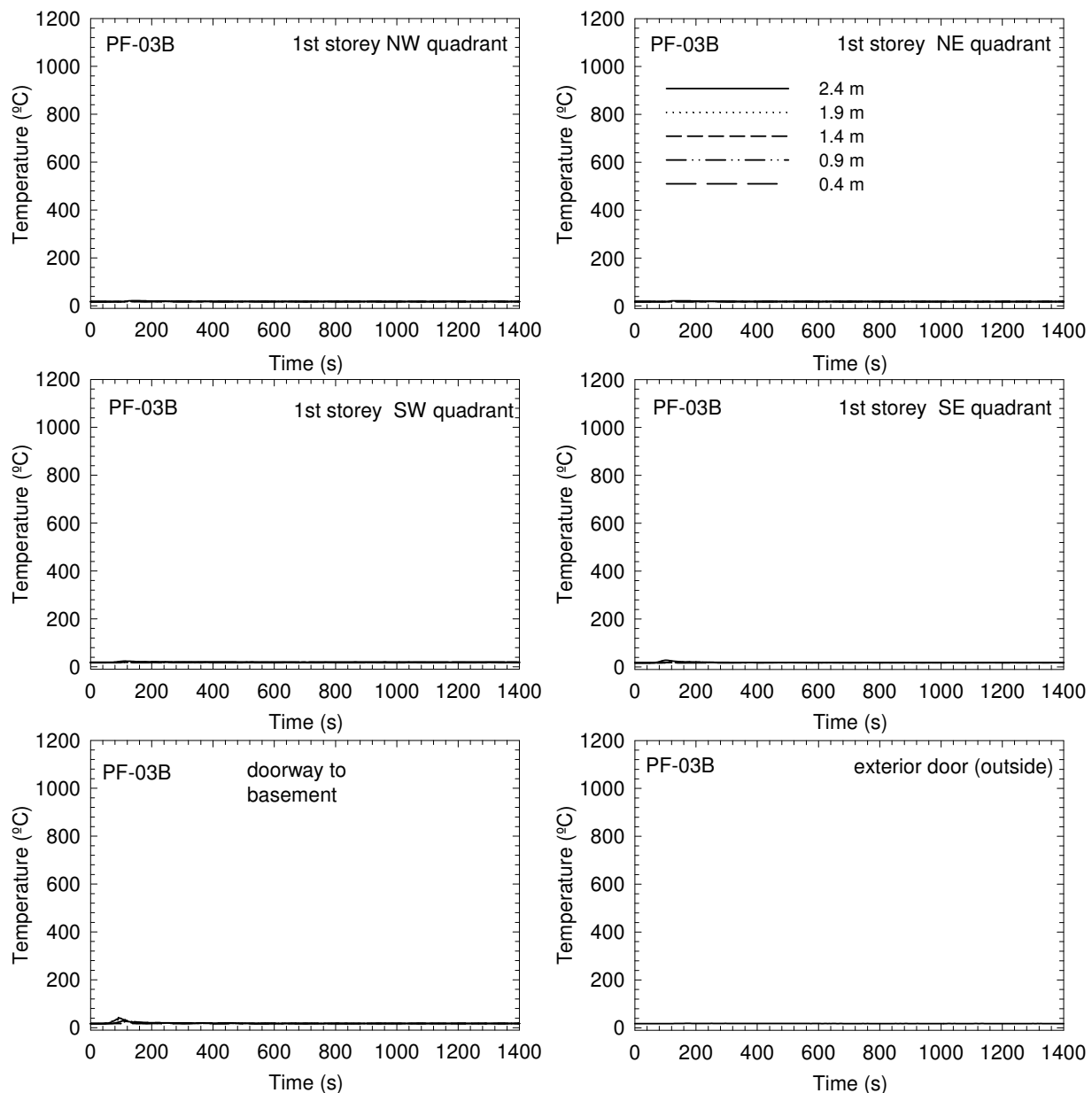
Figure 78. Temperatures on the first storey in Test PF-03B

NRC·CNRC
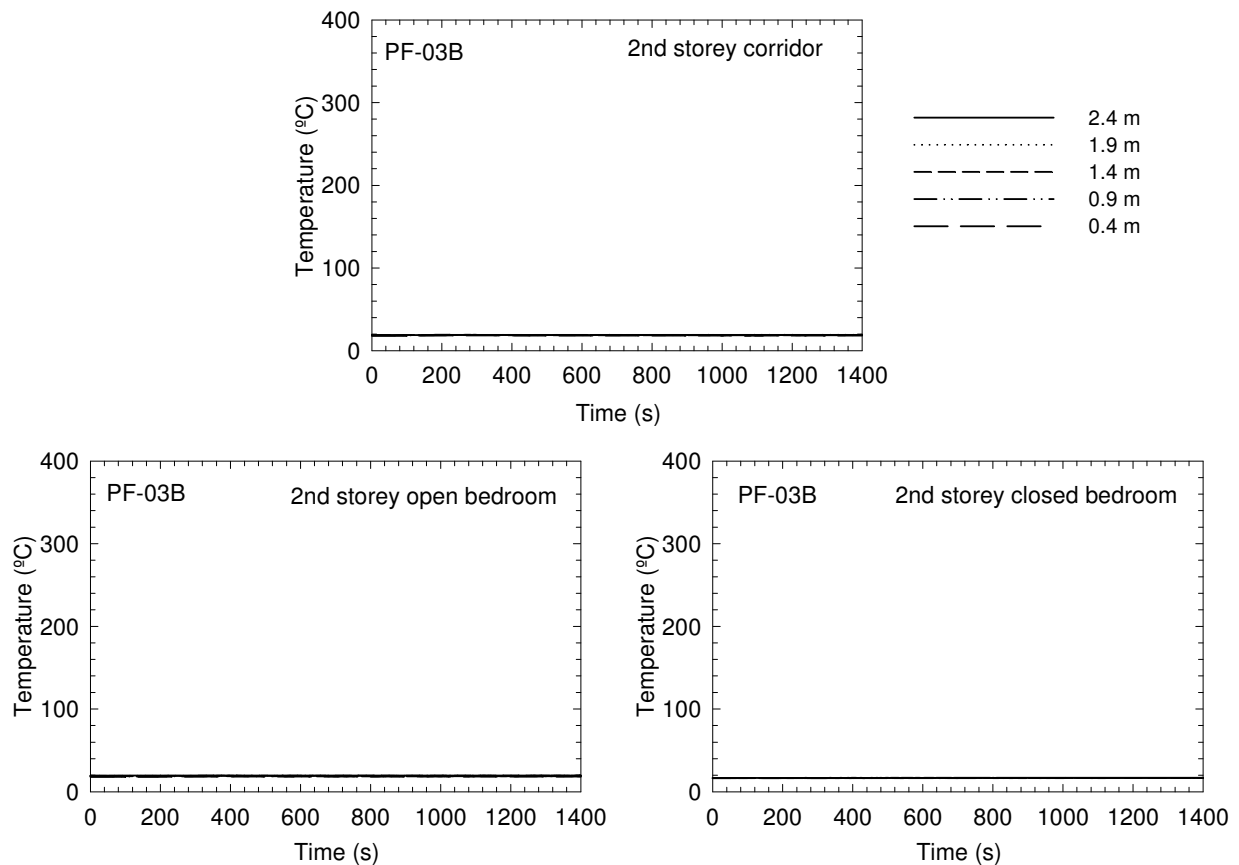
Figure 79. Temperatures on the second storey in Test PF-03B

4.7.6   Performance of Test Assembly

A floor system provides an egress route for occupants and its structural integrity directly impacts the safe evacuation of the occupants from the house during a fire emergency. During the fire experiment, the conditions of the test assembly were monitored.

Figure 80 shows temperatures in the cavities of the test assembly. The thermocouples installed in the six sections of the floor cavities monitored the temperatures within the cavities and provided an indication of the effectiveness of residential sprinkler protection for the test assembly. Depending on the position, the maximum temperatures in the floor cavities were in the range of 55-166°C prior to the sprinkler activation. After sprinkler activation, the temperatures in the floor cavities quickly reduced to close to ambient temperature. There was no ignition of the test assembly during the test.

NRC·CNRC
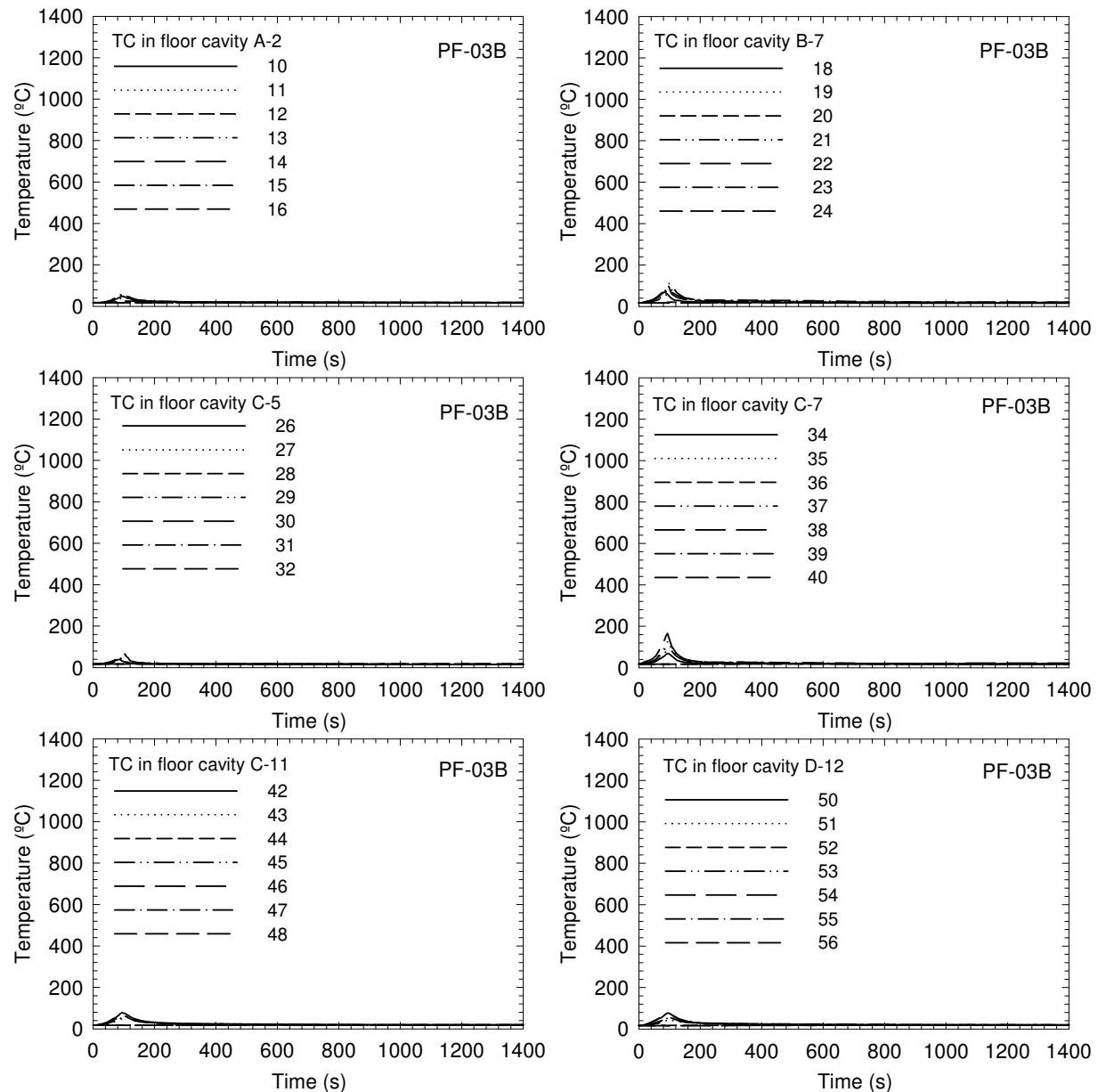
Figure 80. Temperatures in floor cavities in Test PF-03B

Figure 81 shows results of the measurements using thermocouples, flame-sensing devices and deflection devices on the unexposed side the test assembly on the first storey.

The temperature measurements by nine thermocouples under insulated pads on top of the subfloor (on the first storey) are similar to the measurements in the standard fire-resistance test with respect to thermocouple type, installation and layout [29]. There were also four bare thermocouples on top of the subfloor. The increase in these temperatures was less than 5°C during the experiment.

The floor deflection of the test assembly was measured at nine points located in the central area of the test assembly just above the fuel package where the impact of the fire on the assembly was anticipated to be the greatest. There was no floor deflection of the test assembly during the experiment.

The flame-sensing device [19] at the central tongue-and-groove joint on the unexposed side of the OSB subfloor provided detection of flame penetration through the test assembly. There was no noticeable change in the voltage signal.
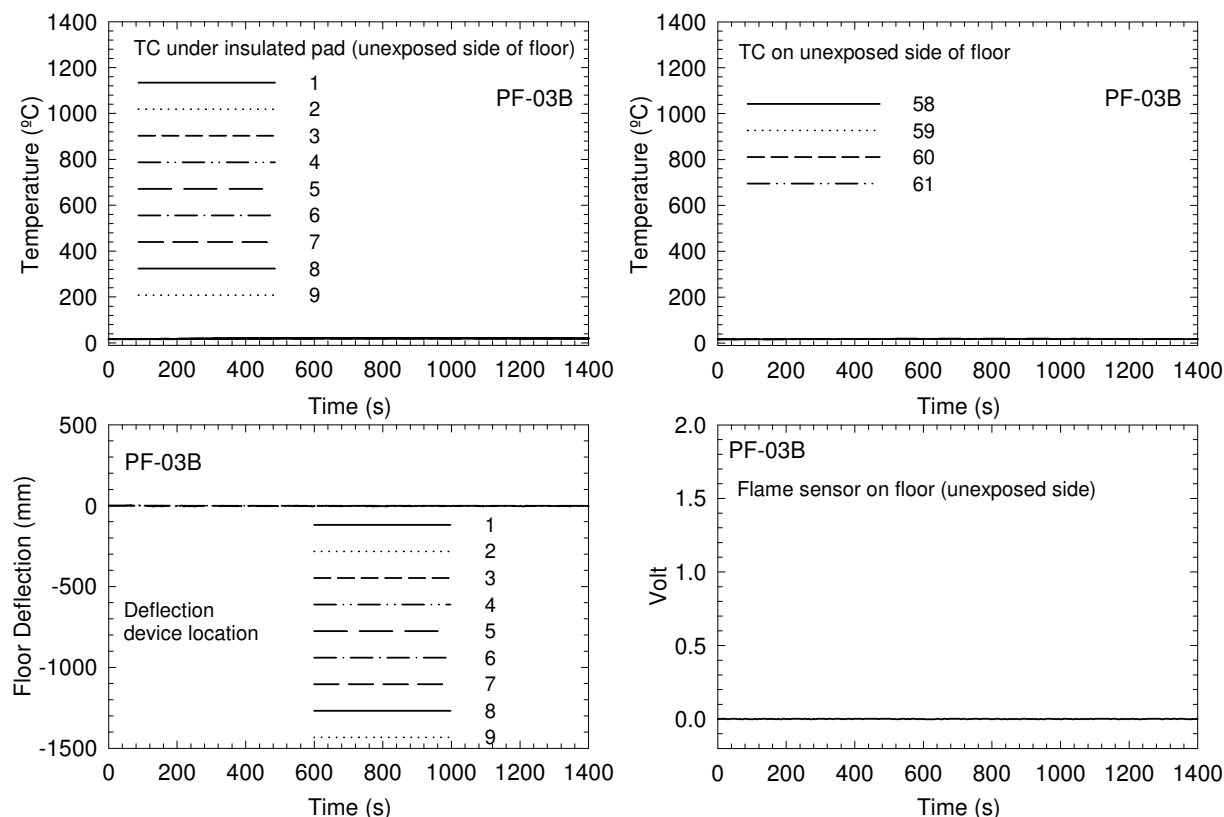
Figure 81. Temperatures, deflections and flame sensor on the unexposed side of the assembly on the first storey in Test PF-03B

4.7.7 Sequence of Events

Table 25 summarizes the results for Test PF-03B. The incapacitation conditions were not reached. Visual observation after the experiment confirmed that, other than soot deposition from the burning of the fuel package, no ignition or damage occurred with the test assembly and the CPVC piping system.

For comparison purposes, Table 25 also shows data from the test conducted in Phase 1 using the same floor structure but no protection (UF-03). The data indicates that the residential sprinkler system maintained tenable conditions and protected the structural integrity of the test assembly during the experiment.

NRC·CNRC

Table 25. Summary of Sequence of Events in Test PF-03B (in seconds)

Assembly Type	Test	First Alarm	OD = 2 m^{-1}	FED=0.3-1 1st storey	FED=0.3-1 2nd storey	Structural Failure
Sprinkler protected wood I-joists	PF-03B*	34	not reached	not reached	not reached	not reached
Unprotected wood I-joists	UF-03	48	183	**205-213**	*225-247*	490

Notes:
1. *The sprinkler activated at 87 s;
2. Values determined using the measurements at 1.5 m height (for gas concentrations and OD) or 1.4 m height (for temperatures);
3. The number with the *Italic* typeface represents the calculated time for reaching the CO incapacitation dose, while the number in **bold** represents the calculated time for reaching the heat incapacitation dose, whichever occurred first.

Additional secondary experiments were conducted using this single-sprinkler arrangement and with the fuel package moved to the southeast corner of the fire room, which are documented in a separate report [18].

4.8 Metal-Web Wood Truss Assembly with Residential Sprinkler Protection – Test PF-06

A metal-web wood truss assembly without any protection had been studied in Phase 1 of the FPH research under the same fire scenario and resulted in the shortest time to reach structural failure. To provide better coverage of the assemblies studied in Phase 1 of the FPH research, the Consortium decided to use the metal-web wood truss assembly for a primary test with residential sprinkler protection (Test PF-06) and, if the assembly was structurally sound after the primary test, a secondary test with regular gypsum board protection. Test PF-06 used the same single-sprinkler system as that in Test PF-03B, with the sprinkler located at the same position and operating under the same flow conditions.

4.8.1 Construction Details of the Test Assembly

The overall dimensions of the metal-web wood truss assembly were 5079 mm x 5150 mm. The assembly had no finished ceiling in the basement – the trusses were exposed in the fire room. Figure 82 and Figure 83 show the test assembly, along with sprinkler and fuel package. The metal-web wood trusses were 302 mm deep, with top and bottom chords of dimensions of 38 mm x 64 mm. The metal webs (20 gauge) had teeth 9.5 mm long and had 0.0171 teeth per square millimeter. The trusses were spaced at 400 mm on centre. The bottom chords of the trusses were reinforced with two strongbacks 38 mm x 140 mm located toward the centre of the span. Based on calculations of maximum strength and deflection, the truss span length chosen was 4.813 m. This span allowed the metal-web wood trusses to extend across the entire length of the fire room (with no need for an intermediate support). Rim boards (headers) 9.5 mm thick x 302 mm deep, were placed around the assembly. In addition, a solid wood 38 mm x 89 mm x 5150 mm member as part of the header was added at the top ends of the trusses to provide lateral support.

NRC·CNRC
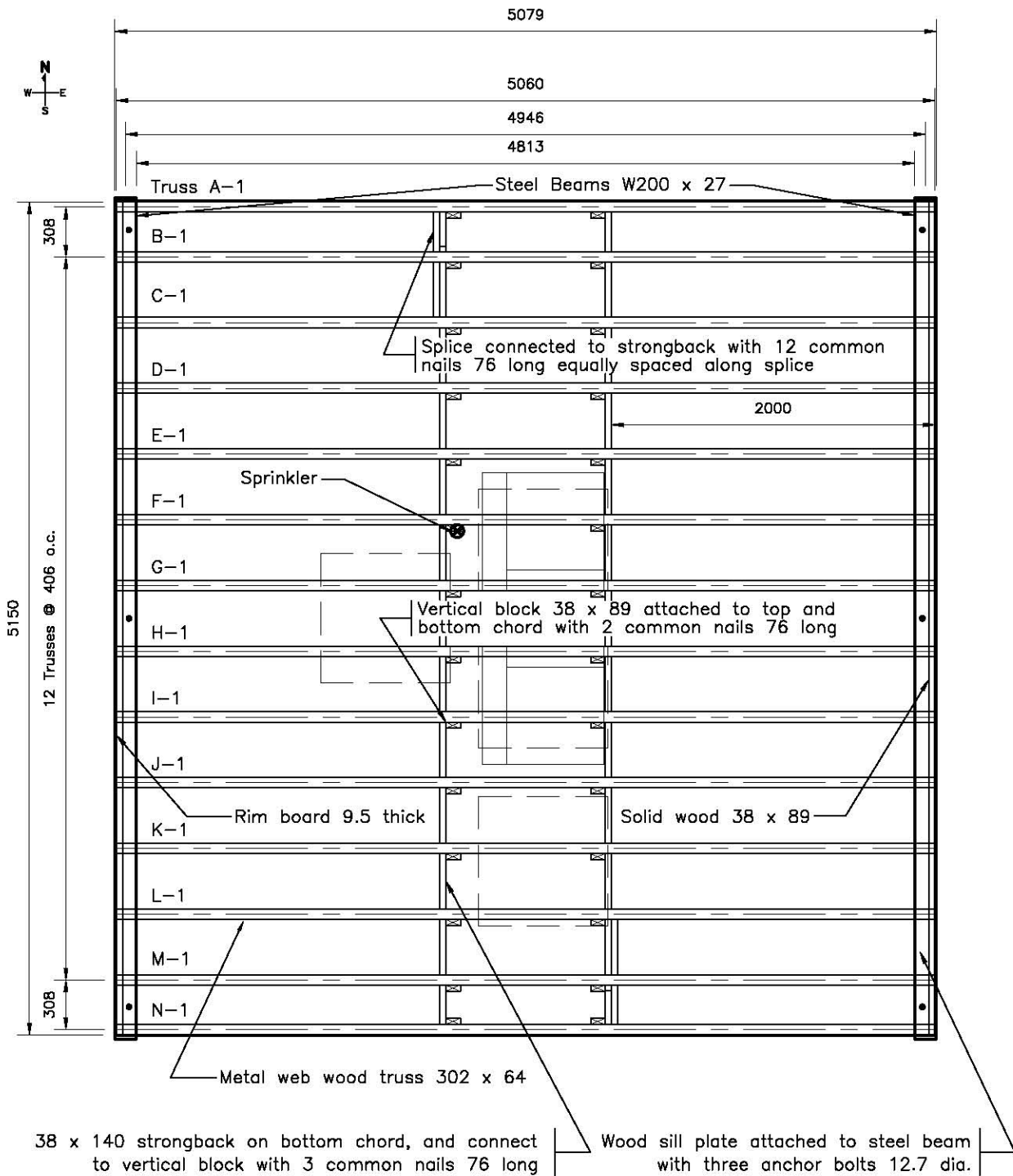
Figure 82. Metal-web wood truss assembly and relative locations for sprinkler and fuel in Test PF-06 (all dimensions in mm)

NRC·CNRC

Figure 83. Metal-web wood truss assembly and sprinkler in Test PF-06

NRC · CNRC

The metal-web wood truss assembly was supported by two horizontal steel beams, each of which was supported by two steel columns (a total of four columns for each assembly). The beams were bolted to the columns, which were stiffened by steel bars and rested stably on the floor under the weight of the assembly and beams. Figure 84 shows the details of the end connection and supporting beams. Ceramic fibre blankets were used to fill any gaps between the assembly and the end walls, also to protect the steel beams and columns.
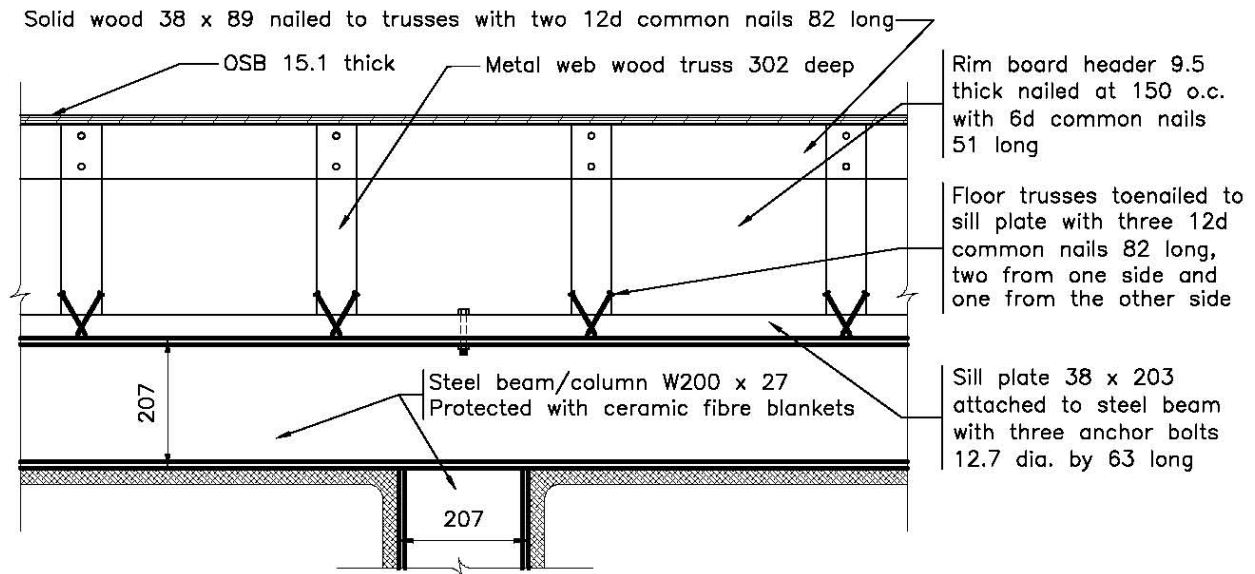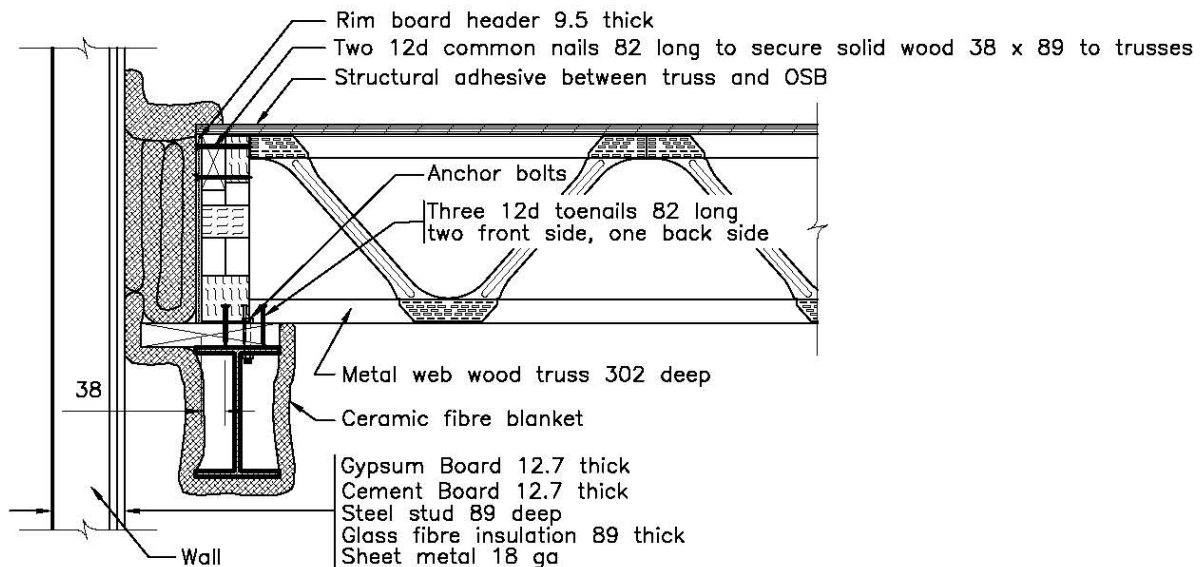
Figure 84. Details of end connection and supports for Test PF-06 (sprinkler protection) (dimensions in mm)
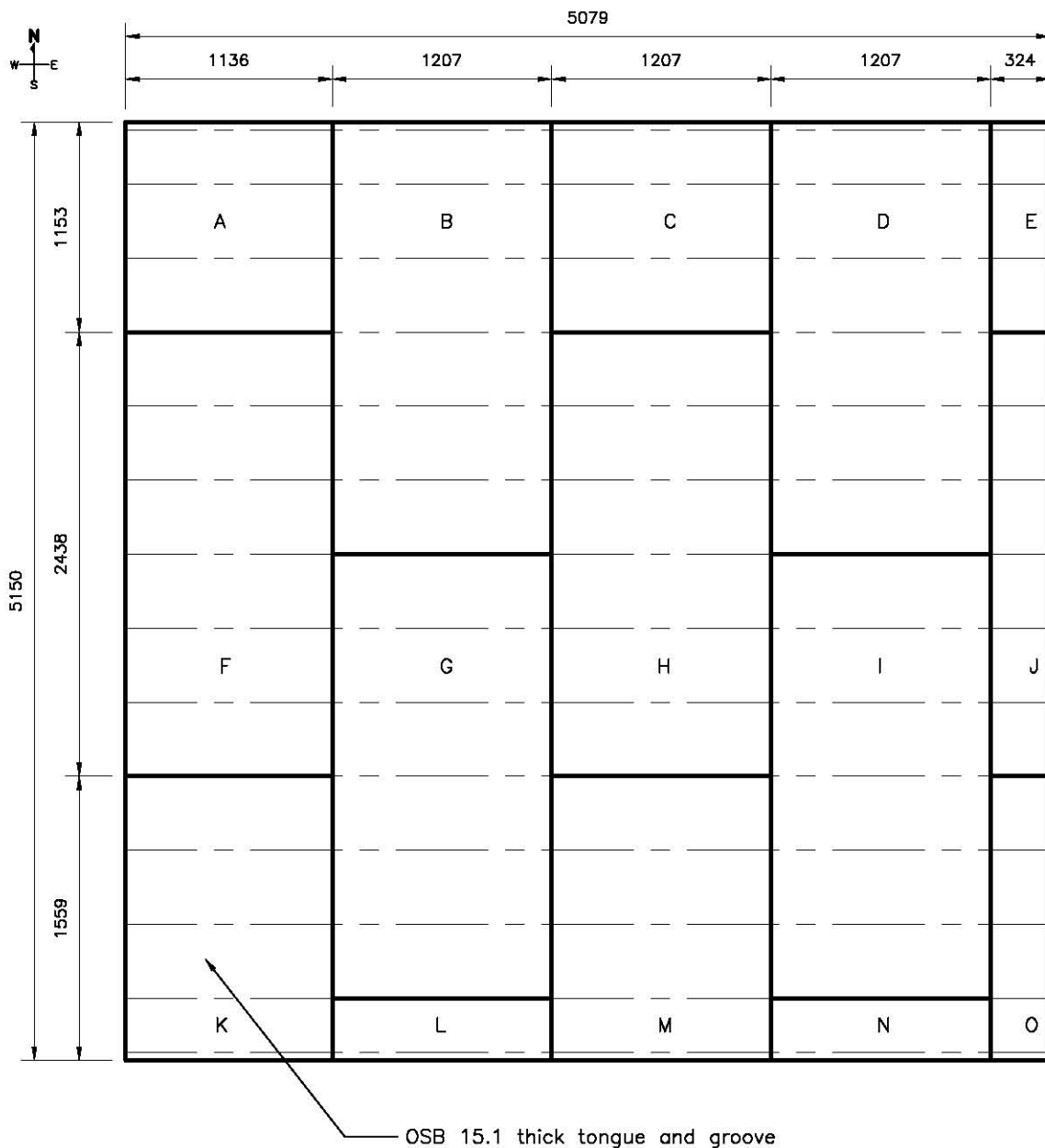
Figure 85. OSB subfloor layout (Tests PF-06 and PF-06C) (all dimensions in mm)

OSB was used as the subfloor material in the test assembly. The specific OSB material used was selected based on a separate study documented in reference [28]. The subfloor panels were 15.1 mm thick, with a full panel size of 1.2 x 2.4 m. The longer panel edges had a tongue-and-groove profile while the short panel edges were square butt ends. Figure 85 shows the layout of the subfloor. The screw pattern and description of screws used to attach the OSB panels to the metal-web wood trusses are shown in Figure 86.
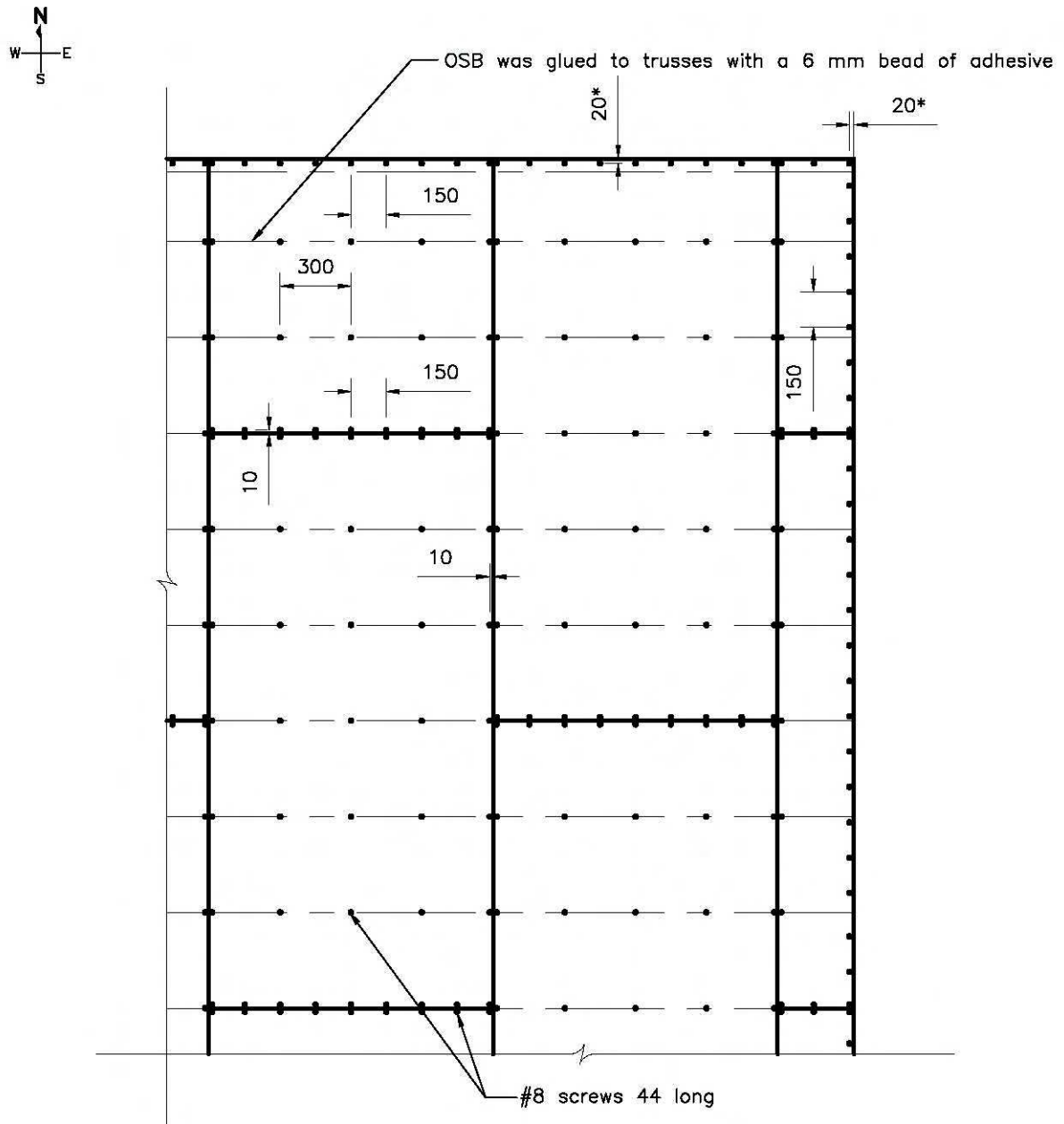
Figure 86. Subfloor screw pattern (Tests PF-06 and PF-06C) (all dimensions in mm)

Sixty-one Type K (20 gauge) chromel-alumel thermocouples, with a thickness of 0.91 mm, were used for measuring temperatures at a number of locations throughout the assembly. The thermocouples were located on the unexposed side and in the cavities of the assembly as shown in Figure 87 and Figure 88. These locations were chosen to monitor the conditions of the assembly at critical locations during the fire tests. The floor deflection was measured at 9 points on the unexposed surface of the test assembly at the locations shown in Figure 13.
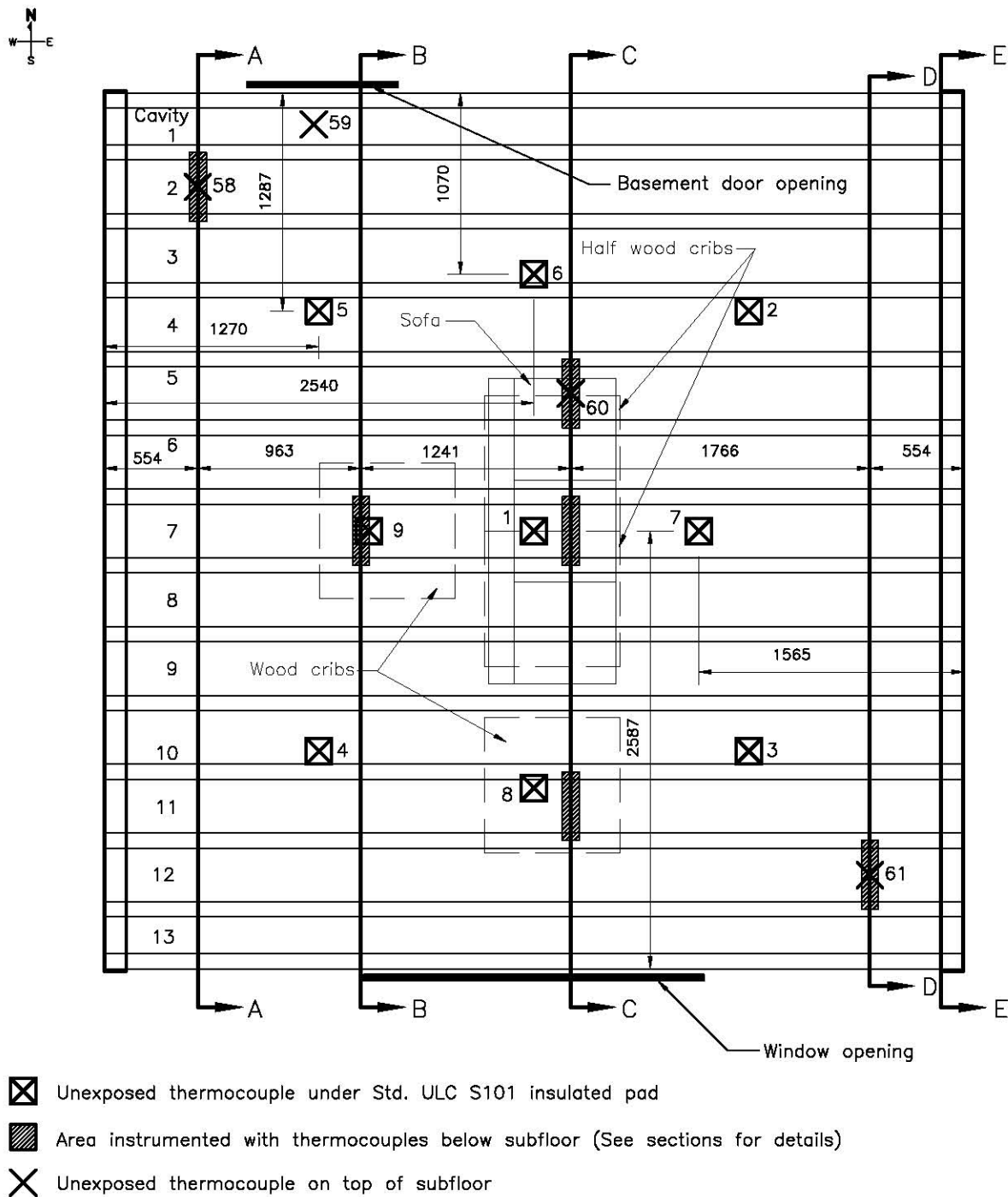
Figure 87. Thermocouples locations (Tests PF-06 and PF-06C) (all dimensions in mm)

NRC·CNRC
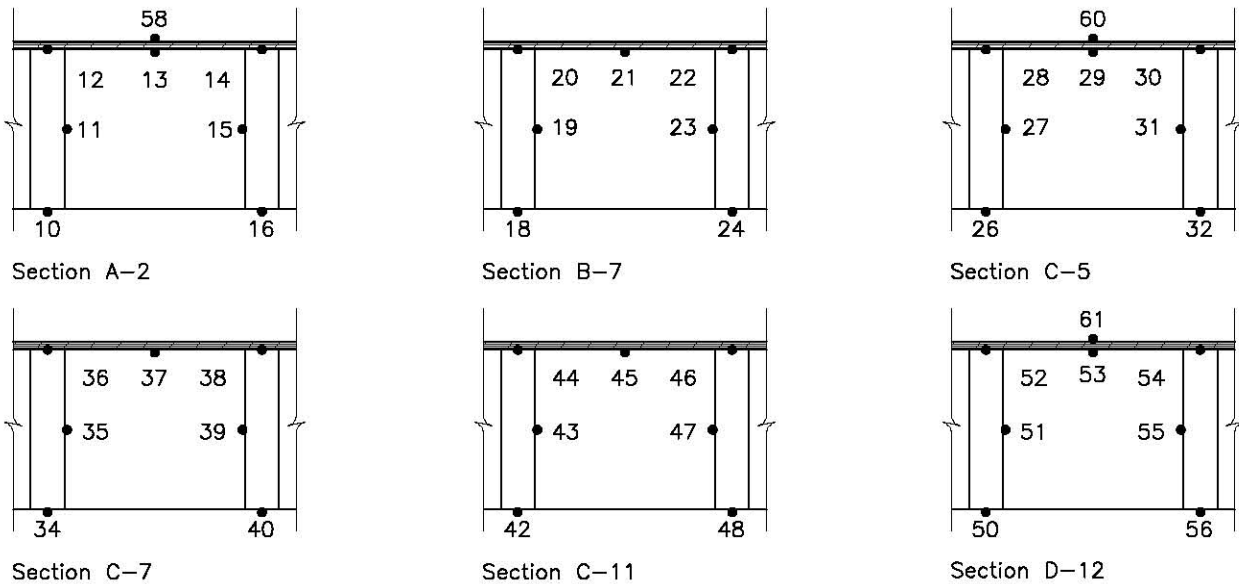
Figure 88. Thermocouples installed in the sections shown in Figure 87 (Test PF-06 only)

4.8.2 Fire Development in Basement

The polyurethane foam used for the mock-up sofa was ignited and dominated the initial fire growth. Figure 89 shows the temperature measured beside the sprinkler in the basement fire room. The sprinkler activated at 87 s and quickly suppressed the fire. Based on observation and video records, visible flame disappeared in the fire room at 200 s. There was no more visible flame afterward. The sprinkler discharge continued for 1800 s (30 min).
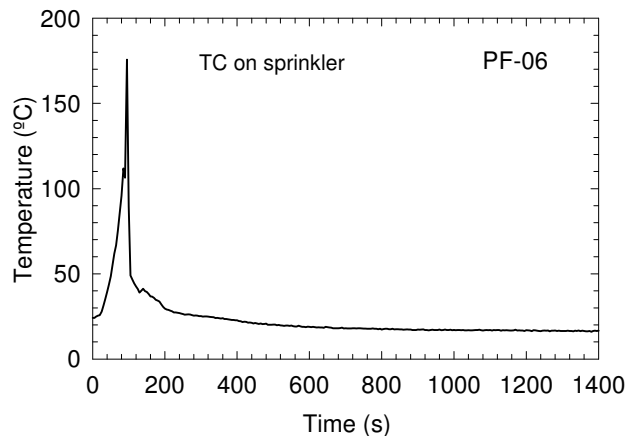
Figure 89. Temperature beside sprinkler in the basement fire room in Test PF-06

Figure 90 shows the temperature profiles measured in the basement fire room. Prior to the sprinkler activation, the peak temperatures at the 2.4 m height were 62°C at the NW quadrant, 59°C at the NE quadrant, 81°C at the SW quadrant, and 76°C at the SE quadrant. The peak temperatures at the window were 126°C. After sprinkler activation, the temperatures in the fire room quickly reduced to close to the ambient temperature. Figure 90 also shows the heat flux measured at the west wall (near the centre, 2.05 m above the floor). The maximum heat flux was 2 kW·m^{-2} prior to the sprinkler activation. The sprinkler discharge was able to suppress the

104

fire and keep the temperature in the fire room close to the ambient level. Because the temperature at the window did not reach 300°C, the noncombustible window covering panel was not removed during the experiment.
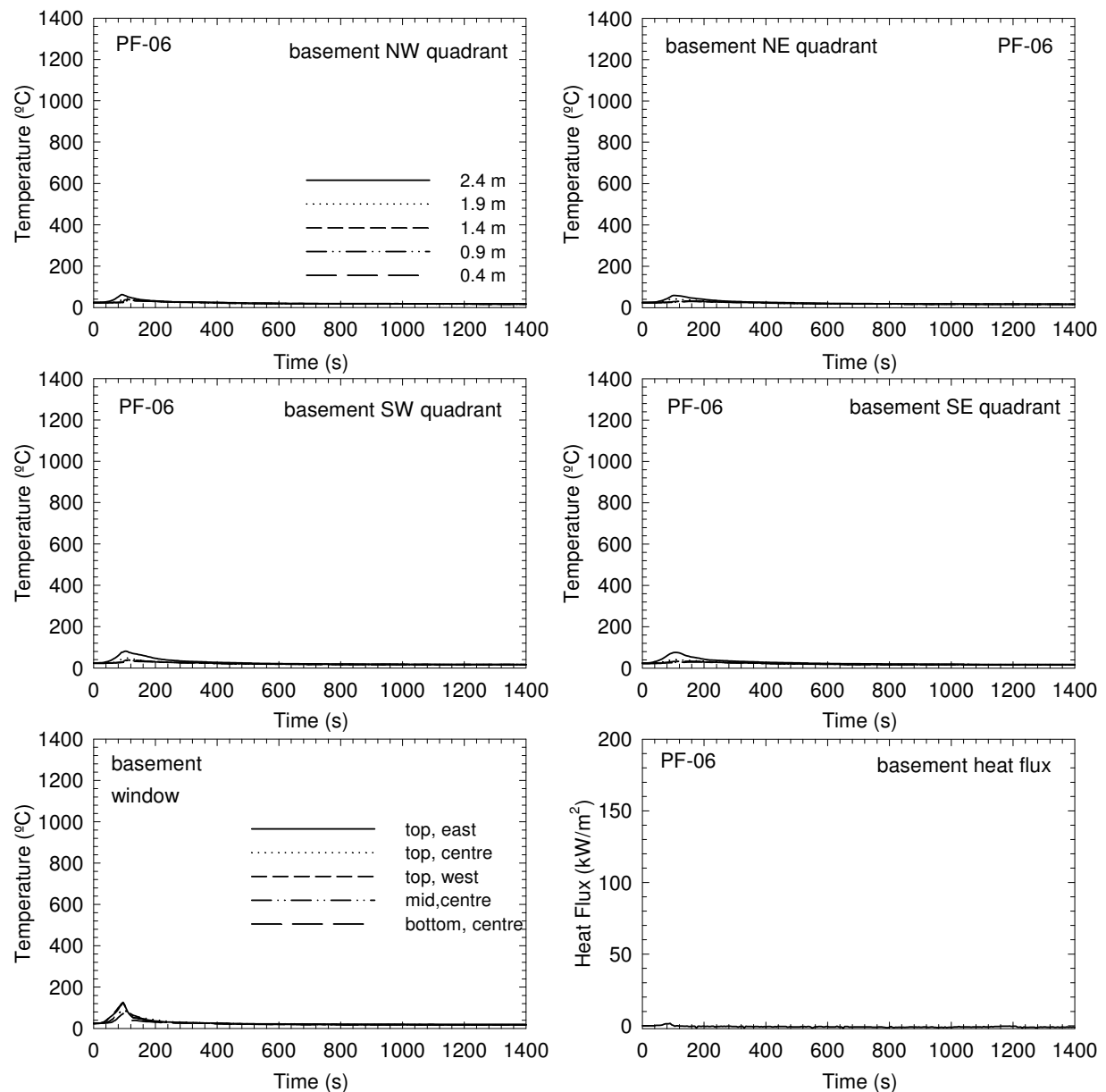
Figure 90. Temperatures and heat flux in the basement fire room in Test PF-06

4.8.3   Visual Obscuration

The optical density was measured at 0.9 and 1.5 m heights (simulating the height of the nose/mouth of an average height individual crawling and standing, respectively) above the floor on the first and second storeys. Figure 91 shows the optical density-time profiles; OD remained under 0.15 m^{-1} throughout the upper storeys during the experiment. At this smoke level, a normal person should still be able to see the surroundings.

NRC·CNRC
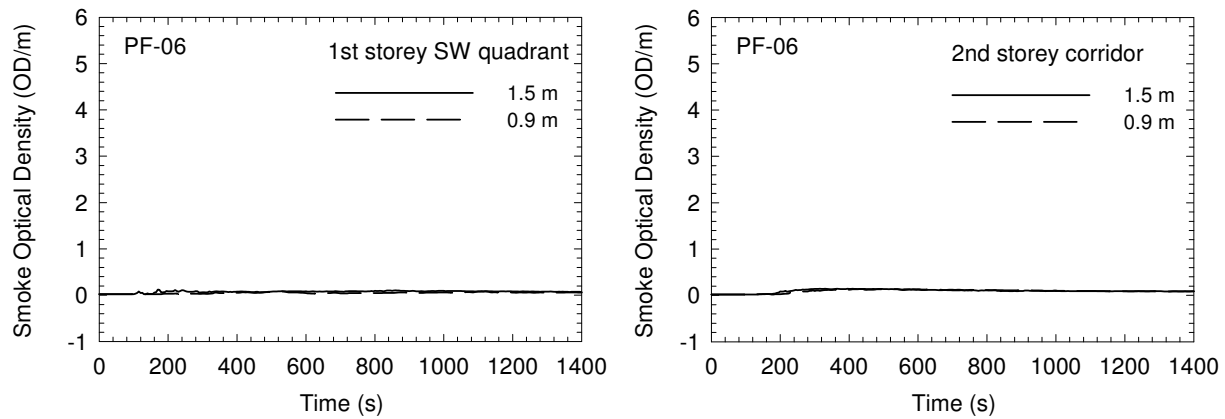
Figure 91. Smoke optical density measurements in Test PF-06

4.8.4   Gas Measurements and Analysis (CO, CO_2 and O_2)

Figure 92 shows the CO, CO_2 and O_2 concentrations at the southwest quarter point on the first storey and at the centre of the corridor on the second story during the experiment. The oxygen concentrations were above 20.5%. The CO_2 concentrations were below 0.25%, and CO below 0.01%. These conditions would not cause incapacitation or any reduction in tenable conditions.
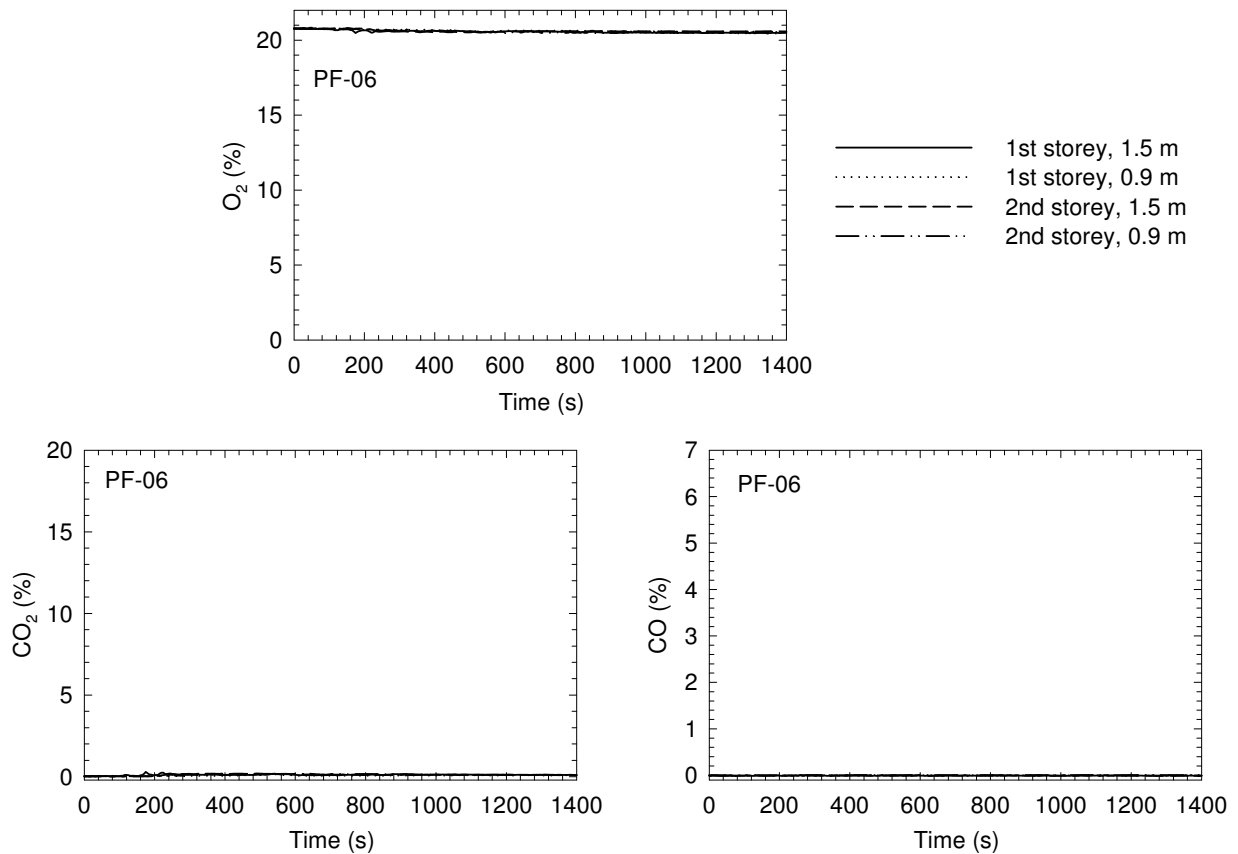
Figure 92. CO, CO_2 and O_2 concentrations in Test PF-06

106

4.8.5 Temperature-Time Profiles on the Upper Storeys

Figure 93 and Figure 94 show temperature profiles measured on the first and second storeys during the experiment. On the first storey, the maximum temperature of 48°C was measured at the doorway to the basement prior to the sprinkler activation; the maximum temperatures at the four quadrants were less than 35°C. After sprinkler activation, the temperatures on the first storey quickly reduced to the ambient temperature. On the second storey, there was minimal temperature change. These conditions would not cause incapacitation or any reduction in tenable conditions.
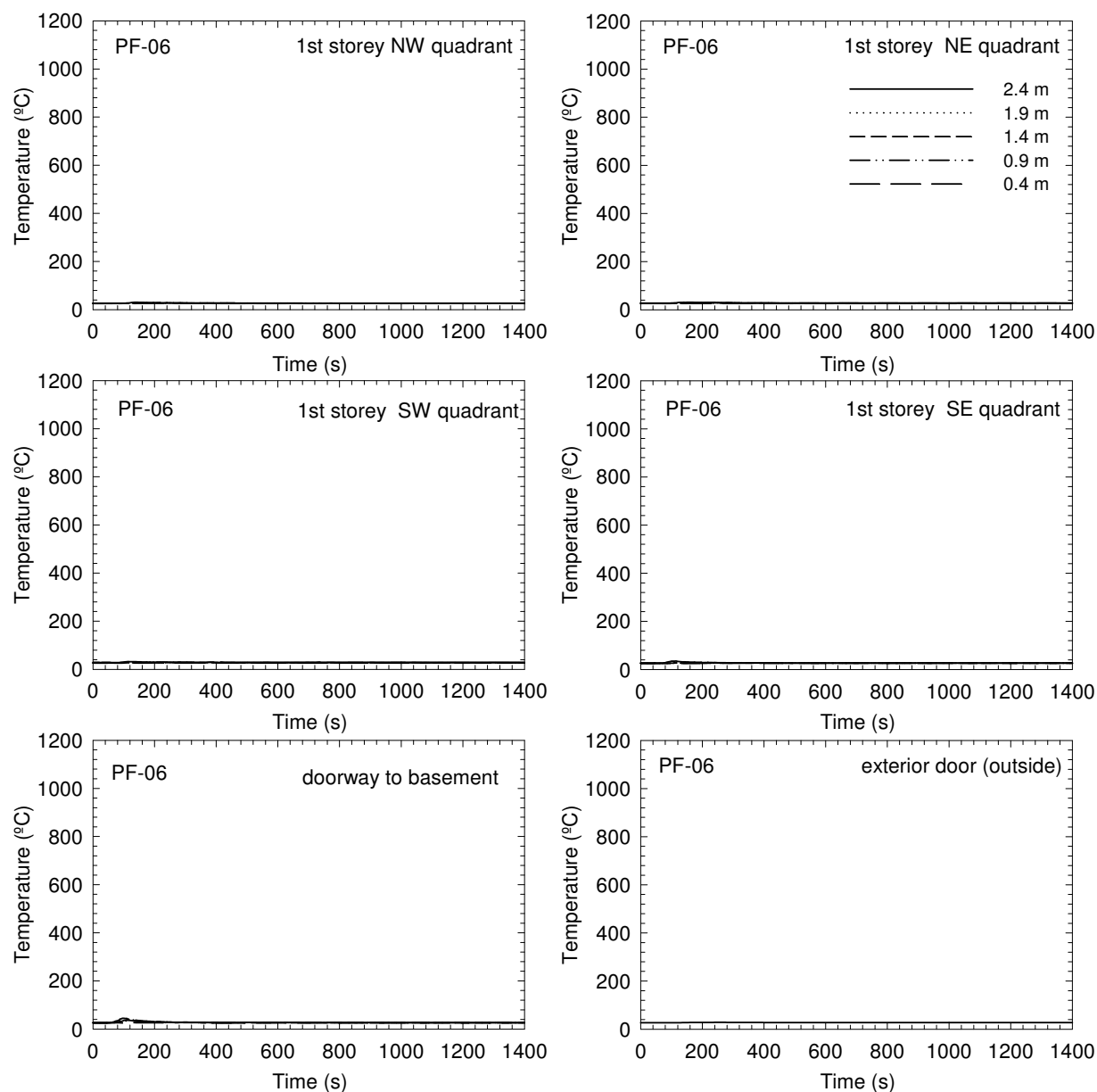
Figure 93. Temperatures on the first storey in Test PF-06
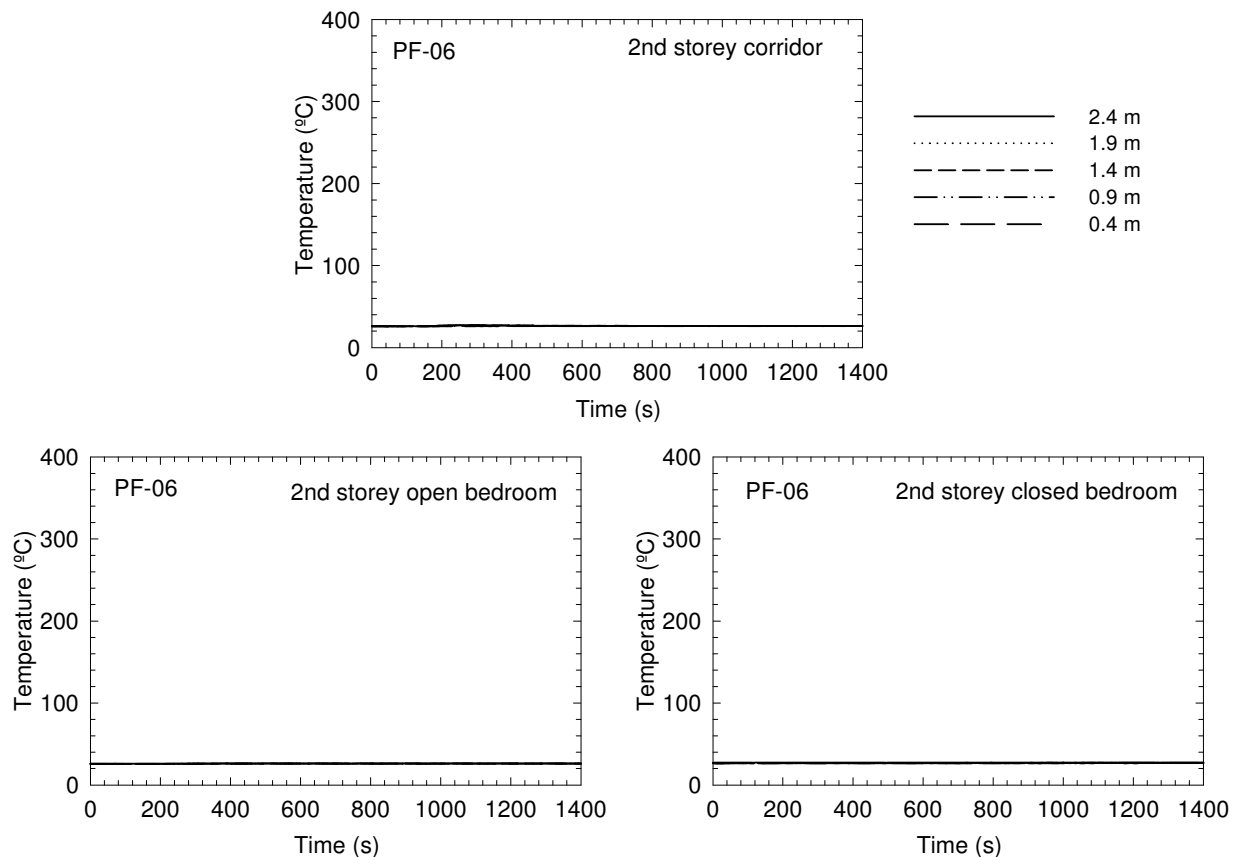
Figure 94. Temperatures on the second storey in Test PF-06

4.8.6 Performance of Test Assembly

A floor system provides an egress route for occupants and its structural integrity directly impacts the safe evacuation of the occupants from the house during a fire emergency. During the fire experiment, the conditions of the test assembly were monitored.

Figure 95 shows temperatures in the cavities of the test assembly. The thermocouples installed in the six sections of the floor cavities monitored the temperatures within the cavities and provided an indication of the effectiveness of residential sprinkler protection for the test assembly. Depending on the position, the maximum temperatures in the floor cavities were in the range of 46-160°C prior to the sprinkler activation. After sprinkler activation, the temperatures in the floor cavities quickly reduced to ambient temperature. There was no ignition of the test assembly during the experiment.

NRC·CNRC
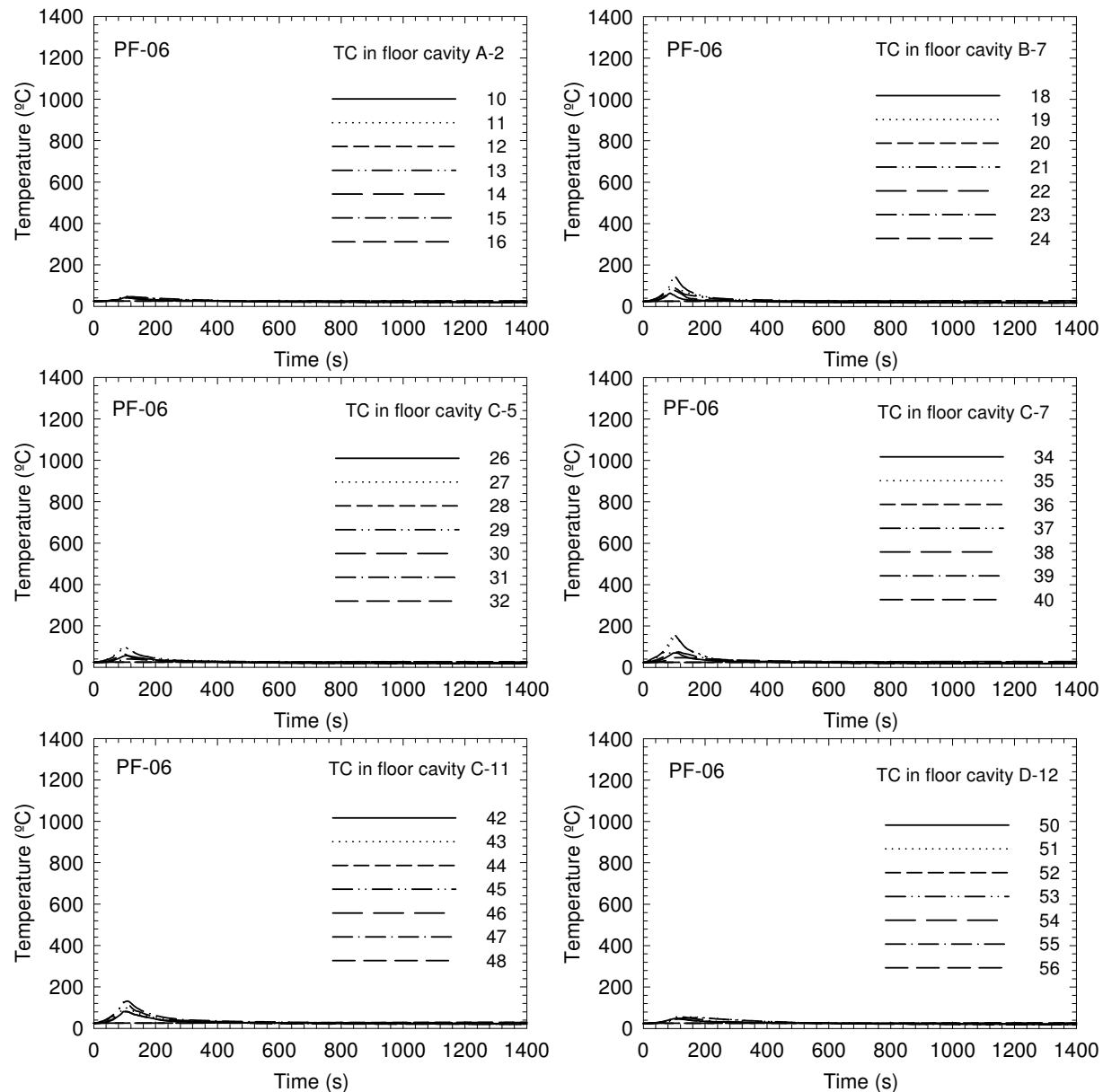
Figure 95. Temperatures in floor cavities in Test PF-06

Figure 96 shows results of the measurements using thermocouples, flame-sensing devices and deflection devices on the unexposed side the test assembly on the first storey.

The temperature measurements by nine thermocouples under insulated pads on top of the subfloor (on the first storey) are analogical to the measurements in the standard fire-resistance test with respect to thermocouple type, installation and layout [29]. There were also four bare thermocouples installed on top of the subfloor. The increase in these temperatures was less than 7°C during the experiment.

The floor deflection of the test assembly was measured at nine points located in the central area of the test assembly just above the fuel package where the impact of the fire on the assembly

was anticipated to be the greatest. There was no floor deflection of the test assembly during the experiment.

The flame-sensing device [19] at the central tongue-and-groove joint on the unexposed side of the OSB subfloor provided detection of flame penetration through the test assembly. There was no noticeable change in the voltage signal.
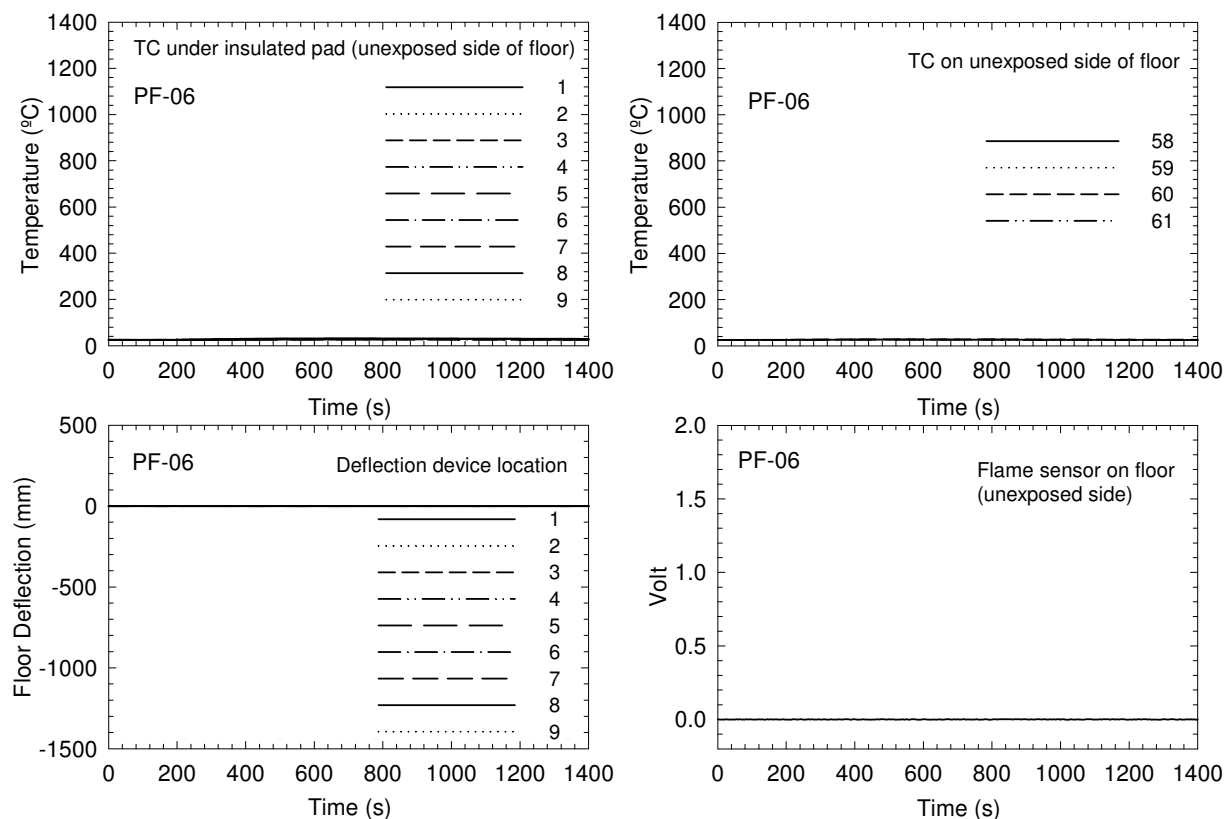
Figure 96. Temperatures, deflections and flame sensor on the unexposed side of the assembly on the first storey in Test PF-06

4.8.7 Sequence of Events

Table 26 summarizes the results for Test PF-06. The incapacitation conditions were not reached. Visual observation after the experiment confirmed that, other than soot deposition from the burning of the fuel package, no ignition or damage occurred with the test assembly and the CPVC piping system.

For comparison purposes, Table 26 also shows data from the test conducted in Phase 1 using the same floor structure but no protection (UF-07). The data indicates that the residential sprinkler system kept tenable conditions and protected the structural integrity of the test assembly during the experiment.

NRC·CNRC

Table 26. Summary of Sequence of Events in Test PF-06 (in seconds)

Assembly Type	Test	First Alarm	OD = 2 m^{-1}	FED=0.3-1 1st storey	FED=0.3-1 2nd storey	Structural Failure
Sprinkler protected wood trusses	PF-06*	55	not reached	not reached	not reached	not reached
Unprotected wood trusses	UF-07	40	170	**192-207**	*230*-**255**	325

Notes:
1. *The sprinkler activated at 87 s;
2. Values determined using the measurements at 1.5 m height (for gas concentrations and OD) or 1.4 m height (for temperatures);
3. The number with the *Italic* typeface represents the calculated time for reaching the CO incapacitation dose, while the number in **bold** represents the calculated time for reaching the heat incapacitation dose, whichever occurred first.

Since this PF-06 test assembly survived the primary fire experiment (Test PF-06), two additional fire experiments (secondary Tests PF-06B and PF-06C) were conducted using this test assembly. Test PF-06C was conducted with the assembly protected with a regular gypsum board ceiling (see next section of this report). Test PF-06B was conducted with the fuel package moved to the southeast corner of the fire room (see separate report for details of Test PF-06B [18]).

4.9   Metal-Web Wood Truss Assembly with Gypsum Protection – Test PF-06C

The metal-web wood truss assembly that survived both of the sprinklered Tests PF-06 (see Section 4.8 of this report) and PF-06B (see separate report [18]) was used again in Test PF-06C but with the automatic residential sprinkler system removed and regular gypsum board installed on the basement side of the assembly, i.e. finished gypsum board ceiling in the fire room (see Figure 97).

Regular gypsum board was installed on the basement side of the PF-06 assembly by being fastened directly to the bottom chords of the metal-web wood trusses. The gypsum board was 12.7 mm thick, with a full sheet size of 1.2 x 2.4 m. Figure 39 and Figure 98 show details of the gypsum board installation and layout, end connection and the supporting beams. The joints of the gypsum board were finished with joint compound and tape. The screw pattern and description of screws used to fasten the gypsum board to the trusses and rim board (header) are shown in Figure 10.

NRC·CNRC
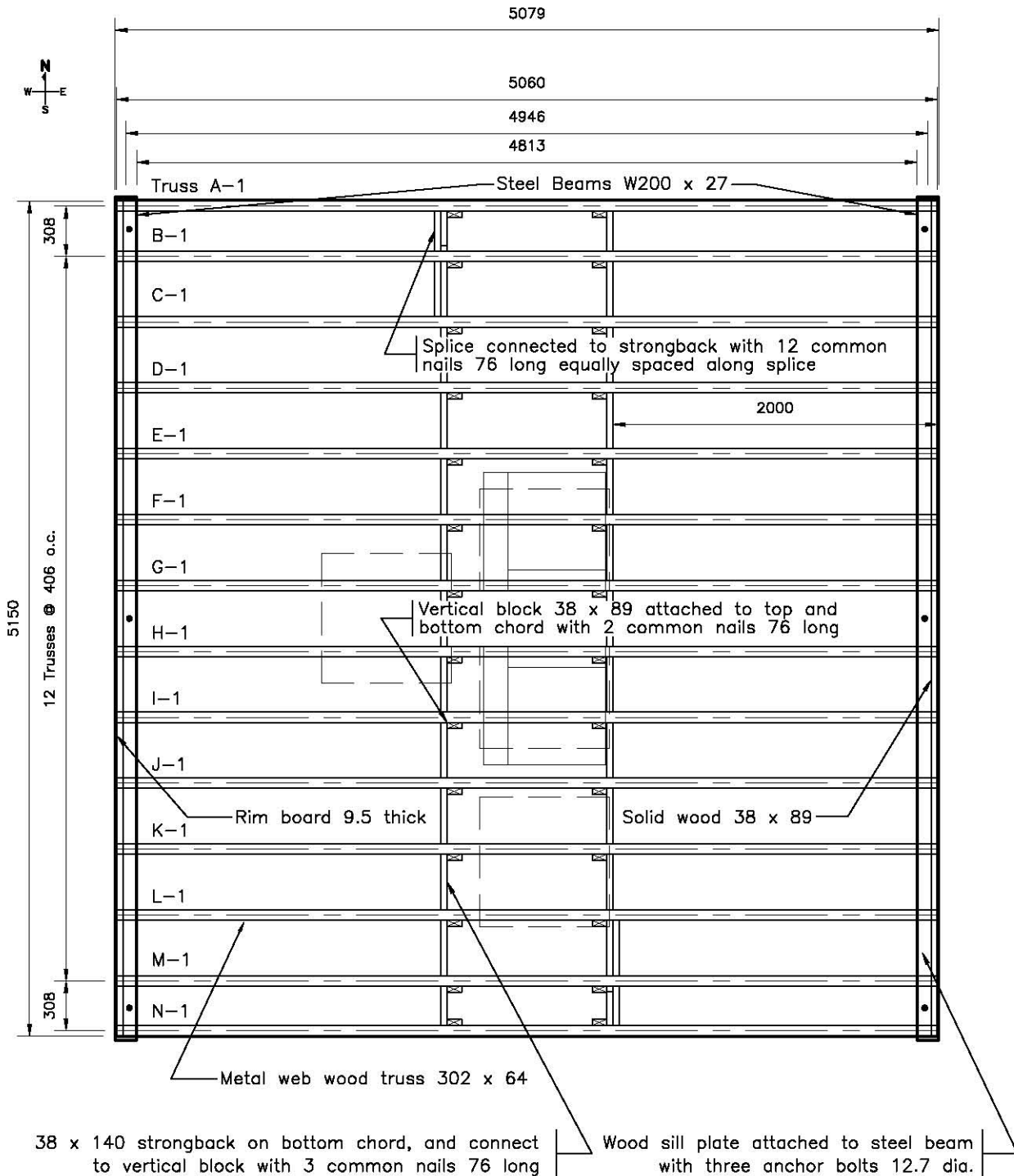
Figure 97. Metal-web wood truss layout details for Tests PF-06 and PF-06C (all dimensions in mm)

NRC·CNRC
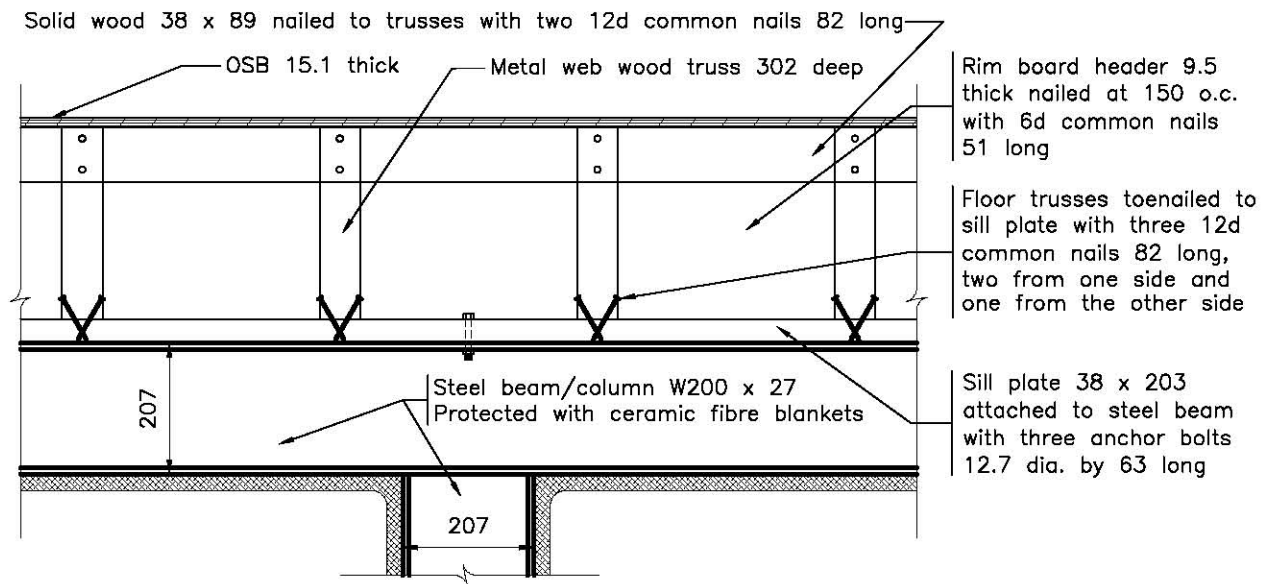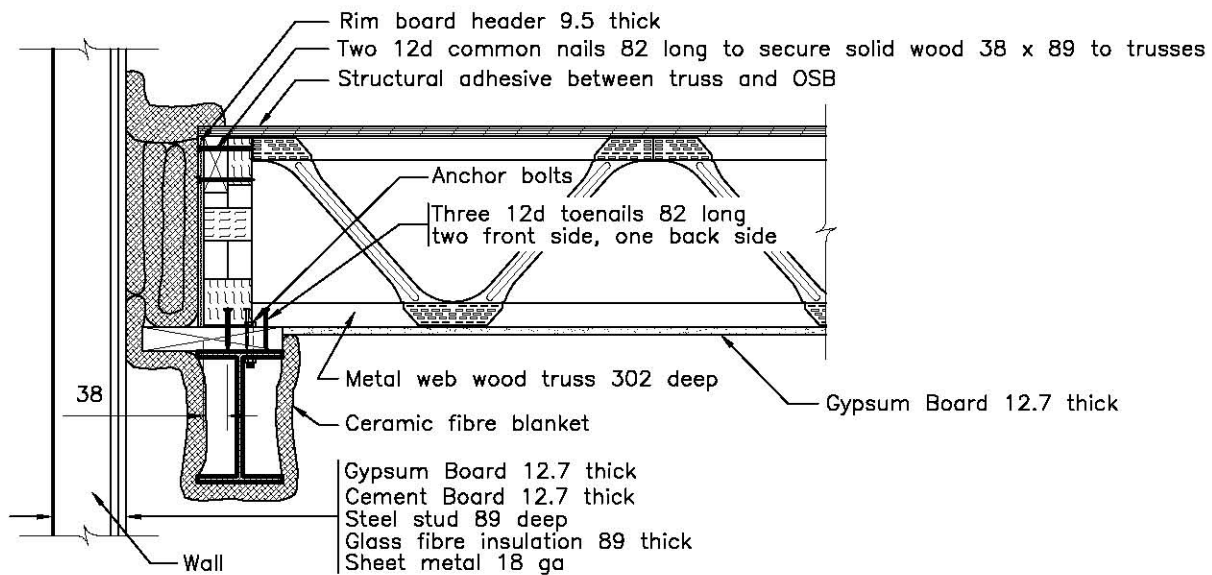
Figure 98. Details of end connection and supports for Test PF-06C (gypsum protection) (all dimensions in mm)

NRC·CNRC

The thermocouples for measuring temperatures throughout the assembly were located on the unexposed side and in the cavities of the assembly as shown in Figure 87 and Figure 99.

58
12 13 14
11   15
17
10   16
Section A–2

20 21 22
19   23
25
18   24
Section B–7

60
28 29 30
27   31
33
26   32
Section C–5

36 37 38
35   39
41
34   40
Section C–7

44 45 46
43   47
49
42   48
Section C–11

61
52 53 54
51   55
57
50   56
Section D–12
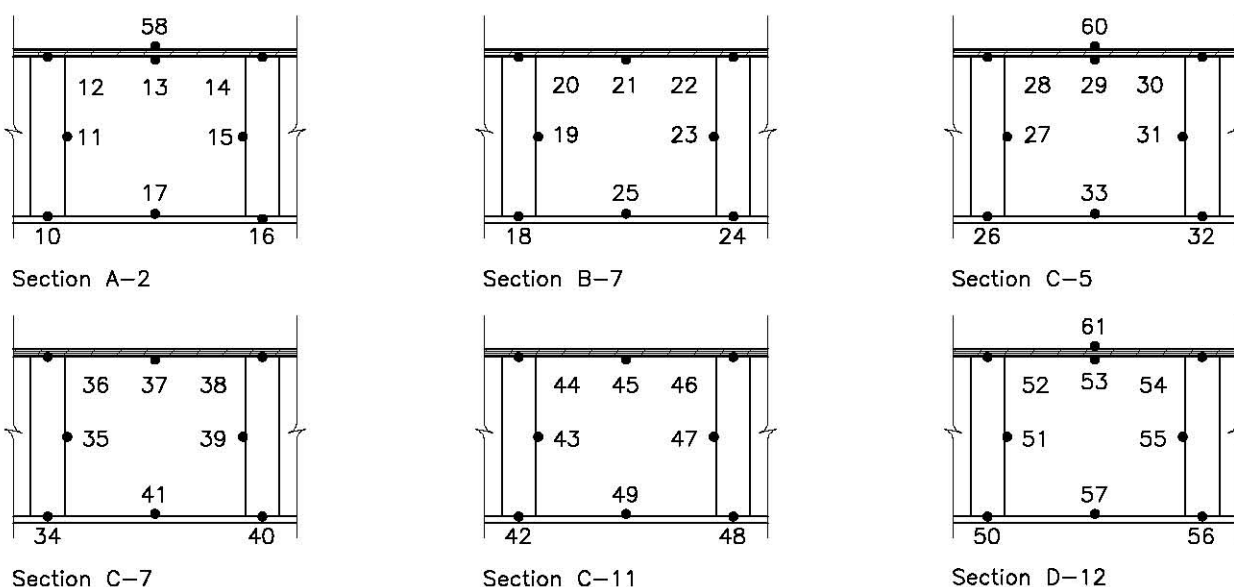
Figure 99. Thermocouples installed in the sections shown in Figure 87 (Test PF-06C only)

4.9.1   Fire Development in Basement

Figure 100 shows the temperature profiles measured in the basement fire room. The polyurethane foam used for the mock-up sofa dominated the initial fire growth. The temperatures at the window quickly reached 300°C and the noncombustible window covering panel was removed at 140 s. The temperatures at the 2.4 m height exceeded 600°C within 170-190 s, indicating that the fire room reached flashover conditions. The fast development of the fire from ignition to attainment of the first temperature peak was consistent with the experiments in Phase 1 of FPH research. Following this initial stage of fire growth, the fire became wood-crib-dominated. There was a quick transition from a well-ventilated flaming fire to an under-ventilated fire. Figure 100 also shows the heat flux measured at the west wall (near the centre, 2.05 m above the floor). The maximum heat flux was 110 kW·m^{-2} near the end of the experiment.

NRC·CNRC
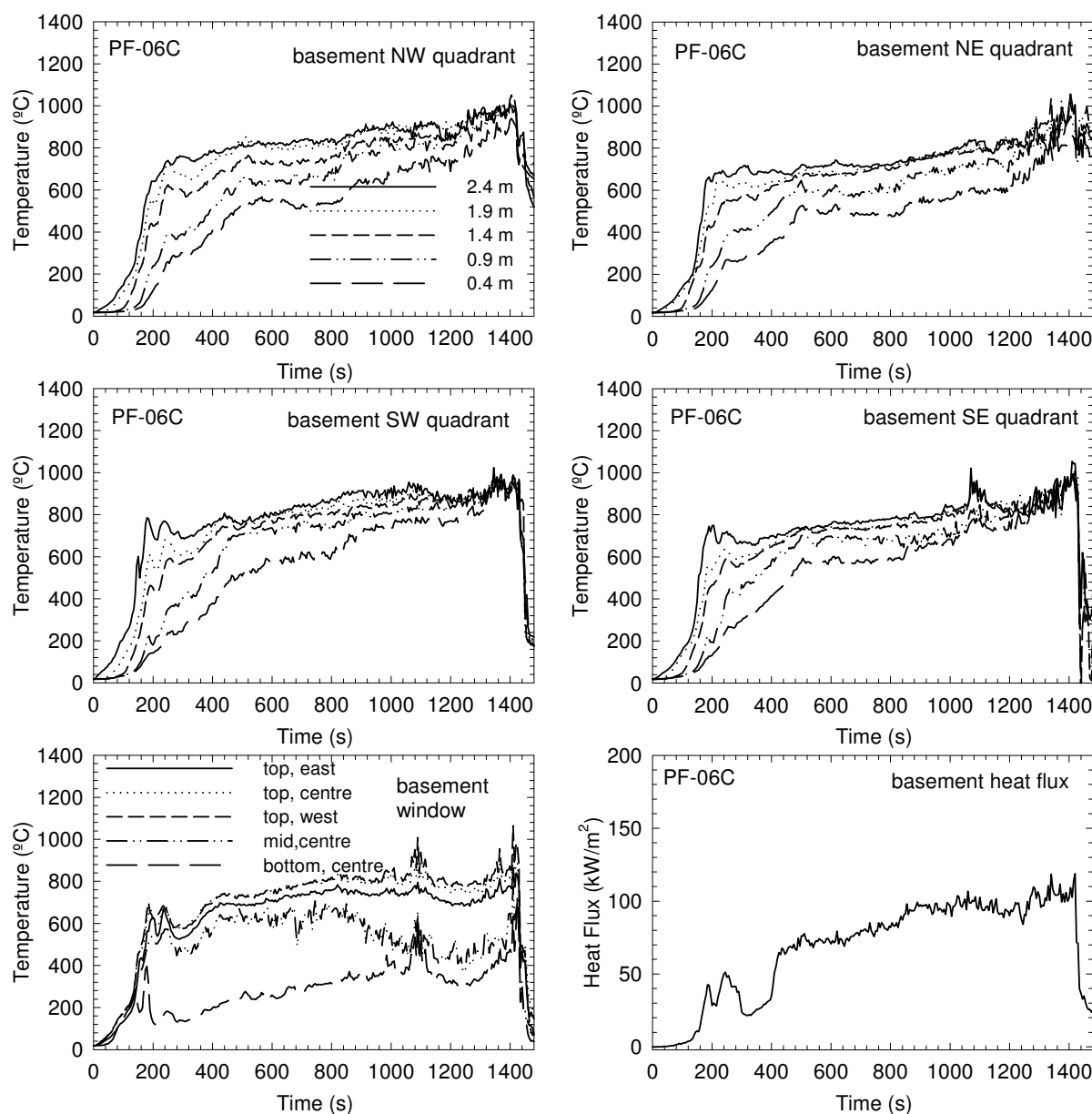
Figure 100. Temperatures and heat flux in the basement fire room in Test PF-06C

4.9.2 Visual Obscuration

The optical density was measured at 0.9 and 1.5 m heights (simulating the height of the nose/mouth of an average height individual crawling and standing, respectively) above the floor on the first and second storeys. Table 27 shows the times to reach OD = 2 m^{-1}. Figure 101 shows the optical density-time profiles. It must be pointed out that the video records show no signs of decrease in the optical density after the first peak, indicating that the smoke density meters started the self-purging cycle after the first peak. The smoke density meter has an operation temperature limit of 80°C in its gas chamber; when this temperature is reached, the

NRC·CNRC

flow is reversed to cool the chamber to protect the electronic components. In this experiment, only the initial part of the curves (up to the first peaks) represents valid measurements.

Table 27. Time (in seconds) to the Smoke Optical Density Limit in Test PF-06C

Test PF-06C	1st storey SW quadrant	2nd storey corridor
OD =	**2 m⁻¹**	**2 m⁻¹**
1.5 m above floor	225	245
0.9 m above floor	n.a	275

Note:
1. n.a. – not available (purging cycle started).
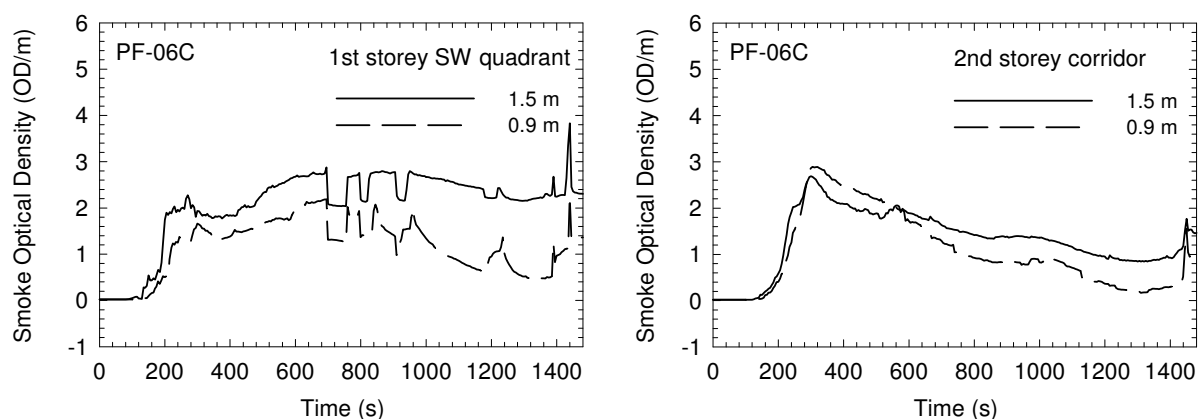
Figure 101. Smoke optical density measurements in Test PF-06C

4.9.3   Gas Measurements and Analysis (CO, CO₂ and O₂)

Figure 102 shows the CO, CO_2 and O_2 concentration-time profiles measured at the southwest quarter point on the first storey and at the centre of the corridor on the second story during the experiment. Within approximately 500 s, oxygen was diminished to below 12% and CO_2 increased to above 8%, which could cause incapacitation and lead to loss of consciousness rapidly due to lack of oxygen alone or due to the CO_2 asphyxiant effect alone [22]. The concentrations were below 8% O_2 and above 12% CO_2 near the end of the experiment. The tenability analysis indicated that the toxic effect of CO would be capable of causing incapacitation at an earlier time than the effect of O_2 vitiation and the asphyxiant effect of CO_2. The times to reach the specified FED for exposure to O_2 vitiation, CO_2 and CO are shown in Table 28.

NRC·CNRC
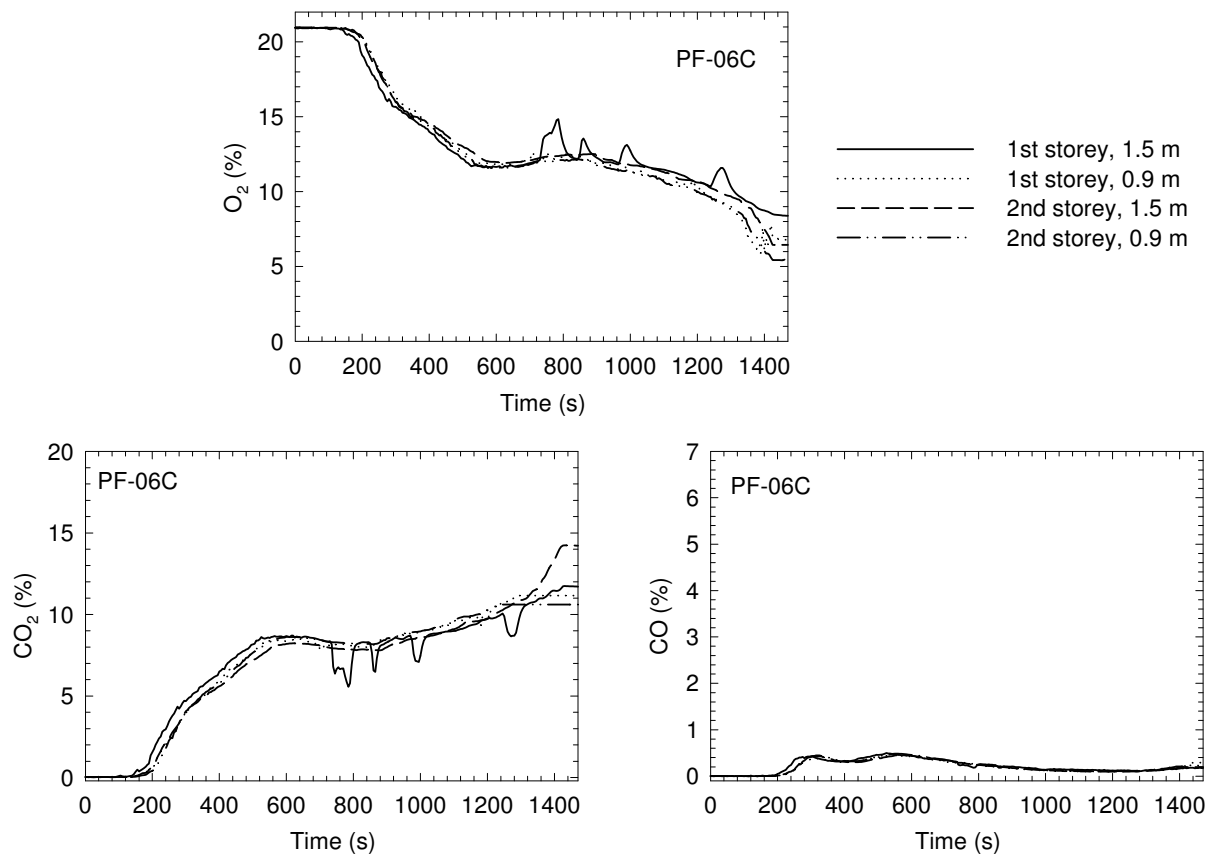
Figure 102. CO, CO_2 and O_2 concentrations in Test PF-06C

Table 28. Time (in seconds) to the Specified FED for Exposure to O_2 Vitiation, CO_2 and CO in Test PF-06C

Fractional Effective Dose	FED = 0.3	FED = 1.0
CO alone – 1st storey	395	780
CO with CO_2 hyperventilation – 1st storey	300±25	430±60
Low O_2 hypoxia – 1st storey	950	1435
CO alone – 2nd storey corridor	420	850
CO with CO_2 hyperventilation – 2nd storey corridor	325±25	470±60
Low O_2 hypoxia – 2nd storey corridor	990	1400
High CO_2 hypercapnia – 1st storey	515	765
High CO_2 hypercapnia – 2nd storey corridor	570	880

Note:
1. Values determined using concentrations at 1.5 m height.

NRC·CNRC

4.9.4   Temperature-Time Profiles on the Upper Storeys

Figure 103 and Figure 104 show temperature profiles measured on the first and second storeys during the experiment. The temperatures depended on the locations inside the test house. In the bedroom with the door closed, the temperatures never exceeded 60°C during the experiment.
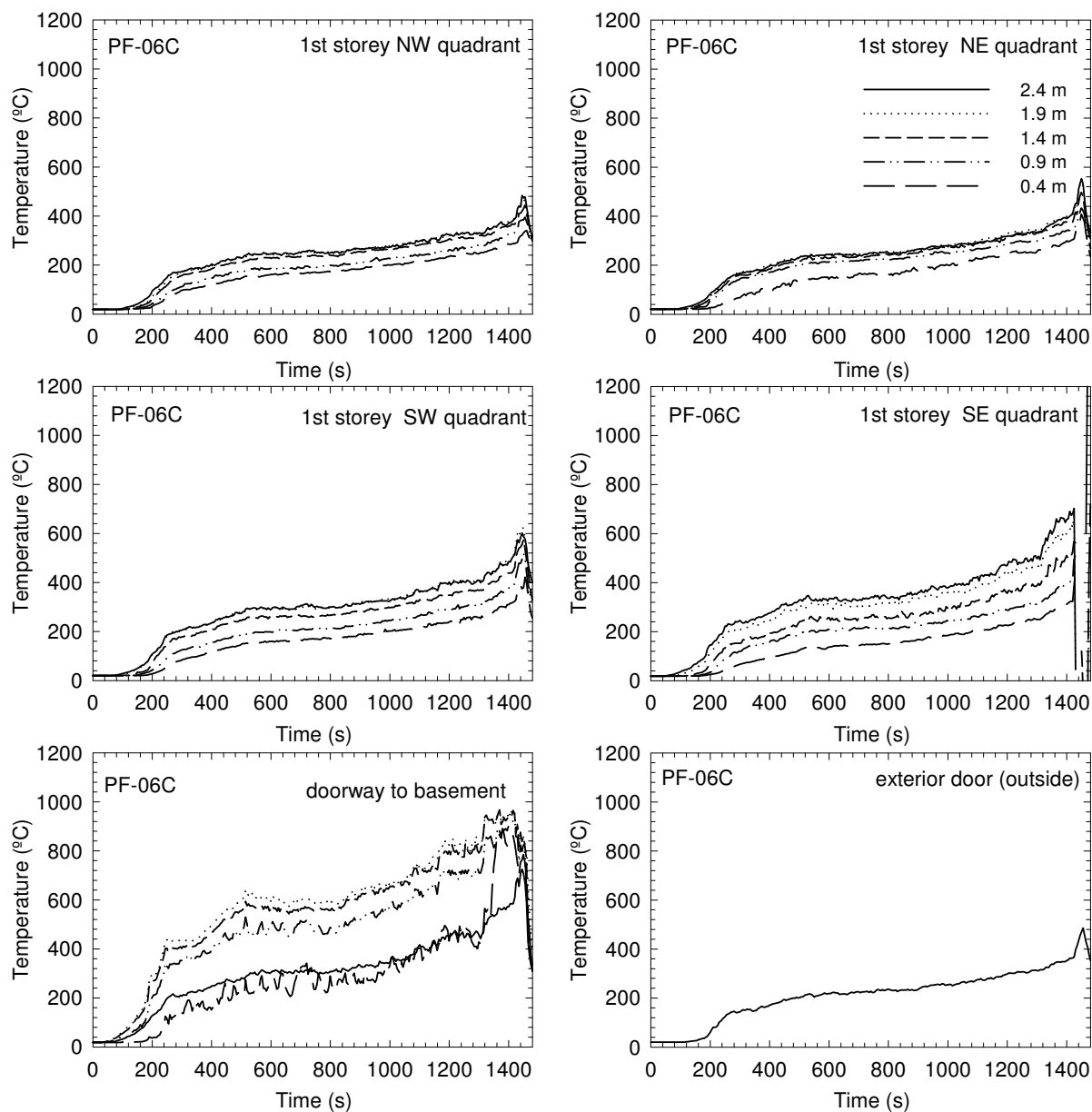
Figure 103. Temperatures on the first storey in Test PF-06C

NRC·CNRC
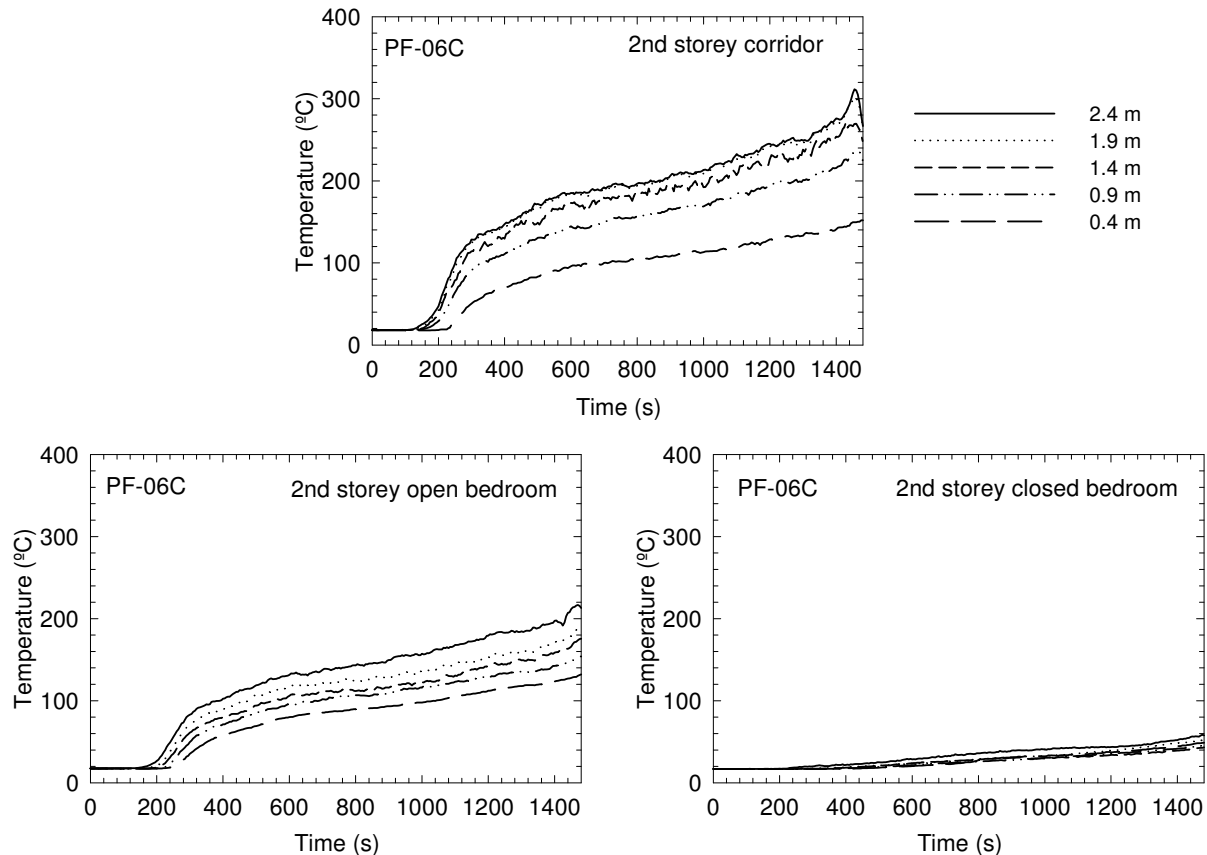
Figure 104. Temperatures on the second storey in Test PF-06C

In the closed bedroom, heat exposure would not cause incapacitation. On the first storey, in the corridor or in the open bedroom on the second storey, the calculated times to incapacitation due to exposure to the convected heat are given in Table 29 for FED = 0.3 and 1. The calculated times to reach the heat incapacitation doses on the first storey were shorter than those for CO exposure; the time difference for FED to change from 0.3 to 1.0 due to the heat exposure was also shorter than that for CO exposure. In the corridor on the second storey, the calculated times to reach the incapacitation doses for heat exposure were similar to those for CO exposure.

Table 29. Time (in seconds) to the Specified FED for Convected Heat in Test PF-06C

Fractional Effective Dose	FED = 0.3	FED = 1.0
1st storey SE quadrant	270	335
1st storey SW quadrant	260±10	315±15
1st storey NE quadrant	280	345
1st storey NW quadrant	285	350
2nd storey corridor	345±20	460±30
2nd storey open bedroom	545	800
2nd storey closed bedroom	not reached (FED < 0.04)	not reached (FED < 0.04)

Note:
1. Values determined using temperatures at 1.4 m height.

119

4.9.5 Estimation of Time to Incapacitation

Table 30 summarizes the results of tenability analysis with the estimated times to the onset of various conditions for Test PF-06C. Smoke obscuration was the first hazard to arise. The calculated time for reaching the specific FED either due to the heat exposure or due to the CO exposure (exacerbated by CO_2-induced hyperventilation), whichever occurred first, is listed in Table 30. Heat exposure reached the specific FED on the first storey at times shorter than for CO exposure. On the second storey (in the corridor), CO exposure and heat exposure reached the specific FED at similar times and the time difference for heat exposure and CO exposure to reach the specific FED was not significant. Note that for the closed bedroom on the second storey, based on the temperatures and the heat exposure calculation, the conditions in the closed bedroom would not reach untenable conditions.

Table 30. Summary of Estimation of Time to Specified FED and OD (in seconds) for Test PF-06C

Test	OD = 2 m^{-1}		FED = 0.3		FED = 1	
	1st storey	2nd storey	1st storey	2nd storey	1st storey	2nd storey
PF-06C	225±5	245±5	**260±10**	*325±25*	**315±15**	**460±30**

Notes:
1. Values determined using the measurements at 1.5 m height (for gas concentrations and OD) or 1.4 m height (for temperatures);
2. The number with the *Italic* typeface represents the calculated time for reaching the CO incapacitation dose, while the number in **bold** typeface represents the calculated time for reaching the heat incapacitation dose, whichever occurred first.

4.9.6 Performance of Test Assembly

A floor system provides an egress route for occupants and its structural integrity directly impacts the safe evacuation of the occupants from the house during a fire emergency. During the fire experiment, the conditions of the test assembly were monitored.

Figure 105 shows temperatures in the cavities of the test assembly. The thermocouples installed in the six sections of the floor cavities monitored the temperatures within the cavities and provided an indication of the effectiveness of gypsum board protection for the test assembly. The moment that the temperatures in the floor cavities approached the fire room temperature indicates the loss of the gypsum board membrane protection for the floor structure. This happened after 900 s depending on the position. This was accompanied by a slow but regular increase in room temperatures in the basement (Figure 100), which was likely a result of an increase in the burning rate due to the additional fuel from ignited areas of the floor assembly that were left exposed to the fire as portions of the gypsum ceiling fell off. Visual observation confirmed that small gypsum board pieces started falling from the centre of the ceiling shortly after 900 s, followed by larger gypsum board pieces falling. Then flame started to involve the joists and subfloor.

NRC·CNRC
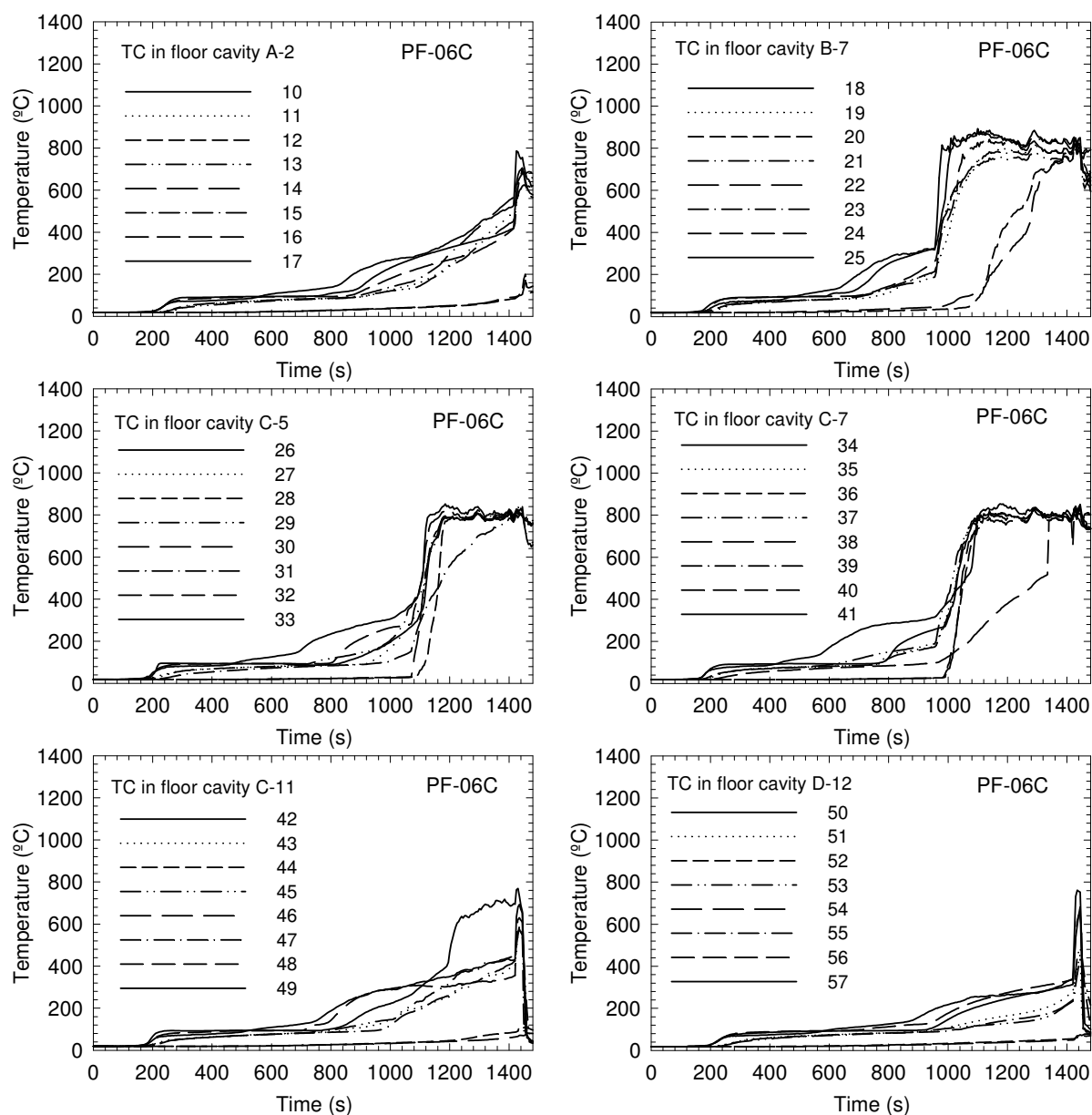
Figure 105. Temperatures in floor cavities in Test PF-06C

Figure 106 shows results of the measurements using thermocouples, flame-sensing devices and deflection devices on the unexposed side the test assembly on the first storey.

The floor deflection of the test assembly was measured at nine points located in the central area of the test assembly just above the fuel package where the impact of the fire on the assembly was anticipated to be the greatest. The test assembly reached the maximum floor deflection (downward) at 1420 s. This deflection occurred prior to the structural collapse of the test assembly. There were some positive signals from four of the nine measurement devices during the experiment, which may indicate some upward movement of the floor but this could not be confirmed.

NRC·CNRC

The temperature measurements by nine thermocouples under insulated pads on top of the subfloor (on the first storey) are analogical to the measurements in the standard fire-resistance test with respect to thermocouple type, installation and layout [29]. A rapid increase in temperature indicates that the test assembly was significantly breached. The subsequent rapid decrease in temperature was due to the termination of the experiment by extinguishing the fire with water. It is worth mentioning that on the basis of temperature, failure under standard fire-resistance test conditions is defined as a temperature rise of 140°C on average of the nine padded thermocouples or a temperature rise of 180°C at any single point. Based on this criterion, the structural failure time would be 1420 s (single-point temperature rise of 180°C). Four bare thermocouples were also installed on the unexposed side of the test assembly for temperature measurements.

The flame-sensing device [19] at the central tongue-and-groove joint on the unexposed side of the OSB subfloor provided detection of flame penetration through the test assembly. The figure shows a voltage signal after 1000 s and a large voltage spike after 1420 s, indicating the device being struck by flames that penetrated through the test assembly. Flame penetration through the test assembly is also a failure criterion in standard fire-resistance testing [29].

Figure 106. Temperatures, deflections and flame sensor on the unexposed side of the assembly on the first storey in Test PF-06C

Visual observation through the window opening of the fire room confirmed the structural failure being at 1424 s. There was a complete collapse of the test assembly into the basement due to the failure of the floor trusses. The OSB subfloor in many areas was still intact after the floor failure.

4.9.7   <u>Sequence of Events</u>

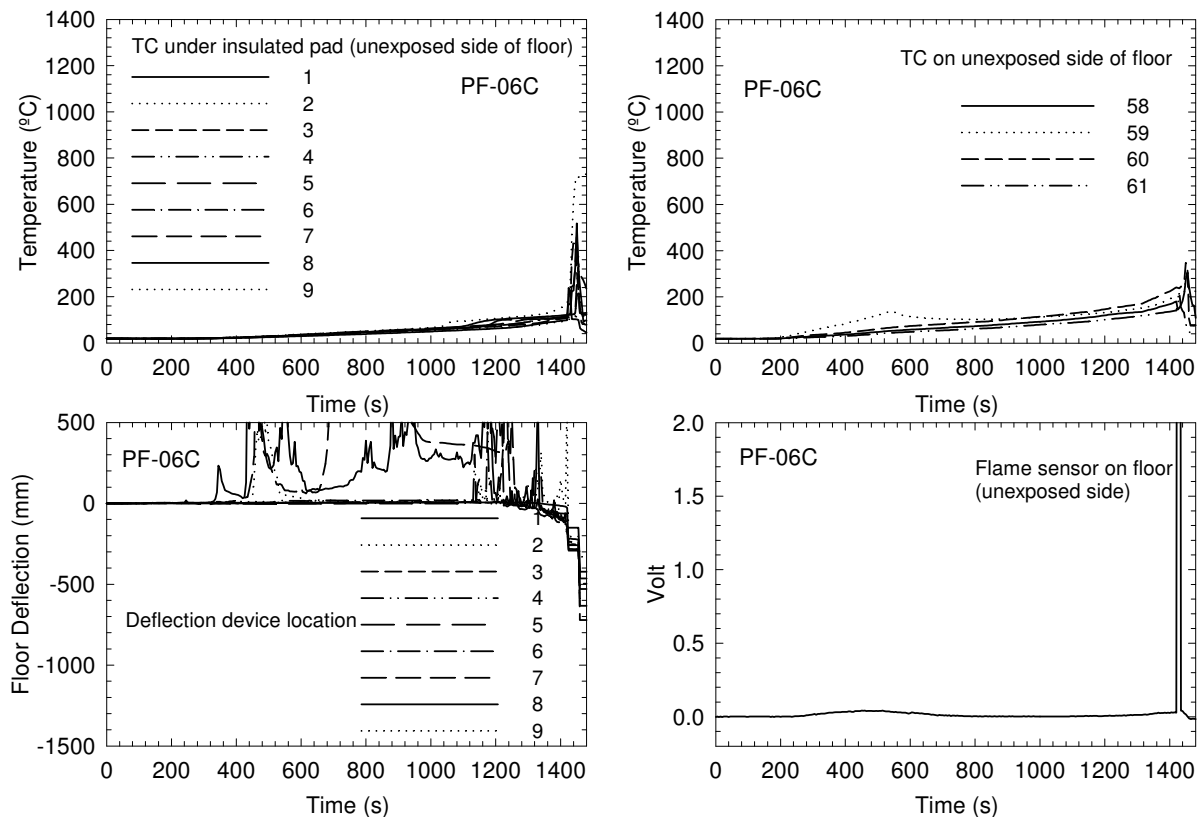Table 31 summarizes the chronological sequence of the fire events in Test PF-06C — fire initiation, smoke alarm activation, onset of untenable conditions, and structural failure of the test assembly. Smoke obscuration was the first hazard to arise. It must be pointed out that people with impaired vision could become disoriented earlier at an optical density lower than 2 m^{-1}. The incapacitation conditions were reached shortly after smoke obscuration. The structural failure of the test assembly occurred well after the untenable conditions were reached.

For comparison purposes, Table 31 also shows data from the test conducted in Phase 1 using the same floor structure but no gypsum board protection (UF-07). The data indicates that tenability conditions are only slightly improved whilst the structural performance is improved significantly with the protected ceiling/floor assembly.

Table 31. Summary of Sequence of Events in Test PF-06C (in seconds)

Assembly Type	Test	First Alarm	OD = 2 m^{-1}	FED=0.3-1 1st storey	FED=0.3-1 2nd storey	Structural Failure
Gypsum protected wood trusses	PF-06C	30	225-245	**260-315**	*325*-**460**	1424*
Unprotected wood trusses	UF-07	40	170	**192-207**	*230*-**255**	325

Notes:
1.   Values determined using the measurements at 1.5 m height (for gas concentrations and OD) or 1.4 m height (for temperatures);
2.   The number with the *Italic* typeface represents the calculated time for reaching the CO incapacitation dose, while the number in **bold typeface** represents the calculated time for reaching the heat incapacitation dose, whichever occurred first;
3.   *Values of the structural failure time of the test assemblies determined by visual observation;
     a.   The maximum deflection capacity of the measurement devices reached at 1420 s;
     b.   A single-point temperature rise of 180°C occurred on the unexposed side of the test assembly at 1420 s;
     c.   A large voltage spike detected using the flame-sensing device at 1420 s.

5   SUMMARY AND CONCLUSIONS

A series of full-scale fire experiments were conducted to investigate the fire performance of protected ceiling/floor assemblies in a basement fire scenario. Four types of floor systems (wood I-joist, steel C-joist and metal-web wood truss assemblies, as well as solid-sawn wood joist assemblies) were selected from the assemblies that had been tested in Phase 1 of the FPH research. The test assemblies were protected on the basement side with direct-applied regular gypsum board, residential sprinkler systems or a suspended ceiling. The study focused on the impact of the protection measures on the life safety and egress of occupants from the perspective of tenability for occupants and integrity of structural elements as egress routes. Table 32 shows a summary of the experimental results.

NRC·CNRC

Table 32. Timelines for All Experiments (in seconds)

Test	Test Assembly	First Alarm	OD = 2 m^{-1}	FED=0.3-1 1st storey	FED=0.3-1 2nd storey	Structural Failure	Increased Time for Structure*
Protection by Gypsum Board							
PF-01	Solid-sawn wood joist	27	192-257	**242-287**	*297-377*	1320	580
PF-02	Steel C-joist	30	345	**255-300**	**320**-420	1320	858
PF-04	Wood I-joist	30	200-220	**235-280**	*295-400*	1247	757
PF-06C	Metal-web wood truss	30	225-245	**260-315**	*325*-**460**	1424	1099
Protection by Suspended Ceiling							
PF-05	Wood I-joist	47	192-222	**220-255**	**282-342**	638	148
Protection by Residential Sprinklers							
PF-03	Wood I-joist	45	not reached	not reached	not reached	not reached	unlimited
PF-03B	Wood I-joist	34	not reached	not reached	not reached	not reached	unlimited
PF-06	Metal-web wood truss	55	not reached	not reached	not reached	not reached	unlimited

Notes:
1. Values determined using the measurements at 1.5 m height (for gas concentrations and OD) or 1.4 m height (for temperatures);
2. The number with the *Italic* typefacet represents the calculated time for reaching the CO incapacitation dose, while the number in **bold** typeface represents the calculated time for reaching the heat incapacitation dose, whichever occurred first;
3. * The increase in the time taken to reach structural failure from the unprotected assembly to the protected assembly.

For the experiments using the test assemblies with regular gypsum board protection (Tests PF-01, PF-02, PF-04 and PF-06C), the chronological sequence of the fire events is the same — fire initiation, smoke alarm activation, onset of untenable conditions, and structural failure of the test assemblies. The sequence was the same between the experiments conducted in this series of the full-scale fire experiments and also the same as the experiments conducted in Phase 1 of the FPH research for the fire scenario with the open basement doorway. Smoke obscuration was the first hazard to arise. The incapacitation (untenable) conditions were reached shortly after smoke obscuration. Compared to the experiments conducted in Phase 1 using the same floor structures without gypsum board protection, the times during which tenable conditions were maintained were similar or only slightly improved whilst the structural

NRC·CNRC

performance was improved significantly with the gypsum-board-protection. The times taken to reach structural failure for the gypsum-board-protected ceiling/floor assemblies were much longer than those Phase 1 experiments with no protection. Table 32 shows the increase in the time taken to reach structural failure from the unprotected assemblies (tested in Phase 1 of the FPH research) to the protected assemblies. Also, with regular gypsum board protection, all test assemblies provided similar durations of structural fire endurance under the test fire scenario.

The experiment with the suspended ceiling (Test PF-05) followed the same sequence of fire events and similar tenability conditions compared with the gypsum-board-protected assemblies. The benefit of the suspended ceiling as a protection measure was marginal. The structural collapse of the test assembly was only delayed by 148 s, compared to the same test assembly without protection.

For the experiments with residential sprinkler-protected assemblies (Tests PF-03, PF-03B and PF-06), the residential sprinkler systems protected the structural integrity of the test assemblies and effectively suppressed the fire. No ignition, structural failure or damage occurred with the test assemblies during the experiments. The residential sprinkler systems maintained tenable conditions in the test house during the experiments. Additional experiments were conducted using the single-sprinkler arrangement with a more challenging fuel package and/or fire location. The results of these experiments are documented in a separate report [18].

6   REFERENCES

1. Bénichou, N., Su, J.Z., Bwalya, A.C., Lougheed, G.D., Taber, B.C., Leroux, P., Kashef, A., McCartney, C., Thomas, J.R., "Fire Performance of Houses, Phase I, Study of Unprotected Floor Assemblies in Basement Fire Scenarios, Part 1 - Results of Tests UF-01 and UF-02 (Solid Wood Joists)," Institute for Research in Construction, National Research Council of Canada, Research Report 246, 2009, http://www.nrc-cnrc.gc.ca/obj/irc/doc/pubs/rr/rr246/rr246.pdf

2. Su, J.Z., Bénichou, N., Bwalya, A.C., Lougheed, G.D., Taber, B.C., Leroux, P., Kashef, A., Thomas, J.R., "Fire Performance of Houses, Phase I, Study of Unprotected Floor Assemblies in Basement Fire Scenarios, Part 2 - Results of Tests UF-03 and UF-09 (Wood I-Joists A)," Institute for Research in Construction, National Research Council of Canada, Research Report 247, 2009, http://www.nrc-cnrc.gc.ca/obj/irc/doc/pubs/rr/rr247/rr247.pdf

3. Bénichou, N., Su, J.Z., Bwalya, A.C., Lougheed, G.D., Taber, B.C., Leroux, P., Kashef, A., Thomas, J.R., "Fire Performance of Houses, Phase I, Study of Unprotected Floor Assemblies in Basement Fire Scenarios, Part 3 - Results of Test UF-04 (Steel C-Joists)," Institute for Research in Construction, National Research Council of Canada, Research Report 248, 2009, http://www.nrc-cnrc.gc.ca/obj/irc/doc/pubs/rr/rr248/rr248.pdf

4. Su, J.Z., Bénichou, N., Bwalya, A.C., Lougheed, G.D., Taber, B.C., Leroux, P., Kashef, A., Thomas, J.R., "Fire Performance of Houses, Phase I, Study of Unprotected Floor Assemblies in Basement Fire Scenarios, Part 4 - Results of Test UF-05 (Metal-Plate Wood Trusses)," Institute for Research in Construction, National Research Council of Canada, Research Report 249, 2009, http://www.nrc-cnrc.gc.ca/obj/irc/doc/pubs/rr/rr249/rr249.pdf

5. Bénichou, N., Su, J.Z., Bwalya, A.C., Lougheed, G.D., Taber, B.C., Leroux, P., Thomas, J.R., "Fire Performance of Houses, Phase I, Study of Unprotected Floor Assemblies in Basement Fire Scenarios, Part 5 - Results of Tests UF-06, UF-06R and UF-06RR (Wood

NRC·CNRC

I-Joists B)," Institute for Research in Construction, National Research Council of Canada, Research Report 250, 2009, http://www.nrc-cnrc.gc.ca/obj/irc/doc/pubs/rr/rr250/rr250.pdf

6. Su, J.Z., Bénichou, N., Bwalya, A.C., Lougheed, G.D., Taber, B.C., Leroux, P., Thomas, J.R., "Fire Performance of Houses, Phase I, Study of Unprotected Floor Assemblies in Basement Fire Scenarios, Part 6 - Results of Tests UF-07 and UF-08 (Metal-Web Wood Trusses)," Institute for Research in Construction, National Research Council of Canada, Research Report 251, 2009, http://www.nrc-cnrc.gc.ca/obj/irc/doc/pubs/rr/rr251/rr251.pdf

7. Su, J.Z., Bénichou, N., Bwalya, A.C., Lougheed, G.D., Taber, B.C., Leroux, P., Proulx, G., Kashef, A., McCartney, C., Thomas, J.R., "Fire Performance of Houses, Phase I, Study of Unprotected Floor Assemblies in Basement Fire Scenarios, Summary Report," NRC Institute for Research in Construction, Research Report 252, 2008, http://www.nrc-cnrc.gc.ca/obj/irc/doc/pubs/rr/rr252/rr252.pdf

8. Bwalya, A. C., "An Extended Survey of Combustible Contents in Canadian Residential Living Rooms," Institute for Research in Construction, National Research Council of Canada, Research Report 176, 2004.

9. Canadian Commission on Building and Fire Codes, National Building Code of Canada, National Research Council of Canada, Ottawa, Canada, 2010.

10. Bwalya, A.C., Carpenter, D.W., Kanabus-Kaminska, J.M., Lougheed, G.D., Su, J.Z., Taber, B.C., Bénichou, N., Kashef, A., McCartney, C., Bounagui, A., Thomas, J.R., "Development of a Fuel Package for Use in the Fire Performance of Houses Project," Institute for Research in Construction, National Research Council of Canada, Research Report 207, 2006.

11. Bwalya, A.C., Lougheed, G.D., Su, J.Z., Taber, B.C., Bénichou, N., Kashef, A., "Development of a fuel package for use in the fire performance of houses project," 2007 Fire and Materials Conference (San Francisco, January 29, 2007), pp. 1-14, January 29, 2007.

12. ASTM E1537-02a: Standard Test Method for Fire Testing of Upholstered Furniture", American Society for Testing and Materials, PA, USA, 2002.

13. Su, J.Z., Bwalya, A.C., Lougheed, G.D., Bénichou, N., Taber, B.C., Thomas, J.R., "Fire Scenario Tests in Fire Performance of Houses Test Facility - Data Analysis," Institute for Research in Construction, National Research Council of Canada, Research Report 210, 2007.

14. EC1, Eurocode 1, "Basis of design and design actions on structures", Part 2-2: Actions on Structures Exposed to Fire, ENV 1991-2-2, European Committee for Standardization, Brussels, Belgium, 1994.

15. SNZ, "Code of practice for the general structural design and design loadings for buildings", SNZ 4203, Standards New Zealand, Wellington, New Zealand. 1992.

16. AS/NZS, "Structural design actions, Part 0: General principles", AS/NZS 1170.0, Australia/New Zealand Standard, 2002.

17. ASCE 7-98, ASCE Standard, "Minimum design loads for buildings and other structures", American Society of Civil Engineering, Reston, Virginia, 2000.

18. Su, J.Z., Taber, B.C., Leroux, P., Bénichou, N., Lougheed, G.D., Bwalya, A.C., "Experiments of Sprinkler Protected Ceiling/Floor Assemblies in A Basement Fire Scenario," NRC Institute for Research in Construction, Research Report 308, 2011, http://www.nrc-cnrc.gc.ca/obj/irc/doc/pubs/rr/rr308.pdf

NRC·CNRC

19. Crampton, G.P., "The Design and Construction of a Flame Conductivity Device to Measure Flame Penetration through Floor Systems," Institute for Research in Construction, National Research Council of Canada, Research Report 223, 2006.

20. Forte, N., Crampton, G.P., "The Design and Construction of Electronic Deflection Gauges to Measure the Movement of Floor Assemblies in a Fire," Institute for Research in Construction, National Research Council of Canada, Research Report 202, 2005.

21. ISO 13571, "Life-threatening Components of Fire—Guidelines for the Estimation of Time Available for Escape Using Fire Data," International Organization for Standardization, Geneva, 2007.

22. Purser, D.A., "Toxicity Assessment of Combustion Products," in The SFPE Handbook of Fire Protection Engineering, ed. P.J. DiNenno, D. Drysdale, C.L. Beyler, W.D. Walton, R.L.P. Custer, J.R. Hall, Jr. and J.M. Watts, Jr., 3rd edition, Society of Fire Protection Engineers /National Fire Protection Association, Quincy, Massachusetts, 2002, Section 2, Chapter 6.

23. Christopher J. Wieczorek and Nicholas A. Dembsey, "Human Variability Correction Factors for Use with Simplified Engineering Tools for Predicting Pain and Second Degree Skin Burns", Journal of Fire Protection Engineering, Vol. 11, No. 2, 88-111, 2001

24. Jin, T., "Visibility and Human Behavior in Fire Smoke," in The SFPE Handbook of Fire Protection Engineering, ed. P.J. DiNenno, D. Drysdale, C.L. Beyler, W.D. Walton, R.L.P. Custer, J.R. Hall, Jr. and J.M. Watts, Jr., 3rd edition, Society of Fire Protection Engineers /National Fire Protection Association, Quincy, Massachusetts, 2002, Section 2, Chapter 4.

25. Babrauskas, V., "Combustion of Mattresses Exposed to Flaming Ignition Sources, Part I. Full-Scale Tests and Hazard Analysis," NBSIR 77-1290, National Bureau of Standards, Washington, DC, September 1977.

26. Babrauskas, V., "Full-Scale Burning Behavior of Upholstered Chairs," NBS Technical Note 1103, National Bureau of Standards, Washington, DC, August 1979.

27. Bukowski, R.W., Peacock, R.D., Averill, J.D., Cleary, T.G., Bryner, N.P., Walton, W.D., Reneke, P.A., Kuligowski, E.D., "Performance of Home Smoke Alarms - Analysis of the Response of Several Available Technologies in Residential Fire Settings," NIST Technical Note 1455, National Institute of Standards and Technology, December 2003.

28. Leroux, P., Kanabus-Kaminska, J.M., Seguin, Y.P., Henrie, J.P., Lougheed, G.D., Bwalya, A.C., Su, J.Z., Benichou, N., Thomas, J.R., "Small-scale and Intermediate-scale Fire Tests of Flooring Materials and Floor Assemblies for the Fire Performance of Houses Project," Institute for Research in Construction, National Research Council of Canada, Research Report 211, 2007.

29. CAN/ULC-S101-04, Standard Methods of Fire Endurance Tests of Building Construction and Materials, Underwriters' Laboratories of Canada, Scarborough, Canada, 2004.

30. Sultan, M.A., Seguin, Y.P., Latour, J.C., Leroux, P. and Henrie, J.P., Intermediate-scale Furnace: A New Fire Resistance Test Facility at the National Research Council Canada, Research Report 213, Institute for Research in Construction, National Research Council, Ottawa, ON, 2006.

31. NFPA 13D, "Standard for the Installation of Sprinkler Systems in One- and Two-Family Dwellings and Manufactured Homes," National Fire Protection Association, Quincy, Massachusetts, 2007

32. APA Technical Note, Form J745, "Sprinkler Pipe Installation for APA Performance Rated I-Joists," APA - The Engineered Wood Association, Tacoma, WA, June 2009.

NRC·CNRC